frontiers | Research Topics

Bone health and development in children and adolescents, volume II

Edited by
Fátima Baptista and Federico Baronio

Published in
Frontiers in Endocrinology

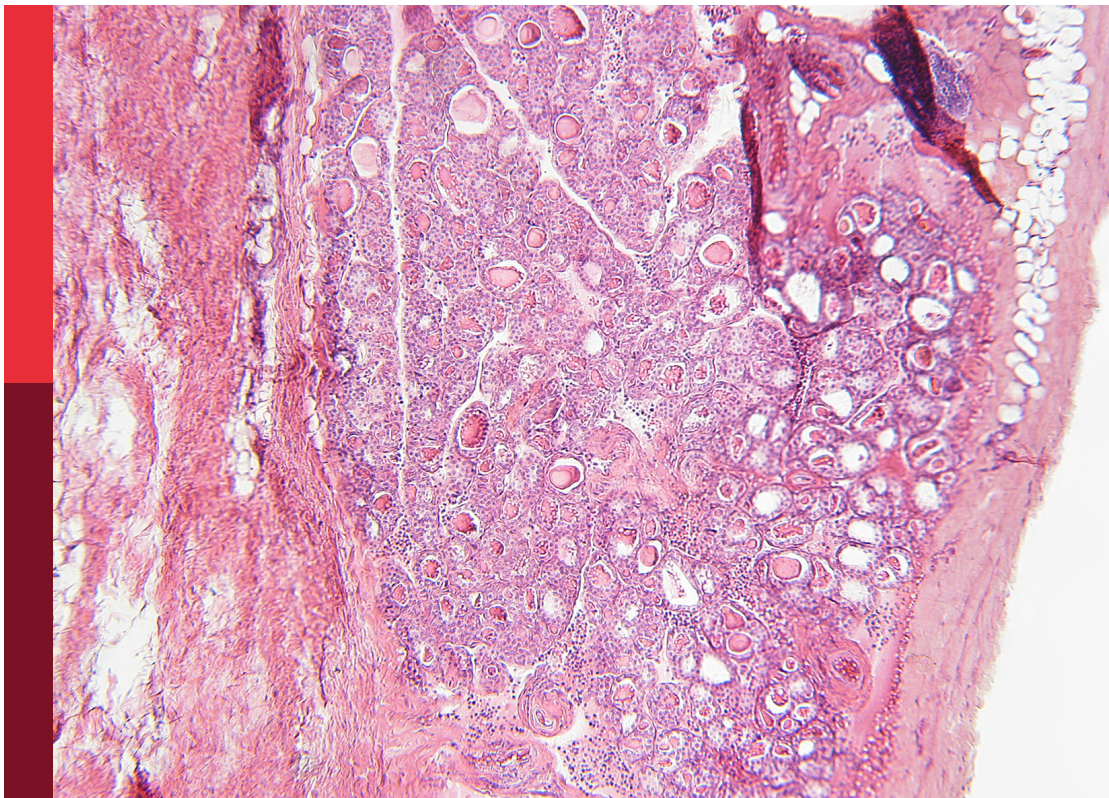

ISSN 1664-8714
ISBN 978-2-8325-7103-3
DOI 10.3389/978-2-8325-7103-3

Generative AI statement
Any alternative text (Alt text) provided alongside figures in the articles in this ebook has been generated by Frontiers with the support of artificial intelligence and reasonable efforts have been made to ensure accuracy, including review by the authors wherever possible. If you identify any issues, please contact us.

About Frontiers

Frontiers is more than just an open access publisher of scholarly articles: it is a pioneering approach to the world of academia, radically improving the way scholarly research is managed. The grand vision of Frontiers is a world where all people have an equal opportunity to seek, share and generate knowledge. Frontiers provides immediate and permanent online open access to all its publications, but this alone is not enough to realize our grand goals.

Frontiers journal series

The Frontiers journal series is a multi-tier and interdisciplinary set of open-access, online journals, promising a paradigm shift from the current review, selection and dissemination processes in academic publishing. All Frontiers journals are driven by researchers for researchers; therefore, they constitute a service to the scholarly community. At the same time, the *Frontiers journal series* operates on a revolutionary invention, the tiered publishing system, initially addressing specific communities of scholars, and gradually climbing up to broader public understanding, thus serving the interests of the lay society, too.

Dedication to quality

Each Frontiers article is a landmark of the highest quality, thanks to genuinely collaborative interactions between authors and review editors, who include some of the world's best academicians. Research must be certified by peers before entering a stream of knowledge that may eventually reach the public - and shape society; therefore, Frontiers only applies the most rigorous and unbiased reviews. Frontiers revolutionizes research publishing by freely delivering the most outstanding research, evaluated with no bias from both the academic and social point of view. By applying the most advanced information technologies, Frontiers is catapulting scholarly publishing into a new generation.

What are Frontiers Research Topics?

Frontiers Research Topics are very popular trademarks of the *Frontiers journals series*: they are collections of at least ten articles, all centered on a particular subject. With their unique mix of varied contributions from Original Research to Review Articles, Frontiers Research Topics unify the most influential researchers, the latest key findings and historical advances in a hot research area.

Find out more on how to host your own Frontiers Research Topic or contribute to one as an author by contacting the Frontiers editorial office: frontiersin.org/about/contact

Bone health and development in children and adolescents, volume II

Topic editors

Fátima Baptista — Universidade de Lisboa, Portugal

Federico Baronio — IRCCS AOU S.Orsola-Malpighi, Dpt Hospital of Woman and Child, Italy

Citation

Baptista, F., Baronio, F., eds. (2025). *Bone health and development in children and adolescents, volume II*. Lausanne: Frontiers Media SA.

doi: 10.3389/978-2-8325-7103-3

Table of contents

frontiers | Frontiers in Endocrinology

TYPE Editorial
PUBLISHED 20 October 2025
DOI 10.3389/fendo.2025.1720995

OPEN ACCESS

EDITED AND REVIEWED BY
Alberto Falchetti,
Santa Maria della Misericordia, Italy

*CORRESPONDENCE
Fátima Baptista
fbaptista@fmh.ulisboa.pt

RECEIVED 08 October 2025
ACCEPTED 09 October 2025
PUBLISHED 20 October 2025

CITATION
Baptista F and Baronio F (2025) Editorial: Bone health and development in children and adolescents, volume II.
Front. Endocrinol. 16:1720995.
doi: 10.3389/fendo.2025.1720995

Editorial: Bone health and development in children and adolescents, volume II

Fátima Baptista[1]* and Federico Baronio[2]

[1]CIPER, Faculdade de Motricidade Humana, Universidade de Lisboa, Lisbon, Portugal, [2]Pediatric Unit, Istituto di Ricovero e Cura a Carattere Scientifico (IRCCS) Azienda Ospedaliero-Universitaria di Bologna, Bologna, Italy

KEYWORDS

mechanical loading, metabolic regulation, cardiometabolic index, bone mineral density (BMD), extracellular vesicles, cerebral palsy, pediatric densitometry, pycnodysostosis

Editorial on the Research Topic
Bone health and development in children and adolescents, volume II

Bone health and development in children and adolescents are key factors for lifelong skeletal strength. During adolescence, about half of an adult's bone mineral content is accumulated, with over 80% of peak bone mass usually reached by age 18. This phase is vital not only for maintaining a healthy diet and establishing healthy eating habits but also for engaging in sufficient physical activity. Mechanical loading influences bone size and structure, while metabolic and hormonal factors control accrual and remodeling. Despite significant progress, gaps remain in understanding how modifiable and inherent factors interact *in vivo* and how to best evaluate bone health in a rapidly changing skeleton. This Research Topic compiles studies exploring the mechanical, metabolic, and psychosocial influences, as well as clinical conditions and diagnostic advancements, offering a comprehensive view of bone development during growth.

In this context, Erlandson et al. followed children engaged in recreational (non-competitive) gymnastics and observed sustained benefits at the distal radius, sites that are typically less exposed to habitual loading. Participants accumulated greater bone area, mineral content, and estimated strength at the wrist, with no apparent differences at the radial shaft or tibia. The pattern suggests modeling responses driven primarily by bone size rather than density, a distinction that matters for fracture resistance at a site where injuries peak during growth. These findings underscore the value of diverse, upper–limb loading in childhood, when rapid linear growth precedes mineral accrual and fragility transiently increases.

By contrast, Agostinete et al. examined adolescent competitive swimmers and found lower areal bone mineral density (aBMD) at the lower limbs and whole body compared with non–athletes, but significantly higher aBMD at the upper limbs. This regional pattern underscores the osteogenic role of muscular contractions in the arms, which experience repetitive loading despite the hypo-gravitational nature of swimming. Training load, defined as session rating of perceived exertion multiplied by training volume, was negatively associated with aBMD; however, inflammatory markers (IL-6, CRP) did not

mediate this relationship. Swimmers presented with higher levels of calcium, vitamin D, and IGF-1, but were leaner and slightly shorter than the control group. Because DXA–derived aBMD is size –dependent, the absence of explicit height adjustment warrants caution when interpreting group differences. It provides a natural bridge to a dedicated study on pediatric densitometry.

Magallares et al. directly addressed this challenge by testing whether the height-for-age Z-score (HAZ) adjustment, following the approach of Zemel et al. (1), should be applied routinely in pediatric DXA interpretation. In 103 children and adolescents, discrepancies of up to 7% emerged between unadjusted and HAZ–adjusted Z–scores at the lumbar spine and whole body. Adjustment reduced misclassification at both ends of the height spectrum, correcting the underestimation of bone density in shorter individuals and the overestimation in taller ones, where bone size may confound aBMD. The study strengthens the case for systematic size correction in pediatric densitometry to improve diagnostic accuracy and comparability across cohorts.

Hodgson et al. used peripheral quantitative computed tomography to characterize tibial structure in children and adolescents with cerebral palsy and other neuromotor impairments. They reported markedly smaller and thinner long bones, with Z –scores for bone and muscle parameters ranging from -2.7 to -1.1. Deficits were greatest in those with poorer motor function. They reflected reduced periosteal expansion and cortical thickness rather than impaired cortical mineralization, an imprint consistent with reduced weight–bearing and attenuated muscular loading. These data reinforce the fundamentally mechanical nature of bone deficits in this population and support the use of targeted, weight-bearing, and muscle-strengthening strategies to reduce fracture risk.

Turning to metabolism, Liu et al. analyzed NHANES data from 1,514 adolescents aged 12–19 years. They observed an inverse association between the cardiometabolic index (a composite of triglycerides, HDL–cholesterol, and waist–to–height ratio) and BMD at the lumbar spine and femoral neck, but not at other proximal femur sites. These predominantly trabecular regions could be more metabolically sensitive to systemic dysregulation of lipid and glucose pathways. Notably, associations persisted after adjustment for BMI and physical activity, suggesting that cardiometabolic risk is related to impaired bone accrual in adolescence, particularly in individuals with central adiposity and an unfavorable lipid profile.

He et al. expanded the scope to include psychosocial factors by studying extracellular vesicle (EV) microRNAs (miRNAs) in participants with a history of early-life stress treated at a psychosomatic clinic. Twenty-two EV-miRNAs were differentially expressed compared to controls, with several associated with bone formation (P1NP), resorption (CTx), or turnover (osteocalcin). Notably, miR-26b-5p and miR-421, both involved in osteogenic differentiation but playing opposite roles —miR-26b-5p promotes and miR-421 inhibits osteogenesis —were linked to bone turnover markers in adjusted models. These results suggest that early psychosocial stress may influence the balance between bone formation and resorption through epigenetic regulation mediated by extracellular vesicle microRNAs, a hypothesis that calls for further mechanistic investigation.

Together, these studies illustrate a complex landscape where bone health during growth depends on the interaction of mechanical loading, metabolic regulation, and psychosocial factors. This physiological framework aids in understanding clinical cases where development is hindered by chronic disease, neuromotor impairment, or genetic predisposition, conditions in which the same biological mechanisms that support normal adaptation, when disrupted, can cause skeletal fragility.

Within clinical contexts, Alsaghier et al. reported a series of eight Saudi patients with pycnodysostosis due to a shared CTSK mutation (NM_000396.3(CTSK):c.244–29A>G) - seven of eight experienced fractures, pseudotumor cerebri, or hypophosphatemia. Response to growth hormone therapy was variable, underscoring the need for individualized care. The authors argue for early genetic screening and a multidisciplinary approach to optimize outcomes.

Cao et al. synthesized evidence on Modic changes in the lumbar spine across 25 studies, estimating an overall occurrence of ~35%. Age, disc degeneration, endplate changes, spondylolisthesis, reduced anterior lumbar lordosis, and a history of physical labor were significant risk factors, whereas sex, BMI, and smoking showed no consistent associations. These insights provide a framework for earlier recognition and targeted management of spine pathology.

Chutani et al. investigated an enriched botanical extract, Fortified Withaferin A (FWA), as a potential enhancer of endochondral bone repair. In rodents, the healing time was reduced from 23–24 days to approximately 12 days, with FWA downregulating osteoclast-related genes, promoting anabolic responses, and reducing inflammation, effects that exceeded those of parathyroid hormone in regulating osteoclasts. While further translational steps are needed, the data support assessing FWA as a cost-effective adjunct in the healing of delayed or osteoporotic fractures.

Cun et al. evaluated the systemic inflammatory response index (SIRI) in 8–19-year-olds and, contrary to many adult reports, observed positive associations with BMD in the pelvis, trunk, and whole body. The authors speculate that moderate inflammation may accompany remodeling during growth, whereas excessive inflammation may be harmful. Sex, age, and BMI influenced these associations, with more favorable outcomes in males and less so in those with obesity, highlighting SIRI as a potential biomarker for early, personalized risk assessment.

In a heterogeneous clinical cohort of children and adolescents referred for bone health assessment, Magallares et al. reported that over 96% of the 103 patients who already exhibited a risk factor showed two or more, which were often unnoticed. The prevalence of low bone mass for chronological age was 10.5%, and childhood osteoporosis was 4.8%. Male sex was positively associated with vertebral BMD, while a sedentary lifestyle and previous fractures were negatively correlated with whole-body and head BMD. Physical inactivity proved to be the most modifiable risk factor,

supporting the routine use of DXA morphometry and targeted interventions.

Zhang et al. focused on transfusion-dependent β-thalassemia and showed that the initially high prevalence of low bone mass (31.6%) decreased to 15.8% after height-adjusted BMD correction. Increasing age was a consistent risk factor; in unadjusted models, IGF-1 levels below -2 SD and hypogonadism were prominent risks, whereas, after adjustment, normal BMI and higher albumin levels were found to be protective. The study highlights the clinical utility of height–adjusted BMD, alongside assessment of the growth hormone axis, gonadal function, and nutritional status.

Wang et al. combined a challenging case with a systematic review to clarify surgical timing in Blount's disease. For children with onset before four years, conservative management followed by timely osteotomy achieves recovery rates of up to 80%. In those over ten years, growth potential assessment guides the strategy: hemiepiphysiodesis is suitable for patients with at least two years of remaining growth, while osteotomy is preferred otherwise. Delayed or inappropriate interventions increase the risk of recurrence and burden, emphasizing the importance of personalized planning.

The collective evidence presented in this Research Topic emphasizes the connection between physiological adaptation and clinical vulnerability. Advances in understanding how mechanical loading, metabolic status, and mental health interact with bone modeling are enhanced by improved diagnostic tools, such as size-adjusted pediatric DXA. Protecting skeletal health during growth, therefore, requires combining these perspectives to encourage diverse physical activity, balanced nutrition, metabolic fitness, and psychosocial well-being, ensuring that growth benefits translate into lifelong skeletal resilience.

Author contributions

FaB: Writing – original draft, Writing – review & editing. FeB: Writing – original draft, Writing – review & editing.

Conflict of interest

The authors declare that the research was conducted in the absence of any commercial or financial relationships that could be construed as a potential conflict of interest.

Generative AI statement

The author(s) declare that no Generative AI was used in the creation of this manuscript.

Any alternative text (alt text) provided alongside figures in this article has been generated by Frontiers with the support of artificial intelligence and reasonable efforts have been made to ensure accuracy, including review by the authors wherever possible. If you identify any issues, please contact us.

Publisher's note

Reference

1. Zemel BS, Leonard MB, Kelly A, Lappe JM, Gilsanz V, Oberfield S, et al. Height adjustment in assessing dual energy x-ray absorptiometry measurements of bone mass and density in children. *J Clin Endocrinol Metab*. (2010) 95:1265–73. doi: 10.1210/jc.2009-2057

frontiers | Frontiers in Endocrinology

TYPE Original Research
PUBLISHED 25 February 2025
DOI 10.3389/fendo.2025.1537574

OPEN ACCESS

EDITED BY
Federico Baronio,
IRCCS AOU S.Orsola-Malpighi, Italy

REVIEWED BY
Rawad El Hage,
University of Balamand, Lebanon
Yongzhi Cui,
Shanghai Jiao Tong University, China

*CORRESPONDENCE
Ziwei Jiang
jiangziwei1686@gzucm.edu.cn

RECEIVED 01 December 2024
ACCEPTED 07 February 2025
PUBLISHED 25 February 2025

CITATION
Cun D, Yang N, Zhou L, Zeng W, Chen B, Pan Z, Feng H and Jiang Z (2025) Relationship between systemic inflammatory response index and bone mineral density in children and adolescents aged 8-19 years: a cross-sectional study based on NHANES 2011-2016.
Front. Endocrinol. 16:1537574.
doi: 10.3389/fendo.2025.1537574

Relationship between systemic inflammatory response index and bone mineral density in children and adolescents aged 8-19 years: a cross-sectional study based on NHANES 2011-2016

Dejun Cun[1], Nan Yang[1], Lin Zhou[1], Wenxing Zeng[1], Bin Chen[2], Zichen Pan[3], Huang Feng[4] and Ziwei Jiang[4]*

[1]Department of Traditional Chinese Medicine, The First Clinical College of Guangzhou University of Chinese Medicine, Guangzhou, China, [2]Department of Traditional Chinese Medicine, The First Clinical College of Yunnan University of Traditional Chinese Medicine, Kunming, China, [3]College of First Clinical Medicine, Shandong University of Traditional Chinese Medicine, Jinan, Shandong, China, [4]Department of Lower Limb Trauma Orthopedics, The First Affiliated Hospital of Guangzhou University of Traditional Chinese Medicine, Guangzhou, China

Objective: This study aims to investigate the relationship between the Systemic Inflammatory Response Index (SIRI) and bone mineral density (BMD) in children and adolescents aged 8-19 years.

Methods: A cross-sectional design was used, utilizing NHANES data from 2011-2016, including 3,205 participants aged 8 to 19 years. Weighted multivariable regression analysis was conducted to assess the association between SIRI and BMD at the lumbar spine, pelvis, trunk, and whole body. Additionally, smooth curve fitting was applied to examine the nonlinear relationship between SIRI and BMD, and subgroup analyses were performed to explore potential interaction effects and modifiers.

Results: SIRI was significantly positively correlated with BMD at the pelvis, trunk, and whole body ($p < 0.05$). After adjusting for covariates, a one-unit increase in ln (SIRI) was associated with increases in BMD of 0.018 g/cm^2, 0.006 g/cm^2, and 0.005 g/cm^2 for the pelvis, trunk, and whole body, respectively. Nonlinear analysis revealed a saturation effect between ln(SIRI) and BMD, with a more pronounced impact at specific threshold values. Subgroup analysis indicated that gender, age, BMI and total calcium levels modulated the relationship between SIRI and BMD.

Conclusion: SIRI is significantly associated with BMD in children and adolescents, with a positive effect on BMD at specific threshold levels. This finding suggests

that SIRI may serve as a potential biomarker for assessing the risk of low bone mineral density, offering theoretical support for the prevention and intervention of bone health issues such as osteoporosis.

KEYWORDS

systemic inflammatory response index, bone mineral density, children and adolescents, NHANES, cross-sectional study

Introduction

BMD is a crucial indicator of bone health and fracture risk (1), particularly during childhood and adolescence, which are critical periods for peak bone mass (PBM) development (2). PBM represents the highest bone density in an individual's lifetime and has been shown to be a key determinant of osteoporosis and fragility fractures in later life (3, 4). Childhood and adolescence are key stages for maximizing bone accumulation, with optimal bone growth during puberty not only determining adult bone health but also providing some protection against age-related bone loss and osteoporosis-related diseases (5, 6). However, the factors influencing bone health are multifaceted (7), including genetic, nutritional, hormonal, and environmental influences.

In recent years, systemic inflammation has increasingly been recognized as an important factor influencing bone remodeling (8, 9). Systemic inflammation may promote bone resorption by activating osteoclasts while inhibiting osteoblast differentiation and function, leading to reduced bone formation. This mechanism is particularly pronounced in chronic inflammatory states and may have profound effects on bone homeostasis and structural integrity. The Systemic Inflammatory Response Index (SIRI), introduced by Qi et al. in 2016 (10), is a novel inflammatory marker calculated based on neutrophil, lymphocyte, and monocyte counts. SIRI can distinguish between the immune-inflammatory responses of three different pathways in the body, reflecting the overall state of inflammation and immune balance. Initially used to predict the survival of pancreatic cancer patients undergoing gemcitabine chemotherapy, SIRI has since been expanded to assess mortality, severity, and sepsis risk in stroke patients (11), and as a reliable immune-inflammatory marker to differentiate between myelin oligodendrocyte glycoprotein antibody-associated diseases (MOGAD) and aquaporin-4 immunoglobulin G-positive neuromyelitis optica spectrum disorders (NMOSD) (12). Furthermore, studies have shown that SIRI is significantly associated with various chronic diseases, such as cardiovascular diseases, metabolic disorders, and chronic inflammation (13, 14). However, the potential impact of SIRI on bone health during the rapid growth phases of children and adolescents remains underexplored. Adolescence is a critical period for rapid skeletal growth, with significant bone turnover, and inflammation may uniquely and importantly affect this process. Yet, research on the relationship between SIRI and BMD in children and adolescents is still lacking.

The National Health and Nutrition Examination Survey (NHANES) provides nationally representative data to study the association between SIRI and BMD. This study utilizes NHANES data from 2011 to 2016 to explore the relationship between SIRI levels and BMD in U.S. children and adolescents aged 8-19 years, with an in-depth analysis of nonlinear relationships, subgroup differences, saturation effects, and threshold effects. The findings will elucidate the potential mechanisms by which SIRI influences skeletal development, providing scientific evidence to optimize bone health and reduce future fracture risk. We hypothesize that, within a moderate range of inflammation levels, elevated SIRI is associated with increased BMD in children and adolescents.

Methods

Study design and population

This study is based on data from the 2011-2016 National Health and Nutrition Examination Survey (NHANES), utilizing a cross-sectional design. NHANES is an ongoing survey program led by the National Center for Health Statistics (NCHS), aimed at obtaining nationally representative samples of the health and nutrition status of the U.S. civilian, non-institutionalized population through complex, multi-stage probability sampling. The survey includes various demographic subgroups, encompassing different ages, genders, races/ethnicities, and socioeconomic backgrounds, ensuring the data's broad representativeness and validity. NHANES data are collected through both household interviews and mobile examination centers (MECs). During the household interview phase, respondents answer a range of questions regarding health, socioeconomic status, lifestyle, and other factors to provide detailed background information. Subsequently, participants visit the MEC for comprehensive physical exams and laboratory tests, including blood analysis and dual-energy X-ray absorptiometry (DXA), among others. This rigorous process enables NHANES to accurately assess health indicators and provide consistent biomarker data. Comprehensive NHANES information can be accessed at http://www.cdc.gov/nhanes.

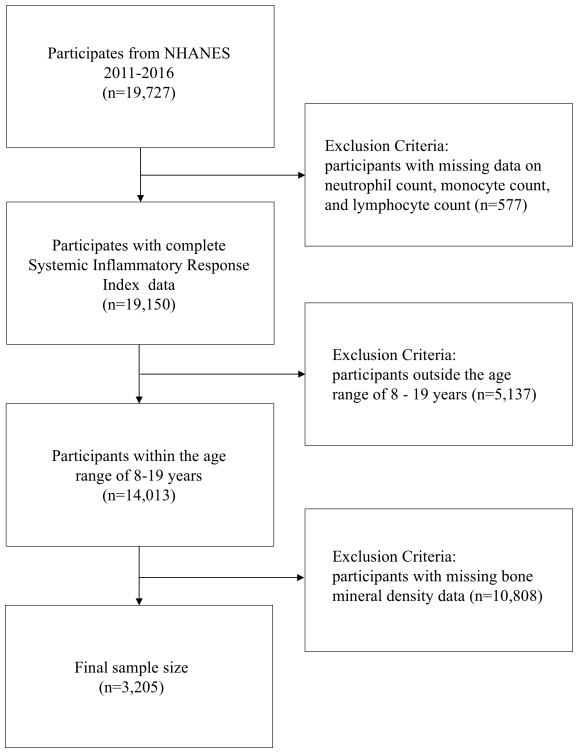

FIGURE 1
Participant inclusion and exclusion criteria flowchart for NHANES.

Data for this study were obtained from three cycles of NHANES (2011-2016), involving 19,727 participants. After excluding 577 participants due to the lack of systemic inflammatory response index (SIRI) data, 5,137 participants who were outside the age range of 8-19 years, and 10,590 participants without available BMD data, the final study sample consisted of 3,205 participants (Figure 1). This study adhered to the Strengthening the Reporting of Observational Studies in Epidemiology (STROBE) guidelines for reporting (15).

Definition of variables

Systemic inflammatory response index

The Systemic Inflammatory Response Index (SIRI) is the primary exposure variable in this study, calculated based on the counts of neutrophils, monocytes, and lymphocytes. The formula for calculating SIRI in this study is as follows: (Neutrophil count × Monocyte count)/ Lymphocyte count. These white blood cell count data were derived from the complete blood count (CBC) and white blood cell differentiation tests in NHANES. NHANES laboratory tests adhere to strict standards for sample collection, processing, and analysis. Blood samples were obtained via venipuncture and processed in laboratories within the mobile examination centers (MECs). CBC and white blood cell differentiation tests were conducted using automated blood analyzers that are regularly calibrated and subject to the quality control standards of the National Health and Nutrition Examination Survey (NHANES) to ensure data accuracy and consistency. Given that inflammatory markers typically exhibit a skewed distribution, a natural logarithmic transformation (ln) of SIRI was applied (Figure 2) to normalize the data, reduce the influence of extreme values, and meet the assumptions for statistical analysis. The transformed ln(SIRI) was then used in multivariable regression models to assess its association with BMD.

Lumbar, pelvis, trunk, and total bone mineral density

The outcome variable in this study is BMD, which includes measurements at four specific sites: lumbar spine (Lumbar BMD), pelvis (Pelvis BMD), trunk (Trunk BMD), and total body (Total BMD). BMD was assessed using dual-energy X-ray absorptiometry (DXA) with a Hologic Discovery model densitometer (Hologic, Inc., Bedford, Massachusetts) and analyzed using Apex version 3.2 software. All BMD values were expressed in grams per square centimeter (g/cm^2) and were standardized according to NHANES

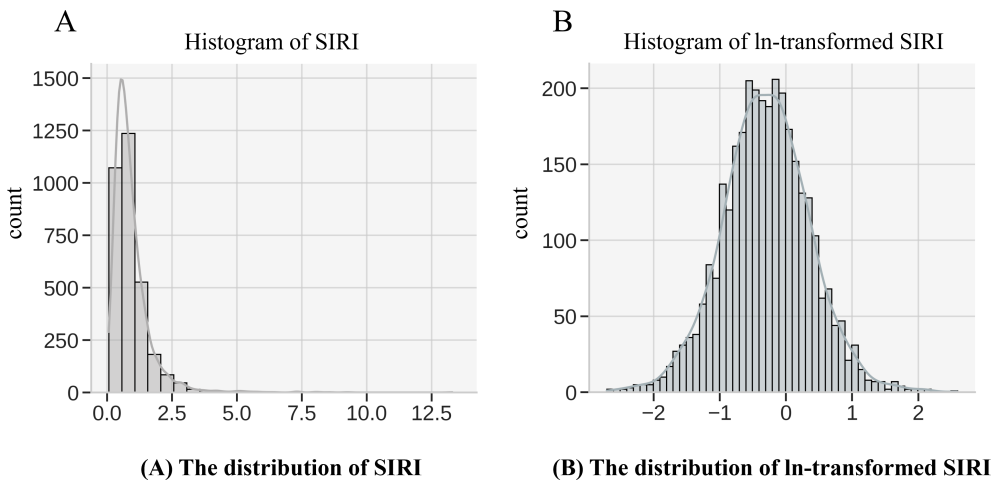

FIGURE 2
Logarithmic transformation of SIRI. **(A)** SIRI **(B)** ln(SIRI).

procedures. BMD data were collected and processed by trained technicians, and the standardized data can be accessed in the NHANES dataset.

Covariates

The selection of covariates was based on theoretical reasoning and research on the relationship between inflammation and bone health. Covariates included age, sex, race/ethnicity, the ratio of family income to poverty (PIR), the number of days per week with at least 60 minutes of physical activity, serum 25-hydroxyvitamin D (X25.OH.D), phosphorus, total calcium, and alkaline phosphatase (ALP). Physical activity specifically refers to activities that elevate the participant's heart rate and result in slight breathlessness. With the exception of sex, race/ethnicity, and the number of days of at least 60 minutes of physical activity per week, all other covariates were treated as continuous variables. Race/ethnicity was categorized into five groups: non-Hispanic White, non-Hispanic Black, Mexican American, other Hispanic, and other ethnicities. The number of days per week with at least 60 minutes of physical activity was categorized from 0 to 7 days. Detailed measurement techniques for the study variables can be found on the Centers for Disease Control and Prevention (CDC) website at www.cdc.gov/nchs/nhanes/.

Statistical analysis

All statistical analyses were conducted using R software version 4.2.1 and EmpowerStats 2.0. To minimize bias introduced by missing data, the random forest imputation method was used to fill in missing values. Descriptive statistics were used to analyze the basic characteristics of the sample, with continuous variables expressed as mean ± standard deviation or median (interquartile range), and categorical variables presented as frequencies and percentages. To compare baseline characteristics, weighted linear regression was applied to continuous variables to ensure sample representativeness and improve the accuracy of estimates, while weighted chi-square tests were used for categorical variables to better reflect the distribution of the target population. In multivariable regression analysis, the SIRI was log-transformed (ln) to correct for its skewed distribution. The transformed ln (SIRI) was treated as the primary exposure variable and grouped into quartiles: Quartile 1 (Q1) for values below the 25th percentile, Quartile 2 (Q2) for the 25th to 50th percentile, Quartile 3 (Q3) for the 50th to 75th percentile, and Quartile 4 (Q4) for the 75th to 100th percentile. The association between ln(SIRI) in each quartile and BMD at the lumbar spine, pelvis, trunk, and total body was assessed, and regression coefficients (β values) along with 95% confidence intervals (CI) were calculated. To control for potential confounders, three progressively adjusted regression models were constructed: Model 1 (unadjusted), Model 2 (adjusted for age, sex, and race/ethnicity), and Model 3 (further adjusted for PIR, the number of days per week of at least 60 minutes of physical activity, X25.OH.D, phosphorus, total calcium, and ALP). To explore potential effect modification by age, sex, race/ethnicity, total calcium, and ALP in the relationship between ln(SIRI) and BMD, total calcium and ALP were categorized into low, medium, and high levels for stratified analysis, and interaction tests were conducted in the models to assess potential modifying effects at different levels. Threshold effect analysis was performed to determine the saturation point in the relationship between ln(SIRI) and BMD. Finally, sensitivity analyses were performed to ensure the robustness of the results. All statistical tests were two-sided, with a p-value < 0.05 considered statistically significant.

Ethics and consent

This study utilized publicly available data from the National Health and Nutrition Examination Survey (NHANES), conducted by the National Center for Health Statistics (NCHS), and approved by the NCHS Research Ethics Review Board. All NHANES participants provided written informed consent prior to data collection, and the study protocol adhered to the ethical principles outlined in the Declaration of Helsinki.

Results

Basic characteristics of participants

A total of 3,205 participants aged 8 to 19 years were included in this study, with a mean age of 13.11 ± 3.44 years. Of these, 52.45% were male and 47.55% were female. The average ln(SIRI) of all participants was -0.30 ± 0.66. The mean BMD values for the lumbar spine, pelvis, trunk, and total body were 0.87 ± 0.19 g/cm², 1.05 ± 0.23 g/cm², 0.77 ± 0.16 g/cm², and 0.95 ± 0.16 g/cm², respectively. Significant differences in baseline characteristics, including age, race, PIR, total calcium, phosphorus, ALP, and the number of days per week of at least 60 minutes of physical activity, were observed across the quartiles of ln(SIRI) (all $p < 0.05$). Compared to the lowest quartile (Q1), Participants in the highest quartile (Q4) were significantly older and had higher BMI indices, more likely to be non-Hispanic White ($p < 0.001$), and engaged in more days of at least 60 minutes of physical activity per week. Furthermore, participants in the Q4 group had lower levels of total calcium, phosphorus, ALP, and PIR compared to those in the Q1 group (Table 1).

Analysis of the relationship between BMD and SIRI

Table 2 presents the results of the weighted multivariable regression analysis, showing a significant positive association between SIRI levels and BMD in all models, except for lumbar BMD ($p < 0.05$). After adjusting for all covariates, each unit increase in ln(SIRI) was associated with a significant increase in pelvic, trunk, and total body BMD. Specifically, pelvic BMD increased by 0.018 g/cm², trunk BMD increased by 0.006 g/cm², and total body BMD increased by 0.005 g/cm².

TABLE 1 Baseline Characteristics of Participants Stratified by Quartiles of ln(SIRI).

Characteristic	Quartiles of ln (SIRI)				P-Value
	Q1	Q2	Q3	Q4	
	N=801	N = 799	N = 801	N = 804	
Age,(years)	12.51 ± 3.31	12.82 ± 3.41	13.20 ± 3.42	13.90 ± 3.47	<0.001
Sex, (%)					0.186
Male	55.06	53.32	51.56	49.88	
Female	44.94	46.68	48.44	50.12	
Race/ethnicity, (%)					<0.001
Mexican American	15.73	20.90	22.85	26.12	
Other Hispanic	7.24	12.02	13.48	16.42	
Non-Hispanic White	18.98	26.41	28.84	27.11	
Non-Hispanic Black	41.95	23.78	19.35	16.29	
Other Race	16.10	16.90	15.48	14.05	
PIR	2.13 ± 1.51	1.98 ± 1.46	1.99 ± 1.46	1.88 ± 1.40	0.009
Total calcium, (mg/dL)	9.61 ± 0.24	9.60 ± 0.22	9.60 ± 0.25	9.54 ± 0.26	<0.001
Phosphorus, (mg/dL)	4.72 ± 0.61	4.64 ± 0.59	4.55 ± 0.59	4.37 ± 0.63	<0.001
ALP, (IU/L)	208.18 ± 98.78	192.53 ± 97.85	177.65 ± 102.05	154.55 ± 90.45	<0.001
25(OH)D, (nmol/L)	57.29 ± 19.37	58.68 ± 19.41	59.41 ± 20.57	57.66 ± 20.06	0.130
BMI, (kg/m^2)	20.65 ± 4.92	21.90 ± 5.51	23.00 ± 5.99	24.05 ± 6.75	<0.001
Days physically active at least 60 min, (%)					<0.001
0	3.12	3.00	2.37	3.73	
1	1.87	2.63	2.75	2.86	
2	2.87	3.25	4.12	3.23	
3	9.86	10.89	15.11	16.17	
4	24.47	24.53	20.85	24.63	
5	19.35	22.15	18.48	19.78	
6	3.12	4.26	6.99	4.48	
7	35.33	29.29	29.34	25.12	
Lumbar BMD, (g/cm^2)	0.84 ± 0.19	0.85 ± 0.19	0.87 ± 0.20	0.90 ± 0.19	<0.001
Pelvis BMD, (g/cm^2)	1.01 ± 0.23	1.04 ± 0.24	1.07 ± 0.23	1.10 ± 0.23	<0.001
Trunk BMD, (g/cm^2)	0.75 ± 0.15	0.76 ± 0.16	0.78 ± 0.16	0.80 ± 0.15	<0.001
Total BMD, (g/cm^2)	0.93 ± 0.16	0.93 ± 0.16	0.95 ± 0.16	0.97 ± 0.15	<0.001

Further analysis was conducted by categorizing ln(SIRI) from a continuous variable into quartiles (Q1 to Q4). Compared to the lowest quartile (Q1), the highest quartile (Q4) was associated with increases in pelvic, trunk, and total body BMD of 0.037 g/cm^2 (β: 0.037; 95% CI: 0.021–0.052, $p < 0.00001$), 0.015 g/cm^2 (β: 0.015; 95% CI: 0.005–0.025, $p = 0.00326$), and 0.013 g/cm^2 (β: 0.013; 95% CI: 0.004–0.022, $p = 0.00559$), respectively. These findings further support a positive association between SIRI and BMD. However, after separately adjusting for BMI and body weight, the effect of SIRI on BMD was no longer significant ($P > 0.05$). This suggests that BMI and body weight may play a more significant role in predicting BMD, potentially masking the independent effect of SIRI (Supplementary Tables 1, 2).

Subgroup analysis and interaction tests

The study results indicate that the association between SIRI levels and pelvic, trunk, and total BMD varied across subgroups (Tables 3). In the subgroup analysis stratified by sex, the correlation

10.3389/fendo.2025.1537574

TABLE 2 Association between ln(SIRI) and Bone Mineral Density.

Exposure	Model 1[β (95%CI)]	Model 2[β (95%CI)]	Model 3[β (95%CI)]
Lumbar BMD (continuous)	0.038 (0.028, 0.048)	0.011 (0.004, 0.017)	0.004 (-0.002, 0.010)
Lumbar BMD (quartile)			
Quartile 1	Reference	Reference	Reference
Quartile 2	0.020 (0.002, 0.039)	0.015 (0.003, 0.027)	0.011 (-0.001, 0.022)
Quartile 3	0.054 (0.036, 0.073)	0.025 (0.013, 0.036)	0.016 (0.004, 0.027)
Quartile 4	0.080 (0.061, 0.098)	0.028 (0.016, 0.040)	0.016 (0.005, 0.028)
p for trend	<0.00001	0.00123	0.20331
Pelvis BMD (continuous)	0.056 (0.044, 0.069)	0.025 (0.016, 0.033)	0.018 (0.010, 0.027)
Pelvis BMD (quartile)			
Quartile 1	Reference	Reference	Reference
Quartile 2	0.041 (0.018, 0.064)	0.035 (0.019, 0.050)	0.029 (0.013, 0.044)
Quartile 3	0.073 (0.050, 0.095)	0.039 (0.024, 0.055)	0.030 (0.014, 0.045)
Quartile 4	0.109 (0.086, 0.132)	0.050 (0.034, 0.065)	0.037 (0.021, 0.052)
p for trend	<0.00001	<0.00001	0.00002
Trunk BMD (continuous)	0.032 (0.024, 0.040)	0.011 (0.005, 0.016)	0.006 (0.001, 0.012)
Trunk BMD (quartile)			
Quartile 1	Reference	Reference	Reference
Quartile 2	0.020 (0.005, 0.036)	0.016 (0.006, 0.026)	0.012 (0.003, 0.022)
Quartile 3	0.042 (0.027, 0.057)	0.020 (0.010, 0.030)	0.014 (0.004, 0.023)
Quartile 4	0.063 (0.048, 0.079)	0.023 (0.013, 0.033)	0.015 (0.005, 0.025)
p for trend	<0.00001	0.00014	0.02017
Total BMD (continuous)	0.031 (0.023, 0.039)	0.010 (0.005, 0.015)	0.005 (0.000, 0.010)
Total BMD (quartile)			
Quartile 1	Reference	Reference	Reference
Quartile 2	0.020 (0.005, 0.035)	0.017 (0.007, 0.026)	0.013 (0.004, 0.022)
Quartile 3	0.040 (0.025, 0.055)	0.020 (0.011, 0.029)	0.014 (0.005, 0.023)
Quartile 4	0.061 (0.046, 0.076)	0.021 (0.012, 0.031)	0.013 (0.004, 0.022)
p for trend	<0.00001	0.00010	0.03120

Model 1: Unadjusted. Model 2: Adjusted for age, sex, and race. Model 3: Adjusted for age, sex, race, PIR, physical activity (≥60 minutes/week), X25.OH.D, phosphorus, total calcium, and ALP.

between ln(SIRI) and pelvic and total BMD showed significant differences (p for interaction < 0.05). Specifically, for each one-unit increase in ln(SIRI), pelvic BMD increased by 0.0271 g/cm² (β: 0.0271; 95% CI: 0.0160–0.0382, p < 0.0001) and total BMD increased by 0.0100 g/cm² (β: 0.0100; 95% CI: 0.0036–0.0164, p = 0.0023) in males. However, in females, the increase in ln(SIRI) did not have a significant effect on either pelvic or total BMD (p > 0.05). Trunk BMD, on the other hand, did not show any significant differences (p for interaction > 0.05). In the subgroup analysis stratified by BMI, the correlation between ln(SIRI) and total BMD showed significant differences (p for interaction < 0.05). In the BMI ≥ 25 kg/m² group, the relationship between SIRI and total BMD was significant (P < 0.05), with each one-unit increase in ln(SIRI) associated with a decrease of 0.013 g/cm² in total BMD (β: -0.013; 95% CI: -0.022, -0.003; p = 0.0087). Moreover, interaction tests revealed that race, age, total calcium, ALP, and the number of physical activity days per week did not significantly influence the association between SIRI and BMD in the stratified analyses (Table 3, all p for interaction > 0.05).

In the interaction test between BMI and SIRI, we performed subgroup analyses stratified by sex and age. The results showed that the interaction between SIRI and BMI had a significant effect on total BMD (p for interaction < 0.05). In the male group with BMI ≥ 18.5 & < 25, the relationship between SIRI and total BMD was significant (P < 0.05), with each one-unit increase in ln (SIRI) associated with an increase of 0.01 g/cm² in total BMD (β: 0.01; 95% CI: 0.001, 0.019). In the male group with BMI ≥ 25, each one-unit increase in ln (SIRI) was associated with a decrease of 0.015 g/cm² in

10.3389/fendo.2025.1537574

TABLE 3 Subgroup analysis of the association between ln(SIRI) and bone mineral density, adjusted for age, sex, race, PIR, physical activity (≥60 minutes/week), X25.OH.D, phosphorus, total calcium, BMI and ALP.

Subgroup	Pelvis BMD [β (95%CI)]	P for interaction	Trunk BMD [β (95%CI)]	P for interaction	Total BMD [β (95%CI)]	P for interaction
Sex		0.0068		0.0508		0.0077
Male	0.027 (0.016, 0.038)		0.010 (0.003, 0.017)		0.010 (0.0036, 0.0164)	
Female	0.004 (-0.009, 0.017)		-0.0005 (-0.008, 0.007)		-0.003 (-0.0105, 0.0041)	
Race/ethnicity		0.4471		0.6184		0.6274
Mexican American	0.029 (0.006, 0.051)		0.008 (-0.007, 0.022)		0.008 (-0.005, 0.021)	
Other Hispanic	0.034 (0.004, 0.064)		0.020 (0.002, 0.039)		0.017 (0.000, 0.034)	
Non-Hispanic White	0.011 (-0.001, 0.023)		0.004 (-0.003, 0.012)		0.003 (-0.003, 0.010)	
Non-Hispanic Black	0.019 (-0.001, 0.040)		0.005 (-0.008, 0.018)		0.002 (-0.009, 0.014)	
Other Race	0.028 (-0.002, 0.058)		0.005 (-0.014, 0.024)		0.005 (-0.012, 0.022)	
Age		0.1475		0.0807		0.1873
8–10 years old	0.004 (-0.017, 0.024)		-0.004 (-0.016, 0.009)		-0.003 (-0.015, 0.008)	
11–13 years old	0.019 (0.002, 0.036)		0.004 (-0.006, 0.015)		0.009 (-0.001, 0.019)	
14–16 years old	0.033 (0.017, 0.048)		0.016 (0.006, 0.026)		0.013 (0.004, 0.022)	
17–19 years old	0.023 (0.009, 0.037)		0.010 (0.001, 0.019)		0.008 (-0.001, 0.016)	
Total calcium		0.4051		0.3583		0.3216
7.30–9.499	0.024 (0.008, 0.040)		0.009 (-0.001, 0.019)		0.002 (-0.007, 0.012)	
9.50–9.68	0.014 (0.000, 0.027)		0.003 (-0.005, 0.012)		0.005 (-0.003, 0.013)	
9.681–11.3	0.026 (0.012, 0.040)		0.012 (0.003, 0.020)		0.011 (0.003, 0.019)	
ALP		0.2386		0.0963		0.5211
31-105	0.015 (0.002, 0.028)		0.002 (-0.006, 0.010)		0.003 (-0.004, 0.011)	
106-240.4	0.027 (0.014, 0.040)		0.013 (0.005, 0.022)		0.009 (0.001, 0.016)	
240.52-740	0.012 (-0.002, 0.026)		0.002 (-0.007, 0.011)		0.004 (-0.005, 0.012)	
BMI		0.1903		0.0300		0.0036
BMI< 18.5	-0.001(-0.015,0.012)		-0.003 (-0.013,0.006)		-0.003 (-0.012,0.005)	
BMI ≥ 18.5 & < 25	0.008 (-0.002,0.018)		0.006(-0.001,0.013)		0.006 (-0.000, 0.013)	
BMI ≥ 25	-0.008 (-0.023,0.007)		-0.009 (-0.019, 0.001)		-0.013 (-0.022, -0.003)	
Days physically active at least 60 min		0.2848		0.1641		0.1251
0	-0.034 (-0.096, 0.027)		-0.023 (-0.062, 0.015)		-0.018 (-0.055, 0.018)	
1	0.013 (-0.051, 0.077)		0.002 (-0.038, 0.042)		0.003 (-0.034, 0.041)	
2	0.065 (0.008, 0.122)		0.047 (0.011, 0.082)		0.036 (0.002, 0.069)	
3	0.018 (-0.010, 0.045)		-0.001 (-0.018, 0.016)		-0.002 (-0.018, 0.014)	
4	0.014 (-0.004, 0.031)		0.004 (-0.007, 0.015)		0.002 (-0.008, 0.012)	
5	0.031 (0.015, 0.048)		0.012 (0.002, 0.022)		0.010 (0.001, 0.020)	
6	0.018 (-0.015, 0.051)		-0.002 (-0.023, 0.019)		-0.012 (-0.031, 0.008)	
7	0.016 (0.002, 0.030)		0.008 (-0.000, 0.017)		0.009 (0.001, 0.017)	

total BMD (β: -0.015; 95% CI: -0.028, -0.001; P < 0.05). In the female group with BMI ≥ 25, each one-unit increase in ln (SIRI) was associated with a decrease of 0.017 g/cm² in total BMD (β: -0.017; 95% CI: -0.029, -0.004; P < 0.05). In other BMI groups, the effect of SIRI on total BMD was not significant (P > 0.05). In the male and female groups with BMI ≥ 25, the effect of SIRI on total BMD was statistically significant (P < 0.05). In the subgroup analysis stratified by age, in the 8–10 years age group, when BMI < 18.5, each one-unit increase in ln (SIRI) was associated with a decrease of 0.010 g/cm² in total BMD (95% CI: -0.019, -0.001, P < 0.05). No significant effect of SIRI on other BMD sites (Pelvis BMD, Trunk BMD) was observed (P > 0.05). When BMI ≥ 18, the effect of SIRI on all BMD sites was not significant (P > 0.05). In the 11–13 years age group, no significant effect of SIRI on any BMD sites was observed (P > 0.05). In the 14–16 years age group, when BMI ≥ 18.5 & < 25, each one-unit increase in ln (SIRI) was associated with an increase of 0.018 g/cm² in total BMD (95% CI: 0.005, 0.032, P < 0.05). When BMI < 18.5 & ≥ 25, the effect of SIRI on all BMD sites was not significant (P > 0.05). In the 17–19 years age group, when BMI ≥ 25, each one-unit increase in ln (SIRI) was associated with a decrease of 0.017 g/cm² in total BMD (95% CI: -0.033, -0.002, P < 0.05). When BMI < 25, the effect of SIRI on all BMD sites was not significant (P > 0.05) (Table 4).

Analysis of nonlinear, threshold, and saturation effects in the relationship between SIRI and bone mineral density

Figure 3 shows the nonlinear relationship and saturation effects between ln (SIRI) and pelvic, trunk, and total BMD, as demonstrated by smooth curve fitting. Among all participants,

TABLE 4 Interaction between ln SIRI and BMI, and subgroup analysis stratified by sex and age.

Subgroup	Pelvis BMD [β (95%CI)]	P for interaction	Trunk BMD [β (95%CI)]	P for interaction	Total BMD [β (95%CI)]	P for interaction
Stratified by sex						
Male		0.0550		0.0416		0.0094
BMI< 18.5	0.004 (-0.013,0.02)		-0.001(-0.013,0.011)		0.000 (-0.011, 0.012)	
BMI ≥ 18.5 & < 25	0.012 (-0.002, 0.026)		0.008 (-0.002, 0.018)		0.010 (0.001, 0.019)	
BMI ≥ 25	-0.018(-0.039, 0.003)		-0.014 (-0.029, 0.001)		-0.015(-0.028, -0.001)	
Female		0.4665		0.2187		0.0849
BMI< 18.5	-0.015 (-0.035, 0.005)		-0.010 (-0.024, 0.003)		-0.012(-0.025, 0.000)	
BMI ≥ 18.5 & < 25	-0.000 (-0.015, 0.015)		0.001 (-0.009, 0.011)		-0.001(-0.010, 0.009)	
BMI ≥ 25	-0.010 (-0.030, 0.010)		-0.011 (-0.024, 0.002)		-0.017(-0.029, -0.004)	
Stratified by age						
8–10 years old		0.4984		0.8719		0.4691
BMI< 18.5	-0.004 (-0.016, 0.009)		-0.006 (-0.015, 0.002)		-0.010(-0.019, -0.001)	
BMI ≥ 18.5 & < 25	-0.015 (-0.033, 0.003)		-0.005 (-0.017, 0.006)		-0.003(-0.016, 0.010)	
BMI ≥ 25	-0.018 (-0.066, 0.030)		-0.013 (-0.044, 0.017)		0.007 (-0.027, 0.041)	
11–13 years old		0.9661		0.6322		0.3273
BMI< 18.5	0.006 (-0.013, 0.025)		0.003 (-0.010, 0.015)		0.004 (-0.008, 0.016)	
BMI ≥ 18.5 & < 25	0.002 (-0.018, 0.022)		-0.003 (-0.017, 0.010)		0.010 (-0.003, 0.023)	
BMI ≥ 25	0.003 (-0.035, 0.041)		-0.009 (-0.035, 0.016)		-0.010(-0.034, 0.014)	
14–16 years old		0.3124		0.1934		0.0641
BMI< 18.5	0.016 (-0.023, 0.055)		-0.001 (-0.013, 0.011)		0.004 (-0.021, 0.030)	
BMI ≥ 18.5 & < 25	0.025 (0.004, 0.045)		0.008 (-0.002, 0.018)		0.018 (0.005, 0.032)	
BMI ≥ 25	-0.004 (-0.036, 0.028)		-0.014 (-0.029, 0.001)		-0.010(-0.031, 0.011)	
17–19 years old		0.2029		0.0617		0.0072
BMI< 18.5	0.033 (-0.027, 0.093)		0.019 (-0.023, 0.060)		0.030 (-0.008, 0.069)	
BMI ≥ 18.5 & < 25	0.012 (-0.002, 0.026)		0.011 (-0.004, 0.025)		0.010 (-0.004, 0.023)	
BMI ≥ 25	0.011 (-0.010, 0.032)		-0.013 (-0.030, 0.003)		-0.017(-0.033, -0.002)	

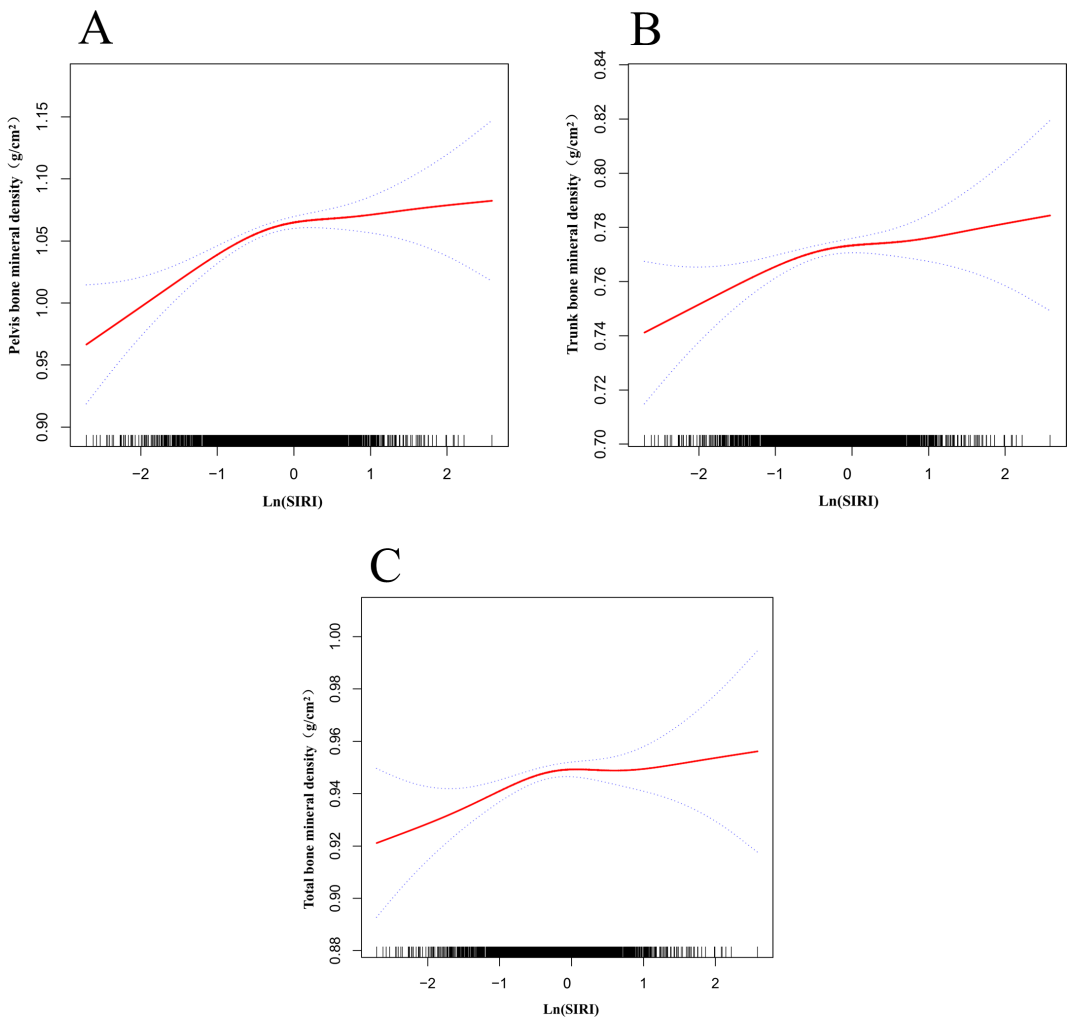

FIGURE 3
Nonlinear relationship between ln(SIRI) and bone mineral density. The red solid line represents the smooth curve fit, and the dashed lines indicate the 95% confidence interval. **(A)** Relationship between ln(SIRI) and pelvic BMD; **(B)** Relationship between ln(SIRI) and trunk BMD; **(C)** Relationship between ln(SIRI) and total BMD.

the saturation point for the relationship between ln(SIRI) and pelvic BMD was -0.336 (Table 5). When ln(SIRI) was below -0.336, the effect size was 0.050 (95% CI: 0.032–0.067, $p < 0.0001$), indicating a significant positive effect of ln(SIRI) on pelvic BMD. However, when ln(SIRI) exceeded -0.336, the increase in ln(SIRI) no longer significantly affected pelvic BMD ($p > 0.05$), exhibiting a saturation effect. Similarly, for trunk BMD, the saturation point for ln(SIRI) was -0.258. When ln(SIRI) was below -0.258, the effect size was 0.018 (95% CI: 0.008–0.029, $p = 0.0004$), showing a significant positive correlation. However, when ln(SIRI) exceeded -0.258, the effect size became -0.004 (95% CI: -0.013, 0.005, $p = 0.3749$), indicating that the effect on trunk BMD was not significant. For total BMD, the saturation point for ln(SIRI) was -0.26. When ln (SIRI) was below -0.26, the effect size was 0.019 (95% CI: 0.010–0.028, $p < 0.0001$), significantly increasing total BMD. When ln (SIRI) exceeded -0.26, the effect size became -0.006 (95% CI: -0.015, 0.002, $p = 0.1454$), suggesting that the increase in ln(SIRI) no longer had a significant effect on total BMD. In summary, ln(SIRI) exhibited nonlinear and saturation effects on pelvic, trunk, and total BMD. with significant increases in BMD below the threshold and no significant effect above the threshold.

All participants were grouped by sex, and smooth curve and threshold effect evaluations were conducted (Table 5, Figure 4A). The results showed that for trunk BMD in males, when ln(SIRI) < -0.357, each unit increase in ln(SIRI) was associated with an increase of 0.020 g/cm² in trunk BMD (95% CI: 0.005, 0.035, $p = 0.0110$). In contrast, for individuals with ln(SIRI) > -0.357, the correlation between ln(SIRI) and trunk BMD was not significant (β: 0.003; 95% CI: -0.010, 0.015, $p = 0.6794$). In females, the relationship between ln(SIRI) and trunk BMD displayed a significant threshold effect. When ln(SIRI) < -0.821, each unit increase in ln(SIRI) was associated with a significant increase in trunk BMD (β: 0.038; 95% CI: 0.012, 0.064, $p = 0.0044$). However, when ln(SIRI) exceeded -0.821, each unit increase in ln(SIRI) resulted in a decrease of 0.009 g/cm² in trunk BMD (β: -0.009; 95% CI: -0.018, -0.001, $p = 0.0385$), indicating that above this threshold, increases in ln(SIRI) may have a negative impact on female BMD. Participants were grouped by age into four categories

10.3389/fendo.2025.1537574

TABLE 5 Saturation and threshold effects of ln(SIRI) on bone mineral density, with stratified results by sex, age, and total calcium levels, adjusted for age, sex, race, PIR, days of at least 60 minutes of physical activity per week, X25.OH.D, phosphorus, total calcium, and ALP.

Subgroup	Pelvis BMD [β (95%CI)]	P for interaction	Trunk BMD [β (95%CI)]	P for interaction	Total BMD [β (95%CI)]	P for interaction
Sex		0.0068		0.0508		0.0077
Male	0.027 (0.016, 0.038)		0.010 (0.003, 0.017)		0.010 (0.0036, 0.0164)	
Female	0.004 (-0.009, 0.017)		-0.0005 (-0.008, 0.007)		-0.003 (-0.0105, 0.0041)	
Race/ethnicity		0.4471		0.6184		0.6274
Mexican American	0.029 (0.006, 0.051)		0.008 (-0.007, 0.022)		0.008 (-0.005, 0.021)	
Other Hispanic	0.034 (0.004, 0.064)		0.020 (0.002, 0.039)		0.017 (0.000, 0.034)	
Non-Hispanic White	0.011 (-0.001, 0.023)		0.004 (-0.003, 0.012)		0.003 (-0.003, 0.010)	
Non-Hispanic Black	0.019 (-0.001, 0.040)		0.005 (-0.008, 0.018)		0.002 (-0.009, 0.014)	
Other Race	0.028 (-0.002, 0.058)		0.005 (-0.014, 0.024)		0.005 (-0.012, 0.022)	
Age		0.1475		0.0807		0.1873
8–10 years old	0.004 (-0.017, 0.024)		-0.004 (-0.016, 0.009)		-0.003 (-0.015, 0.008)	
11–13 years old	0.019 (0.002, 0.036)		0.004 (-0.006, 0.015)		0.009 (-0.001, 0.019)	
14–16 years old	0.033 (0.017, 0.048)		0.016 (0.006, 0.026)		0.013 (0.004, 0.022)	
17–19 years old	0.023 (0.009, 0.037)		0.010 (0.001, 0.019)		0.008 (-0.001, 0.016)	
Total calcium		0.4051		0.3583		0.3216
7.30–9.499	0.024 (0.008, 0.040)		0.009 (-0.001, 0.019)		0.002 (-0.007, 0.012)	
9.50–9.68	0.014 (0.000, 0.027)		0.003 (-0.005, 0.012)		0.005 (-0.003, 0.013)	
9.681–11.3	0.026 (0.012, 0.040)		0.012 (0.003, 0.020)		0.011 (0.003, 0.019)	
ALP		0.2386		0.0963		0.5211
31-105	0.015 (0.002, 0.028)		0.002 (-0.006, 0.010)		0.003 (-0.004, 0.011)	
106-240.4	0.027 (0.014, 0.040)		0.013 (0.005, 0.022)		0.009 (0.001, 0.016)	
240.52-740	0.012 (-0.002, 0.026)		0.002 (-0.007, 0.011)		0.004 (-0.005, 0.012)	
Days physically active at least 60 min		0.2848		0.1641		0.1251
0	-0.034 (-0.096, 0.027)		-0.023 (-0.062, 0.015)		-0.018 (-0.055, 0.018)	
1	0.013 (-0.051, 0.077)		0.002 (-0.038, 0.042)		0.003 (-0.034, 0.041)	
2	0.065 (0.008, 0.122)		0.047 (0.011, 0.082)		0.036 (0.002, 0.069)	
3	0.018 (-0.010, 0.045)		-0.001 (-0.018, 0.016)		-0.002 (-0.018, 0.014)	
4	0.014 (-0.004, 0.031)		0.004 (-0.007, 0.015)		0.002 (-0.008, 0.012)	
5	0.031 (0.015, 0.048)		0.012 (0.002, 0.022)		0.010 (0.001, 0.020)	
6	0.018 (-0.015, 0.051)		-0.002 (-0.023, 0.019)		-0.012 (-0.031, 0.008)	
7	0.016 (0.002, 0.030)		0.008 (-0.000, 0.017)		0.009 (0.001, 0.017)	

(8-10 years, 11-13 years, 14-16 years, 17-19 years), and smooth curve and saturation effect evaluations were conducted (Table 5, Figure 4B). The analysis revealed that the saturation effect between ln(SIRI) and pelvic, trunk, and total BMD was most pronounced in the 14-16-year age group. For pelvic BMD, when ln(SIRI) < -0.233, each unit increase in ln(SIRI) was associated with an increase of 0.081 g/cm² (β: 0.081; 95% CI: 0.049, 0.114, p < 0.0001). In contrast, when ln(SIRI) > -0.233, the increase in ln(SIRI) did not significantly affect pelvic BMD (β: -0.016; 95% CI: -0.047, 0.016, p = 0.3279). In the relationship between ln(SIRI) and trunk BMD, when ln(SIRI) < -0.146, each unit increase in ln(SIRI) was associated with a 0.040 g/cm² increase in trunk BMD (β: 0.040; 95% CI: 0.020, 0.060, p < 0.0001). However, when ln(SIRI) > -0.146, the increase in ln(SIRI) did not significantly affect trunk BMD (β: -0.012; 95% CI: -0.035,

10.3389/fendo.2025.1537574

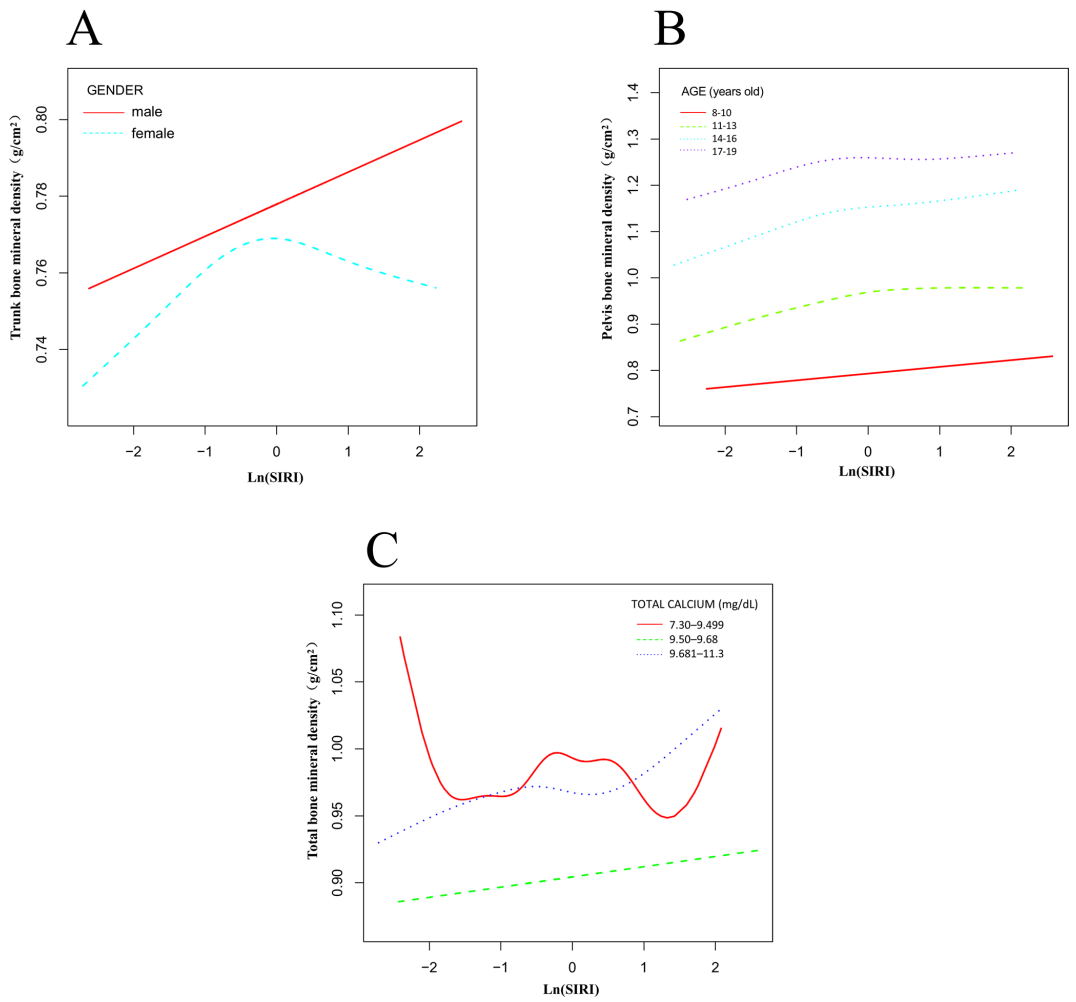

FIGURE 4
Nonlinear association between ln(SIRI) and bone mineral density stratified by sex, age, and total calcium levels. **(A)** Stratified by sex; **(B)** Stratified by age; **(C)** Stratified by total calcium levels.

0.010, p = 0.2796). For total BMD, when ln(SIRI) < -0.197, each unit increase in ln(SIRI) was associated with a 0.032 g/cm² increase in total BMD (β: 0.032; 95% CI: 0.013, 0.050, p = 0.0011). When ln (SIRI) > -0.197, the increase in ln(SIRI) did not significantly affect total BMD (β: -0.008; 95% CI: -0.027, 0.012, p = 0.4475). Participants were divided into three groups based on total calcium levels (7.30–9.499 mg/dL, 9.50–9.68 mg/dL, 9.681–11.3 mg/dL), and smooth curve and threshold effect evaluations were conducted (Table 5, Figure 4C). The analysis revealed that in the 7.30–9.499 mg/dL group, the threshold effects between ln(SIRI) and pelvic, trunk, and total BMD were most pronounced. For total BMD, when ln(SIRI) < 0.255, each unit increase in ln(SIRI) was associated with a 0.020 g/cm² increase in total BMD (β: 0.020; 95% CI: 0.006, 0.035, p = 0.0057). In contrast, when ln(SIRI) > 0.255, the increase in ln(SIRI) was significantly negatively correlated with total BMD, with each unit increase in ln(SIRI) associated with a 0.042 g/cm² decrease in total BMD (β: -0.042; 95% CI: -0.067, -0.017, p = 0.0011). Notably, in this total calcium group, only total BMD exhibited a significant threshold effect, while the threshold effect analysis for pelvic and trunk BMD did not reach statistical significance (p > 0.05). This suggests that at lower total calcium levels, increases in ln(SIRI) have a more pronounced effect on total BMD, particularly showing a significant negative effect above the threshold.

Discussion

This study, using data from the NHANES 2011-2016, explored the association between the Systemic Inflammation Response Index (SIRI) and BMD in children and adolescents aged 8–19. To our knowledge, this is the first study to investigate the relationship between SIRI levels and BMD during the crucial bone growth phases of childhood and adolescence, using a large, nationally representative sample in a cross-sectional design. Our findings indicate a significant association between SIRI levels and BMD, showing a nonlinear relationship, threshold effects, and saturation effects. These results provide new insights into the complex interactions between systemic inflammation and bone health, particularly during key stages of skeletal growth. According to

research by Teresa Iantomas et al., in postmenopausal women with osteoporosis, elevated peripheral blood monocyte levels spontaneously differentiate into osteoclasts and secrete pro-inflammatory cytokines such as IL-1, IL-6, and TNF-α, which further stimulate osteoclast differentiation and activity, leading to an increase in osteoclast numbers and enhanced bone resorption (16, 17). The increased expression of nuclear factor kappa B (NF-κB) ligand receptor activator (RANKL) and RANK in inflammatory neutrophils is closely associated with decreased BMD and increased osteoclast bone resorption (18). T lymphocytes and B lymphocytes participate in bone metabolism by secreting cytokines and regulating the RANKL/OPG balance (19–21). T cells promote osteoclastogenesis by expressing RANKL and secreting pro-inflammatory cytokines such as IL-17 and TNF-α, while B cells, in an inflammatory environment, secrete GCSF and RANKL to accelerate bone resorption. Regulatory T cells (Tregs) and regulatory B cells (Bregs) secrete anti-inflammatory cytokines such as TGF-β and IL-10 to suppress osteoclast activity and promote osteoblast function, thus maintaining the dynamic balance of bone homeostasis (22, 23). This complex balance mechanism determines the dual role of lymphocytes in regulating bone density.

Chronic low-grade inflammation is a core factor in the development of osteoporosis, and its significant role in the pathophysiological mechanisms primarily lies in its disruption of the dynamic balance of bone metabolism (24). Recent studies have emphasized the key role of inflammatory cytokines and immune cells in regulating bone metabolism, which may help explain the complex relationship between systemic inflammation and BMD. Specifically, studies on RANKL, a key regulator of osteoclastogenesis, have shown that its expression is significantly regulated by inflammatory cytokines such as TNF-α, IL-6, and IL-1. Under systemic inflammatory conditions, elevated levels of these cytokines can promote osteoclast differentiation, leading to increased bone resorption and a decrease in BMD (25, 26). Furthermore, research on the role of bone marrow endothelial cells (BMECs) in bone homeostasis suggests that these cells not only regulate vascularization but also influence osteoblast and osteoclast activity through the secretion of angiocrine factors, which may further complicate the inflammatory pathways affecting bone health (27). Recent studies have shown that inflammatory markers such as neutrophil/lymphocyte ratio (NLR), monocyte/lymphocyte ratio (MLR), platelet/lymphocyte ratio (PLR), systemic immune-inflammatory index (SII), and SIRI have important clinical value in reflecting systemic inflammatory status, particularly in the study of diseases such as osteoporosis, cardiovascular diseases, cancer, and metabolic syndrome (28, 29). These composite inflammatory indices stand out for their simplicity and cost-effectiveness, and can be easily obtained through routine blood tests. Additionally, they have significant advantages in terms of ease of measurement and stable data, making them widely applied in clinical practice and scientific research (30).

Our study shows that participants in the highest quartile of SIRI (Q4) were significantly older, engaged in more days of moderate-to-vigorous physical activity (MVPA) per week, and had lower levels of total calcium, phosphorus, and ALP compared to those in the lowest quartile (Q1). The observation that participants with higher SIRI levels are older aligns with the trend of increasing systemic inflammation with age (31, 32), which holds true even in children and adolescents. Adolescence is a key period of growth and hormonal fluctuations, closely linked to dynamic changes in immune function and metabolic processes. This may explain why older participants tend to have higher SIRI levels. The age-related increase in systemic inflammation could partially explain the relationship between SIRI and bone density, as older adolescents are closer to the formation stage of peak bone mass (the point at which bone mineral density and bone strength reach their highest levels) (33, 34). During this stage, inflammatory mediators may play an important role in bone metabolism by modulating the dynamic balance between osteoblasts and osteoclasts. The relationship between physical activity and SIRI levels may reflect the combined effects of short-term acute inflammatory responses and long-term anti-inflammatory effects. This phenomenon may be due to a combination of factors, such as the temporary physiological stress induced by high-intensity exercise, the long-term anti-inflammatory effects that are masked by short-term responses, and the stimulatory effects of exercise on bone metabolism. Mechanical loading from physical activity may both enhance bone formation (35, 36) and transiently increase the release of inflammatory mediators, though the specific mechanisms require further investigation. The lower levels of phosphorus and ALP in participants with higher SIRI levels suggest that systemic inflammation may exacerbate bone metabolic imbalance by affecting mineral metabolism and osteoblast function (37), highlighting the importance of controlling inflammation to maintain bone health. Although our results indicate a significant association between SIRI and BMD, after adjusting for BMI and body weight, the effect of SIRI on BMD was no longer significant. This finding suggests that BMI and body weight may play a more critical role in predicting BMD, possibly by modulating inflammatory responses or directly affecting bone metabolism. Previous studies have identified BMI and body weight as important predictors of BMD in children and adolescents, which is consistent with our results. Therefore, we believe that the potential impact of BMI and body weight on SIRI in studies of BMD in children and adolescents warrants further investigation.

In subgroup analysis, the relationship between SIRI and BMD differed significantly by gender, with a stronger positive correlation observed in males compared to females. This difference may be partly due to hormonal and metabolic differences between adolescent males and females during puberty (38). For example, testosterone in males not only promotes bone growth but may also enhance osteoblast activity and sensitivity to inflammatory signals, thereby reinforcing the positive effects of bone metabolism (39, 40). In contrast, estrogen in females has anti-inflammatory and bone-protective effects (41), which may modulate the impact of SIRI on bone metabolism, leading to a weaker effect of SIRI on BMD in females. Saturation and threshold effect analyses further revealed

gender- and site-specific effects of SIRI on BMD. In males, SIRI exhibited a saturation effect in the pelvis, trunk, and total BMD, with a significant positive correlation with bone density below a specific threshold. However, once the threshold was exceeded, this positive effect plateaued or became nonsignificant, suggesting that moderate inflammation may promote bone formation, but high levels of inflammation may no longer be beneficial. In females, the threshold effect was observed only for trunk BMD, where SIRI had a significant positive effect on BMD below the threshold, but after surpassing the threshold, an increase in SIRI was associated with a decrease in bone density, indicating that high levels of inflammation may disrupt bone metabolic balance. Age stratification analysis further showed that the positive correlation between SIRI and BMD was most significant in the 14-16year age group. This age range corresponds to the critical period of PBM formation. According to research by Bonjour JP (42) and others, bone metabolism is highly active during this period, with the bone formation rate peaking, making this stage more sensitive to systemic inflammation and other external factors. Moreover, BMI stratification revealed that in the obese group (BMI $\geq$ 25 kg/m^2), the negative effect of SIRI on total BMD was significant ($P < 0.05$), further supporting the significant role of chronic inflammation in individuals with high BMI. This finding emphasizes the interaction between BMI and inflammation in bone health, suggesting that a combined approach of controlling both BMI and inflammation may be more effective in improving bone mineral density in obese children and adolescents. Additionally, in the interaction test between BMI and SIRI, subgroup analyses stratified by age and different genders showed that, in the higher BMI group, SIRI is an independent predictor of total BMD. The independent predictive role of SIRI on bone density may be modulated by BMI and gender, particularly in the obese population (BMI $\geq$ 25), where its effect is more pronounced. This also supports the idea that obesity, as a progressive disease, may alter the impact of inflammatory status on BMD. In terms of age, in the younger age groups (8-10 years and 11-13 years), the significant effect of SIRI on bone density was concentrated in total BMD, while in the older age groups (14-16 years and 17-19 years), the effects were more complex, showing both significant positive and negative effects. Notably, total BMD was the site most significantly influenced by SIRI, and the combined modulating effects of BMI and age were particularly evident at this site, suggesting that the independent predictive role of SIRI is crucial in specific BMI and age subgroups.

The positive correlation observed between SIRI and BMD in this study is significant because it contrasts sharply with the negative correlation commonly reported in adult populations. In adults, chronic systemic inflammation is typically associated with increased bone resorption and decreased bone formation (43–45), leading to a reduction in bone density. However, this study shows a positive correlation between SIRI levels and pelvic, trunk, and total BMD, independent of lumbar spine BMD. This may be due to differences in metabolic characteristics of different skeletal regions and their sensitivity to systemic inflammatory signals. After adjusting for covariates, this positive correlation remained stable, suggesting that elevated SIRI levels during childhood and adolescence may contribute to an increase in BMD. Notably, this positive correlation is not infinite. Analysis revealed that beyond a certain threshold (e.g., -0.336 for pelvic BMD), the relationship gradually plateaued and even reversed in some cases, especially for total BMD. This saturation effect suggests that systemic inflammation may have a dual role: during the skeletal growth phase, moderate inflammation levels could promote bone remodeling by modulating the activity of bone metabolism-related cells (such as osteoclasts and osteoblasts). However, when inflammation levels exceed a certain threshold, prolonged high systemic inflammation may disrupt the dynamic balance of bone remodeling, inhibiting bone formation or accelerating bone resorption. This phenomenon is consistent with the hypothesis that low-level systemic inflammation in children and adolescents may stimulate bone metabolism through inflammatory cytokines (e.g., TNF-α, IL-6), which regulate the activity of osteoclasts and osteoblasts. This finding provides new insights into the mechanisms by which inflammation and bone metabolism interact at different ages and underscores the importance of maintaining moderate inflammation levels for bone health in children and adolescents. Furthermore, the relationship between SIRI levels and total BMD is significantly modulated by total calcium levels, with individuals in the lowest calcium quartile showing a pronounced threshold effect. At low calcium levels, moderate systemic inflammation may exert a protective effect by promoting bone metabolism, but once inflammation exceeds a threshold, the balance of bone metabolism is disrupted, leading to a significant decrease in bone density. In contrast, individuals with higher calcium levels did not exhibit a significant threshold effect, suggesting that adequate calcium intake may stabilize bone metabolism dynamics, effectively buffering the negative impact of high inflammation levels on BMD. These results indicate that populations with low calcium intake are more sensitive to the negative effects of systemic inflammation, emphasizing the importance of increasing calcium intake and managing inflammation for bone health protection, especially for high-risk groups with inadequate calcium intake (35, 46, 47).

This study has several limitations. First, due to its cross-sectional design, we cannot establish a causal relationship between SIRI levels and BMD in adolescents. Second, data limitations prevented the inclusion of all possible covariates that might influence bone metabolism, so potential confounding factors, such as dietary habits, types of physical activity, and genetic background, may still exist. Third, although the study population is based on the NHANES national sample, which is representative, the external validity of the results may be limited, especially in groups with different demographic characteristics or healthcare systems. Additionally, NHANES data did not include some key inflammatory biomarkers, which limits a comprehensive analysis of the inflammatory mechanisms. Therefore, future longitudinal studies and multi-center cohort studies will help further explore the causal relationship between SIRI and bone density and provide more insight into the underlying biological mechanisms.

Conclusion

This study reveals the relationship between SIRI and BMD in children and adolescents aged 8 to 19 years. The analysis shows a significant positive correlation between SIRI levels and BMD in the pelvis, trunk, and total body, with this relationship demonstrating nonlinearity and saturation effects. Furthermore, subgroup analysis suggests that factors such as sex, age, and BMI may play a moderating role in the relationship between SIRI and BMD. Overall, SIRI is closely related to BMD, with its effects varying across different age groups, sexes, and BMI categories, providing new insights into the inflammatory mechanisms underlying bone density development in children and adolescents. In conclusion, this study suggests that SIRI could be a valuable biomarker, not only as an early tool for predicting changes in bone density but also for identifying high-risk individuals, thus guiding personalized interventions and optimizing bone health management strategies. This finding offers a simple, cost-effective, and widely applicable method for clinical use, potentially playing a key role in the prevention and treatment of bone diseases such as osteoporosis in the future.

Data availability statement

The original contributions presented in the study are included in the article/Supplementary Material. Further inquiries can be directed to the corresponding author.

Ethics statement

The studies involving humans were approved by The ethics review board of the National Center for Health Statistics. The studies were conducted in accordance with the local legislation and institutional requirements. Written informed consent for participation in this study was provided by the participants' legal guardians/next of kin.

Author contributions

DC: Conceptualization, Data curation, Formal analysis, Methodology, Writing – original draft. NY: Investigation, Software, Visualization, Writing – review & editing. LZ: Data curation, Methodology, Resources, Writing – review & editing. WZ: Formal analysis, Investigation, Methodology, Software, Visualization, Writing – review & editing. BC: Data curation, Investigation, Methodology, Resources, Writing – original draft. ZP: Writing – review & editing. HF: Conceptualization, Data curation, Formal analysis, Methodology, Supervision, Writing – review & editing. ZJ: Conceptualization, Formal analysis, Methodology, Supervision, Writing – review & editing.

Funding

The author(s) declare financial support was received for the research, authorship, and/or publication of this article. The 'Program for Cultivating Academic Reserve Talents of Double First-class and High-level Universities' at Guangzhou University of Traditional Chinese Medicine; the 'National Studio Construction Projects for Experts in Traditional Chinese Medicine (HF Studio N75, 2022)'.

Conflict of interest

The authors declare that the research was conducted in the absence of any commercial or financial relationships that could be construed as a potential conflict of interest.

Generative AI statement

The author(s) declare that no Generative AI was used in the creation of this manuscript.

Publisher's note

Supplementary material

The Supplementary Material for this article can be found online at: https://www.frontiersin.org/articles/10.3389/fendo.2025.1537574/full#supplementary-material

SUPPLEMENTARY TABLE 1
The Relationship Between Ln SIRI and BMD After Adjusting for BMI as a Covariate.

SUPPLEMENTARY TABLE 2
The Relationship Between Ln SIRI and BMD After Adjusting for weight as a Covariate.

References

1. León-Reyes G, Argoty-Pantoja AD, Becerra-Cervera A, López-Montoya P, Rivera-Paredez B, Velázquez-Cruz R. Oxidative-stress-related genes in osteoporosis: A systematic review. *Antioxidants (Basel Switzerland).* (2023) 12(4):915. doi: 10.3390/antiox12040915

2. Heaney RP, Abrams S, Dawson-Hughes B, Looker A, Marcus R, Matkovic V, et al. Peak bone mass. *Osteoporosis international: J established as result cooperation between Eur Foundation Osteoporosis Natl Osteoporosis Foundation USA*. (2000) 11:985–1009. doi: 10.1007/s001980070020

3. Baxter-Jones AD, Faulkner RA, Forwood MR, Mirwald RL, Bailey DA. Bone mineral accrual from 8 to 30 years of age: an estimation of peak bone mass. *J Bone mineral research: Off J Am Soc Bone Mineral Res.* (2011) 26:1729–39. doi: 10.1002/jbmr.412

4. Ferrari S, Rizzoli R, Slosman D, Bonjour JP. Familial resemblance for bone mineral mass is expressed before puberty. *J Clin Endocrinol Metab*. (1998) 83:358–61. doi: 10.1210/jcem.83.2.4583

5. Compston JE, McClung MR, Leslie WD. Osteoporosis. *Lancet (London England).* (2019) 393:364–76. doi: 10.1016/s0140-6736(18)32112-3

6. Xiao PL, Cui AY, Hsu CJ, Peng R, Jiang N, Xu XH, et al. Global, regional prevalence, and risk factors of osteoporosis according to the World Health Organization diagnostic criteria: a systematic review and meta-analysis. *Osteoporosis international: J established as result cooperation between Eur Foundation Osteoporosis Natl Osteoporosis Foundation USA*. (2022) 33:2137–53. doi: 10.1007/s00198-022-06454-3

7. Davies JH, Evans BA, Gregory JW. Bone mass acquisition in healthy children. *Arch Dis childhood.* (2005) 90:373–8. doi: 10.1136/adc.2004.053553

8. Epsley S, Tadros S, Farid A, Kargilis D, Mehta S, Rajapakse CS. The effect of inflammation on bone. *Front Physiol*. (2020) 11:511799. doi: 10.3389/fphys.2020.511799

9. Pathak JL, Bakker AD, Luyten FP, Verschueren P, Lems WF, Klein-Nulend J, et al. Systemic inflammation affects human osteocyte-specific protein and cytokine expression. *Calcified Tissue Int*. (2016) 98:596–608. doi: 10.1007/s00223-016-0116-8

10. Qi Q, Zhuang L, Shen Y, Geng Y, Yu S, Chen H, et al. A novel systemic inflammation response index (SIRI) for predicting the survival of patients with pancreatic cancer after chemotherapy. *Cancer*. (2016) 122:2158–67. doi: 10.1002/cncr.30057

11. Zhang Y, Xing Z, Zhou K, Jiang S. The predictive role of systemic inflammation response index (SIRI) in the prognosis of stroke patients. *Clin Interventions aging.* (2021) 16:1997–2007. doi: 10.2147/cia.S339221

12. Wang L, Xia R, Li X, Shan J, Wang S. Systemic inflammation response index is a useful indicator in distinguishing MOGAD from AQP4-IgG-positive NMOSD. *Front Immunol*. (2023) 14:1293100. doi: 10.3389/fimmu.2023.1293100

13. Sun H, Liu H, Li J, Kou J, Yang C. Analysis of the clinical predictive value of the novel inflammatory indices SII, SIRI, MHR and NHR in patients with acute myocardial infarction and their extent of coronary artery disease. *J Inflammation Res*. (2024) 17:7325–38. doi: 10.2147/jir.S479253

14. Li X, Cui L, Xu H. Association between systemic inflammation response index and chronic kidney disease: a population-based study. *Front endocrinology.* (2024) 15:1329256. doi: 10.3389/fendo.2024.1329256

15. von Elm E, Altman DG, Egger M, Pocock SJ, Gøtzsche PC, Vandenbroucke JP. The Strengthening the Reporting of Observational Studies in Epidemiology (STROBE) statement: guidelines for reporting observational studies. *Ann Internal Med*. (2007) 147:573–7. doi: 10.7326/0003-4819-147-8-200710160-00010

16. Iantomasi T, Romagnoli C, Palmini G, Donati S, Falsetti I, Miglietta F, et al. Oxidative stress and inflammation in osteoporosis: molecular mechanisms involved and the relationship with microRNAs. *Int J Mol Sci*. (2023) 24(4):3772. doi: 10.3390/ijms24043772

17. D'Amelio P, Grimaldi A, Pescarmona GP, Tamone C, Roato I, Isaia G. Spontaneous osteoclast formation from peripheral blood mononuclear cells in postmenopausal osteoporosis. *FASEB journal: Off Publ Fed Am Societies Exp Biol.* (2005) 19:410–2. doi: 10.1096/fj.04-2214fje

18. Iking-Konert C, Ostendorf B, Sander O, Jost M, Wagner C, Joosten L, et al. Transdifferentiation of polymorphonuclear neutrophils to dendritic-like cells at the site of inflammation in rheumatoid arthritis: evidence for activation by T cells. *Ann rheumatic diseases.* (2005) 64:1436–42. doi: 10.1136/ard.2004.034132

19. Frase D, Lee C, Nachiappan C, Gupta R, Akkouch A. The inflammatory contribution of B-lymphocytes and neutrophils in progression to osteoporosis. *Cells.* (2023) 12(13):1744. doi: 10.3390/cells12131744

20. Zhang W, Dang K, Huai Y, Qian A. Osteoimmunology: the regulatory roles of T lymphocytes in osteoporosis. *Front endocrinology.* (2020) 11:465. doi: 10.3389/fendo.2020.00465

21. Weitzmann MN, Ofotokun I. Physiological and pathophysiological bone turnover - role of the immune system. *Nat Rev Endocrinology.* (2016) 12:518–32. doi: 10.1038/nrendo.2016.91

22. Sato K, Suematsu A, Okamoto K, Yamaguchi A, Morishita Y, Kadono Y, et al. Th17 functions as an osteoclastogenic helper T cell subset that links T cell activation and bone destruction. *J Exp Med*. (2006) 203:2673–82. doi: 10.1084/jem.20061775

23. Kong YY, Feige U, Sarosi I, Bolon B, Tafuri A, Morony S, et al. Activated T cells regulate bone loss and joint destruction in adjuvant arthritis through osteoprotegerin ligand. *Nature.* (1999) 402:304–9. doi: 10.1038/46303

24. Zhivodernikov IV, Kirichenko TV, Markina YV, Postnov AY, Markin AM. Molecular and cellular mechanisms of osteoporosis. *Int J Mol Sci*. (2023) 24(21):15772. doi: 10.3390/ijms242115772

25. Cui Y, Lv B, Li Z, Ma C, Gui Z, Geng Y, et al. Bone-targeted biomimetic nanogels re-establish osteoblast/osteoclast balance to treat postmenopausal osteoporosis. *Small (Weinheim an der Bergstrasse Germany).* (2024) 20:e2303494. doi: 10.1002/smll.202303494

26. Cui Y, Guo Y, Kong L, Shi J, Liu P, Li R, et al. A bone-targeted engineered exosome platform delivering siRNA to treat osteoporosis. *Bioactive materials.* (2022) 10:207–21. doi: 10.1016/j.bioactmat.2021.09.015

27. Cui Y, Li Z, Guo Y, Qi X, Yang Y, Jia X, et al. Bioinspired nanovesicles convert the skeletal endothelium-associated secretory phenotype to treat osteoporosis. *ACS nano.* (2022) 16:11076–91. doi: 10.1021/acsnano.2c03781

28. Fu Q, Zhang C, Yang Y, Teng R, Liu F, Liu P, et al. Correlation study of multiple inflammatory indices and vertebral compression fracture: A cross-sectional study. *J Clin Trans endocrinology.* (2024) 37:100369. doi: 10.1016/j.jcte.2024.100369

29. Nie YZ, Yan ZQ, Yin H, Shan LH, Wang JH, Wu QH. Osteosarcopenic obesity and its components-osteoporosis, sarcopenia, and obesity-are associated with blood cell count-derived inflammation indices in older Chinese people. *BMC geriatrics.* (2022) 22:532. doi: 10.1186/s12877-022-03225-x

30. Chen S, Sun X, Jin J, Zhou G, Li Z. Association between inflammatory markers and bone mineral density: a cross-sectional study from NHANES 2007-2010. *J orthopaedic Surg Res*. (2023) 18:305. doi: 10.1186/s13018-023-03795-5

31. Thevaranjan N, Puchta A, Schulz C, Naidoo A, Szamosi JC, Verschoor CP, et al. Age-associated microbial dysbiosis promotes intestinal permeability, systemic inflammation, and macrophage dysfunction. *Cell Host Microbe*. (2017) 21:455–66.e4. doi: 10.1016/j.chom.2017.03.002

32. Chung HY, Cesari M, Anton S, Marzetti E, Giovannini S, Seo AY, et al. Molecular inflammation: underpinnings of aging and age-related diseases. *Ageing Res Rev*. (2009) 8:18–30. doi: 10.1016/j.arr.2008.07.002

33. Chevalley T, Rizzoli R. Acquisition of peak bone mass. *Best Pract Res Clin Endocrinol Metab*. (2022) 36:101616. doi: 10.1016/j.beem.2022.101616

34. Bachrach LK. Acquisition of optimal bone mass in childhood and adolescence. *Trends Endocrinol metabolism: TEM.* (2001) 12:22–8. doi: 10.1016/s1043-2760(00)00336-2

35. Ondrak KS, Morgan DW. Physical activity, calcium intake and bone health in children and adolescents. *Sports Med (Auckland NZ).* (2007) 37:587–600. doi: 10.2165/00007256-200737070-00003

36. Karlsson MK, Rosengren BE. Exercise and peak bone mass. *Curr Osteoporos Rep*. (2020) 18:285–90. doi: 10.1007/s11914-020-00588-1

37. Schini M, Vilaca T, Gossiel F, Salam S, Eastell R. Bone turnover markers: basic biology to clinical applications. *Endocrine Rev*. (2023) 44:417–73. doi: 10.1210/endrev/bnac031

38. Vanderschueren D, Laurent MR, Claessens F, Gielen E, Lagerquist MK, Vandenput L, et al. Sex steroid actions in male bone. *Endocrine Rev*. (2014) 35:906–60. doi: 10.1210/er.2014-1024

39. Walsh JS, Eastell R. Osteoporosis in men. *Nat Rev Endocrinology.* (2013) 9:637–45. doi: 10.1038/nrendo.2013.171

40. Al Mukaddam M, Rajapakse CS, Bhagat YA, Wehrli FW, Guo W, Peachey H, et al. Effects of testosterone and growth hormone on the structural and mechanical properties of bone by micro-MRI in the distal tibia of men with hypopituitarism. *J Clin Endocrinol Metab*. (2014) 99:1236–44. doi: 10.1210/jc.2013-3665

41. Emmanuelle NE, Marie-Cécile V, Florence T, Jean-François A, Françoise L, Coralie F, et al. Critical role of estrogens on bone homeostasis in both male and female: from physiology to medical implications. *Int J Mol Sci*. (2021) 22(4):1568. doi: 10.3390/ijms22041568

42. Bonjour JP, Theintz G, Law F, Slosman D, Rizzoli R. Peak bone mass. *Osteoporosis international: J established as result cooperation between Eur Foundation Osteoporosis Natl Osteoporosis Foundation USA*. (1994) 4 Suppl 1:7–13. doi: 10.1007/bf01623429

43. Briot K, Geusens P, Em Bultink I, Lems WF, Roux C. Inflammatory diseases and bone fragility. *Osteoporosis international: J established as result cooperation between Eur Foundation Osteoporosis Natl Osteoporosis Foundation USA*. (2017) 28:3301–14. doi: 10.1007/s00198-017-4189-7

44. Redlich K, Smolen JS. Inflammatory bone loss: pathogenesis and therapeutic intervention. *Nat Rev Drug discovery.* (2012) 11:234–50. doi: 10.1038/nrd3669

45. Chen Y, Yu J, Shi L, Han S, Chen J, Sheng Z, et al. Systemic inflammation markers associated with bone mineral density in perimenopausal and postmenopausal women. *J Inflammation Res*. (2023) 16:297–309. doi: 10.2147/jir.S385220

46. Boot AM, de Ridder MA, Pols HA, Krenning EP, de-Muinck-Keizer-Schrama SM. Bone mineral density in children and adolescents: relation to puberty, calcium intake, and physical activity. *J Clin Endocrinol Metab*. (1997) 82:57–62. doi: 10.1210/jcem.82.1.3665

47. Johnston CC Jr., Miller JZ, Slemenda CW, Reister TK, Hui S, Christian JC, et al. Calcium supplementation and increases in bone mineral density in children. *New Engl J Med*. (1992) 327:82–7. doi: 10.1056/nejm199207093270204

frontiers | Frontiers in Endocrinology

TYPE Original Research
PUBLISHED 26 February 2025
DOI 10.3389/fendo.2025.1515910

OPEN ACCESS

EDITED BY
Fátima Baptista,
Universidade de Lisboa, Portugal

REVIEWED BY
Melanie Haffner-Luntzer,
University of Ulm, Germany
Benjamin Garfinkel,
Alnylam Pharmaceuticals, United States

*CORRESPONDENCE
Yangyang He
yangyang.he@uni-potsdam.de

RECEIVED 23 October 2024
ACCEPTED 03 February 2025
PUBLISHED 26 February 2025

CITATION
He Y, Wuertz-Kozak K, Cazzanelli P, Houtenbos S, Garcia-Carrizo F, Schulz TJ and Wippert P-M (2025) Differential expression of plasma extracellular vesicles microRNAs and exploration of their association with bone metabolism in childhood trauma participants treated in a psychosomatic clinic. *Front. Endocrinol.* 16:1515910. doi: 10.3389/fendo.2025.1515910

Differential expression of plasma extracellular vesicles microRNAs and exploration of their association with bone metabolism in childhood trauma participants treated in a psychosomatic clinic

Yangyang He[1,2]*, Karin Wuertz-Kozak[3,4], Petra Cazzanelli[3], Sanne Houtenbos[1,2], Francisco Garcia-Carrizo[5,6], Tim J. Schulz[5,6,7] and Pia-Maria Wippert[1,2]

[1]Medical Sociology and Psychobiology, University of Potsdam, Potsdam, Germany, [2]Faculty of Health Sciences Brandenburg, Joint Faculty of the University of Potsdam, The Brandenburg, Medical School Theodor Fontane and The Brandenburg University of Technology Cottbus—Senftenberg, Potsdam, Germany, [3]Department of Biomedical Engineering, Rochester Institute of Technology, Rochester, NY, United States, [4]Schoen Clinic Munich Harlaching, Spine Center, Academic Teaching Hospital and Spine Research Institute of the Paracelsus Medical University Salzburg, Munich, Germany, [5]Department of Adipocyte Development and Nutrition, German Institute of Human Nutrition, Potsdam, Germany, [6]German Center for Diabetes Research (DZD), München, Germany, [7]Institute of Nutritional Science, University of Potsdam, Potsdam, Germany

Introduction: Early life stress (ELS) impacts neurotransmitters and cell communication, potentially disrupting neurological and physiological processes. Recently, ELS has been implicated in impaired bone metabolism, with extracellular vesicles (EVs) and their cargo, microRNAs (miRNAs), might affecting this process. This research aimed to elucidate the association between childhood trauma, a specific form of ELS, and bone metabolism through studying miRNA in EVs within three steps: firstly, examining alterations of EV miRNAs between ELS and controls, secondly analyzing associations between altered EV miRNAs and bone markers, and thirdly exploring the target gene prediction and enrichment pathways of altered EV miRNAs.

Methods: This study included a subgroup of the DEPREHA project (total n=208) from a psychosomatic clinic. Firstly, real-time quantitative PCR was performed on plasma EVs isolated from childhood trauma participants with depression (n=6) and matched healthy controls (n=9) to detect the differentially expressed EV miRNAs. Secondly, general linear regression models were employed to investigate the associations between specific EV miRNAs and circulating bone turnover markers (procollagen type 1 amino-terminal propeptide (P1NP), osteocalcin, and β-CrossLaps (CTx)), adjusting for depression as a potential confounder. Thirdly, the miRNA target gene networks and enriched pathways were explored based on altered EV miRNAs.

Results: These analyses could be conducted on n=19 participants from the entire group (11 [57.9%] female; median [IQR] age, 35.00 [26.00] years), but finally n=15

participants were included for analyses. 22 out 380 EV miRNAs were differentially expressed between childhood trauma participants (6 up-regulated and 16 down-regulated) and healthy controls. Among these, miR-25-3p, miR-26b-5p, miR-451a, and miR-421 were associated with P1NP (bone formation marker) and CTx (bone resorption marker). MiR-26b-5p, miR-330-3p, and miR-542-5p were associated with osteocalcin (bone turnover marker). MiRNA target gene network prediction revealed highly associated target genes of dysregulated miRNAs, such as Trinucleotide Repeat Containing Adaptor 6B (*TNRC6B*), and enrichment analysis highlighted pathways including the forkhead box protein O (FoxO) signaling pathway.

Discussions: This study explored the potential associations between childhood trauma and bone metabolism, due to the sample size and experimental group limitations, these associations should be validated in future experiments with larger sample sizes and different control group settings.

KEYWORDS

mental disorder, epigenetics, bone remodeling, osteoporosis, bone turnover markers

Introduction

Stress is a state in which the homeodynamic balance of an organism is threatened (1), and chronic or excessive stress reactions may cause a series of pathological reactions that affect the organism's health. The term early life stress (ELS) refers to a single or a series of adverse events and stressful experiences during childhood, including childhood abuse, neglect, parental illness, separation, and poverty (2). As brain development largely occurs during this early stage of life, stressor exposure can have enduring effects, leading to the development of mental illness later in life (3, 4). Among adult patients suffering from mental illnesses, 53% report having experienced at least one childhood adversity (5), highlighting the high impact of ELS on public health.

ELS involves different moderating factors, including neuroendocrine stress responsiveness, the immune system, epigenetic programming, metabolism, and the transcriptome (6), which can induce biopsychological effects in later life. In this article, childhood trauma will be addressed, which represents a specific form of ELS and is defined as "a traumatic event is one that threatens injury, death, or the physical integrity of self or others and also causes horror, terror, or helplessness at the time it occurs." (7). Accumulating evidence showed that childhood trauma is associated with various mental disorders in a lifetime, for example, posttraumatic stress disorder (8), anxiety (9), and depression (10). It has also been demonstrated that individuals with childhood trauma and during a depressive episode showed deteriorating effects on bone health, such as reduced bone mineral density, regardless of age (11). Previous studies have shown that depression is associated with increased bone loss (12) and fracture risk (13), and is considered a risk factor for osteoporosis (14–16). Bone metabolism consists of a balance between bone-forming osteoblasts and bone-resorbing osteoclasts which helps maintain balanced calcium homeostasis while at the same time ensuring that the skeleton is able to deliver stable mechanical support. Disruptions in this delicate equilibrium, particularly when bone resorption outpaces formation, culminate in pathology, which includes diminished bone mass and structural deterioration, a condition recognized as osteoporosis (17). However, the molecular link between childhood trauma and osteoporosis/bone damage has not been studied so far. Of note, considering that the association between circulating miRNAs and static bone microstructure is weak, and the dynamic changes in bone turnover are better reflected at the level of circulating miRNAs (18), the bone turnover markers were used in the present research to understand the bone metabolism. These markers were selected for the following reasons: procollagen type 1 amino-terminal propeptide (P1NP) is released during the synthesis of type I collagen and is regarded as an indicator of bone formation (19); elevated P1NP levels suggest increased bone formation. Osteocalcin is expressed in the mature stage of osteoblasts and released from the bone matrix during resorption (20); hence, increased osteocalcin levels refer to high bone turnover

Abbreviations: ARHGAP12, Rho GTPase Activating Protein 12; BDI-II, Beck Depression Inventory-II questionnaire; BMI, Body mass index; CTS, Childhood Trauma Screener; CTx, β-CrossLaps; ELS, Early life stress; EVs, Extracellular vesicles; FDR, false discovery rate; FoxO, forkhead box protein O; HPA, hypothalamic pituitary adrenal; hsa-miR, *Homo sapiens* microRNA; IGF-1, Insulin-like growth factor 1; IQR, Interquartile range; KEGG, Kyoto Encyclopedia of Genes and Genomes; miRNA, miR, MicroRNA; mRNA, messenger RNA; NUFIP2, Nuclear FMR1 Interacting Protein 2; P1NP, Procollagen type I N-terminal propeptide; PAP2C, Phospholipid Phosphatase 2; PI3K, Phosphatidylinositol-4,5-bisphosphate 3-kinase; PKB or Akt, protein kinase B; TNRC6B, Trinucleotide Repeat Containing Adaptor 6B; WEE1, WEE1 G2 Checkpoint Kinase; ZBTB18, Zinc Finger And BTB Domain Containing 18

status with both increased bone formation and resorption (21). The collagen fragment β-CrossLaps (CTx) is generated during the bone resorption process (22). Increased CTx levels are indicative of enhanced bone resorption.

It has become increasingly apparent that extracellular vesicles (EVs) are important in cellular communication, leading to a crucial role in many physiological and pathological processes. These vesicles, released by cells into the extracellular environment, are involved in intercellular communication either by acting on cells surrounding the secreting cells or distant cells through the circulation of biofluids (23). Analyzing the cargo of EVs, such as microRNAs (miRNAs), can provide insights into paracrine and endocrine cell regulation and may highlight a link between childhood trauma and the impairment of bone health (24). MiRNAs regulate subsets of targeted messenger RNAs (mRNAs) (25), and are considered as part of epigenetics. There is increasing evidence that dysregulated miRNAs (in biofluids/tissues as well as in EVs) play an essential role in the pathological process of various mental disorders (26–28). In terms of childhood trauma, studies found altered expression levels of miRNAs in different tissues from childhood trauma participants (29, 30). The association between circulating miRNAs and childhood trauma was also identified; for example, a significant association was found between the altered expression of plasma miR-19b-3p and childhood traumatic experiences (31). Moreover, EV miR-450a-2-3p levels are associated with scores of total childhood trauma, emotional abuse, and physical neglect (32). The diverse properties of miRNAs and the fact that their expression in EVs is altered by physiological changes such as disease states make miRNA cargo in EVs a subject of interest to research the association between childhood trauma and bone health. Many miRNA functional annotation tools today can provide more information on potential biological processes and pathways regarding miRNAs, such as DNA Intelligent Analysis (DIANA)-miRPath v4.0 (33). Thus, miRNA informatics tools were used in this study to gain a deeper understanding of the possible roles of miRNA cargo between childhood trauma and bone health.

The present research aimed to explore the association between childhood trauma and bone metabolism by studying the cargo of EVs within three steps. Firstly, it should be analyzed, whether there are differences in miRNA expression in plasma EV between childhood trauma participants and healthy controls. Secondly, the possible associations between the EV miRNAs expression and levels of circulating bone turnover markers should be examined in the same blood samples. Thirdly, altered miRNAs expression in EVs should be used to explore enriched targeted genes and pathways.

Methods

Participants

For this study, data from an interventional study with depressive patients (DEPREHA (34), n=208) were used, some of whom had experienced childhood trauma. The inclusion criteria were strictly defined, resulting in a homogeneous cohort with minimal confounding variables and were as follows: individuals aged 18-65 years with a diagnosis of depressive episode (ICD-10 F32.x or F33.x), dysthymia (F34.1), or adjustment disorder with prolonged depressive reaction (F43.21); Inability to work for more than 21 days in the last 12 months due to the above diagnosis. Exclusion criteria were: Pregnancy; Hormone therapy (excluding hormonal contraception); Intellectual disability (ICD-10 F70-89); Compliance with other primary diagnoses, e.g., Hormonal/endocrine metabolic disorders (diabetes mellitus, thyroid dysfunction, renal, hepatic disorders, etc.); Neurological disorders; Dementia (ICD-10 F00-F03); Psychotropic drug dependence syndrome (ICD-10 F1x.2); Schizophrenia (ICD-10 F20); Psychotic, stress, and somatoform disorders (F40-49, unless they fall within the inclusion criteria); Emotionally unstable personality disorder (ICD-10 F60.3x) and other personality and behavioral disorders (F61-F69); Acute infections; Immune system disorders; Unstable remitting addictions other than nicotine; Acute drug abuse other than nicotine. The control group consisted of healthy volunteer participants, all of them were without the diagnosis of a depressive episode or early childhood trauma. Furthermore, the same exclusion criteria as mentioned above were applied to the control group. This enabled a comparison between depressed individuals with and without childhood trauma, alongside a control group without childhood trauma.

Ethical statement

All participants in this study were informed of the purpose and content of the study verbally and in written form, and their permission was requested to complete the questionnaire and sign the consent form to participate. The clinical investigations were conducted according to the principles of the Declaration of Helsinki. Final ethical approval was provided on (11.05.2021) from the Ethics Review Board of the University of Potsdam, Germany (number 19/2021).

Psychometric measures

For the assessment of depressive symptoms and severity, the Beck Depression Inventory-II (BDI-II) questionnaire (35, 36) was used. The BDI is a questionnaire consisting of a 21-item self-report questionnaire that addresses current affective, cognitive, motivational, and physiological symptoms of depression. Internal consistency in the sample was Cronbach's Alpha 0.948. The assessment of the experience, severity, and different types of childhood trauma was driven by the Childhood Trauma Screener (CTS) (37), a 5-item screening tool derived from the Childhood Trauma Questionnaire, a retrospective 28-item self-report inventory tool (38, 39). All items from CTS were referred to as "When I was growing up (age<16 years old)." These 5 items were answered, including "never true" (1), "rarely true" (2), "sometimes true" (3), "often true" (4), and "very often true" (5). These 5-items

from CTS were used to assess five types of childhood maltreatment, including emotional, physical, sexual abuse, emotional, and physical neglect. In accordance with Glaesmer et al. (37), we classified participants at risk if they rated at least mild forms of childhood abuse or neglect. We additionally controlled for response bias by the 3-item Minimization-Denial subscale from the Childhood Trauma Questionnaire, and excluded participants when indicated. Cronbach's Alpha was previously specified with 0.76 (40).

Plasma sample collection

Participants were instructed to stay abstinent and only drink water during the last 12 hours before assessment. Participants were also instructed to avoid high amounts of coffee, tea, and certain foods (e.g., bananas, cheese, almonds, nuts, vanilla, and citrus fruits) as well as intense exercise and unscheduled medication the previous day. About 10 ml blood was drawn into the EDTA blood tubes (Sarstedt, Germany). The blood was stored at 4°C for 30 minutes and centrifuged at 1500 g for 20 minutes to isolate the platelet-poor plasma (41). After being divided into 500 µl aliquots, EDTA-plasma samples were stored at -80°C for subsequent analyses. The hemolytic blood samples were excluded from the analysis.

EV harvest

EVs from human plasma were isolated using Systems Bioscience's thrombin and ExoQuick solutions (SBI, USA). Plasma samples were thawed, centrifuged at 3,000 g for 15 minutes to remove cells and cell debris, incubated with 5 µl (611U/ml) Thrombin (SBI, USA) (5 µl per 500 µl of plasma, RT, 5 minutes), and then centrifuged at 10,000 rpm for 5 minutes in order to remove the fibrin pellet. The supernatants (i.e., de-fibrinated plasma) were treated with 120 µl ExoQuick (SBI, USA) for 30 min at 4°C and centrifuged at 13,000 rpm for 2 minutes to pellet the EVs.

EV RNA isolation

The SeraMir RNA Columns (SBI, USA) were used according to the manufacturer's instruction for EV RNA isolation. Briefly, the EV pellet was resuspended in 350 µl Lysis Buffer, mixed with 200 µl 100% Ethanol (PanReac AppliChem, Germany), transferred to the spin column and centrifuged at 13,000 rpm for 1 minute. Then, 400 µl Wash Buffer was added and the samples were centrifuged at 13,000 rpm for 1 minute. This washing step was repeated twice. Finally, the 30 µl Elution Buffer was added in the spin column and first centrifuged at 2,000 rpm for 2 minutes to load the buffer. The spin columns were centrifuged at 13,000 rpm for 1 minute to elute the EV RNA finally.

The Agilent 2100 Bioanalyzer and RNA 6000 Pico chip Kits (Agilent Technologies, USA) were used to assess the quantity and quality of isolated EV RNA. Plasma samples with insufficient EV RNA quantity (<2 ng/ml) were discarded.

EV RNA reverse transcription and miRNA real-time quantitative PCR

5 µl total exoRNA eluted from spin column was reverse transcribed (cDNA synthesis) using SeraMir Kits (SBI, USA) according to the manufacturer's instructions. Real-time quantitative PCR was conducted on the CFX384 Touch Real-Time PCR Detection System (Bio-Rad Laboratories, USA) using 384-well SeraMir Profiler (SBI, USA) with and 2X Maxima SYBR Green/ROX qPCR Master Mix (Thermo Scientific, USA). The protocol was as follows: 50°C/2 min, 95°C/10 min, 40 cycles; 95°C/15 s, 60°C/1 min; data read at 60°C/1 min. The global mean normalization was applied for calculate the miRNA expression levels to reduce the influence of batch effects.

Bone markers measurement

Measurements of P1NP, osteocalcin, and CTx were conducted directly on plasma samples with electrochemiluminescence immunoassays "ECLIA" from Roche COBAS Elecsys 2010 MODULARANALYTICS E170 according to the manufacturer's protocol (REF 12149133 122 for osteocalcin, REF 03141071 190 for P1NP and REF 11972308122 for CTx, F. Hoffmann-La Roche, Ltd., Basel, Switzerland).

Predicting the target genes of differently expressed miRNAs

The target genes of differently expressed miRNAs were predicted based on databases Targetscan (42), miRtarbase (43), and miRDB (44). To minimize the false positive rate and enhance result reliability, only the overlap of the predicted genes from the three databases was selected by Venn plot. The results from three databases were then imported into the Cytoscape software for constructing and visualizing the miRNA-mRNA interaction network. In Cytoscape, miRNA and mRNAs were represented as nodes, and the edges between nodes illustrated the interactions between miRNAs or mRNAs. The key mRNAs with the most interconnections, extracted using cytoHubba (version 0.1) (45), tend to highly connected to multiple miRNAs and virtual nodes in biological networks.

Enriched biological pathway analysis

To better understand the childhood trauma related biological process, we performed enriched biological pathway analysis for the altered EV miRNAs. DIANA-miRPath v4.0 (33) software was used to identify the enriched pathways by both up-regulated and down-regulated miRNAs between CTS and healthy controls. This software identifies the targeted biological pathways via the "Kyoto Encyclopedia of Genes and Genomes (KEGG)", providing a systematic analysis of miRNA functions, connecting genomic data with functional annotations. KEGG PATHWAY database (https://www.genome.jp/kegg/pathway.html) was applied to classify the category of miRNA-related pathways. The "pathways union"

option of the miRPath software was performed. Given the database bias toward cancer/tumor-related pathways, these were excluded from the analysis for providing a more balanced assessment regarding mental health disorders.

Statistical analysis

Due to the non-normal distribution of continuous variables such as age and body mass index (BMI) differences between groups were assessed using the Mann-Whitney U test, with results presented as median (interquartile range, IQR). Categorical variables (sex, smoking, alcohol use) were analyzed using the Chi-Square test, with results reported as frequencies.

For the first study objective, real-time PCR data on EV miRNA expression levels were analyzed using qbase+ software. The expression of miRNAs in plasma EVs from childhood trauma patients was calculated relative to expression of miRNAs in plasma EVs from healthy controls, using the $2^{-\Delta\Delta Ct}$ method. And the global mean normalization in qbase+ minimized technical variability, allowing for more accurate comparisons of gene expression levels across samples. The non-parametric Mann-Whitney U-test was used for differential miRNA expression analysis. The adjusted *p*-values were calculated using the FDR multiple comparison methods based on Benjamini and Hochberg methods (46). Criteria thresholds for significantly differential miRNA expression between the childhood trauma participants and healthy controls were set as adjusted *p*-values (FDR) < 0.05 and $\log_2$ fold change > 2 or < -2. As generated by the qbase+, bar graphs display the mean and 95% confidence intervals for comparing the miRNA expression levels in each group.

For the second objective, general linear regression models were employed to investigate the associations between specific EV miRNA and circulating bone markers and presented in three different models: model 1 was unadjusted regarding possible confounder variables. Given that age and sex impact circulating miRNAs (47, 48), and EV cargoes (49), model 2 was adjusted for age and sex. As our CTS group was combined with depression (depressive patients without CTS was excluded due to small sample size for statistical analysis), we adjusted in model 3 for the BDI-II score for controlling the influence of depression. The analysis was conducted using the IBM SPSS Statistics program (IBM SPSS 23.0).

For the third study objective regarding pathway exploration, *P*-values were obtained by the Fisher's exact test as an enrichment analysis method, and the FDR was estimated.

Results

The miRNA analysis was conducted in a total of n= 45 participants, but finally data of n=19 persons could analyze and are presented here due to a low detectable miRNA amount in EVs. Depressive patients with CTS, n=6; depressive patients without CTS, n=4; healthy individuals without CTS, n=9. Since the small size of the subgroup of depressive patients without CTS, this group was excluded from further analyses. And a descriptive overview is provided in the Supplementary Table S1.

First step: analysis of differentially expressed miRNA in plasma EVs

The expression of 380 miRNAs was analyzed in plasma samples from $n = 6$ people with childhood trauma (age: *Median* = 50.00 (*IQR* = 22.00), BDI: *Median* = 21.00 (*IQR* = 23.00), female: 66.7%) and compared to $n = 9$ people without childhood trauma as controls (age: *Median* = 28.00 (*IQR* = 15.00), BDI: *Median* = 5.00 (*IQR* = 10.00), female: 55.6%). The two groups differ descriptively but not statically significant in basic characteristics such as age, gender or BMI (*P*-value > 0.05) (for further sample characteristics see Table 1).

TABLE 1 Demographic and clinical characteristic of childhood trauma subjects and healthy controls.

Variables	*N*	All (IQR)	*N*	CTS (IQR)	*N*	Controls (IQR)	Mann-Whitney U	Chi-Square	*p*-value
Sex (M/F)	15	6/9	6	2/4	9	4/5		0.185	0.667
Age (years)	15	30.00 (25.00)	6	50.00 (22.00)	9	28.00 (15.00)	11.5		0.066
Weight (Kg)	15	67.00 (14.00)	6	70.30 (24.42)	9	66.00 (9.00)	16.5		0.224
Height (cm)	15	170.00 (16.00)	6	166.50 (18.00)	9	173.00 (10.50)	20.5		0.456
BMI (kg/m^2)	15	22.60 (5.60)	6	25.88 (5.40)	9	20.70 (2.35)	13		0.113
Smoking (no/yes)	15	14/1	6	5/1	9	9/0		1.607	0.205
Alcohol (no/yes)	15	9/6	6	5/1	9	4/5		2.269	0.132
BDI	15	11.00 (15.00)	6	21.00 (23.00)	9	5.0 (10.00)	2.5		0.002
P1NP (µg/l)	14	54.90 (22.38)	6	46.10 (35.10)	8	57.75 (18.22)	35.5		0.142
Osteocalcin (ng/ml)	13	16.40 (7.40)	6	17.65 (8.75)	7	13.20 (5.40)	12		0.234
CTx (ng/ml)	14	0.57 (0.14)	6	0.48 (0.31)	8	0.58 (0.07)	36		0.142

Mann-Whitney U values are reported for comparisons of continuous variables. Chi-square values are reported for comparisons of categorical variables. BMI, Body mass index; CTS, Childhood Trauma Screener; P1NP, Procollagen type I N-terminal propeptide; CTx, β-CrossLaps; IQR, Interquartile Range; BDI, Beck Depression Inventory-II questionnaire.

We identified 22 miRNAs that showed a significant differential expression between childhood trauma participants and healthy controls. Of these, 6 were significantly up-regulated (miR-518e-3p, miR-421, miR-520h, miR-330-3p, miR-105-5p, and miR-542-5p) and 16 were significantly down-regulated (miR-26b-5p, miR-19a-3p, miR-25-3p, miR-195-5p, miR-451a, miR-16-5p, miR-106a-5p, miR-140-3p, miR-20b-5p, miR-24-3p, miR-126-3p, miR-223-3p, miR-17-5p, miR-19b-3p, miR-18a-5p, and miR-23a-3p) in childhood trauma participants (Figures 1A, B). Two miRNAs (one up-regulated and one down-regulated) were showed based on their association with bone marker after adjustments (Figures 1C, D). The bar diagrams for all dysregulated miRNAs see Supplementary Figures S1 and S2.

Second step: the association between EV miRNAs with circulating bone markers

Results with a significant association are highlighted in Table 2 (full association results are shown in Supplementary Table S2). In model 1 (unadjusted), miR-25-3p, miR-26b-5p, miR-451a, and miR-421 were associated with P1NP and CTx (all p-values < 0.05). Next, it was checked if age, sex and depression affect the association. The significant association of miR-25-3p and miR-451a with P1NP or CTx no longer existed in both models 2 (adjusted age and sex) and 3 (adjusted BDI), all p-values > 0.05, suggesting that age, sex and depression have influenced their observed association. Moreover, in model 2, miR-26b-5p positively associated with P1NP (p=0.029) and CTx (p=0.033). MiR-330-3p positively associated with osteocalcin (p=0.044). MiR-421 negatively associated with P1NP (p=0.007), and miR-542-5p positively associated with osteocalcin (p=0.038). In model 3, miR-26b-5p positively associated with P1NP (p=0.039), osteocalcin (p=0.037), and CTx (p=0.022). MiR-421 negatively associated with P1NP (p=0.006) and CTx (p=0.03).

Third step: exploration of the predicted target genes of differentially expressed miRNAs

In order to predict the highly associated target mRNAs of those altered miRNAs and further explore their potential role in bone

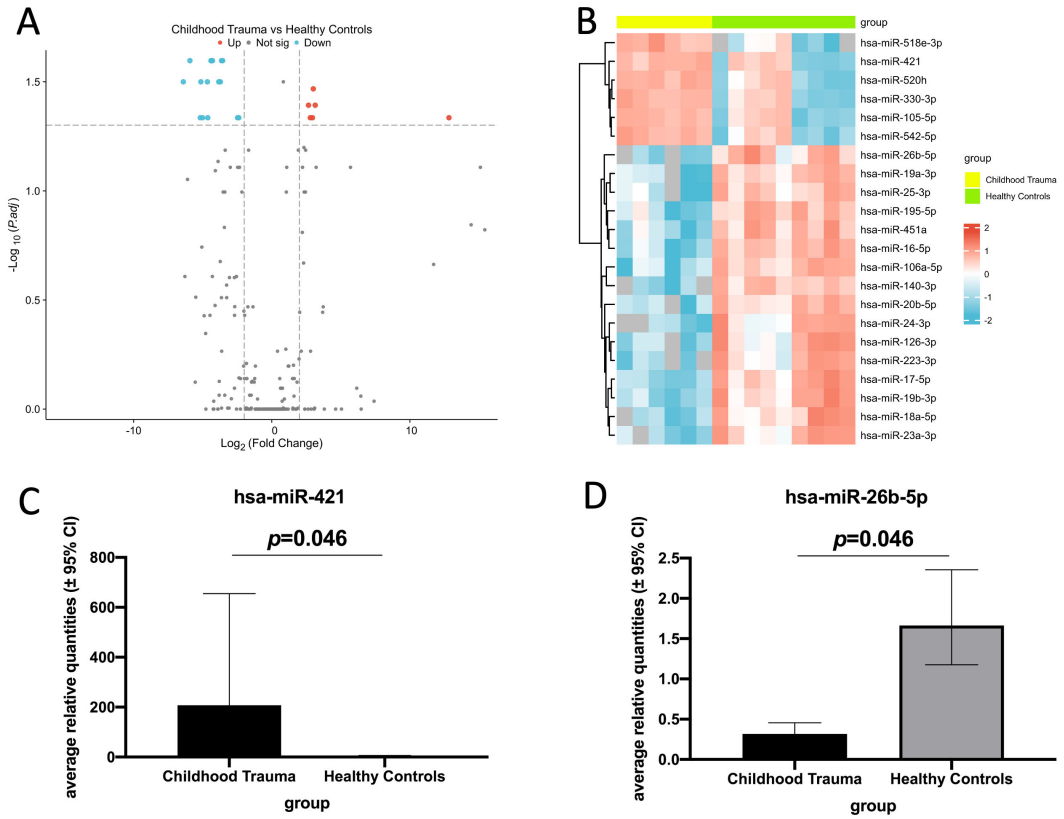

FIGURE 1
Real-time quantitative PCR analysis of differentially expressed EV miRNAs in childhood trauma participants compared to healthy controls (log_2 fold change > 2 or < -2, adjusted p-value threshold: 0.05). **(A)** Volcano plot of all dysregulated EV miRNAs between childhood trauma and healthy controls. Blue: down-regulated expression; gray: no significant difference in the expression; red: up-regulated expression. **(B)** Heat map analysis shows all the differentially expressed EV miRNAs. Blue: down-regulated expression; red: up-regulated expression. **(C)** Bar diagram shows one up-regulated EV miRNA in childhood trauma. (hsa-miR-421, all miRNAs see Supplementary Figure S1). **(D)** Bar diagram shows one down-regulated EV miRNA in childhood trauma. (hsa-miR-26b-5p, all miRNAs see Supplementary Figure S2).

10.3389/fendo.2025.1515910

TABLE 2 Association of EV miRNA expression levels with bone marker levels.

		Model 1[a]		Model 2[b]		Model 3[c]	
Linear regression (Listwise)	*N*	Regression coefficient	*p*-value	Adj. regression coefficient	*p*-value	Adj. regression coefficient	*p*-value
hsa-miR-25-3p							
P1NP	13	**12.261**	0.025*	9.127	0.082	12.658	0.092
osteocalcin	12	0.481	0.815	-1.201	0.603	1.572	0.577
CTx	13	**0.116**	0.021*	0.088	0.075	0.118	0.086
hsa-miR-26b-5p							
P1NP	12	**13.838**	0.009**	**14.095**	0.029*	**13.348**	0.039*
osteocalcin	11	2.051	0.146	1.332	0.449	**3.651**	0.037*
CTx	12	**0.138**	0.005**	**0.143**	0.033*	**0.139**	0.022*
hsa-miR-451a							
P1NP	14	**5.618**	0.049*	3.395	0.234	5.107	0.217
osteocalcin	13	-0.246	0.795	-1.051	0.307	0.45	0.746
CTx	14	**0.055**	0.036*	0.038	0.166	0.068	0.078
hsa-miR-330-3p							
P1NP	14	-2.817	0.45	-0.975	0.771	-0.344	0.933
osteocalcin	13	1.657	0.158	**2.275**	0.044*	1.574	0.239
CTx	14	-0.04	0.231	-0.026	0.42	-0.29	0.457
hsa-miR-421							
P1NP	14	**-0.069**	0.001**	**-0.055**	0.007**	**-0.67**	0.006**
osteocalcin	13	-0.003	0.69	0.002	0.838	-0.003	0.69
CTx	14	**-0.001**	0.011*	0	0.057	**-0.001**	0.03*
hsa-miR-542-5p							
P1NP	14	-1.569	0.621	-0.459	0.869	0.885	0.799
osteocalcin	13	1.594	0.101	**1.925**	0.038*	1.581	0.158
CTx	14	-0.027	0.35	-0.018	0.499	-0.015	0.661

[a]Model 1 was not adjusted.
[b]Model 2 was adjusted for age and sex.
[c]Model 3 was adjusted for BDI.
Significant Regression coefficients are bold (p<0.01, p<0.05, two sided testing); significance level: **P<0.01, *P<0.05

metabolism, the miRNA-mRNA interaction network was constructed based on the target gene prediction of Targetscan, miRtarbase, and miRDB by Cytoscape (Supplementary Figure S3). According to the prediction, the most associated target mRNAs of these differentially expressed miRNAs in childhood trauma group, in order, were Trinucleotide Repeat Containing Adaptor 6B (*TNRC6B*), Nuclear FMR1 Interacting Protein 2 (*NUFIP2*), Phospholipid Phosphatase 2 (*PAP2C*), Rho GTPase Activating Protein 12 (*ARHGAP12*), WEE1 G2 Checkpoint Kinase (*WEE1*), and Zinc Finger And BTB Domain Containing 18 (*ZBTB18*), shown in Figure 2. Among, these *TNRC6B* (50), *NUFIP2* (51, 52), *ARHGAP12* (53), and *ZBTB18* (54) are known to be involved in bone metabolism.

Third step: enriched pathways identified by DIANA-miRPath software

A total of 166 significantly enriched pathways of 22 dysregulated miRNAs with adjusted *p*-value <0.05 was explored (Supplementary Figure S4), and the top 10 enriched pathways based on miRNA numbers and adjusted *p*-value was showed in Supplementary Table S3. According to the KEGG pathway results, five pathways were Cellular Processes-related (three were associated with Cell growth and death, one was associated with Cellular community - eukaryotes, and one was associated with Transport and catabolism). Two pathways were Environmental

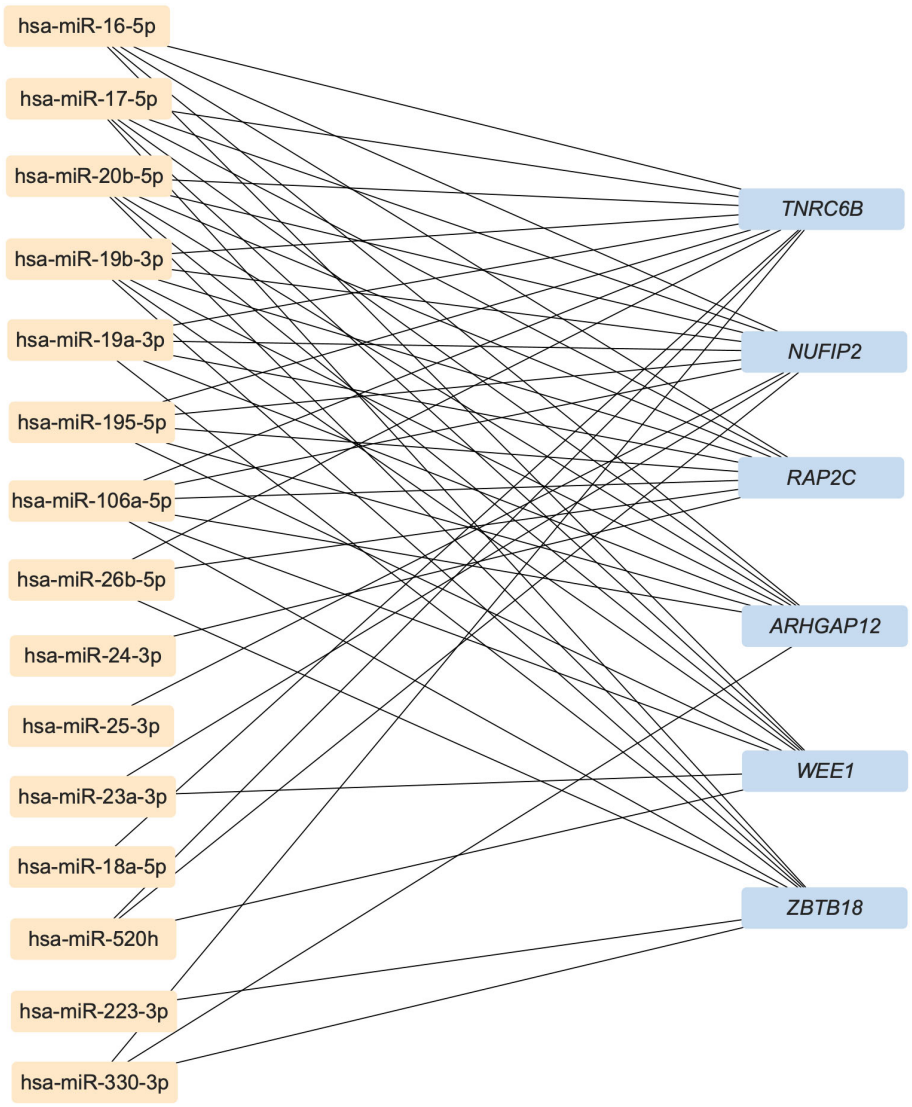

FIGURE 2
The most associated target mRNAs of these differently expressed miRNAs in childhood trauma group. TNRC6B, Trinucleotide Repeat Containing Adaptor 6B; NUFIP2, Nuclear FMR1 Interacting Protein 2; PAP2C, Phospholipid Phosphatase 2; ARHGAP12, Rho GTPase Activating Protein 12; WEE1, WEE1 G2 Checkpoint Kinase; ZBTB18, Zinc Finger And BTB Domain Containing 18.

Information Processing-related (forkhead box protein O (FoxO) and Phosphatidylinositol-4,5-bisphosphate 3-kinase (PI3K)/protein kinase B (Akt) signaling pathway, both were associated with signal transduction), one pathway was Human Diseases-related (Infectious disease: bacterial), one pathway was Organismal Systems-related (Nervous system), and one pathway was Genetic Information Processing-related (Folding, sorting and degradation).

Discussion

This study explored the association between childhood trauma and bone metabolism through EVs, specifically their miRNA cargo. In total, 22 differentially expressed EV miRNAs were identified between childhood trauma participants and healthy controls. Among them, Van der Auwera et al. (55) found that miR-26b-5p is negatively associated with CTS score, and a significant association between altered miR-19b-3p expression and childhood traumatic experiences in bipolar depression was found (31).

Regarding the associations between those altered EV miRNAs and bone turnover markers, miR-26b-5p and miR-421 showed associations with bone turnover markers in multiple models. Therefore, a more detailed literature search was conducted to determine the possible biological role of miR-26b-5p and miR-421. Previous research showed that miR-26b-5p can alter neurite growth and synaptogenesis by targeting methyl-CpG-binding protein-2 in mouse neural stem cells (56). Therefore, miR-26b-5p may also have the potential to influence structural and functional deficits in the developing brain and thus may involve in childhood trauma processes. In addition, miR-421 is involved in regulating plasminogen activator inhibitor-1 (57), which is known to induce neuronal apoptosis (58), suggesting a possible role of miR-421 in

the long-lasting process of brain development. As we aim to explore whether EVs altered due to childhood trauma may impact bone metabolism, the role of miR-26b-5p and miR-421 in bone tissue homeostasis and remodeling is of specific relevance to us. MiR-26b-5p was found up-regulated during osteogenic differentiation, and functional analysis showed that miR-26b-5p positively regulates osteogenic differentiation (59), which may explain the decrease in miR-26b-5p level found in bone samples from osteoporosis patients (60). Thus, the down-regulated miR-26b-5p can potentially affect bone tissue by impacting osteogenic differentiation. MiR-421 was found to have the ability to inhibit osteogenic differentiation of pre-osteoblasts, and an up-regulated miR-421 expression in bone tissue of osteoporosis patients was found (61). Considering these data in the context of our findings, we assume that childhood trauma may lead to reduced miR-26b-5p and increased miR-421 levels in circulating EVs, which reach bone tissues via the circulation and both lead to a weakened osteogenic differentiation, resulting in a net-decrease of bone formation.

Our results also showed that miR-26b-5p, which was down-regulated in childhood trauma participants, was positively associated with P1NP and CTx. Furthermore, miR-421, which was up-regulated in childhood trauma participants, was negatively associated with P1NP and CTx. Both suggest a reduced bone turnover (both bone formation and resorption) due to childhood trauma. It should be noted that the association between miR-26b-5p and osteocalcin became significant (p = 0.037) after BDI-II score adjustment in model 3, which may give notice that the direct relationship between miR-26b-5p and osteocalcin was isolated by controlling for this confounding factor (depression). This also suggests the repression of bone turnover in the context of childhood trauma. All demonstrated that altered circulating EV miRNAs due to childhood trauma could deliver specific, detrimental information on bone metabolism.

Regarding the exploration of target genes of those altered EV miRNAs, *TNRC6B* has to be highlighted due to its possible contribution to bone physiology. A single-nucleotide polymorphism in the *TNRC6B* gene has been identified as being associated with a lower spine bone mineral density and increased risk of fractures (50). The *TNRC6B* gene is also involved in bone physiology-related pathways (62), such as the Wnt signaling pathway (63). Furthermore, previous research showed the role of other observed target genes (*NUFIP2*, *ARHGAP12*, and *ZBTB18)* in bone metabolism (51–54), which showed a prospective network in the pathophysiology of childhood trauma leading to dysregulated bone metabolism (summarized in Figure 3). Considered those enriched pathways of miRNAs, FoxOs may be regulated by serotonin or norepinephrine signaling and the HPA axis, both are associated with stress development (64). FoxOs are also crucial in governing an array of critical functions in bone cells; for example, FoxOs promote osteogenesis and suppress osteoclastogenesis or adipogenesis by reducing levels of reactive oxygen species (65). Numerous studies have demonstrated the function of PI3K in synaptic plasticity, memory consolidation, and major depression (66, 67). Moreover, the various roles of the PI3K/Akt signaling pathway in bone metabolism have also been recognized (68). In summary, both FoxO and PI3K/Akt signaling pathways may involved in the process of childhood trauma leading to dysregulated bone metabolism. Overall, those bioinformatic analyses provided additional information for our experimental conclusions. It's important to note that the use of miRNA informatics tools in our study is only for functional annotation purposes, and they are employed to fill the gap in the roles of miRNA, instead of conducting any form of data validation.

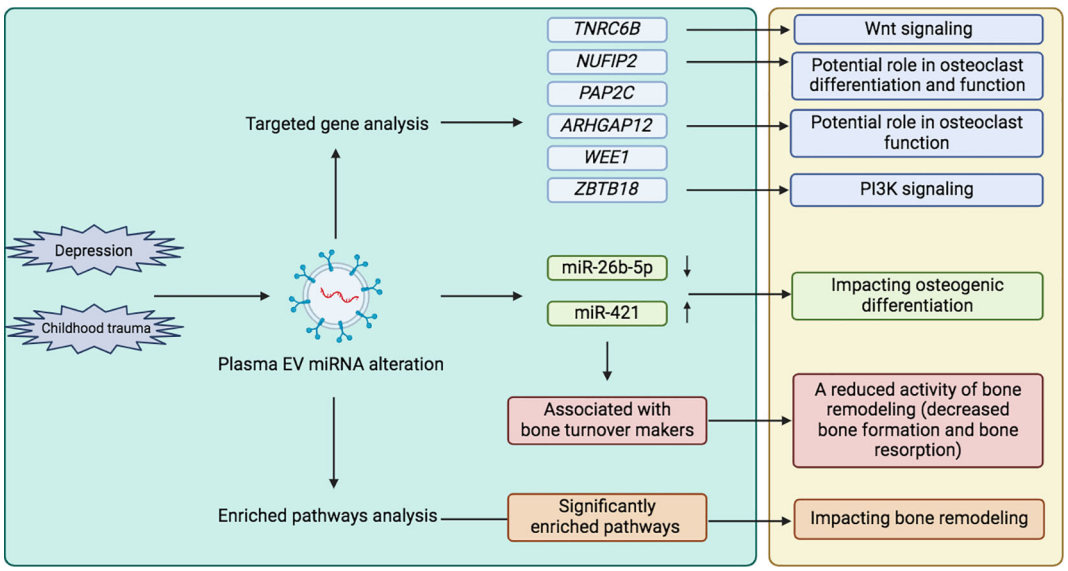

FIGURE 3
Exploring the association between childhood trauma and bone metabolism through EVs. (left green box: our research, right yellow box: combined other research from literature review). TNRC6B, Trinucleotide Repeat Containing Adaptor 6B; NUFIP2, Nuclear FMR1 Interacting Protein 2; PAP2C, Phospholipid Phosphatase 2; ARHGAP12, Rho GTPase Activating Protein 12; WEE1, WEE1 G2 Checkpoint Kinase; ZBTB18, Zinc Finger And BTB Domain Containing 18; EV, Extracellular vesicle; micro RNA, miR.

Nowadays, there has been a growing interest in the research of EVs and their cargo, considering the ability of miRNAs to be efficiently transfected in cells, and the epigenetic control mechanism of miRNA-mediated silencing of mRNAs make miRNAs a key research topic among EVs-carrying cargoes (69). Some differentially expressed circulating EV miRNAs due to childhood trauma have been reported (32), but the potential for EV-based pathophysiological interaction between childhood trauma and other diseases has not been elucidated. The present study focused on differentially expressed EV miRNAs and their association with bone markers in cases of childhood trauma, thus exploring the potential relationship between childhood trauma and bone metabolism via EVs.

Strengths and limitations of the experimental study

Our sample size is relatively small because a highly controlled patient inclusion was used. We have controlled multiple variables that might affect the robustness of this research; for example, demographic and clinical characteristic variables (e.g., age, gender, BMI) were controlled between case and controls. Some variables were adjusted (age, gender, BDI) in the linear regression to control the effects on the association between miRNAs and bone markers. In a future analysis of a larger sample set, other possible influencing covariates, such as medication, smoking, alcohol, and BMI, could be considered. And while the use of model 3 (BDI-II score adjustment) helps isolate the role of depression in the association between ELS and circulating biomarkers, it does not directly address the question regarding the effects of depression on miRNA expression. Further studies compare miRNA alterations in depression, with and without ELS, would provide more insights into these associations.

Despite our efforts to match the clinical characteristics between the childhood trauma participants and healthy controls, control group participants tended to be overall younger (n=0.066). To investigate the potential impact of age differences on our results, we conducted a sub-analysis comparing the three oldest and three youngest participants in both groups, which showed no significant differences in bone biomarkers between these age subgroups, suggesting that age is unlikely to be a major confounding factor in our study. Nevertheless, to account for any potential confounding effects of age, we included age as a covariate in our regression models (model 2).

Moreover, participants were asked to avoid specific beverages and foods that are known to influence blood chemistry, and depressed patients in clinic have followed the nutrition protocol, thus reducing the influence of nutritional status. The rigorous selection process was applied to collect a highly controlled cohort, thus minimizing the impact of confounding variables and enhancing the internal validity of our findings. Furthermore, as bone mineral density test is an important indicator of bone health, we performed this test on a subgroup of study participants throughout the DEPEHA project. However, due to a limited quantity of EV RNA in some plasma samples (<2 ng/ml), the sample size for comparing bone mineral density was reduced. Thus, the direct comparison between childhood trauma participants and controls was not included in this analysis. A subgroup of participants with depression but without CTS was initially included to better investigate the effects of childhood trauma on bones; however, this group was excluded from the analysis due to its limited size.

As the enriched target gene exploration was based on database predictions, and supplementary bioinformatic analysis tool derived from online software, additional functional and mechanistic studies should be conducted in the future to substantiate this potential molecular link between childhood trauma and bone metabolism.

Conclusion

As an exploratory study, the present study provides a prospective investigation of the relationship between childhood trauma and skeletal disorders, and hopefully provides guidance for early preventive measures, such as stress management aimed at alleviating the long-term impact of ELS on bone health. Our experimental data showed the association between dysregulated EV miRNAs and bone turnover markers, suggesting a possible role of altered miRNAs due to childhood trauma in bone metabolism. Aligned with our experimental data, this complementary bioinformatic analysis noted the potential link between childhood trauma and bone metabolism.

Data availability statement

The raw data supporting the conclusions of this article will be made available by the authors, without undue reservation.

Ethics statement

The studies involving humans were approved by Ethics Review Board of the University of Potsdam, Germany. The studies were conducted in accordance with the local legislation and institutional requirements. The participants provided their written informed consent to participate in this study.

Author contributions

YH: Data curation, Methodology, Writing – original draft, Formal Analysis, Funding acquisition, Software. KW-K: Conceptualization, Methodology, Resources, Supervision, Writing – review & editing, Investigation. PC: Methodology, Writing – review & editing, Software. SH: Data curation, Formal Analysis, Writing – review & editing. FG-C: Methodology, Writing – review & editing. TJ:

Funding acquisition, Methodology, Resources, Writing – review & editing. P-MW: Conceptualization, Investigation, Methodology, Project administration, Resources, Supervision, Writing – review & editing.

Funding

The author(s) declare that financial support was received for the research, authorship, and/or publication of this article. YH was funded by CHINA SCHOLARSHIP COUNCIL, grant number 202008430179. We acknowledge the support from the Deutsche Forschungsgemeinschaft (DFG) – Project number 427826188.

Conflict of interest

The authors declare that the research was conducted in the absence of any commercial or financial relationships that could be construed as a potential conflict of interest.

Generative AI statement

The author(s) declare that no Generative AI was used in the creation of this manuscript.

Publisher's note

Supplementary material

The Supplementary Material for this article can be found online at: https://www.frontiersin.org/articles/10.3389/fendo.2025.1515910/full#supplementary-material

References

1. Chrousos GP. Stress and disorders of the stress system. *Nat Rev Endocrinol*. (2009) 5:374–81. doi: 10.1038/nrendo.2009.106

2. Pechtel P, Pizzagalli DA. Effects of early life stress on cognitive and affective function: an integrated review of human literature. *Psychopharmacol (Berl)*. (2011) 214:55–70. doi: 10.1007/s00213-010-2009-2

3. Jawahar MC, Murgatroyd C, Harrison EL, Baune BT. Epigenetic alterations following early postnatal stress: a review on novel aetiological mechanisms of common psychiatric disorders. *Clin Epigenet*. (2015) 7:122. doi: 10.1186/s13148-015-0156-3

4. Lopatina OL, Panina YA, Malinovskaya NA, Salmina AB. Early life stress and brain plasticity: from molecular alterations to aberrant memory and behavior. *Rev Neurosci*. (2021) 32:131–42. doi: 10.1515/revneuro-2020-0077

5. Green JG, McLaughlin KA, Berglund PA, Gruber MJ, Sampson NA, Zaslavsky AM, et al. Childhood adversities and adult psychiatric disorders in the national comorbidity survey replication I: associations with first onset of DSM-IV disorders. *Arch Gen Psychiatry*. (2010) 67:113–23. doi: 10.1001/archgenpsychiatry.2009.186

6. Agorastos A, Pervanidou P, Chrousos GP, Baker DG. Developmental trajectories of early life stress and trauma: A narrative review on neurobiological aspects beyond stress system dysregulation. *Front Psychiatry*. (2019) 10:118. doi: 10.3389/fpsyt.2019.00118

7. Association AP. *Diagnostic and statistical manual of mental disorders: DSM-5*. Washington, DC: American Psychiatric Association (2013).

8. Yehuda R, Halligan SL, Grossman R. Childhood trauma and risk for PTSD: relationship to intergenerational effects of trauma, parental PTSD, and cortisol excretion. *Dev Psychopathol*. (2001) 13:733–53. doi: 10.1017/S0954579401003170

9. McKay MT, Cannon M, Chambers D, Conroy RM, Coughlan H, Dodd P, et al. Childhood trauma and adult mental disorder: A systematic review and meta-analysis of longitudinal cohort studies. *Acta Psychiatr Scand*. (2021) 143:189–205. doi: 10.1111/acps.v143.3

10. Kuzminskaite E, Penninx B, Harmelen van AL, Elzinga BM, Hovens J, Vinkers CH. Childhood trauma in adult depressive and anxiety disorders: an integrated review on psychological and biological mechanisms in the NESDA cohort. *J Affect Disord*. (2021) 283:179–91. doi: 10.1016/j.jad.2021.01.054

11. Wuertz-Kozak K, Roszkowski M, Cambria E, Block A, Kuhn GA, Abele T, et al. Effects of early life stress on bone homeostasis in mice and humans. *Int J Mol Sci*. (2020) 21. doi: 10.3390/ijms21186634

12. Yirmiya R, Goshen I, Bajayo A, Kreisel T, Feldman S, Tam J, et al. Depression induces bone loss through stimulation of the sympathetic nervous system. *Proc Natl Acad Sci*. (2006) 103:16876–81. doi: 10.1073/pnas.0604234103

13. Wu Q, Liu B, Tonmoy S. Depression and risk of fracture and bone loss: an updated meta-analysis of prospective studies. *Osteoporos Int*. (2018) 29:1303–12. doi: 10.1007/s00198-018-4420-1

14. Lee CW, Liao CH, Lin CL, Liang JA, Sung FC, Kao CH. Increased risk of osteoporosis in patients with depression: a population-based retrospective cohort study. *Mayo Clin Proc*. (2015) 90:63–70. doi: 10.1016/j.mayocp.2014.11.009

15. Tolea MI, Black SA, Carter-Pokras OD, Kling MA. Depressive symptoms as a risk factor for osteoporosis and fractures in older Mexican American women. *Osteoporosis Int*. (2007) 18:315–22. doi: 10.1007/s00198-006-0242-7

16. Cizza G, Primma S, Csako G. Depression as a risk factor for osteoporosis. *Trends Endocrinol Metab*. (2009) 20:367–73. doi: 10.1016/j.tem.2009.05.003

17. NIH Consensus Development Panel on Osteoporosis Prevention. *Diagnosis, and Therapy, March 7-29, 2000: highlights of the conference. South Med J*. (2001) 94:569–73.

18. Feichtinger X, Muschitz C, Heimel P, Baierl A, Fahrleitner-Pammer A, Redl H, et al. Bone-related Circulating MicroRNAs miR-29b-3p, miR-550a-3p, and miR-324-3p and their Association to Bone Microstructure and Histomorphometry. *Sci Rep*. (2018) 8. doi: 10.1038/s41598-018-22844-2

19. Schini M, Vilaca T, Gossiel F, Salam S, Eastell R. Bone turnover markers: basic biology to clinical applications. *Endocr Rev*. (2023) 44:417–73. doi: 10.1210/endrev/bnac031

20. Singer FR, Eyre DR. Using biochemical markers of bone turnover in clinical practice. *Cleve Clin J Med*. (2008) 75:739–50. doi: 10.3949/ccjm.75.10.739

21. Liu Z, Chen R, Jiang Y, Yang Y, He L, Luo C, et al. A meta-analysis of serum osteocalcin level in postmenopausal osteoporotic women compared to controls. *BMC Musculoskelet Disord*. (2019) 20:532. doi: 10.1186/s12891-019-2863-y

22. Garnero P, Ferreras M, Karsdal MA, Nicamhlaoibh JRisteli R, Borel O, et al. The type I collagen fragments ICTP and CTX reveal distinct enzymatic pathways of bone collagen degradation. *J Bone Miner Res*. (2003) 18:859–67. doi: 10.1359/jbmr.2003.18.5.859

23. Herrmann IK, Wood MJA, Fuhrmann G. Extracellular vesicles as a next-generation drug delivery platform. *Nat Nanotechnology*. (2021) 16:748–59. doi: 10.1038/s41565-021-00931-2

24. He Y, Wuertz-Kozak K, Kuehl LK, Wippert PM. Extracellular vesicles: potential mediators of psychosocial stress contribution to osteoporosis? *Int J Mol Sci*. (2021) 22. doi: 10.3390/ijms22115846

25. Diener C, Keller A, Meese E. Emerging concepts of miRNA therapeutics: from cells to clinic. *Trends Genet*. (2022) 38:613–26. doi: 10.1016/j.tig.2022.02.006

26. Ivanova E, Bozhilova R, Kaneva R, Milanova V. The dysregulation of microRNAs and the role of stress in the pathogenesis of mental disorders. *Curr Top Med Chem*. (2018) 18:1893–907. doi: 10.2174/1568026619666181130135253

27. Saeedi S, Israel S, Nagy C, Turecki G. The emerging role of exosomes in mental disorders. *Transl Psychiatry*. (2019) 9:122. doi: 10.1038/s41398-019-0459-9

28. Kong L, Zhang D, Huang S, Lai J, Lu L, Zhang J, et al. Extracellular vesicles in mental disorders: A state-of-art review. *Int J Biol Sci*. (2023) 19:1094–109. doi: 10.7150/ijbs.79666

29. Dickson DA, Paulus JK, Mensah V, Lem J, Saavedra-Rodriguez L, Gentry A, et al. Reduced levels of miRNAs 449 and 34 in. *sperm mice men exposed to early Life stress. Transl Psychiatry*. (2018) 8:101. doi: 10.1038/s41398-018-0146-2

30. Van der Auwera S, Ameling S, Wittfeld K, Rowold ED, Nauck M, Völzke H, et al. Association of childhood traumatization and neuropsychiatric outcomes with altered plasma micro RNA-levels. *Neuropsychopharmacology*. (2019) 44:2030–7. doi: 10.1038/s41386-019-0460-2

31. Chen Y, Shi J, Liu H, Wang Q, Chen X, Tang H, et al. Plasma microRNA Array Analysis Identifies Overexpressed miR-19b-3p as a Biomarker of Bipolar Depression Distinguishing From Unipolar Depression. *Front Psychiatry*. (2020) 11. doi: 10.3389/fpsyt.2020.00757

32. Ran LY, Kong YT, Xiang JJ, Zeng Q, Zhang CY, Shi L, et al. Serum extracellular vesicle microRNA dysregulation and childhood trauma in adolescents with major depressive disorder. *Bosn J Basic Med Sci*. (2022) 22:959–71. doi: 10.17305/bjbms.2022.7110

33. Tastsoglou S, Skoufos G, Miliotis M, Karagkouni D, Koutsoukos I, Karavangeli A, et al. *DIANA-miRPath v4.0: expanding target-based miRNA functional analysis in cell-type and tissue contexts. Nucleic Acids Res.* (2023) 51:W154–9. doi: 10.1093/nar/gkad431

34. Wippert PM, Block A, Mansuy IM, Peters EMJ, Rose M, Rapp MA, et al. Alterations in bone homeostasis and microstructure related to depression and allostatic load. *Psychother Psychosom*. (2019) 88:383–5. doi: 10.1159/000503640

35. Beck AT, Steer RA, Brown G. "Beck depression inventory–II", In: *Psychological Assessment*. (1996). doi: 10.1037/t00742-000

36. Wintjen L, Petermann F. Beck-depressions-inventar revision (BDI–II). *Z für Psychiatrie Psychol und Psychotherapie*. (2010) 58:243–5. doi: 10.1024/1661-4747.a000033

37. Glaesmer H, Schulz A, Häuser W, Freyberger HJ, Brähler E, Grabe H-J. Der childhood trauma screener (CTS)–entwicklung und validierung von schwellenwerten zur klassifikation. *Psychiatrische Praxis*. (2013) 40:220–6. doi: 10.1055/s-0033-1343116

38. Bernstein D, Fink L. *Childhood Trauma Questionnaire: A retrospective self-report questionnaire and manual*. San Antonio, TX: The Psychological Corporation (1998).

39. Wingenfeld K, Spitzer C, Mensebach C, Grabe HJ, Hill A, Gast U, et al. Die deutsche version des childhood trauma questionnaire (CTQ): erste befunde zu den psychometrischen Kennwerten. *PPmP-Psychotherapie· Psychosomatik· Medizinische Psychol*. (2010) 60:442–50. doi: 10.1055/s-0030-1247564

40. Grabe HJ, Schulz A, Schmidt CO, Appel K, Driessen M, Wingenfeld K, et al. A brief instrument for the assessment of childhood abuse and neglect: the childhood trauma screener (CTS). *Psychiatrische Praxis*. (2012) 39:109–15. doi: 10.1055/s-0031-1298984

41. Kuo WP, Jia S. *Extracellular vesicles: methods and protocols* Vol. 1660. New York, NY: Springer (2017).

42. McGeary SE, Lin KS, Shi CY, Pham TM, Bisaria N, Kelley GM, et al. The biochemical basis of microRNA targeting efficacy. *Science*. (2019) 366. doi: 10.1126/science.aav1741

43. Huang HY, Lin YC, Li J, Huang KY, Shrestha S, Hong HC, et al. *miRTarBase 2020: updates to the experimentally validated microRNA-target interaction database. Nucleic Acids Res.* (2020) 48:D148–54. doi: 10.1093/nar/gkz896

44. Chen Y, Wang X. *miRDB: an online database for prediction of functional microRNA targets. Nucleic Acids Res*. (2020) 48:D127–31. doi: 10.1093/nar/gkz757

45. Chin CH, Chen SH, Wu HH, Ho CW, Ko MT, Lin CY. *cytoHubba: identifying hub objects and sub-networks from complex interactome. BMC Syst Biol*. (2014) 8 Suppl 4:S11. doi: 10.1186/1752-0509-8-S4-S11

46. Benjamini Y, Hochberg Y. Controlling the false discovery rate - a practical and powerful approach to multiple testing. *J R Stat Soc Ser B-Statistical Method*. (1995) 57:289–300. doi: 10.1111/j.2517-6161.1995.tb02031.x

47. Meder B, Backes C, Haas J, Leidinger P, Stahler C, Grossmann T, et al. Influence of the confounding factors age and sex on microRNA profiles from peripheral blood. *Clin Chem*. (2014) 60:1200–8. doi: 10.1373/clinchem.2014.224238

48. Ameling S, Kacprowski T, Chilukoti RK, Malsch C, Liebscher V, Suhre K, et al. Associations of circulating plasma microRNAs with age, body mass index and sex in a population-based study. *BMC Med Genomics*. (2015) 8:61. doi: 10.1186/s12920-015-0136-7

49. Noren Hooten N, Byappanahalli AM, Vannoy M, Omoniyi V, Evans MK. Influences of age, race, and sex on extracellular vesicle characteristics. *Theranostics*. (2022) 12:4459–76. doi: 10.7150/thno.72676

50. Karasik D, Zillikens MC, Hsu YH, Aghdassi A, Akesson K, Amin N, et al. Disentangling the genetics of lean mass. *Am J Clin Nutr*. (2019) 109:276–87. doi: 10.1093/ajcn/nqy272

51. Rehage N, Davydova E, Conrad C, Behrens G, Maiser A, Stehklein JE, et al. Binding of NUFIP2 to Roquin promotes recognition and regulation of ICOS mRNA. *Nat Commun*. (2018) 9:299. doi: 10.1038/s41467-017-02582-1

52. Gigliotti CL, Boggio E, Clemente N, Shivakumar Y, Toth E, Sblattero D, et al. ICOS-ligand triggering impairs osteoclast differentiation and function *in vitro* and *in vivo*. *J Immunol*. (2016) 197:3905–16. doi: 10.4049/jimmunol.1600424

53. van Wesenbeeck L, Odgren PR, Mackay CA, Hul Van W. Localization of the gene causing the osteopetrotic phenotype in the incisors absent (ia) rat on chromosome 10q32.1. *J Bone Miner Res*. (2004) 19:183–9. doi: 10.1359/jbmr.2004.19.2.183

54. Xie B, Khoyratty TE, Abu-Shah E, Cespedes PF, MacLean AJ, Pirgova G, et al. The zinc finger protein zbtb18 represses expression of class I phosphatidylinositol 3-kinase subunits and inhibits plasma cell differentiation. *J Immunol*. (2021) 206:1515–27. doi: 10.4049/jimmunol.2000367

55. Van der Auwera S, Ameling S, Nauck M, Voelzke H, Voelker U, Grabe HJ. Association between different dimensions of childhood traumatization and plasma micro-RNA levels in a clinical psychiatric sample. *J Psychiatr Res*. (2021) 139:113–9. doi: 10.1016/j.jpsychires.2021.05.023

56. Shyamasundar S, Ramya S, Kandilya D, Srinivasan DK, Bay BH, Ansari SA, et al. Maternal Diabetes Deregulates the Expression of Mecp2 via miR-26b-5p in Mouse Embryonic Neural Stem Cells. *Cells*. (2023) 12. doi: 10.3390/cells12111516

57. Marchand A, Proust C, Morange PE, Lompre AM, Tregouet DA. miR-421 and miR-30c inhibit SERPINE 1 gene expression in human endothelial cells. *PloS One*. (2012) 7:e44532. doi: 10.1371/journal.pone.0044532

58. Soeda S, Oda M, Ochiai T, Shimeno H. Deficient release of plasminogen activator inhibitor-1 from astrocytes triggers apoptosis in neuronal cells. *Brain Res Mol Brain Res*. (2001) 91:96–103. doi: 10.1016/S0169-328X(01)00133-4

59. Trompeter HI, Dreesen J, Hermann E, Iwaniuk KM, Hafner M, Renwick N, et al. MicroRNAs miR-26a, miR-26b, and miR-29b accelerate osteogenic differentiation of unrestricted somatic stem cells from human cord blood. *BMC Genomics*. (2013) 14:111. doi: 10.1186/1471-2164-14-111

60. De-Ugarte L, Yoskovitz G, Balcells S, Güerri-Fernández R, Martinez-Diaz S, Mellibovsky L, et al. MiRNA profiling of whole trabecular bone: identification of osteoporosis-related changes in MiRNAs in human hip bones. *BMC Med Genomics*. (2016) 8:1–11. doi: 10.1186/s12920-015-0149-2

61. Wang Z, Zhang H, Li Q, Zhang L, Chen L, Wang H, et al. Long non-coding RNA KCNQ1OT1 alleviates postmenopausal osteoporosis by modulating miR-421-3p/mTOR axis. *Sci Rep*. (2023) 13:2333. doi: 10.1038/s41598-023-29546-4

62. Carro Vazquez D, Emini L, Rauner M, Hofbauer C, Grillari J, Diendorfer AB, et al. Effect of anti-osteoporotic treatments on circulating and bone microRNA patterns in osteopenic ZDF rats. *Int J Mol Sci*. (2022) 23. doi: 10.3390/ijms23126534

63. Wang Y, Li YP, Paulson C, Shao JZ, Zhang X, Wu M, et al. Wnt and the Wnt signaling pathway in bone development and disease. *Front Biosci (Landmark Ed)*. (2014) 19:379–407. doi: 10.2741/4214

64. Rana T, Behl T, Sehgal A, Mehta V, Singh S, Sharma N, et al. Elucidating the possible role of foxO in depression. *Neurochem Res*. (2021) 46:2761–75. doi: 10.1007/s11064-021-03364-4

65. Ma X, Su P, Yin C, Lin X, Wang X, Gao Y, et al. The roles of foxO transcription factors in regulation of bone cells function. *Int J Mol Sci*. (2020) 21. doi: 10.3390/ijms21030692

66. Budni J, Lobato KR, Binfare RW, Freitas AE, Costa AP, Martin-de-Saavedra MD, et al. Involvement of PI3K, GSK-3beta and PPARgamma in the antidepressant-like effect of folic acid in the forced swimming test in mice. *J Psychopharmacol*. (2012) 26:714–23. doi: 10.1177/0269881111424456

67. Horwood JM, Dufour F, Laroche S, Davis S. Signalling mechanisms mediated by the phosphoinositide 3-kinase/Akt cascade in synaptic plasticity and memory in the rat. *Eur J Neurosci*. (2006) 23:3375–84. doi: 10.1111/j.1460-9568.2006.04859.x

68. Xi JC, Zang HY, Guo LX, Xue HB, Liu XD, Bai YB, et al. The PI3K/AKT cell signaling pathway is involved in regulation of osteoporosis. *J Receptors Signal Transduction*. (2015) 35:640–5. doi: 10.3109/10799893.2015.1041647

69. Munir J, Yoon JK, Ryu S. Therapeutic miRNA-enriched extracellular vesicles: current approaches and future prospects. *Cells*. (2020) 9. doi: 10.3390/cells9102271

frontiers | Frontiers in Endocrinology

TYPE Original Research
PUBLISHED 09 April 2025
DOI 10.3389/fendo.2025.1587382

OPEN ACCESS

EDITED BY
Federico Baronio,
IRCCS AOU S.Orsola-Malpighi, Italy

REVIEWED BY
Giorgio Radetti,
Ospedale di Bolzano, Italy
Giuseppe Cannalire,
Guglielmo da Saliceto Hospital, Italy

*CORRESPONDENCE
Berta Magallares
bmagallares@santpau.cat
Helena Codes-Méndez
hcodes@santpau.cat

RECEIVED 04 March 2025
ACCEPTED 19 March 2025
PUBLISHED 09 April 2025

CITATION
Magallares B, Malouf J, Codes-Méndez H, Park HS, Betancourt J, Fraga G, Quesada-Masachs E, López-Corbeto M, Torrent M, Marín A, Herrera S, Gich I, Boronat S, Casademont J, Corominas H and Cerdá D (2025) Pediatric densitometry: is the Z score adjustment necessary in all cases? *Front. Endocrinol.* 16:1587382. doi: 10.3389/fendo.2025.1587382

Pediatric densitometry: is the Z score adjustment necessary in all cases?

Berta Magallares[1,2,3,4]*, Jorge Malouf[5], Helena Codes-Méndez[1,3]*, Hye Sang Park[1,3,4], Jocelyn Betancourt[3,6], Gloria Fraga[3,6], Estefanía Quesada-Masachs[2,7], Mireia López-Corbeto[7], Montserrat Torrent[6], Ana Marín[5], Silvia Herrera[3,5], Ignasi Gich[3,8,9], Susana Boronat[3,6], Jordi Casademont[3,4,10], Hector Corominas[1,3,4] and Dacia Cerdá[11]

[1]Department of Rheumatology, Hospital de la Santa Creu i Sant Pau, Barcelona, Spain, [2]Department of Rheumatology, Universitari Dexeus-Grupo Quirón Salud Hospital, Barcelona, Spain, [3]Institut de Recerca Sant Pau (IR SANT PAU), Sant Quintí 77-79, Barcelona, Spain, [4]Medicine Faculty, Universitat Autònoma de Barcelona (UAB), Cerdanyola del Vallès, Spain, [5]Department of Mineral Metabolism Unit - Internal Medicine, Hospital de la Santa Creu i Sant Pau, Barcelona, Spain, [6]Department of Pediatrics, Hospital de la Santa Creu i Sant Pau, Barcelona, Spain, [7]Department of Pediatric Rheumatology, Vall d'Hebrón Barcelona Hospital, Barcelona, Spain, [8]Centro de Investigación Biomédica en Red de Enfermedades Raras (CIBERER), Madrid, Spain, [9]Department of Clinical Epidemiology and Public Health, Hospital de la Santa Creu i Sant Pau, Barcelona, Spain, [10]Department of Internal Medicine, Hospital de la Santa Creu i Sant Pau, Barcelona, Spain, [11]Department of Rheumatology, Hospital Sant Joan Despí Moisès Broggi, Barcelona, Spain

Background: The International Society for Clinical Densitometry recommends adjusting the bone mineral density (BMD) Z-score in children with short stature or growth delay. However, it is not clear whether height-for-age Z-score (HAZ) adjustment is required in all children. The aim of this study was to determine whether HAZ adjustment is necessary by examining variability in unadjusted and adjusted Z-scores for the main regions of interest in a large pediatric cohort.

Methods: We evaluated 103 patients ≤ 20 years of age who underwent lumbar spine and whole-body dual-energy x-ray absorptiometry (DXA) at our tertiary care hospital from 2016 to 2018. The formula proposed by Zemel was used to calculate the HAZ.

Results: A total of 103 participants were included (54 females; 52.4%). The mean age was 9.8 years. Height percentiles were ≤ 3 or ≥ 97 in seven (6.8%) and five (4.9%) patients. Diagnostic criteria for low bone mineral density (LBMD; BMD Z-score ≤ −2) were met in 8 lumbar spine scans and 10 whole-body scans. After HAZ adjustment, the prevalence of LBMD decreased from 8.2% (n=8) to 6.4% (n=6) in the lumbar spine scans and from 10.5% (n=10) to 7.2% (n=8) in the whole-body scans. Agreement between the adjusted and non-adjusted HAZ data was 0.498 for the lumbar spine and 0.557 for the whole body. The diagnostic discrepancy rate for LBMD diagnosis was 7%. After HAZ adjustment, 5% patients no longer met LBMD criteria while conversely 2% met LBMD criteria only after adjustment.

Conclusions: The high diagnostic discrepancy rate (7%) for LBMN in this unselected pediatric cohort underscores the value of performing HAZ

10.3389/fendo.2025.1587382

adjustment of Z-scores to improve diagnostic accuracy. This divergence between adjusted and unadjusted Z-scores suggests that all pediatric patients, not only those with short stature or growth retardation, may benefit from densitometric size adjustment. This is especially true in individuals whose stature is at the upper end of the range, where size may obscure a diagnosis of LBMD.

KEYWORDS

pediatric densitometry, height-for-age z-score, bone mineral density, low bone mineral mass, DXA (dual-energy x-ray absorptiometry)

1 Introduction

Several imaging techniques are currently available to monitor bone disease in the pediatric population (1). The gold standard for measuring bone mineral content (BMC) and bone mineral density (BMD) is dual-energy X-ray absorptiometry (DXA) (2, 3). DXA has several advantages, including low radiation doses (4–27 μSv), a short scanning time, widespread availability, high reproducibility, and an extensive body of pediatric reference data (4). Moreover, DXA plays a key role in assessing pediatric bone health because the definition of low bone mineral density (LBMD) is based on densitometric criteria (3, 5).

Interpreting DXA results in children can be challenging due to the dynamic nature of the growing skeleton. Unlike adults, children's bones grow and change their tridimensional shape over time, and growth is highly variable depending on the individual and the developmental stage (5). DXA is a two-dimensional (2D) imaging technique that relies on differential X-ray absorption to distinguish between tissues of varying densities. Unfortunately, it cannot measure the depth of bones, the third dimension. As a result, BMD is calculated as a 2D projection of a 3D structure, expressed in g/cm2 (5, 6). Because BMD is not a volumetric measure, it is influenced by the size of the bone being assessed. Consequently, smaller bones may appear to have a lower BMD than larger bones, even if their actual volumetric density is identical (5), which means that DXA-derived areal BMD tends to underestimate true volumetric BMD (g/cm^3) in children with short stature while overestimating BMD in taller children (7, 8). For this reason, in 2019, the International Society for Clinical Densitometry (ISCD) officially recommended adjusting BMD Z-scores for bone size in children with growth impairment (3).

Several different approaches have been developed to adjust BMD Z-scores to more accurately determine BMD in children of all statures. Some of the more common techniques include adjustments based on height, weight, bone mineral apparent density, and the height-for-age Z-score (HAZ). While all of these methods have been shown to more accurately predict fracture risk in the pediatric population compared to unadjusted techniques (9), the HAZ-adjustment technique developed by Zemel et al. is considered to be the least biased method (2).

Beyond HAZ-based adjustments, other techniques have been explored to mitigate the impact of bone size on BMD measurements. These include adjustments based on bone age, pubertal stage, lean body mass, and vertebral body height. Some DXA systems also estimate bone volume using dimensional indices of the scanned region, enabling the calculation of volumetric BMD (vBMD) under simplified anatomical assumptions. For example, Kröger et al. proposed a method that considers the vertebrae as a cube or cylinder, using the formula: vBMD = aBMD × [4/(π × width)], where aBMD is areal BMD and width is the measured vertebral body width (10). In addition, new imaging technologies such as Radiofrequency Echographic Multi Spectrometry (REMS) are emerging as potential alternatives to DXA, with the advantage of assessing bone quality and fracture risk without being influenced by bone size (11). However, these technologies ae still undergoing validation and are not yet widely available in routine pediatric clinical practice.

In this context, the aim of this study was to compare standard BMD Z-scores to HAZ-adjusted Z-scores in a real-life cohort of pediatric patients. The study was carried out in the context of routine clinical practice in an unselected population. We sought to determine whether there were discrepancies in the diagnosis of LBMD based on HAZ adjusted and non-adjusted Z-scores for the main regions of interest.

2 Materials and methods

2.1 Study population

This was a cross-sectional, single-center study based on data from spine and whole-body DXA scans performed between 2016 and 2018. The study population included patients ≤ age 20 referred to the pediatric rheumatology outpatient clinic at our hospital for bone health assessment due to the presence of one or more of the following risk factors: malabsorption syndrome or food

10.3389/fendo.2025.1587382

allergies; juvenile idiopathic arthritis; nephropathy; hematological disorders; systemic autoimmune or autoinflammatory disease; endocrinopathy; treatment with drugs that alter bone metabolism (e.g., glucocorticosteroids or immunosuppressants); lack of physical activity; or insufficient calcium intake.

The study was approved by the ethics committee at our hospital (IIBSP-FRA-2016-11). Informed consent was obtained from all patients and/or their legal guardians prior to recruitment.

2.2 Data collection and study variables

The following data were collected: date of birth; weight; height; and calculated height and weight percentiles. The presence of any of the aforementioned risk factors for developing low bone mass was recorded. Densitometric measurements included total body and subtotal body less head BMD; L1-L4 vertebrae BMD; and Z-scores for both total body and L1-L4 vertebrae. We did not include Z-scores for the total body less head (TBLH), as our densitometer lacks population-based normative data required for this calculation, a common issue in real-world clinical settings at many hospitals. HAZ adjustment for lumbar spine and total body Z-score values was applied in all cases using the formulas developed by Zemel et al. (8). Densitometric measurements were obtained with the Hologic Discovery densitometer scanner (Hologic, Inc., Bedford, MA, USA).

2.3 Statistical analysis

The IBM-SPSS software package (v. 26.0) was used to perform the statistical analyses. Quantitative variables are presented as means with standard deviation (SD) and categorical variables are presented as absolute frequencies with percentages. Distribution normality for the study variables was assessed using the Shapiro-Wilk test. Depending on the distribution, the differences in mean BMD according to Z-scores and HAZ scores were analyzed using the following tests, as appropriate: T-test, Mann-Whitney U test, Kruskal-Wallis test, or ANOVA for continuous variables; and Chi-square test or Fisher's exact test for categorical variables. Pearson's linear correlation coefficient or Spearman's correlation coefficient were used to examine correlations between BMD values and HAZ-adjusted and unadjusted Z-scores. Analyses were conducted as two-tailed tests with a significance level set at 5% (α=0.05).

3 Results

3.1 Baseline characteristics and densitometric measurements

A total of 103 patients were included in the study. The mean age was 9.8 years. Height percentiles were ≤ 3 or ≥ 97 in seven (6.8%) and five (4.9%) patients. The baseline characteristics of the study population are shown in Table 1.

TABLE 1 Baseline characteristics.

Variable	n (%)
Sex, female	54 (52.4)
Age (years; range)	
Early childhood (2-3)	9 (8.7)
Childhood (4-9)	33 (32)
Adolescence (10-17)	55 (53.4)
Young adulthood (18-20)	6 (5.8)
Ethnicity	
Caucasian	82 (79.6)
Hispanic	10 10.7)
Arab-Berber	7 (6.8)
Other	3 (2.9)
Anthropometric characteristics	
Height ≤ 3rd percentile	7 (6.8)
Height ≥ 97th percentile	5 (4.9)
Weight ≤ 3rd percentile	8 (8.7)
Weight ≥ 97th percentile	9 (8.7)
Comorbid disease	99 (96.1)
Malabsorption/food allergies	47 (46.6)
Juvenile idiopathic arthritis	18 (17.5)
Nephropathy	18 17.5)
Hematological disorder	6 (6.8)
Systemic autoimmune disease	9 (7.8)
Autoinflammatory disease	3 (2.9)
Endocrinopathy	1 (1)

Densitometric data according to the region of interest are presented in Tables 2, 3. Table 2 shows BMD and BMC values for the lumbar spine with raw and HAZ Z-scores. Table 3 provides BMD and BMC values for the whole body and TBLH with raw and HAZ Z-scores.

Correlations between anthropometric measures and bone mineral density

TABLE 2 Densitometric data for the lumbar spine.

	n	Mean	SD	Median	Range
BMC, g	102	29	15.89	25.52	6.20 – 90.40
BMD, g/cm^2	102	0.64	0.18	0.61	0.36 – 1.06
Z-score	99	-0.46	1.08	-0.40	-3.20 – 1.80
HAZ-adjusted Z-score	95	-0.43	0.96	-0.41	-2.77 – 1.65

SD, standard deviation; BMC, bone mineral content; BMD, bone mineral density; HAZ, height-for-age Z-score.

10.3389/fendo.2025.1587382

TABLE 3 Densitometric data for the whole-body.

	n	Mean	SD	Median	Range
BMC, g	103	1172.2	520.6	1083.8	190.5 – 2326.4
BMC less head, g	98	861.9	443.8	775.7	244.4 – 1899.9
BMD, g/cm^2	98	0.81	0.16	0.81	0.53 – 1.17
BMD less head, g/cm^2	98	0.69	0.17	0.70	0.39 – 1.01
Z-score	96	-0.32	1.18	-0.20	-3.20 – 2.10
HAZ-adjusted Z-score	92	-0.40	1.02	-0.32	-3.41 – 1.77

SD, standard deviation; BMC, bone mineral content; BMD, bone mineral density; HAZ, height-for-age Z-score.

Both weight and height were significantly correlated with BMD at all three main locations (p<0.001 in all cases). Correlation coefficients for weight and height, respectively, were as follows: lumbar spine BMD: 0.855 and 0.824; whole body BMD: 0.889 and 0.899; and TBLH BMD: 0.908 and 0.935.

LBMD criteria (Z-score ≤2) were met by 8.2% (n=8) of the sample in the lumbar spine and 10.5% (n=10) in the whole-body. After HAZ adjustment, these values decreased to 6.4% (n=6) and 7.2% (n=8), respectively.

3.2 Comparison of unadjusted and HAZ-adjusted Z-scores

No significant differences (p=0.913) were observed in the mean unadjusted (-0.44 +/- 1.07) or HAZ-adjusted (-0.43 +/- 0.96) lumbar spine Z-scores. The correlation coefficient between the two scores was 0.78 (p<0.001), with a mean difference of 0.0075. However, the unadjusted Z-score was more variable than the HAZ-adjusted spine Z-score with a difference of 0.67.

The relationship between these variables is graphically illustrated in Figure 1. Despite the close correlation between the HAZ adjusted and unadjusted measures, there was a difference in the diagnosis of LBMD in 7% of the patients. More specifically, in 5% (n=5) of the patients, the unadjusted lumbar spine Z-score was ≤ -2 but the adjusted score was > -2. By contrast, in 2% (n=2) of patients, the HAZ-adjusted Z-score was ≤ -2 with an adjusted score > -2. At the LBMD threshold (≤ -2), the concordance index between the unadjusted and HAZ-adjusted lumbar spine Z-scores was 0.498.

No significant differences (p=0.367) were observed between the unadjusted (-0.34 ± 1.19), and HAZ-adjusted (-0.40 ± 1.02) whole body Z-scores, with a mean difference of 0.063 (-0.34 unadjusted vs -0.4 HAZ-adjusted Z-scores). The difference between the two measures in terms of SD was 0.66, indicating less dispersion in the HAZ-adjusted Z-score. The correlation between these variables was 0.82, as shown in Figure 1.

Two patients (2%) with a HAZ-adjusted whole-body Z-score ≤ -2 (LBMD threshold), had an unadjusted Z-score > -2. Similarly, 5 patients (5%) with an unadjusted Z-score ≤ -2, had a HAZ-adjusted Z-score > -2. The concordance between the unadjusted and the HAZ-adjusted whole-body Z-scores at the LBMD threshold was 0.557.

4 Discussion

The aim of this study was to determine whether size adjustment should be performed only in children with short stature (height < 3rd percentile), as currently recommended, or if it should always be adjusted when performing pediatric bone densitometry. This study was prompted by real-world clinical observations at our center, which led us to believe that the diagnostic accuracy of LBMD could be improved in other groups by performing HAZ adjustments, particularly in children with tall stature.

In this context, we determined the variability in densitometric Z-scores for the main ROIs, with and without HAZ Z-score adjustment, in a cohort of children who were not pre-selected based on height. We adjusted all Z scores, regardless of the individual's height or weight percentile. We found no significant

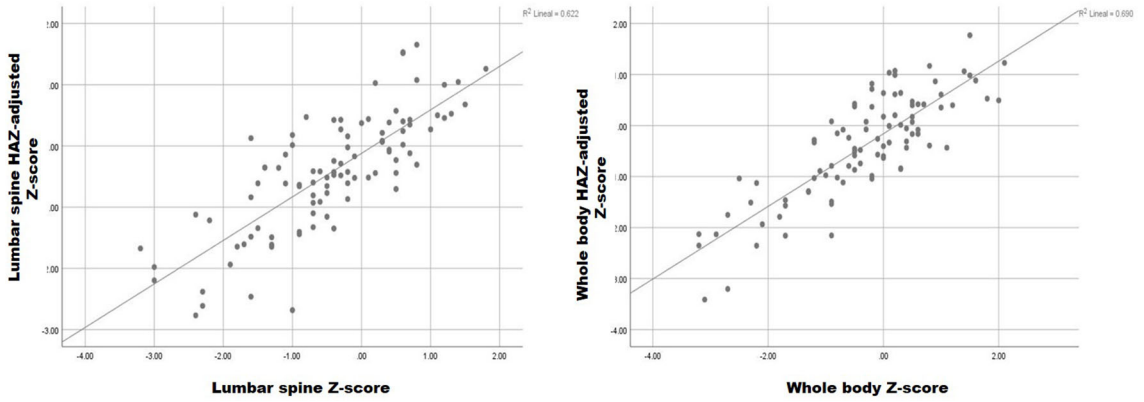

FIGURE 1
Relationship between HAZ-adjusted and unadjusted lumbar spine and whole-body Z-score.

differences in the mean adjusted and unadjusted Z-scores for the main ROIs (i.e., spine and whole body). However, the HAZ-adjusted Z-scores showed less dispersion (based on SD values), indicating reduced variability.

At the LBMD threshold (Z-score ≤ -2), the discordance rate between HAZ-adjusted and unadjusted measurements was 7% in the two ROIs (lumbar spine and whole body). After HAZ adjustment, 5% of patients who had met diagnostic criteria for LBMD (based on unadjusted values) no longer met those criteria and 2% of patients whose Z-scores were considered normal actually met LBMD criteria.

After HAZ adjustment, 5% of patients who initially met diagnostic criteria for LBMD no longer did, likely corresponding to those on the lower end of the height percentile. Conversely, 2% of patients who now met LBMD criteria post-adjustment were likely on the higher end of the height percentile. These findings suggest a strong correlation between HAZ-adjusted and unadjusted Z-scores given that both scores measure the same parameter. However, the reduced variability in the HAZ-adjusted Z-scores, particularly at the diagnostic threshold, is an important advantage of using adjusted scores because it reduces both underdiagnosis or overdiagnosis.

These findings are consistent with previous studies supporting size correction in children with growth disturbances, and they also reinforce the utility of methods such as bone volume estimation using geometric modeling approximations, as described by Kröger et al. (10). Nonetheless, these techniques also rely on certain assumptions and may not be routinely available in all clinical settings. Moreover, while newer imaging modalities like REMS may offer size-independent assessment (11), they are still not routinely available and further validation is required before widespread implementation in pediatric care.

Given these results, we believe that densitometric size adjustment should be applied to the whole pediatric population, regardless of stature or growth status. Size adjustment could be particularly beneficial in individuals whose height falls in the upper percentiles as unadjusted scores in this group are more likely to appear within the normal range, thus masking an LBMD diagnosis and delaying appropriate follow-up or treatment. Therefore, we recommend that clinicians consider applying size adjustment for all pediatric densitometry in all patients.

4.1 Strengths and limitations

The main limitation this study is the single-center design, which may limit the generalizability of our findings to other clinical settings or populations. Notwithstanding that limitation, the study hospital is a tertiary care referral center for rheumatic diseases, with a broad catchment area (> 450,000 residents), thus ensuring a diverse patient population. Another limitation is technical in nature, related to the DXA software used at the time of the study, which prevented us from performing Z-score evaluations for the TBLH projections. As a result, we were unable to obtain standardized assessments for those measurements. To overcome this limitation, we included both raw BMD values and Z-scores, which improves transparency and allows for a more nuanced interpretation of bone health in this population. It should be noted that this limitation is common in routine clinical practice at many hospitals, where lumbar spine DXA scans are often the only assessment performed. Despite this limitation, we believe it is important to present our data to encourage other centers to perform whole-body assessments, as this can provide important information until new software becomes available for TBLH projections (12). Clearly, these limitations should be considered when interpreting our findings. More research is needed with the latest DXA technology and standardized protocols across various populations to validate our findings.

This study has several strengths. First, several previous studies have concluded that size adjustment for DXA measurements should be performed in specific populations with growth disturbances (6, 13, 14). To our knowledge, however, our study is the first to investigate the need to perform size adjustments for all pediatric DXAs and the first to compare diagnostic discrepancies between adjusted and unadjusted measurements. By evaluating the impact of HAZ adjustment of Z-scores in a diverse, unselected pediatric cohort, our study provides evidence to support the benefits of size adjustment in improving the accuracy of the LBMD diagnosis. The inclusion of both raw and adjusted Z-scores further enhances the robustness of our analysis and supports the application of these findings in clinical practice.

4.2 Conclusion

In this study, we found discrepancies between HAZ-adjusted and unadjusted Z-scores in terms of the diagnosis of LBMD. More specifically, we found that the diagnosis differed in 7% of patients according to whether the adjusted or unadjusted scores were used. In 5% of cases, the patients no longer met criteria for a diagnosis of LDMD after HAZ adjustment. In 2% of cases, patients who originally had normal Z-scores met LBMD criteria after adjustment. These findings highlight the critical importance of performing size adjustment in all pediatric DXA measures to avoid both underdiagnosis and overdiagnosis. These findings suggest that Z-scores should be size adjusted for in all pediatric cases, especially in children in the top height percentiles, to improve the accuracy and reliability of the LBMD diagnosis.

Data availability statement

The original contributions presented in the study are included in the article. Further inquiries can be directed to the corresponding author/s.

Ethics statement

The studies involving humans were approved by Institutional Ethics Committee of Hospital de la Santa Creu I Sant Pau, Barcelona, Spain (IIBSP-FRA-2016-11). The studies were

conducted in accordance with the local legislation and institutional requirements. Written informed consent for participation in this study was provided by the participants' legal guardians/next of kin.

Author contributions

BM: Conceptualization, Formal analysis, Methodology, Project administration, Validation, Writing – original draft, Writing – review & editing. JM: Conceptualization, Methodology, Project administration, Writing – review & editing. HC-M: Methodology, Project administration, Validation, Visualization, Writing – review & editing. HP: Methodology, Writing – review & editing. JB: Methodology, Writing – review & editing. GF: Methodology, Writing – review & editing. EQ-M: Methodology, Writing – review & editing. ML-C: Methodology, Writing – review & editing. MT: Writing – review & editing. AM: Investigation, Writing – review & editing. SH: Investigation, Writing – review & editing. IG: Data curation, Software, Writing – review & editing. SB: Writing – review & editing. JC: Writing – review & editing. HC: Writing – review & editing. DC: Writing – review & editing.

Funding

The author(s) declare that financial support was received for the research and/or publication of this article.

Acknowledgments

We thank Bradley Londres for professional language editing.

Conflict of interest

The authors declare that the research was conducted in the absence of any commercial or financial relationships that could be construed as a potential conflict of interest.

Generative AI statement

The author(s) declare that no Generative AI was used in the creation of this manuscript.

Publisher's note

References

1. Lalayiannis AD, Crabtree NJ, Fewtrell M, Biassoni L, Milford DV, Ferro CJ, et al. Assessing bone mineralisation in children with chronic kidney disease: what clinical and research tools are available? *Pediatr Nephrol (Berlin Germany).* (2020) 35:937–57. doi: 10.1007/s00467-019-04271-1

2. Gordon CM, Leonard MB, Zemel BS. Pediatric Position Development Conference: executive summary and reflections. *J Clin densitometry: Off J Int Soc Clin Densitometry*. (2013) 17:219–24. doi: 10.1016/j.jocd.2014.01.007

3. Shuhart CR, Yeap SS, Anderson PA, Jankowski LG, Lewiecki EM, Morse LR, et al. Executive summary of the 2019 ISCD position development conference on monitoring treatment, DXA cross-calibration and least significant change, spinal cord injury, peri-prosthetic and orthopedic bone health, transgender medicine, and pediatrics. *J Clin densitometry: Off J Int Soc Clin Densitometry.* (2019) 22:453–71. doi: 10.1016/j.jocd.2019.07.001

4. Bachrach LK, Sills IN. Clinical report-bone densitometry in children and adolescents. *Pediatrics.* (2011) 127:189–94. doi: 10.1542/peds.2010-2961

5. Binkovitz LA, Henwood MJ. Pediatric DXA: technique and interpretation. *Pediatr radiology.* (2007) 37:21–31. doi: 10.1007/s00247-006-0153-y

6. Salem N, Bakr A. Size-adjustment techniques of lumbar spine dual energy X-ray absorptiometry measurements in assessing bone mineralization in children on maintenance hemodialysis. *J Pediatr Endocrinol metabolism: JPEM.* (2021) 34:1291–302. doi: 10.1515/jpem-2021-0081

7. Crabtree N, Ward K. Bone densitometry: current status and future perspective. *Endocrine Dev.* (2015) 28:72–83. doi: 10.1159/000223689

8. Zemel BS, Leonard MB, Kelly A, Lappe JM, Gilsanz V, Oberfield S, et al. Height adjustment in assessing dual energy x-ray absorptiometry measurements of bone mass and density in children. *J Clin Endocrinol Metab.* (2010) 95:1265–73. doi: 10.1210/jc.2009-2057

9. Crabtree NJ, Hogler W, Cooper MS, Shaw NJ. Diagnostic evaluation of bone densitometric size adjustment techniques in children with and without low trauma fractures. *Osteoporosis international: J established as result cooperation between Eur Foundation Osteoporosis Natl Osteoporosis Foundation USA.* (2013) 24:2015–24. doi: 10.1007/s00198-012-2263-8

10. Kröger H, Vainio P, Nieminen J, Kotaniemi A. Comparison of different models for interpreting bone mineral density measurements using DXA and MRI technology. *Bone.* (1995) 17:157–9. doi: 10.1016/S8756-3282(95)00162-X

11. Fuggle NR, Reginster J-Y, Al-Daghri N, Bruyere O, Burlet N, Campusano C, et al. Radiofrequency echographic multi spectrometry (REMS) in the diagnosis and management of osteoporosis: state of the art. *Aging Clin Exp Res.* (2024) 36:135. doi: 10.1007/s40520-024-02784-w

12. Zemel BS, Shepherd JA, Grant SFA, Lappe JM, Oberfield SE, Mitchell JA, et al. Reference ranges for body composition indices by dual energy X-ray absorptiometry from the Bone Mineral Density in Childhood Study Cohort. *Am J Clin Nutr.* (2023) 118:792–803. doi: 10.1016/j.ajcnut.2023.08.006

13. Kor D, Bulut FD, Kılavuz S, Şeker Yılmaz B, Köşeci B, Kara E, et al. Evaluation of bone health in patients with mucopolysaccharidosis. *J Bone mineral Metab.* (2022) 40:498–507. doi: 10.1007/s00774-021-01304-4

14. Ali F, Cole CR, Hornung L, Mouzaki M, Wasserman H, Kalkwarf HJ. Age-related trajectory of bone density in children with intestinal failure: A longitudinal retrospective cohort study. *JPEN J parenteral enteral Nutr.* (2023) 47:736–45. doi: 10.1002/jpen.v47.6

frontiers | Frontiers in Endocrinology

TYPE Case Report
PUBLISHED 09 April 2025
DOI 10.3389/fendo.2025.1547679

OPEN ACCESS

EDITED BY
Federico Baronio,
Dpt Hospital of Woman and Child, Italy

REVIEWED BY
Djandan Tadum Arthur Vithran,
Hunan Provincial People's Hospital, China
Andrei Feier,
Sciences and Technology of Târgu Mureş, Romania

*CORRESPONDENCE
Haining Sun
shnjjzy@163.com

†These authors share first authorship

RECEIVED 18 December 2024
ACCEPTED 20 March 2025
PUBLISHED 09 April 2025

CITATION
Wang B, Miao Z, Yu X, Zhou K, Liu N, Zhai K, Zheng S and Sun H (2025) Case Report: Surgical timing for Blount's disease: a case report and systematic review. *Front. Endocrinol.* 16:1547679. doi: 10.3389/fendo.2025.1547679

Case Report: Surgical timing for Blount's disease: a case report and systematic review

Bing Wang†, Zukang Miao†, Xiuchun Yu, Ke Zhou, Ning Liu, Kai Zhai, Shu Zheng and Haining Sun*

Department of Orthopedics, 960th Hospital of the People's Liberation Army, Jinan, China

Background: Currently, Blount's disease is treated in a variety of ways, but the optimal timing of treatment and the choice of optimal treatment regimen have yet to be determined. We report a case of a patient who failed multiple surgical treatments and underwent 3D-printed osteotomy guide-assisted proximal tibial orthopedic external fixation in adulthood to restore normal lower limb mechanical axis and suggest optimal treatment modalities in light of the systematic literature.

Methods: A case of Blount's disease patient who was misdiagnosed and missed and underwent multiple surgical treatments was retrospectively studied. According to the PRISMA statement, a systematic review of electronic databases such as PubMed, Embase, and Web of Science was conducted to explore the optimal timing of surgery for Blount's disease from 2010.

Results: A boy born in 2001 was found to have a varus deformity in his left knee joint at the age of 2 years, which was not diagnosed. At the age of 7 years, he was diagnosed with Blount's disease and underwent multiple surgeries over the following years, all of which resulted in recurrences. At the age of 21 years, he underwent high osteotomy and external fixation of the proximal left tibia using a 3D-printed guide plate in our hospital. At present, the external fixation has been taken out, and the lower limb force line has recovered well. The timing and choice of treatment for Blount's disease are important for the patient's prognosis. The systematic review analyzed a total of 23 studies with a combined sample size of 679 cases, it provides recommendations for treatment strategies based on patient age.

Conclusion: The patient's age and degree of deformity are key in determining the timing and treatment plan. For patients with early-onset, who are under four years old, they may begin with a conservative treatment strategy, moving to a timely osteotomy if the initial approach proves ineffective. For patients with late-onset, 4-10 years old, there are no recommendations for definitive treatment at this time. Patients over 10 years old should have their bone age and growth potential evaluated, with epiphysiodesis recommended for those with a growth potential greater than 2 years and osteotomy recommended for those with less than 2 years to achieve a complete correction of the deformity.

KEYWORDS

blount's disease, operation timing, treatment, osteotomy, early-onset; late-onset

Introduction

Blount's disease is a spontaneous condition that causes an abnormal unilateral or bilateral growth of the medial proximal tibia, leading to severe tibial varus deformity. The disease is classified into two main categories based on age at onset: Early-onset, detected before the age of four years, and late-onset, detected after this age (1). A more specific classification further segments the late-onset category into early-onset/infantile (less than 4 years old), juvenile (4–10 years old), and adolescent (more than 10 years old) (2). Prognosis, intervention timing, and treatment modalities for Blount's disease can vary significantly, as evidenced by domestic and international studies. Thus, based on the diagnosis, treatment process, and prognosis of a Blount's disease patient treated at our hospital, and in combination with relevant literature, we aimed to discuss the most recent strategies for the timing of Blount's disease treatment.

Case presentation

A male patient, born in March 2001, presented with a varus deformity in his left knee joint that has existed since the age of two. No genetic disease in the patient's family. Initial consultation at a local healthcare facility raised suspicions of rickets, leading to a three-year regimen of intermittent calcium and vitamin D tablets, not treated with conservative treatment such as knee ankle foot orthosis(KAFO). However, this treatment failed to substantially alleviate his symptoms, and the varus deformity progressively worsened. In May 2008, at the age of seven, the patient underwent further diagnostic imaging at a second medical institution. The clinical presentation and subsequent diagnostic results confirmed a diagnosis of Blount's disease. Following appropriate surgical considerations, the patient underwent high osteotomy and external fixation of the left tibia. In December 2011, he received a navigational surgery at another hospital to open the left proximal tibial medial epiphysis, followed by high proximal tibial osteotomy and internal fixation (Figures 1A, B). Post-operatively, the leg was immobilized in plaster for two months and weight-bearing was gradually introduced. Despite these measures, the varus deformity persisted. The patient presented to our institution in July 2013 for internal fixation (Figures 1C, D). X-ray shows medial step-like changes in the proximal tibial metaphysis. Blood biochemical parameters were normal, physiologic knee inversion and rickets were ruled out, and the diagnosis of blount's disease was once again made definitively. Upon removal of the fixation, the varus deformity of his knee deteriorated further. Given this history of left tibial varus deformity lasting over 14 years and recent onset left knee joint pain of one-month duration, our surgical team performed high osteotomy and external fixation of the proximal left tibia using a 3D printed guide plate on April 8, 2022. Follow-up appointments showed promising prognosis, and the external fixator was successfully removed on January 31, 2023.

Upon admission on March 29, 2022, physical examination revealed the following parameters: height, 178 cm; weight, 104 kg; and a body mass index (BMI) of 32.82 kg/m2. Notable findings included a claudicating gait and a varus deformity of the left knee.

FIGURE 1
(A) Full-length X-ray of both lower limbs (October 2011, preoperative): Demonstrates varus deformity of the left tibia, wedge-shaped thinning of the medial epiphysis of the proximal tibia, and uneven osteogenesis of the proximal metaphysis. The MAA is 148°. **(B)** (December 2011, post-secondary surgery): Shows solid internal fixation in an optimal position, MAA: 170°. **(C)** Photograph of the left lower leg (July 2013, pre-internal fixation removal): Prominent varus deformity with a well-healed 15 cm incision on the anterior aspect of the tibia. **(D)** Full-length X-ray of both lower limbs (July 2013, pre-internal fixation removal): Reveals good healing of the osteotomy end and stable internal fixation, MAA: 164°.

There was a visible surgical scar, measuring 20 cm in length, proximal to the left tibia, with no associated tenderness around the incision or the left knee joint. The left lower limb was 3 cm shorter than the right. Both knee joints exhibited a normal range of motion, and muscle strength, tension, and skin sensation were normal in both lower limbs. Physiological reflexes were present and no pathological reflexes were noted (Figure 2A). Laboratory tests revealed: white blood cell (WBC) count, 6.44 x 109/L; red blood cell (RBC) count, 5.69 x 109/L; Hemoglobin (Hb), 165 g/L; Platelet count (Plt), 217 x 109/L; C-reactive protein (CRP), 16.5 mg/L; and uric acid (UA), 466 μmol/L. Full-length X-rays of both lower limbs demonstrated leg length discrepancy, with the right lower limb being 2.3 cm longer than the left. There was malformation in the left lower limb, with irregular bone structure in the proximal tibia, multiple cystic low-density areas, and misalignment of the femur and tibia. The pelvis appeared slightly tilted to the left (Figure 2B). A full-length CT scan of both lower limbs confirmed the irregular proximal bone structure of the left tibia, the presence of multiple cystic lucencies internally, and disordered trabecular bone structure. The medial condyle of the tibia was undersized, and there was poor alignment and asymmetry of the left knee joint space. The left fibula exhibited a localized bony protrusion and an enlarged mid-section, with no other evident abnormalities.

The proposed diagnoses included (1): left tibial varus deformity; (2) Blount's disease; (3) postoperative tibial osteotomy. Noteworthy physical examination results revealed significant deformity on the affected side with a femorotibial mechanical axis angle (MAA) of 158°. Considering the patient's multiple anterior and posterior surgeries, heavy deformity, and poor bone quality, the design of osteotomy guides using 3D printing technology was able to minimize surgical trauma and achieve precision in osteotomy. A 3D-printed osteotomy guide plate was fabricated based on comprehensive CT scans of both lower limbs. The distraction angle was set to approximately 35 degrees (Figure 2C). Using C-arm fluoroscopy, the mechanical axis of the lower limbs was restored. Subsequently, a circular external fixator was applied, an allogenic bone graft was inserted at the osteotomy site, and a drainage tube was placed *in situ* (Figure 2D). The procedure was executed and concluded successfully. Postoperative management included standard anti-inflammatory, analgesic, and antithrombotic regimens. The surgical incision healed well, and sutures were removed without complications (Figures 3A–C). Regular follow-ups were scheduled every three months post-operation. The external fixator was removed and installed internal fixation to prevent fracture in January 2023.The strength line of the affected limb basically returned to normal (MAA: 174°). The physicians and the patient's family observed that the walking posture was significantly improved. The patient said there is no obvious pain and discomfort during walking. and basically returned to normal study and life without assistance.Everyone was very satisfied with the results of the surgery. On March 10, 2025, the patient reported no significant discomfort and had resumed normal exercise and life with no significant deformity of the affected limb (Figures 3D, E).

Systematic review

Literature search

A search of PubMed, Embase, and Web of Science electronic databases was conducted to screen for Blount's disease. The language of publications was limited to English. Publication dates were after 2010. The search terms were ("blount's disease" OR "blount disease" OR "congenital knee inversion deformity") AND ("treatment" OR "surgery" OR "postoperative recurrence") by title/

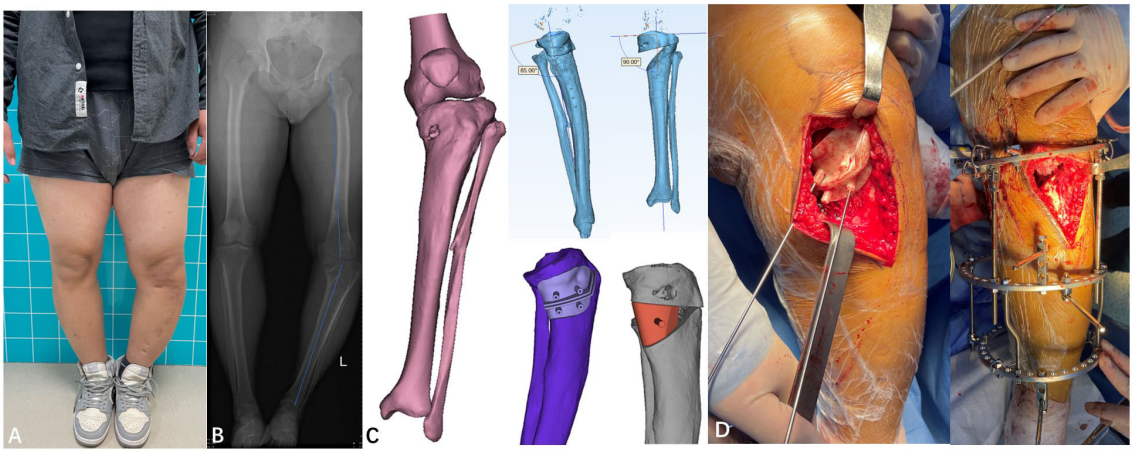

FIGURE 2
(A) Photograph (March 2022, prior to third surgery). **(B)** Full-length X-ray of both lower limbs (March 2022, prior to third surgery): Shows left knee joint varus deformity, uneven tibial plateau with multiple cystic low-density shadows, and disorder in the trabecular structure, MAA: 158°.
(C) Preoperative 3D-printed osteotomy design plan, Intraoperative image showing a 3D-printed osteotomy guide plate assisting in the osteotomy.
(D) Simulation of the preoperative osteotomy angle adjustment, Intraoperative image showing osteotomy and fixation using an external fixator.

FIGURE 3
(A) Full-length X-ray of both lower limbs (April 2022, post-third surgery): Features the external fixator in a good position, normal force lines of both lower limbs, aligned osteotomy ends, the defect filled with high-density bone, and the left limb being shorter than the right by 1 cm, MAA: 176°. **(B)** Photograph (June 2022, post-third surgery): Shows the lower limb deformity completely corrected and fixed with an external fixator, with no obvious discomfort observed. **(C)** X-ray of left tibia and fibula (January 2023, post-third surgery): Demonstrates a medial bone defect in the proximal tibia, good alignment of the osteotomy ends, and a well-positioned external fixator ten months following surgery. **(D)** Photograph (February 2023): Image captured after the removal of the external fixator. **(E)** X-ray(February 2023):MAA:174°.

abstract. An additional search was performed for references cited in all relevant articles.

Data extraction

Data extracted from eligible papers included baseline characteristics, orthopaedic investigations, imaging findings, treatment options and clinical follow-up results. Data collection was conducted independently by two reviewers using a standard form. If disagreements persisted, arbitration was conducted by a third review author.

Literature selection and quality assessment

The initial search revealed 247 studies. After removal of duplicates, exclusion by title and abstract, and exclusion by full text, a total of 23 documents were finally included (Figure 4). All of the literature was assessed by the JBI quality assessment tool to be of adequate quality level.

Data analysis

We reviewed the Blount's disease previously reported (Table 1) (3–25). The selection consisted of 23 articles, including 18

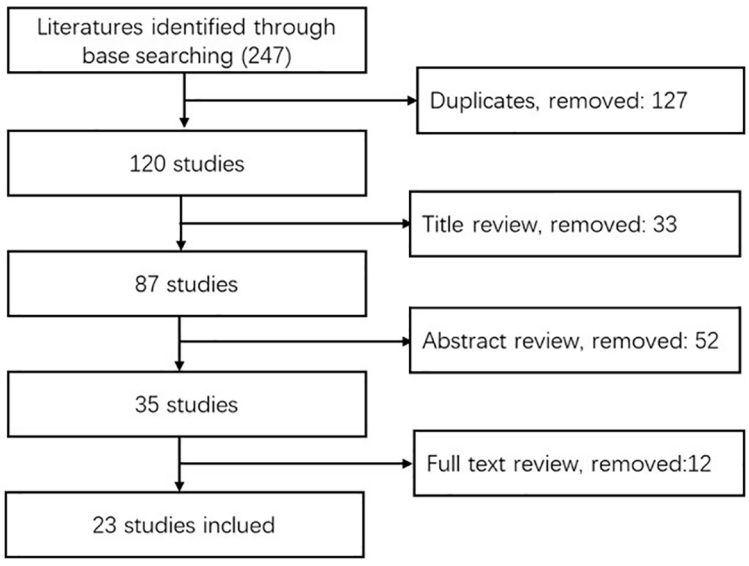

FIGURE 4
PRISMA Flow-chart.

TABLE 1 Cases in the literature.

NO.	Study	Country	Design	Limbs	Age (year)	Typing	Langenskiö-ld stage	Treatment	Fllowing (year)	Conclusion
1	Chandankere etal 2023 (3)	India	Retrospective	8	9.4 (8–11)	Infantile	IV-VI	Medial hemi-plateau elevation and metaphyseal osteotomy	3-8	It is crucial to achieve proper correction of all deformity components during surgery, with epiphysiodesis on the lateral side to prevent further recurrence.
2	Miraj etal 2023 (4)	Indonesia	Retrospective	25	8.8 (6-14)	infantile	III-VI	Acute correction with simultaneous hemiepiphysiodesis of lateral proximal tibia	3	Acute correction with simultaneous hemiepiphysiodesis of lateral proximal tibia physis is an effective technique to prevent deformity recurrence
3	Mare etal 2022 (5)	South Africa	Retrospective	25	12.5 (7-17)	15 Early-onset 10 Late-onset		Gradual correction with a computer-assisted hexapod external fixator	0.5-5.6	Recurrence remains a concern if correction is performed before skeletal maturity
4	Assan etal 2021 (6)	Benin	Retrospective	24	3-12	infantile		Guided growth or Tibial Osteotomy	>1	Guided growth appears to be the best treatment for early stage of disease in squelletically immature patients.
5	Baraka etal 2021 (7)	Egypt	Retrospective	21	10.3 (8.2 - 13.6)	infantile	V	Single-stage medial plateau elevation and metaphyseal osteotomies	5.1 (3.2-8.3)	It significantly improved the clinical and radiographic parameters and PODCI score in advanced infantile Blount's disease and precluded the use of external immobilization, with no evidence of deformity recurrence.
6	Nada etal 2021 (8)	Egypt	Prospective	11	13.5 (11.5 - 15)	infantile	IV,V	Acute Correction and Plate Fixation	2.2 ± 0.5	This single-stage double osteotomy technique has been shown to be successful for this sample of patients and yielded acceptable clinical and radiological outcomes, without significant major complications.
7	Zein etal 2021 (9)	Egypt	Retrospective	32	13-22	Adolescent		Minimally invasive osteotomy and simple circular fixation	>2	Acute correction and simple circular frame fixation is an excellent treatment choice for cases of late-onset tibia vara, especially in severe deformities
8	Griswold etal 2020 (10)	USA	Retrospective	17	3.2 ± 1.4	infantile		Guided growth	≤2: 4.11 ± 2.2 ≥ 3: 4.81 ± 1.8	Caution should be used with the consideration of guided growth forchildren presenting with Langenskiold stage ≥3 due to high rate of recurrent deformity and need for subsequent surgeries
9	Musikachart etal 2020 (11)	Thailand	Retrospective	72	2.9 (2.2–3.9)	Infantile	II	Dome or wedge-shaped proximal tibial osteotomy	4.77 ± 2.78	Don't demonstrate significant differences in the posterior tibial slope (PTS) angle.

(Continued)

10.3389/fendo.2025.1547679

TABLE 1 Continued

NO.	Study	Country	Design	Limbs	Age (year)	Typing	Langenskiö-ld stage	Treatment	Fllowing (year)	Conclusion
10	Marine etal 2020 (12)	USA	Case report	1	5 years 4 months	Infantile	IV	Lateral proximal physeal tethering and medial hemiplateau elevation osteotomy	2	These procedures allow for correction of alignment while preserving growth potential.
11	Danino etal 2020 (13)	Israel	Retrospective	55	9.5 (1.58 -14.83)	11 Infantile, 12 Juvenile, 32 Adolescent		Temporal hemiepiphysiodesis	2(0.3- 3.5)	Adolescent Blount has the best chance of achieving full correction while same treatment is less effective in infantile Blount.
12	Miraj etal 2019 (14)	Indonesia	Retrospective	27	7.8	Infantile	III-VI	Step Cut "V" osteotomy	1	The method can produce an accurate correction, high union rate and early weight bearing with no complication as a result that would be achieved at the end of treatment.
13	Jain etal 2019 (15)	USA	Retrospective	61	9.6 (3.3 -14.8)	19 Early-Onset; 42 Late-Onset		Tension Band Plate (TBP)-guided Hemiepiphysiodesis	3.1 (0.6-9.9)	TBP still needs to be proven but 41% surgical failure rate in our study does not restrict the use of TBP as first choice implant in Blount disease.
14	Terjesen etal 2018 (16)	Norway	Case report	1	13	Unknown		Intraepiphyseal osteotomy with elevation of the medial plateau of the tibia	65	The method can be recommended in older children with pronounced varus deformity.
15	Tsibidakis etal 2017 (17)	Italy	Retrospective	24	7.5 (3–14)	Unknown		Proximal tibial osteotomy and Taylor Spatial Frame	3-6	TSF allows safe gradual correction and is an accurate and well-tolerated method for the treatment of the Blount disease at any age
16	Shawn etal 2015 (18)	USA	Retrospective	38	11.5 (7.5 ~ 15.2)	Late-Onset		Staple or Plate Hemiepiphysiodesis	3 (1.1 -5.3)	There was no difference in success between implant types and hemiepiphysiodesis is not recommended for morbidly obese patients with severe deformity
17	Liu etal 2015 (19)	China	Retrospective	7	1.4 -5.2	Infantile	II-IV	Femur,tibia and fibula osteotomies	3 -16	Femur, tibia and fibula osteotomies are useful for correction of Blount's disease. The complication is less and can get satisfied result.
18	Sabharwal etal 2014 (20)	USA	Retrospective	70	Early-Onset 7.1 (5.3-8.9); Late-Onset 12.8 (12.0-13.5)	33 Early-onset 37 Late-onset	II	Osteotomy; Hemiepiphyseodesis; Epiphyseodesis; Hardware removal	4 (3.25-4.7)	The BMI of the majority of children with Blount's disease increased over time and obesity needed to deal with.
19	Eamsobhana etal 2014 (21)	Thailand	Retrospective	65	2.8 (2.5–3.3)	Infantile	II	Dome osteotomy	3	There was no relationship between the amount of overcorrection to a valgus position and the recurrence.

(Continued)

10.3389/fendo.2025.1547679

10.3389/fendo.2025.1547679

TABLE 1 Continued

NO.	Study	Country	Design	Limbs	Age (year)	Typing	Langenskiö-ld stage	Treatment	Fllowing (year)	Conclusion
20	Abdelgawad 2013 (22)	USA	Case report	2	3	Infantile	II	Lateral tension band plate (eight plate) and distal tibial external rotation osteotomy	1	this combination as the method of treatment for early stages of Blount's disease as it corrects both elements of the disease and in the same time avoids the complications of proximal tibial osteotomy.
21	Oto etal 2012 (23)	Turkey	Retrospective	6	13 (12–14)	Adolescent		Eight-plate (Orthofix) hemiepiph-ysiodesis	1.8(1-2.6)	Don't recommend the use of a tension band plate hemiepiphyseodesis (eight-plate, Orthofix) to treat severe adolescent Blount's disease in obese children.
22	Putzeys etal 2012 (24)	France	Case report	1	14	Late-Onset	VI	Triple proximal tibial osteotomy	1	Late-onset Blount's disease can be treated by a one-time procedure with internal stabilisation devices.
23	Kawu etal 2011 (25)	Nigeria	Retrospective	86	9.7 ± 3.9	Unkown	IV	Wedge, dome or chevron osteotomy	2	Postoperative MDA is a good outcome measure for surgical treatment of Blount disease and surgical correction should aim at producing post MDA ≤10°.

retrospective studies, 4 case reports, and 1 prospective study, encompassing a total of 679 cases: infantile or early-onset, with 358 cases at Langenskiöld stages II through VI; and late-onset, with 210 cases, distributed among juveniles (12 cases), adolescents (70 cases), unclassified (128 cases), and those with unclear categorization (111 cases). The age range was 1.4 to 17 years. Treatments involved conservative management, osteotomy, hemiepiphysiodesis, epiphysiodesis, hardware removal, internal/external fixation and hemiplateau elevation.

Discussion

Blount's disease characteristically induces progressive and three-dimensional deformities, such as proximal tibial varus, flexion, and internal rotation (26). Prolonged, untreated, or recurrent varus deformity increases the risk of degenerative osteoarthritis. Nonetheless, the pathogenesis of Blount's disease remains unclear. Potential contributing factors encompass patient ethnicity, excessive knee joint pressure due to obesity or early weight-bearing, congenital varus development, nutritional status, genetics, histology, and intra-articular alterations (27).

Treatment approaches for Blount's disease aim not only at correcting limb deformities but also restoring lower limb alignment, balancing leg length disparities, and ensuring post-maturity bone stability. The choice of treatment timing and mode is typically predicated on patient classification and deformity severity.

Clinical manifestations of infantile Blount's disease (≤4 years old) often range from proximal tibial varus deformity and increased internal tibial rotation to notable "beak protrusion" of the medial epiphysis and metaphysis of the proximal tibia, and leg length discrepancy. Blount's disease can be diagnosed when the metaphyseal-diaphyseal angle (MDA) of the affected limb is >16° in conjunction with corresponding physical changes (28). In the reported case, the patient displayed unilateral knee varus deformity around the age of two. Originally misdiagnosed with rickets at a primary care hospital. The X-ray of the patient's knee joint before the second operation showed varus deformity of the left knee joint, sharp varus angulation of the metaphysis, and beak-like changes, MDA:19°. There were no skeletal deformities such as chicken breast and square skull, so rickets was not considered.The subsequent progression led to the identification of the condition as Blount's disease.

Blount's disease in infancy, characterized by epiphyseal-metaphyseal distortion, can be stratified into six stages according to Langenskiöld's classification, primarily based on imaging results (29). Early intervention may prove beneficial for these patients, specifically with the application of orthopedic braces. Existing literature suggests that patients aged less than three years and those classified within Langenskiöld stage III or below may experience advantages from the extended use of anti-varus orthopedic braces (30). The knee ankle foot orthosis (KAFO) and the ankle foot orthosis (AFO) are the commonly chosen braces (31). Consequently, an early diagnosis and prompt initiation of brace treatment could potentially curtail the progression of the deformity, or even avert the necessity for subsequent surgical intervention.

Initial studies have identified certain risk factors contributing to the failure of conservative treatment, including obesity (body weight >90%), varus thrust, patient age (>3 years at treatment onset), bilateral involvement, and severe illness (Langenskiöld stage >III). For children under four with high-risk factors like high body mass index, persistent abnormalities following conservative treatment, or progressive worsening, osteotomies are necessary. These interventions can yield a total recovery rate of up to 80% (32, 33). Miraj (14) introduced a novel osteotomy approach termed the "Stepcut V" osteotomy, which has proven effective for patients under four with moderate to high deformities. The patient's age at the time of the osteotomy is significantly associated with the recurrence rate. A delay in treatment until after age four can notably increase the recurrence rate (34, 35), with long-term recurrence rates ranging between 55% and 88% (25). These findings underscore the efficacy of early surgical intervention in controlling disease recurrence. Notably, there is no significant difference in the sagittal sequence among patients who underwent different osteotomy methods (11), eliminating the need for deliberate correction toward a valgus state, which does not affect the long-term recurrence (21). However, when the disease progresses to Langenskiöld stages V or VI, characterized by medial tibial plateau depression or medial tibial bone growth stagnation, osteotomy alone will not rectify the issue. It might lead to unequal lower limb length, exacerbating the deformities. Even with repeated osteotomy, deformities can recur before bone maturity. Successful interventions have been reported for Langenskiöld stage >IV patients under seven years of age, where epiphysiolysis of the proximal medial tibia combined with valgus osteotomy resulted in an over 80% success rate (36). An isolated case reported success with guided growth and hemiplateau elevation in treating advanced Blount's disease, correcting the varus deformity, and preserving the affected limb's growth potential. Postoperative strategies to manage patients' BMI can further reduce the knee joint burden and the probability of recurrence (20). Therefore, for infantile-type patients unresponsive to ongoing conservative treatment or presenting high failure risk factors, timely osteotomy and orthopedic surgery can significantly improve prognosis. Alternative treatments for early-onset cases like growth modulation, hemiplateau elevation, and guided growth with hemiplateau elevation, despite their potential, have not been extensively studied, presenting various complications, uncertain outcomes, and limitations. These are currently subjects of debate within the field (21, 37, 38), yet their use highlights the significance of early intervention.

Late-onset patients with knee varus deformity, typically aged between 4 and 10 years, can be classified as having Juvenile Blount's disease. This group's specific treatment is contentious due to growth spurts and early growth plate fusion occurring between 6 and 8 years of age (32), and is usually discussed in conjunction with patients who develop the disease post age 10.

Blount's disease occurring after the age of 10 is classified as Adolescent Blount's disease. Roughly one third of varus deformities may be attributed to the distal femur (26), and the incidence is high among Caribbean African populations, most of whom are obese. Conservative treatment is generally deemed ineffective, which is strongly associated with patient age and size. Therefore, in order to fully correct deformities and prevent or delay the onset of osteoarthritis, surgical intervention, including osteotomy and hemiepiphyseodeses, is often considered.

Hemiepiphyseodeses and guided growth systems, known for their minimal invasiveness, target and correct deformities at the epiphyseal level. This correction process leverages the growth of the remaining healthy epiphysis while curbing the growth rate of the lateral epiphysis to achieve angular rectification. Barry et al. (13) suggested that lateral tibial hemiepiphyseodeses, based on a multicenter retrospective analysis, serve as a successful primary therapy for Blount's disease. Adolescent Blount's disease, particularly in those over 10 years old, is more likely to achieve full correction. Conversely, this treatment exhibits less effectiveness in infantile/juvenile Blount's disease. The success rate of this intervention is reported to range from 50% to 88% (39), denoting considerable variance. A literature review posits that tibial hemiepiphyseodeses are most suitable for younger patients with mild varus deformity and less severe obesity, including those with a BMI below 40 kg/m2, body weight less than 100 kg, and

TABLE 2 Results in the literature.

Typing		Time of diagnosis	Stage	Treatment
Early-onset		<4years	≤III	Conservative treatment/Osteotomy
			>III	Hardware removal/Hemiplateau Elevation etal+ Osteotomy
		>4years		Surgical intervention is not recommended, When there is no growth potential, one-time osteotomy is feasible
Late-onset	Juvenile(4-10years)			There is no definite treatment plan, and the same as above is recommended
	Adolescent(>10years)	Growth potential≥2years		Hemiepiphyseodesis
		Growth potential<2years	Tibial varus <15°	Acute corrective osteotomy
			Tibial varus >15°	Gradual corrective osteotomy

varus deformity under 15° (18). Literature also suggests that hemiepiphyseodeses procedures should be considered when the patient's growth potential is ensured for a minimum of 2–4 years, and the medial epiphyseal plate is still open and functional. Even if a recurrence transpires, remedial measures remain accessible (40, 41). In recent years, the tension band plate (TBP) has been predominantly utilized in surgery, considerably reducing the risk of postoperative complications compared to previously used transphyseal screws or staples (25, 42). This approach does not damage the original bone structure, ensuring minimal invasiveness. If orthopedic failure occurs, osteotomy can be selected as the final resort.

Osteotomy represents a definitive surgical intervention aimed at rectifying patients' deformities, encompassing both acute and gradual corrective procedures. This surgical technique is particularly effective in addressing three-dimensional deformities in the lower extremities. Various osteotomy methods exist including open-wedge, close-wedge, oblique, dome, serrated, and inclined osteotomies, each boasting unique advantages (7). Notably, the prognosis for patients is relatively consistent across these methods. Gradual correction via osteotomy has been found to provide superior correction effects with fewer complications as compared to acute correction (43). Techniques such as the monolateral L-shaped lock, the Ilizarov apparatus, and Taylor Spatial Frame (TSF) are employed for external fixation, allowing for the gradual adjustment and restoration of normal lower limb anatomy. Despite extending the healing time, this method reduces the incidence of complications such as common peroneal nerve paralysis and osteofascial compartment syndrome (44). Previous studies suggest that acute correction is the preferred method when tibial varus is less than 15°, due to its lower trauma and cost implications. For more severe cases, gradual correction via external fixation is recommended. The most recent research underscores the relevance of bone maturity in patients with Blount's disease in informing surgical correction strategies. The discrepancy between bone age and chronological age narrows with growth, impacting the severity of lower limb deformities and the necessary corrective measures. A regression study found that the bone age in 33 children with Blount's disease was advanced by an average of 16 months (26 months in the early-onset group and 10 months in the late-onset group) (45). Therefore, a re-evaluation of preoperative bone age should be considered when treating children with Blount's disease to facilitate the planning of an appropriate surgical technique, ultimately enabling effective deformity correction. At present, the study does have some limitations, the correction of deformity is mostly evaluated from both coronal and sagittal directions, and the adjustment of tibial rotation deformity has not been clearly studied. At present, there are some limitations in the study. The correction of deformity is mostly evaluated from both coronal and sagittal directions, while the adjustment of tibial rotation deformity has not been clearly studied.

The patient of this study was not given a clear diagnosis at the time of the initial visit. If orthopedic braces or necessary surgical treatment had been given in time, a one-time clinical cure might have been achieved. The patient first underwent an osteotomy at the age of seven. However, a recurrence occurred a year post-operation, necessitating a second internal fixation osteotomy at a different hospital. Despite this, the patient still exhibited a certain degree of varus deformity. The patient underwent several surgical procedures during this time, but postoperative recurrence was perhaps unavoidable due to the potential for continued growth of the patient's unclosed epiphyseal plate. By the age of 20, when the epiphyses were fully closed and the bones fully matured, a final external fixation osteotomy was performed to achieve complete correction. Therefore, within this developmental stage from rapid growth to epiphyseal maturation, a sequence of traditional osteotomies and fixations appears unable to achieve desired surgical outcomes, often resulting in relapse or incomplete orthopedic results. This process can substantially increase both the physical trauma and financial burden on patients, indicating that traditional osteotomy may not be an ideal choice during this stage of patient growth and development, especially when the epiphysis has not yet closed.

Conclusion

Consequently, the anomalous proliferation rate of the medial and lateral epiphyses in Blount's disease patients invariably results in recurrent tibial varus. Thus, in early-onset Blount's disease, prompt detection and treatment are paramount: osteotomy should be administered as soon as practicable when non-invasive treatments prove ineffective in patients below four years old, and a combined surgical approach should be timely considered in cases that are at or above Langenskiöld stage III. For patients who are older than four years or fall within the juvenile age range (4–10 years) but exhibit negligible growth potential, a single-instance osteotomy is performed. Adolescents (>10 years) with considerable growth potential are recommended to undergo hemiepiphysiodesis in conjunction with osteotomy upon maturity of epiphyseal closure (Table 2).

Data availability statement

The original contributions presented in the study are included in the article/Supplementary Material. Further inquiries can be directed to the corresponding author.

Ethics statement

The studies involving humans were approved by 960th Hospital of PLA, Jinan, China. The studies were conducted in accordance with the local legislation and institutional requirements. Written informed consent for participation in this study was provided by the participants' legal guardians/next of kin. Written informed consent was obtained from the individual(s) for the publication of any potentially identifiable images or data included in this article.

Author contributions

BW: Data curation, Writing – review & editing. ZM: Data curation, Formal Analysis, Supervision, Writing – original draft, Writing – review & editing. XY: Supervision, Writing – review & editing. KeZ: Supervision, Writing – review & editing. NL: Supervision, Writing – review & editing. KaZ: Supervision, Writing – review & editing. SZ: Supervision, Writing – review & editing. HS: Supervision, Validation, Visualization, Writing – review & editing.

Funding

The author(s) declare that no financial support was received for the research and/or publication of this article.

Conflict of interest

The authors declare that the research was conducted in the absence of any commercial or financial relationships that could be construed as a potential conflict of interest.

Generative AI statement

The author(s) declare that no Generative AI was used in the creation of this manuscript.

Publisher's note

Supplementary material

The Supplementary Material for this article can be found online at: https://www.frontiersin.org/articles/10.3389/fendo.2025.1547679/full#supplementary-material

References

1. Thompson GH, Carter JR. Late-onset tibia vara (Blount's disease). *Curr concepts Clin Orthop Relat Res.* (1990) 255:24–35. doi: 10.1097/00003086-199006000-00004

2. Sabharwal S. Blount disease. *J Bone Joint Surg Am.* (2009) 91:1758–76. doi: 10.2106/JBJS.H.01348

3. Chandankere V, Reddy MV, Reddy AVG. Outcomes of late-stages infantile Blount's disease managed by acute single stage: medial hemi-plateau elevation and metaphyseal osteotomy. Eight case series. *J Pediatr Orthop B.* (2024) 33:560–7. doi: 10.1097/BPB.0000000000001143

4. Miraj F, Karda IWAM, Erwin US, Pratama IK. Can acute correction with simultaneous hemiepiphysiodesis of lateral proximal tibia physis prevent recurrence in neglected infantile Blount's disease? *Eur J Orthop Surg Traumatol.* (2024) 34:529–37. doi: 10.1007/s00590-023-03699-4

5. Mare PH, Marais LC. Gradual deformity correction with a computer-assisted hexapod external fixator in blount's disease. *Strategies Trauma Limb Reconstr.* (2022) 17:32–7. doi: 10.5005/jp-journals-10080-1549

6. Assan BR, Simon AL, Adjadohoun S, Segbedji GGP, Souchet P, Metchioungbe CS, et al. Guided growth vs.Tibial osteotomy at early stage of Blount disease in squelletically immature patients. *J Orthop.* (2021) 25:140–4. doi: 10.1016/j.jor.2021.05.006

7. Baraka MM, Hefny HM, Mahran MA, Fayyad TA, Abdelazim H, Nabil A. Single-stage medial plateau elevation and metaphyseal osteotomies in advanced-stage Blount's disease: a new technique. *J Child Orthop.* (2021) 15:12–23. doi: 10.1302/1863-2548.15.200157

8. Nada AA, Hammad ME, Eltanahy AF, Gazar AA, Khalifa AM, El-Sayed MH. Acute correction and plate fixation for the management of severe infantile blount's disease: short-term results. *Strategies Trauma Limb Reconstr.* (2021) 16:78–85. doi: 10.5005/jp-journals-10080-1527

9. Zein AB, Elhalawany AS, Ali M, Cousins GR. Acute correction of severe complex adolescent late-onset tibia vara by minimally invasive osteotomy and simple circular fixation: a case series with 2-year minimum follow-up. *BMC Musculoskelet Disord.* (2021) 22:681. doi: 10.1186/s12891-021-04496-y

10. Griswold BG, Shaw KA, Houston H, Bertrand S, Cearley D. Guided growth for the Treatment of Infantile Blount's disease: Is it a viable option? *J Orthop.* (2020) 20:41–5. doi: 10.1016/j.jor.2020.01.007

11. Musikachart P, Eamsobhana P. Do different tibial osteotomy techniques affect sagittal alignment in children with blount disease? *Orthop Surg.* (2020) 12:770–5. doi: 10.1111/os.12674

12. Bolliet MP, Bovid KM, Bauler LD. Guided growth with hemiplateau elevation as an alternative to epiphysiodesis for treatment of a young patient with advanced infantile blount disease: A case report. *JBJS Case Connect.* (2020) 10:e1900643. doi: 10.2106/JBJS.CC.19.00643

13. Danino B, Rödl R, Herzenberg JE, Shabtai L, Grill F, Narayanan U, et al. The efficacy of guided growth as an initial strategy for Blount disease treatment. *J Child Orthop.* (2020) 14:312–7. doi: 10.1302/1863-2548.14.200070

14. Miraj F, Ajiantoro, Arya Mahendra Karda IW. Step cut "V" osteotomy for acute correction in Blount's disease treatment: A case series. *Int J Surg Case Rep.* (2019) 58:57–62. doi: 10.1016/j.ijscr.2019.03.044

15. Jain MJ, Inneh IA, Zhu H, Phillips WA. Tension band plate (TBP)-guided hemiepiphysiodesis in blount disease: 10-year single-center experience with a systematic review of literature. *J Pediatr Orthop.* (2020) 40:e138–43. doi: 10.1097/BPO.0000000000001393

16. Terjesen T, Anticevic D. Blount's disease successfully treated with intraepiphyseal osteotomy with elevation of the medial plateau of the tibia-a case report with 65 years' follow-up. *Acta Orthop.* (2018) 89:699–701. doi: 10.1080/17453674.2018.1516179

17. Tsibidakis H, Panou A, Angoules A, Sakellariou VI, Portinaro NM, Krumov J, et al. The role of taylor spatial frame in the treatment of blount disease. *Folia Med (Plovdiv).* (2018) 60:208–15. doi: 10.1515/folmed-2017-0082

18. Funk SS, Mignemi ME, Schoenecker JG, Lovejoy SA, Mencio GA, Martus JE. Hemiepiphysiodesis implants for late-onset tibia vara: A comparison of cost, surgical success, and implant failure. *J Pediatr Orthop.* (2016) 36:29–35. doi: 10.1097/BPO.0000000000000388

19. Liu J, Cao L, Guo SF, Xue W, Chen ZX, Tai HP, et al. Melt-metaphyseal and diphyseal osteotomy for correction of infantile Blount's disease: a long-term follow-up study. *Int J Clin Exp Med.* (2015) 8:2480–3.

20. Sabharwal S, Zhao C, Sakamoto SM, McClemens E. Do children with Blount disease have lower body mass index after lower limb realignment? *J Pediatr Orthop.* (2014) 34:213–8. doi: 10.1097/BPO.0b013e3182a11d59

21. Eamsobhana P, Kaewpornsawan K, Yusuwan K. Do we need to do overcorrection in Blount's disease? *Int Orthop.* (2014) 38:1661–4. doi: 10.1007/s00264-014-2365-3

22. Abdelgawad AA. Combined distal tibial rotational osteotomy and proximal growth plate modulation for treatment of infantile Blount's disease. *World J Orthop.* (2013) 4:90–3. doi: 10.5312/wjo.v4.i2.90

23. Oto M, Yılmaz G, Bowen JR, Thacker M, Kruse R. Adolescent Blount disease in obese children treated by eight-plate hemiepiphysiodesis. *Eklem Hastalik Cerrahisi.* (2012) 23:20–4. doi: 10.3109/03008207.2011.636160

24. Putzeys P, Wilmes P, Merle M. Triple tibial osteotomy for the correction of severe bilateral varus deformity in a patient with late-onset Blount's disease. *Knee Surg Sports Traumatol Arthrosc.* (2013) 21:731–5. doi: 10.1007/s00167-012-2061-z

25. Kawu AA, Salami OO, Olawepo A, Ugbeye MA, Yinusa W, Odunubi OO. Outcome analysis of surgical treatment of Blount disease in Nigeria. *Niger J Clin Pract*. (2012) 15:165–7. doi: 10.4103/1119-3077.97340

26. Sabharwal S, Lee J Jr, Zhao C. Multiplanar deformity analysis of untreated Blount disease. *J Pediatr Orthop*. (2007) 27:260–5. doi: 10.1097/BPO.0b013e31803433c3

27. Banwarie RR, Hollman F, Meijs N, Arts JJ, Vroemen P, Moh P, et al. Insight into the possible aetiologies of Blount's disease: a systematic review of the literature. *J Pediatr Orthop B*. (2020) 29:323–36. doi: 10.1097/BPB.0000000000000677

28. Chkili S, Simoni P. Blount disease. *J Belg Soc Radiol*. (2021) 105:51. doi: 10.5334/jbsr.2557

29. Langenskioeld A, Riska EB. Tibia vara (Osteochondrosis deformans tibiae): a survey of seventy-one cases. *J Bone Joint Surg*. (1964) 46:1405–20. doi: 10.2106/00004623-196446070-00002

30. Richards BS, Katz DE, Sims JB. Effectiveness of brace treatment in early infantile Blount's disease. *J Pediatr Orthop*. (1998) 18:374–80. doi: 10.1097/01241398-199805000-00020

31. Inaba Y, Saito T, Takamura K. Multicenter study of Blount disease in Japan by the Japanese Pediatric Orthopaedic Association. *J Orthop Sci*. (2014) 19:132–40. doi: 10.1007/s00776-013-0489-8

32. Janoyer M. Blount disease. *Orthopaedics Traumatology: Surg Res*. (2019) 105: S111–21. doi: 10.1016/j.otsr.2018.01.009

33. Herring JA. Genu varum. In: *Tachdjian's pediatric orthopedics, 3rd ed*. Saunders Press, Philadelphia (2002). p. 839–55.

34. Pheddy P, Siregar PU. Osteotomy for deformities in blount disease: A systematic review. *J Orthopaedics*. (2016) 13:207–9. doi: 10.1016/j.jor.2015.03.003

35. Ferriter P, Shapiro F. Infantile tibia vara: factors affecting outcome following proximal tibia osteotomy. *J Pediatr Orthop*. (1987) 7:1–7. doi: 10.1097/01241398-198701000-00001

36. Andrade N, Johnston CE. Medial epiphysiolysis in severe infantile tibia vara. *J Pediatr Orthop*. (2006) 26:652–8. doi: 10.1097/01.bpo.0000230338.03782.75

37. Burghardt RD, Specht SC, Herzenberg JE. Mechanical failures of eight-plateguided growth system for temporary hemiepiphysiodesis. *J Pediatr Orthop*. (2010) 30:594–7. doi: 10.1097/BPO.0b013e3181e4f591

38. van Huyssteen AL, Hastings CJ, Olesak M, Hoffman EB. Double-elevating osteotomy for late-presenting infantile Blount's disease: the importance of concomitant lateral epiphysiodesis. *J Bone Joint Surg Br*. (2005) 87:710–5. doi: 10.1302/0301-620X.87B5.15473

39. Park SS, Gordon JE, Luhmann SJ, Dobbs MB, Schoenecker PL. Outcome of hemiepiphyseal stapling for late-onset tibia vara. *J Bone Joint Surg Am*. (2005) 87:2259–66. doi: 10.2106/JBJS.C.01409

40. de Pablos J, Arbeloa-Gutierrez L, Arenas-Miquelez A. Update on treatment of adolescent Blount disease. *Curr Opin Pediatr*. (2018) 30:71–7. doi: 10.1097/MOP.0000000000000569

41. Birch JG. Blount disease. *J Am Acad Orthopaedic Surgeons*. (2013) 21:408–18. doi: 10.5435/JAAOS-21-07-408

42. Stevens PM. Guided growth: 1933 to the present. *Strategies Trauma Limb Reconstruction*. (2006) 1:29–35. doi: 10.1007/s11751-006-0003-3

43. Feldman DS, Madan SS, Ruchelsman DE, Sala DA, Lehman WB. Accuracy of correction of tibia vara: acute versus gradual correction. *J Pediatr Orthop*. (2006) 26:794–8. doi: 10.1097/01.bpo.0000242375.64854.3d

44. Gilbody J, Thomas G, Ho K. Acute versus gradual correction of idiopathic tibia vara in children: a systematic review. *J Pediatr Orthop*. (2009) 29:110–4. doi: 10.1097/BPO.0b013e31819849aa

45. Sabharwal S, Sakamoto SM, Zhao C. Advanced bone age in children with Blount disease: a case-control study. *J Pediatr Orthop*. (2013) 33:551–7. doi: 10.1097/BPO.0b013e318285c524

frontiers | Frontiers in Endocrinology

TYPE Review
PUBLISHED 17 April 2025
DOI 10.3389/fendo.2025.1517840

OPEN ACCESS

EDITED BY
Federico Baronio,
IRCCS AOU S.Orsola-Malpighi, Italy

REVIEWED BY
Mariateresa Falco,
Ospedali Riuniti San Giovanni di Dio e Ruggi d'Aragona, Italy
Niladri Das,
Nil Ratan Sircar Medical College and Hospital, India

*CORRESPONDENCE
Afaf Alsagheir
ASagheir@kfshrc.edu.sa
Bassam Bin-Abbas
b.binabbas@gmail.com

RECEIVED 27 October 2024
ACCEPTED 02 April 2025
PUBLISHED 17 April 2025

CITATION
Alsagheir A, Alhuthil R, Alissa AT, Joueidi F, Sayed AG, Al-Amoudi W, Alabdulhadi AS and Bin-Abbas B (2025) Pycnodysostosis: a case series of eight Saudi patients with cathepsin K gene mutation and a literature review. *Front. Endocrinol.* 16:1517840. doi: 10.3389/fendo.2025.1517840

Pycnodysostosis: a case series of eight Saudi patients with cathepsin K gene mutation and a literature review

Afaf Alsagheir[1*], Raghad Alhuthil[1], Ahmad T. Alissa[2], Faisal Joueidi[2], Ahmed G. Sayed[2], Waleed Al-Amoudi[2], Alanoud S. Alabdulhadi[2] and Bassam Bin-Abbas[1,2*]

[1]Department of Pediatrics, King Faisal Specialist Hospital and Research Centre, Riyadh, Saudi Arabia, [2]College of Medicine, Alfaisal University, Riyadh, Saudi Arabia

Pycnodysostosis, a rare osteopetrosis subtype, is mainly caused by homozygous or compound heterozygous biallelic pathogenic mutation of the cathepsin K (*CTSK*) gene. The cohort included eight patients (four males and four females) with a mean current age of 13 years (SD ± 3.6) and a mean age at diagnosis of 5 years (SD ± 2). All patients had a positive family history of pycnodysostosis and were born to consanguineous parents. Genetic analysis revealed that all individuals carried the same mutation: *NM_000396.3(CTSK):c.244-29A>G*. Clinically, they exhibited characteristic craniofacial features and skeletal deformities consistent with the diagnosis. Bone fractures were reported in 7 out of 8 patients, highlighting a significant clinical burden. All affected individuals received growth hormone therapy(GHT), though response to treatment varied among the group. These findings emphasize the importance of early genetic screening, particularly in families with a known history of pycnodysostosis, to enable timely diagnosis and intervention. Although pycnodysostosis is typically described as a nonprogressive skeletal dysplasia, the presence of complications such as osteomyelitis and recurrent fractures may contribute to a more complex and progressive clinical course in some patients.

KEYWORDS

***CTSK* gene, osteopetrosis, skeletal deformities, osteomyelitis, bone fracture**

1 Introduction

Pycnodysostosis, a rare osteopetrosis subtype, was first described by Albers-Schönberg in the 20th century (1). It is mainly caused by a homozygous or compound of heterozygous biallelic pathogenic mutation of the cathepsin K (*CTSK*) gene (2). *CTSK* is a membrane papain-cysteine protease family that encodes polypeptide chain 329 amino acids in chromosome 1q2 (3). It contains a three-dimensional structure with typical papain-like folds comprising L and R domains, with a cleft between the catalytic sites (4). *CTSK* forms a

molecular complex with glycosaminoglycans, representing the collagenolytically active form of protease. In the presence of chondroitin sulfate, this complex arranges into bead-like structures along a strand-like organization that activates the substrate binding site (4). Highly expressive in osteoclasts, *CTSK* regulates bone resorption and osteoclast remodeling (3). Although the pycnodysostosis incidence rate is unknown, studies suggest approximately 1–1.7 cases per million births, with high consanguinity rates contributing to the disease's etiological manifestation (5).

The clinical features of pycnodysostosis present with various systemic skeletal and dental abnormalities, including short stature, facial dysmorphology, maxillary and mandibular hypoplasia, polydactyly, and brachydactyly (1, 6). Truncal deformities comprise scoliosis, kyphosis, and recurrent chest infections (6). Dental features include delayed eruption of permanent teeth, retained deciduous dentition, malposed teeth, narrow and grooved palate, enamel hypoplasia, and abnormal tooth morphology (2, 5). Other systemic manifestations include laryngomalacia, stridor, sleep apnea, and dental manifestations (1). Although pycnodysostosis pathophysiology remains unclarified, studies suggest the involvement of a genetic enzyme encoding *CTSK, which* disrupts and impairs normal osteoclast-mediated bone resorption, resulting in osteosclerosis (2, 5). Low levels or deficiency of *CTSK* causes alterations in lysosomal cysteine protease activity, which can decrease osteoclast expression and impair bone turnover. This disruption affects bone resorption and remodeling, potentially leading to systemic osteosclerosis (3, 5, 7).

Pycnodysostosis diagnosis is established during infancy based on detailed history and physical examination, clinical presentation, radiological investigations, and genetic analysis (8). Its management is nonspecific. However, conservative management such as growth hormones, a multidisciplinary approach including psychiatrists, orthopedic surgeons, and pediatricians, and genetic early screening in families with a history of pycnodysostosis is essential to establish better outcomes (2, 8, 9). The disease is considered nonprogressive in nature, but several complications, including osteomyelitis and bone fracture, may alter the progressiveness of such cases (2).

2 Methods

This retrospective case series research involved eight cases of pycnodysostosis currently receiving care at endocrinology clinics at King Faisal Specialist Hospital and Research Center (KFSHRC) in Riyadh, Saudi Arabia. Data retrieval occurred in December 2023 from our electronic records medical system and included both pediatric and adult patients. Individuals without available genetic testing data were excluded. The study documented patients' demographics, medical history, presentations, management, and investigative results.

Genetic testing was conducted as part of routine clinical practice using DNA extraction from peripheral blood samples, and whole-exome sequencing was carried out at the Molecular Diagnostic Laboratory of the Clinical Genomic Department Center for Genomic Medicine at KFSHRC.

This study was cleared and approved by the Ethics Committee at King Faisal Specialist Hospital and Research Center (No. 2245443). A waiver of consent was granted from the ethics committee, given the retrospective nature of the study.

3 Results

Patient's demographics and presentations are summarized in Tables 1, 2.

3.1 Case 1

A 12-year-old male, referred as a case of pycnodysostosis at the age of six, presented with short stature. At baseline, his height was 102.8 cm (SD −3.17) and his weight was 16.5 kg. His medical history was notable for a congenital heart defect—ventricular septal defect—which was discovered incidentally and surgically corrected. He was born at full term via spontaneous vaginal delivery and exhibited normal cognitive development and age-appropriate developmental milestones. On general examination, the patient was alert and oriented. Craniofacial and skeletal examination revealed dysmorphic features including frontal prominence, prominent eyes, blue sclera, and loosening of the mandibular angle. He also had short, broad hands and fingers, irregular and crowded teeth, and pectus carinatum. The remainder of his systemic examination was unremarkable. Laboratory investigations showed a serum calcium of 2.56 mmol/L, phosphate of 1.24 mmol/L, alkaline phosphatase of 237 IU/L, and a baseline IGF-1 of 120 ng/mL (as shown in Table 3). A full skeletal survey demonstrated features consistent with sclerotic dysplasia, including delayed skeletal maturation and diffuse osteosclerosis. Skull X-ray confirmed loosening of the mandibular angle, while spinal imaging showed a generalized increase in vertebral bone density. Radiographs of the pelvis and lower limbs showed diffuse metaphyseal sclerosis, and X-rays of the upper limbs revealed terminal phalangeal hypoplasia. A chest X-ray demonstrated bilateral clavicular hypoplasia. Following the confirmation of pycnodysostosis based on clinical, radiological, and genetic test, the patient was given a trial of recombinant human growth hormone (rhGH) therapy at a dose of 35 mcg/kg/day. Despite good adherence, there was no significant growth response to therapy (see Table 4). At final follow-up, his height reached 125.5 cm (SD −2.79) with a weight of 25.3 kg.

3.2 Case 2

A 17-year-old male was referred for evaluation of short stature and growth failure. He was previously diagnosed with pycnodysostosis at the age of seven and had a history of obstructive lung disease, for which he was being treated with montelukast (Singulair) and fluticasone/salmeterol (Seretide). At

10.3389/fendo.2025.1517840

TABLE 1 Demographics & genetic test information.

#	Family	Sex	Current Age	Age at diagnosis	Region	Mutation	ACMG classification	Zygosity	Family history	Consanguinity
1	Fam-1	M	12 years	6 years	AlDamam	NM_000396.3 (CTSK): c.244-29A>G	LP	Homo	+ve	yes
2	Fam-1	M	17 years	7 years	AlDamam	NM_000396.3 (CTSK): c.244-29A>G	LP	Homo	+ve	yes
3	Fam-2	F	15 years	3 years	Alqassim, Buridah	NM_000396.3 (CTSK): c.244-29A>G	LP	Homo	+ve	yes
4	Fam-3	M	12 years	3 years	Alqassim, Buridah	NM_000396.3 (CTSK): c.244-29A>G	LP	Homo	+ve	yes
5	Fam-4	F	7 years	4 years	Almadinah	NM_000396.3 (CTSK): c.244-29A>G	LP	Homo	+ve	yes
6	Fam-4	F	14 years	7 years	Almadinah	NM_000396.3 (CTSK): c.244-29A>G	LP	Homo	+ve	yes
7	Fam-4	F	16 years	3 years	Almadinah	NM_000396.3 (CTSK): c.244-29A>G	LP	Homo	+ve	yes
8	Fam-5	M	16 years	8 years	Almadinah	NM_000396.3 (CTSK): c.244-29A>G	LP	Homo	+ve	yes

M, male; F, female; ACMG, American College of Medical Genetics, LP, Likely pathogenic; +ve, positive; Homo, Homozygous.

presentation, his baseline height was 92 cm (SD −3.19) and his weight was 13.4 kg. He was born at full term via spontaneous vaginal delivery and demonstrated normal cognitive development with appropriate developmental milestones. On general examination, the patient was alert and oriented. Head and neck examination revealed dysmorphic features, while the remainder of the systemic examination was unremarkable. Laboratory investigations revealed a calcium level of 2.44 mmol/L, phosphate 1.58 mmol/L, alkaline phosphatase 267.1 IU/L, and a baseline IGF-1 of 100 ng/mL (refer to Table 3). Radiological evaluation revealed normal bone age without overt osteosclerosis. A skull X-ray demonstrated loosening of the mandibular angle and dolichocephaly. Chest imaging revealed generalized increased bone density and hypoplasia of the lateral aspects of the clavicles. A pelvic X-ray also showed generalized osteosclerosis. X-rays of the upper and lower limbs showed hypoplasia and fragmentation of the distal phalanges, particularly involving the right thumb, middle, and ring fingers, as well as the left thumb and middle finger. Additionally, an old, healed fracture was noted in the diaphysis of the right tibia, with evidence of partial periosteal and cortical callus

TABLE 2 Presentations.

#	Family	Deformities	Distinctive facial features	Fractures	Pseudotumor cerbri	Cognitive development	Clavicular dysplasia	Ostesclorosis	BMD z-score if done
1	Fam-1	yes	yes	yes	no	normal	no	yes	not done
2	Fam-1	yes	yes	yes	no	normal	yes	yes	not done
3	Fam-2	yes	yes	yes	yes, treated with acetazolamide	normal	not documented	yes	not done
4	Fam-3	yes	yes	yes	no	normal	no	yes	2.4
5	Fam-4	yes	yes	yes	not documented	normal	not documented	yes	not done
6	Fam-4	yes	yes	No	yes	normal	no	yes	not done
7	Fam-4	yes	yes	yes	no	normal	no	yes	not done
8	Fam-5	yes	yes	yes	no	normal	yes	yes	3.7

10.3389/fendo.2025.1517840

TABLE 3 Growth and biochemical data.

#	Family	Baseline height cm	Baseline height SDS	Last height cm	Last height SDS	growth velocity	ALP (Ref.: 100-300 U/L	Ca (Ref.: 2.10-2.60 mmol/L)	Phosphate (Ref.: 1.00-1.75 mmol/L)	1GF1 ng/mL
1	Fam-1	102.8	-3.17	125.5*	-3.79	4	237	1.24	0.87	120
2	Fam-1	92	–3.19	152*	-3.15	6	267	2.44	1.58	100
3	Fam-2	92.2	-1.59	141*	-3.3	5.6	280.1	2.34	1.52	135
4	Fam-3	85.3	-2.79	132.5	-2.65	6.72	278	2.45	1.75	123
5	Fam-4	95	-5.03	95	-5.6	not documented	not documented	not documented	not documented	not documented
6	Fam-4	102.5	-5.16	118.4*	-4.67	5.6	146.4	2.36	1.67	108
7	Fam-4	76	-5.74	110*	-8.2	2.5	1,280	2.23	0.65	106
8	Fam-5	107	-4.5	146.5*	-3.61	4.7	139.7	2.32	1.34	166

AL, alkaline phosphate; SDS, standard deviation score; Ref., Reference range.
*Final height.

formation. Following confirmation of the diagnosis, the patient was given a trial of recombinant human growth hormone (rhGH) therapy at a dose of 35 mcg/kg/day. He demonstrated good compliance and a positive response to treatment, with an observed growth velocity of 2.3 cm/year. At final follow-up, his height had reached 152 cm (SD −3.15).

3.3 Case 3

A 15-year-old female presented with short stature, skeletal dysplasia, and a 4-month history of headaches. Her medical history was significant for multiple recurrent midshaft fractures of the left tibia (three episodes) and a diagnosis of pseudotumor cerebri at age seven, for which she was treated with acetazolamide (Diamox) 125 mg. She was delivered at term via spontaneous vaginal delivery and had normal cognitive development and achievement of developmental milestones. On physical examination her baseline, height was 92.2 cm (SD −1.59) and weight 11.6 kg, she was alert and oriented. Ophthalmologic evaluation revealed papilledema, while the remainder of her systemic examination was unremarkable. Laboratory findings showed: Calcium: 2.34 mmol/L, Phosphate: 1.52 mmol/L, Alkaline phosphatase: 280.1 IU/L, baseline IGF-1: 135 ng/ml. Imaging studies revealed characteristic skeletal abnormalities consistent with a diagnosis of pycnodysostosis. Skull X-ray demonstrated generalized increased bone density, the presence of intrasutural wormian bones, hypotelorism, and an obtuse mandibular angle. Spinal imaging identified a pars interarticularis defect at the L5–S1 level. Hand and foot X-rays showed acro-osteolysis involving the distal phalanges, consistent with distal tuft resorption. Based on the constellation of clinical presentation, biochemical parameters, and radiological findings, a diagnosis of pycnodysostosis was confirmed. The patient was started on recombinant human growth hormone (rhGH) therapy at a dose of 35 mcg/kg/day. Despite documented adherence to treatment, no significant improvement in growth velocity was observed over the treatment period (see Table 4). Her pseudotumor cerebri resolved with acetazolamide therapy and notably did not recur following initiation of GHT. At her most recent follow-up, she had achieved a final height of 141 cm (SD −2.07).

3.4 Case 4

A 12-year-old boy was referred for evaluation of developmental delay and short stature. He was noted to have a large head, prompting a CT scan at a local hospital, which was reported as normal. At presentation, his height measured 85.3 cm (SD −2.79) and his weight was 13.5 kg. His past medical history included a diagnosis of pseudotumor cerebri at the age of ten, for which he was treated with acetazolamide 250 mg. The patient also reported ongoing bone and knee pain, frequent headaches, and episodes of sleep apnea. Despite these complaints, his cognitive development was appropriate for age, and he began walking at 15 months. However, a speech delay was noted during early childhood. On physical examination, the patient was alert and oriented. Head and neck examination revealed multiple dysmorphic features, including macrocephaly, a prominent nose, absence of the mandibular angle, grooved and fragile nails, wrinkled skin, brachydactyly, an open anterior fontanelle, and crowded teeth. The remainder of the systemic examination was unremarkable. Laboratory evaluation showed a calcium level of 2.45 mmol/L, phosphate level of 1.75 mmol/L, alkaline phosphatase of 278.1 IU/L, and a baseline IGF-1 of 123 ng/mL. Radiological imaging supported the clinical findings. Skull X-ray showed mild microcephaly with increased skull bone density and a persistently open anterior fontanelle. Spine imaging revealed a mild, diffuse increase in bone density involving the cervico-thoraco-lumbosacral vertebrae, along with bilateral hypoplastic clavicles. Pelvic and limb radiographs demonstrated a mild to moderate diffuse increase in bone density. Hand and foot X-rays revealed acro-osteolysis affecting the distal phalanges, and delayed ossification of the carpal bones was also noted. Based on the integration of clinical, biochemical, and radiographic data, a

TABLE 4 Management and outcome.

#	Family	Growth hormone therapy, dose	Compliant to treatment	Treatment response	Complications
1	Fam-1	Yes, 35 mcg/kg/day	yes	poor response	no
2	Fam-1	Yes, 35 mcg/kg/day	yes	poor response	no
3	Fam-2	Yes, 35 mcg/kg/day	yes	poor response	no
4	Fam-3	Yes, 35 mcg/kg/day	yes	poor response	Bone pain, knee pain, headaches, and attacks of sleep apnea
5	Fam-4	Yes, 35 mcg/kg/day	Discontinued After 3 months		Discontinued GH by family, due to side effect (headache).
6	Fam-4	Yes, 35 mcg/kg/day	yes	poor response	no
7	Fam-4	Yes, 35 mcg/kg/day	yes	poor response	no
8	Fam-5	Yes, 35 mcg/kg/day	yes	Beneficial	hip pain, stopped for two weeks then continued

diagnosis of pycnodysostosis was established. The patient was started on recombinant human growth hormone therapy (rhGH) at a dose of 35 mcg/kg/day. Despite adherence to therapy, no significant improvement in linear growth was observed. Notably, the patient's pseudotumor cerebri improved significantly following the initiation of with acetazolamide and has not recurred while on GHT.

3.5 Case 5

A 7-year-old female was referred to the outpatient clinic for evaluation of short stature and faltering growth. At presentation, her baseline height measured 95 cm (SD −5.03) and her weight was 13.75 kg. The patient had a history of multiple recurrent fractures, involving the scapula, tibia, and vertebrae. Family history was significant for first-degree parental consanguinity. She was born at term via spontaneous vaginal delivery, and her cognitive development and developmental milestones were within normal limits. On physical examination, the patient was alert and oriented. Craniofacial examination revealed several dysmorphic features, including frontal bossing, broad nasal bridge, hypertelorism, retrognathia, and brachycephaly. Other systemic examinations were unremarkable. Following confirmation of the diagnosis of pycnodysostosis, The patient was started on recombinant human growth hormone therapy (rhGH) at a dose of 35 mcg/kg/day. Although she was compliant with therapy, she developed headaches and was later diagnosed with atrial fibrillation during the course of treatment (see Table 4). These adverse events were considered potential side effects of therapy and prompted further clinical evaluation and monitoring.

3.6 Case 6

A 14-year-old female presented to the pediatric endocrinology clinic with history of growth failure and short stature. At the time of presentation, her baseline height was 102.5 cm and weight was 16.1 kg. Her medical history was notable for chronic snoring and episodes of apnea during sleep, in addition to a prior diagnosis of pseudotumor cerebri at the age of 10 years, which had been managed with acetazolamide. Family history revealed first-degree consanguinity and a positive familial history of short stature. She was born full term via spontaneous vaginal delivery (SVD) and demonstrated normal cognitive development and timely achievement of developmental milestones. On physical examination, the patient was alert and oriented with craniofacial dysmorphic features. The remainder of her systemic examination was unremarkable. Laboratory investigations revealed calcium of 2.36 mmol/L, phosphate of 1.67 mmol/L, alkaline phosphatase of 146.4 IU/L, and a baseline IGF-1 level of 108 ng/mL (Table 3). Radiographic evaluation supported the clinical suspicion of skeletal dysplasia. Skull X-ray showed a widely persistent open suture line, most prominently involving the posterior sagittal and lambdoid sutures. Spinal imaging revealed grade 1 spondylolisthesis of L5/S1 with mild bilateral clavicular hypoplasia. Pelvic X-ray demonstrated generalized osteosclerosis, and X-rays of the upper and lower limbs showed hypoplasia of the distal phalanges, involving both thumbs and index fingers, as well as the left middle finger and right little finger (Figure 1).

Based on clinical, radiological, and genetic findings, a diagnosis of pycnodysostosis was established. The patient was started on recombinant human growth hormone therapy (rhGH) at a dose of 35 mcg/kg/day and no significant response to growth hormone therapy was noted. Her final recorded height was 118 cm (SD −4.67). Notably, her pseudotumor cerebri showed marked improvement with acetazolamide therapy, with no recurrence or worsening during the course of growth hormone treatment.

3.7 Case 7

A 16-year-old female presented to the pediatric clinic with severe short stature, growth retardation, and skeletal dysplasia. At the age of 3 years, her baseline height was 76 cm, and her weight was 8 kg. Her growth velocity was 2.5 cm per year. The patient had a history of recurrent fracture, neonatal diabetes mellitus (on-off

FIGURE 1
Skeletal X-ray of a male patient done at 11-year-old (Case 6) revealing moderate diffuse increased density of the skeletal bones with persistent open skull sutures, and widenings most prominent of the posterior sagittal and lambdoid sutures, anterior fontanelle, and straight mandible angles with abnormal teeth are noted **(a, b)**. Irregularity at the posterior elements of the C2, C3 are seen **(b)**. Spondylolysis /grade 1 spondylolisthesis of L5-S1 **(c)**. Mild to moderately hypoplastic bilateral acetabulae are noted, with 8 mm lateral uncoverage of the right femur head, 12 mm lateral uncoverage of the left femur head seen **(d)**. Prominent tufts resorptions /distal acro-osteolysis of bilateral feet and hands distal phalanges are noted **(e, f)**. Overall Sclerosis and dysplastic skeletal features are compatible with Pycnodysostosis.

hypoglycemic attacks), seizures, and was on insulin for three months, in addition to her menarche (irregular) having persistent hypophosphatemia on phosphate supplements. Neonatal history showed SVD at full term. The patient exhibited normal cognitive development with normal developmental milestones. On general examination, the patient was alert and oriented. Head and neck examination showed dysmorphic features including large ear, high arch palate, multiple oral ulcers, small face and hands, protruded mandible with midface deficiency, and moderate tenderness over the occipital area radiating the neck and upper back associated with blurred vision, which was suggestive of pseudotumor cerebri. Other systemic examinations were unremarkable. Laboratory investigations showed Ca: 2.23, phosphate: 0.65, alkaline phosphatase 1,280 and baseline IGF1 is 106 (Table 3). A skeletal survey revealed an increase in skeleton density, which was suggestive of osteopetrosis. A skull X-ray showed persistent opening in the sagittal suture with abnormal ossification of the calvarium and fusion of the coronal and lambdoid sutures with significant generalized osteopenia. A pelvic X-ray and x-rays of both limbs revealed bilateral subluxation of the hip joint with mild bilateral cox valga, generalized osteopenia, and prominent trabeculation in the bones. Erosion existed in the tuft of the terminal phalanges of the toes. After the diagnosis of pycnodysostosis, the patient's treatment was initiated with human growth hormone therapy (rhGH) at a dose of 35 mcg/kg/day, but she responded poorly to the treatment and his pseudotumor cerebri showed clinical improvement and did not progress during the course of growth hormone therapy.

3.8 Case 8

A 16-year-old boy has been under follow-up in the pediatric endocrinology clinic for short stature since the age of two years. At baseline, his height was 107 cm (SD −4.5), weight was 16.5 kg, and growth velocity was 4.7 cm/year. His medical history included a left forearm fracture at the age of two years and a deviated nasal septum. Family history revealed first-degree parental consanguinity and two maternal uncles with a confirmed diagnosis of pycnodysostosis. He was born full term via spontaneous vaginal delivery and achieved normal developmental milestones with appropriate cognitive development. On general examination, the patient was alert and

oriented. Head and neck examination was notable for moderate adenoid hypertrophy, with no overt dysmorphic features. Laboratory investigations demonstrated calcium of 2.32 mmol/L, phosphate of 1.34 mmol/L, alkaline phosphatase of 139.7 IU/L, and a baseline IGF-1 level of 166 ng/mL. A skeletal survey revealed a generalized increase in bone density, along with multiple wormian bones in the skull and straightening of the mandibular angle (Figure 2). Radiographs also showed mild to moderate resorption of the distal phalanges of both hands and feet, in association with features of skeletal dysplasia. Following a confirmed diagnosis of pycnodysostosis, the patient was initiated on recombinant human growth hormone (rhGH) therapy at a dose of 35 mcg/kg/day. He demonstrated good adherence to the treatment and responded favorably, with his height at the most recent visit reaching 146.5 cm (SD −3.61) and a height velocity of 3.1 cm/year (Figure 3). During treatment, he developed hip pain, which was managed conservatively.

4 Discussion

This single-center study presents the clinical, radiological, and genetic characteristics of eight patients diagnosed with pycnodysostosis and evaluates their response to growth hormone therapy (GHT). Given that the effectiveness of GHT remains a key predictor of clinical improvement, this analysis provides valuable insights into patient-specific outcomes and therapeutic responses.

The papain family of cysteine proteinases includes several phenotypes—B, H, L, S, and K—that are widely expressed in mammalian tissues. Among these, the K phenotype is encoded by the *CTSK* gene, which plays a critical role in bone resorption through its collagenolytic action on type I collagen molecules (10). The *CTSK* gene spans approximately 12 kb and comprises eight exons. To date, 63 mutations have been identified in *CTSK*, including frameshift, nonsense, missense, and splice-site mutations (6).

Among the reported pathogenic variants, *p.Gly180Ser* has been linked to disruption of cathepsin K activity due to its role in enzymatic structure and function. Similarly, mutations affecting the *p.Ala277* residue, located near the protein's active site, are associated with severe phenotypic features. The splice-site mutation *c.244-29A>G*, identified in all patients in our cohort, appears to be regionally clustered, suggesting a potential founder effect (6). Additionally, the *p.Trp2Ter* mutation results in a premature termination codon, which significantly compromises protein function (6).

Functionally, cathepsin K is a major lysosomal cysteine protease in the bone matrix, essential for osteoclast-mediated bone resorption. Deficiency in this enzyme due to *CTSK* mutations leads to osteoclast dysfunction, contributing to the sclerotic and fragile bone phenotype observed in pycnodysostosis (10). The role of *CTSK* in bone homeostasis has also been supported by murine models, where its absence leads to impaired apoptosis of osteoclasts and an increased number of functionally compromised cells (14).

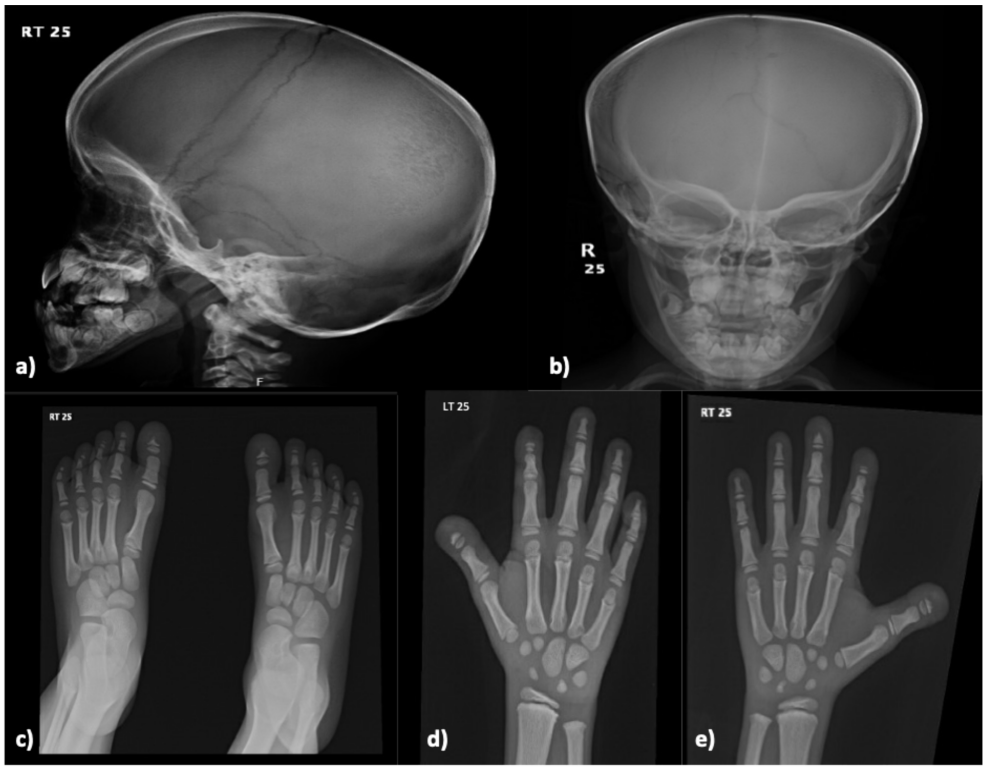

FIGURE 2
Skeletal X-ray of a male patient done at 8-year-old (Case 8) revealing multiple wormian bones identified in the skull with straightening of the mandibular angle **(a, b).** There are mild-to-moderate resorption of the distal phalanges of the hands and feet on both sides **(c–e)**. Findings are consistent with Pycnodysostosis.

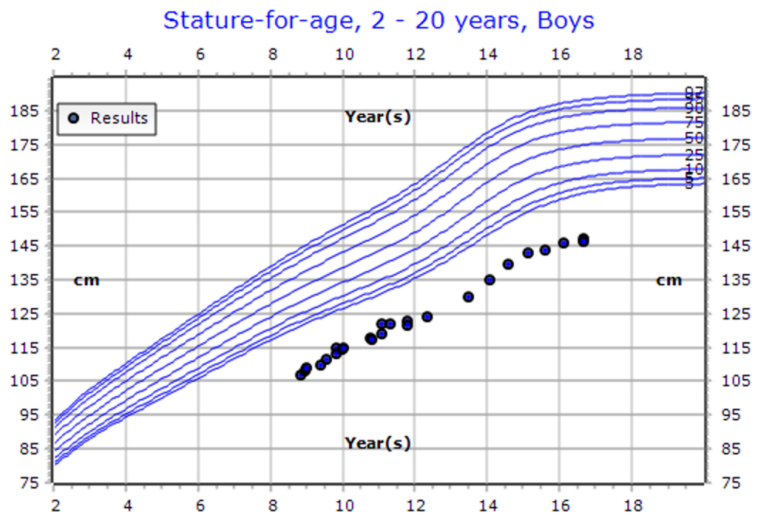

FIGURE 3
CDC Growth chart of a male patient (Case 8). At the presentation (aged 11 years old), his height measured 122 cm (SDS: -3.38, centile: 0.04). At his last visit (aged 16 years old), his height was recorded as 146.5 cm (SDS: -3.61, centile: 0.02). He is currently undergoing growth hormone therapy at a dose of 0.03 mg/kg/day.

Pycnodysostosis was originally described by Maroteaux and Lamy in 1962 as a rare autosomal recessive skeletal dysplasia characterized by distinctive skeletal and dental anomalies (11, 12). The global prevalence is estimated at 1–1.7 cases per million, with a higher frequency reported in consanguineous populations (10, 13).

In our study, all eight patients were homozygous for the *c.244-29A>G* mutation. Clinically, all patients had a positive family history of pycnodysostosis, with most cases arising from first-degree consanguinity. Dysmorphic features, delayed skeletal maturation, and diffuse osteosclerosis were consistent findings. Seven patients experienced recurrent bone fractures, most commonly affecting the scapula, vertebrae, femur, and tibia. Clavicular hypoplasia or dysplasia was observed in five patients, acro-osteolysis in four, osteopetrosis in two, and dental anomalies in two.

Four patients developed pseudotumor cerebri, a known but poorly understood complication in pycnodysostosis, potentially resulting from persistently open cranial sutures and altered cerebrospinal fluid dynamics. While the exact pathophysiology remains unclear, regular ophthalmologic evaluation for signs of raised intracranial pressure is essential (20). For instance, Al Hashmi et al. reported a case of a 13-year-old with visual deterioration due to papilledema, managed successfully with acetazolamide and a ventriculoperitoneal shunt (20).

Radiologically, our findings were consistent with established features of pycnodysostosis, including generalized osteosclerosis, persistent open cranial sutures, clavicular hypoplasia, delayed ossification, and resorption of the distal phalanges (1, 15–17). Dental findings in the literature include enamel hypoplasia, mandibular hypoplasia, hypercementosis, and pulp chamber narrowing (9, 16, 18, 19).

Xue et al. found that short stature was present in 95.9% of patients and increased bone density in 88.7% (19). Similarly, fractures—particularly midshaft fractures of long bones—are among the most common complications, reported in nearly half of affected individuals (2, 15).

Genetic diagnosis is critical for confirming pycnodysostosis, enabling appropriate counseling and guiding management. Molecular testing not only confirms the clinical diagnosis but also allows for investigation of genotype-phenotype correlations. In addition to *CTSK*, genes such as *IL6R* and *MCL1*, located within the same chromosomal region, have been implicated in monocyte/macrophage differentiation and osteoclastogenesis, suggesting a broader genetic landscape influencing disease variability (13, 14).

The clinical features of pycnodysostosis span a range of skeletal and dental manifestations, including osteosclerosis, bone fragility, acro-osteolysis of the distal phalanges, frontal bossing, open fontanelles, mandibular retraction, clavicular anomalies, and skull deformities with delayed suture closure (1, 15–17). Dental abnormalities frequently include enamel hypoplasia, mandibular hypoplasia, and other defects (9, 16, 18, 19).

In our cohort, in addition to the core skeletal phenotype, four patients developed pseudotumor cerebri and one experienced persistent hypophosphatemia. The frequency and diversity of complications underscore the need for comprehensive evaluation and individualized care plans.

The diagnosis of pycnodysostosis relies on a combination of clinical, radiological, and molecular findings. Once confirmed, management must involve a multidisciplinary approach that includes pediatric endocrinology, orthopedics, dentistry, and genetics (21). Genetic counseling is particularly important for families from high-consanguinity backgrounds.

This study confirms that although the phenotypic presentation of pycnodysostosis is relatively consistent, the severity of complications and variability in response to treatment—particularly growth hormone therapy (GHT)—can be significant. GHT has demonstrated promising outcomes in managing growth challenges in pediatric patients with

pycnodysostosis (22). Several studies have reported improvements in disproportionate growth, linear height gains, and a reduction in skeletal complications when GHT is administered (1).While the optimal timing for initiating GHT remains undefined, early treatment appears to mitigate disease progression and reduce the risk of fractures and other complications (23). Soliman et al. found that early GHT leads to increased IGF-1 secretion, enhances osteoclast differentiation, and promotes restoration of linear growth and skeletal proportions, helping patients achieve normal or near-normal stature (22). In contrast, delayed therapy often results in limited efficacy, underscoring the need for early evaluation and intervention in children presenting with reduced growth velocity (17, 22). A recent study reported that five out of six patients achieved a final height exceeding 150 cm following GHT. Similarly, Sulaiman et al. documented near-normal height (−2.25 SDS) after 18 months of therapy, with substantial improvement in long-bone growth and correction of skeletal disproportions, suggesting an excellent response to treatment (Table 5) (22). Despite these encouraging reports, our study demonstrated mixed outcomes. Among the eight patients treated with GHT at a dose of 35 mcg/kg/day, only three showed a positive response with improvements in height, bone density, and growth velocity. Four patients showed poor response and experienced adverse effects such as headache, bone pain, and sleep apnea. Three others showed no measurable response, leading to discontinuation or adjustment of therapy. These findings highlight the variability in GHT response, which may be influenced by the age of initiation, treatment duration, genotype differences, or hormonal sensitivity.

Orthopedic management in pycnodysostosis poses additional challenges due to the inherent bone fragility and sclerotic architecture. Early surgical intervention, including internal plate fixation or intramedullary nailing, may be necessary to address fractures, deformities, or scoliosis and should be tailored to the patient's condition (21). Hald et al. (1), in their review of 27 cases from France, reported a high frequency of fractures, surgical interventions, sleep apnea, and psychomotor delays, further emphasizing the need for GHT and multidisciplinary care, including mental health support (1).

Dental care is also essential. Although none of the patients in our cohort developed severe dental or maxillofacial complications, previous literature reports significant risks. Maintaining oral hygiene, implementing preventive dental strategies, and adopting careful procedural planning are critical due to the risk of mandibular and craniofacial complications (5, 18). For instance, Moroni et al. described a case of mandibular osteonecrosis in a patient with pycnodysostosis, highlighting the susceptibility of these individuals to severe dental and maxillofacial complications, particularly following dental interventions (18).

Thus, this study provides a comprehensive clinical, radiological, and genetic analysis of pycnodysostosis cases, but it has some limitations. The small sample size limits generalizability, and variation in treatment duration, adherence, and response to GHT restricts conclusions regarding its overall benefit. Future studies with larger cohorts and longer follow-up periods are needed to establish standardized protocols for treatment.

5 Conclusion

Pycnodysostosis is a rare skeletal dysplasia primarily associated with consanguineous populations and families. Recent advancements in our understanding have provided valuable insights into pathophysiology, management, and potential therapeutic targets. It requires prompt care from the specialized pediatric team. It is still an expandable entity that integrates complex mechanisms and requires prompt care, follow-up, genetic counseling, and careful observation for the patient's family to reach optimal outcomes for the patient and

TABLE 5 A descriptive summary of reported pycnodysostosis cases in the literature.

Article	Age	Gender	Symptoms	Gene	Management	Complications
Khoja et al. (2015) (5)	13-year-old	Female	Short stature, euryprospic with deficient midface, frontal bossing, suture diastasis, absence of upper incisor with mispositioning of teeth,	–	Cemented upper bonded expander with midline screw expansion	Not reported
Verma et al. (2020) (8)	7-year-old	Female	Short stature, poor weight gain, dysmorphic nails, multiple dental caries and grooved palate, hepatoslenomegaly	Homozygous missense variant CTSK:C.890G>C.	Growth hormone 0.16 mg/kg/week, levothyroxine 50 µg/day	Not reported
Sulaiman & Thalange (2021) (22)	22-month-old	Male	Short stature, failure to thrive, jaundice gaping fontanelle, lumbar lordosis, short limbs	Homozygous frameshift mutation of CTSK gene in exon 4 (c.338delG)	Growth hormone 1 µg/kg/d; 0.5 mg	Not reported
Aynaou et al. (2016) (15)	12-year-old	Female	Short stature, multiple fractures of long bones, dysplastic nails, frontal and occipital bossing, groove palate, impacted and deciduose teeth, maxillary hypoplasia	–	Oral hygiene, psychiatric support	Not reported

future offspring. We recommend multidisciplinary approaches for clinical management alongside the contributions of colleagues, which is crucial for improving outcomes and quality of life.

Author contributions

AA: Conceptualization, Investigation, Validation, Writing – review & editing. RA: Methodology, Visualization, Writing – original draft. AA: Methodology, Visualization, Writing – original draft. FJ: Data curation, Investigation, Writing – original draft. AS: Data curation, Investigation, Writing – original draft. WA: Data curation, Methodology, Writing – original draft. AA: Data curation, Methodology, Writing – original draft. BB: Conceptualization, Investigation, Validation, Writing – review & editing.

Funding

The author(s) declare that no financial support was received for the research and/or publication of this article.

Conflict of interest

The authors declare that the research was conducted in the absence of any commercial or financial relationships that could be construed as a potential conflict of interest.

Generative AI statement

The author(s) declare that no Generative AI was used in the creation of this manuscript.

Publisher's note

References

1. Hald JD, Beck-Nielsen S, Gregersen PA, Gjørup H, Langdahl B. Pycnodysostosis in children and adults. *Bone*. (2023) 169:116674. doi: 10.1016/j.bone.2023.116674

2. Sharma A, Upmanyu A, Parate AR, Kasat VO. Pycnodysostosis-a rare disorder with distinctive craniofacial dysmorphia. A case report. *J Biol Craniofacial Res*. (2021) 11:529–35. doi: 10.1016/j.jobcr.2021.07.006

3. Naeem M, Sheikh S, Ahmad W. A mutation in CTSK gene in an autosomal recessive pycnodysostosis family of Pakistani origin. *BMC Med Genet*. (2009) 10:1–5. doi: 10.1186/1471-2350-10-76

4. Kirschke H, Cathepsin S. *In Handbook of proteolytic enzymes*. United States: Elsevier (2013) p. 1824–30. doi: 10.1016/B978-008055232-3.63060-0

5. Khoja A, Fida M, Shaikh A. Pycnodysostosis with special emphasis on dentofacial characteristics. *Case Rep Dent*. (2015) 2015:817989. doi: 10.1155/2015/817989

6. Mushiba AM, Faqeih E, Saleh MA, Ramzan K, Imtiaz F, Al-Owain M, et al. The genotypic and phenotypic spectrum of pycnodysostosis in Saudi Arabia: Novel variants and clinical findings. *Am J Med Genet Part A*. (2021) 185:2455–63. doi: 10.1002/ajmg.a.62230

7. Dai R, Wu Z, Chu HY, Lu J, Lyu A, Liu J, et al. Cathepsin K: the action in and beyond bone. *Front Cell Dev Biol*. (2020) 8:433. doi: 10.3389/fcell.2020.00433

8. Verma V, Singh RK. A case report of pycnodysostosis associated with multiple pituitary hormone deficiencies and response to treatment. *J Clin Res Pediatr Endocrinology*. (2020) 12:444–9. doi: 10.4274/jcrpe.galenos.2020.2019.0194

9. LeBlanc S, Savarirayan R. Pycnodysostosis. In: Adam MP, Feldman J, Mirzaa GM, Pagon RA, Wallace SE, Bean LJH, Gripp KW, Amemiya A, editors. *GeneReviews®*. University of Washington, Seattle, Seattle (WA (2020). p. 1993–2024.

10. Rantakokko J, Kiviranta R, Eerola R, Aro HT, Vuorio E. Complete genomic structure of the mouse cathepsin K gene (Ctsk) and its localization next to the Arnt gene on mouse chromosome 3. *Matrix Biol*. (1999) 18:155–61. doi: 10.1016/s0945-053x(99)00010-4

11. Maroteaux P, Lamy M. La pycnodysostose. *Presse Med*. (1962) 70:999.

12. Andrrn L, Dymling JF, Hogeman KE, Wendeberg B. Osteopetrosis, acro-osteolytica: A syndrome of osteopetrosis, acro-osteolysis and open sutures of the skull. *Acta Chir Scand*. (1962) 124:496–507.

13. Gelb BD, Edelson JG, Desnick RJ. Linkage of pycnodysostosis to chromosome 1q21 by homozygosity mapping. *Nat Genet*. (1995) 10:235–7. doi: 10.1038/ng0695-235

14. Chen W, Yang S, Abe Y, Li M, Wang Y, Shao J, et al. Novel pycnodysostosis mouse model uncovers cathepsin K function as a potential regulator of osteoclast apoptosis and senescence. *Hum Mol Genet*. (2007) 16:410–23. doi: 10.1093/hmg/ddl474

15. Aynaou H, Skiker I, Latrech H. Short stature revealing a pycnodysostosis: a case report. *J Orthopaedic Case Reports*. (2016) 6:43. doi: 10.13107/jocr.2250-0685.426

16. Rodrigues C, Gomes FA, Arruda JA, Silva L, Álvares P, da Fonte P, et al. Clinical and radiographic features of pycnodysostosis: a case report. *J Clin Exp dentistry*. (2017) 9:e1276. doi: 10.4317/jced.54105

17. Soliman AT, Ramadan MA, Sherif A, Bedair ES, Rizk MM. Pycnodysostosis: clinical, radiologic, and endocrine evaluation and linear growth after growth hormone therapy. *Metabolism-Clinical Experimental*. (2001) 50:905–11. doi: 10.1053/meta.2001.24924

18. Moroni A, Brizola E, Di Cecco A, Tremosini M, Sergiampietri M, Bianchi A, et al. Pathological mandibular fracture complicated by osteonecrosis in an adult patient with pycnodysostosis: Clinical report and review of the literature. *Eur J Med Genet*. (2023) 22:104904. doi: 10.1016/j.ejmg.2023.104904

19. Xue Y, Cai T, Shi S, Wang W, Zhang Y, Mao T, et al. Clinical and animal research findings in pycnodysostosis and gene mutations of cathepsin K from 1996 to 2011. *Orphanet J rare diseases*. (2011) 6:1–0. doi: 10.1186/1750-1172-6-20

20. Hashmi Al, Padidela R, Skae M, Mughal MZ. Raised intracranial pressure in a boy with Pycnodysostosis with open fontanelles. *Bone Abstracts*. (2017) 6. doi: 10.1530/boneabs.6.P072

21. Taka TM, Lung B, Stepanyan H, So D, Yang S. Orthopedic treatment of pycnodysostosis: a systematic review. *Cureus*. (2022) 14(4):e24275. doi: 10.7759/cureus.24275

22. Sulaiman HO, Thalange NK. Pycnodysostosis: a growth hormone responsive skeletal dysplasia. *AACE Clin Case Reports*. (2021) 7:231–5. doi: 10.1016/j.aace.2021.02.006

23. Ünsal Y, Atar S. Evaluation of clinical characteristics and growth hormone response in a rare skeletal dysplasia: pycnodysostosis. *Cureus*. (2023) 15(9):e44823. doi: 10.7759/cureus.44823

frontiers | Frontiers in Endocrinology

TYPE Original Research
PUBLISHED 25 April 2025
DOI 10.3389/fendo.2025.1540237

OPEN ACCESS

EDITED BY
Federico Baronio,
IRCCS AOU S.Orsola-Malpighi, Italy

REVIEWED BY
Maushma Atteeq,
George Mason University, United States
AnneMarie Brescia,
Nemours Children's Health Delaware, United States

*CORRESPONDENCE
Ritu Trivedi
ritu_trivedi@cdri.res.in;
ritu_pgi@yahoo.com

RECEIVED 05 December 2024
ACCEPTED 27 March 2025
PUBLISHED 25 April 2025

CITATION
Chutani K, Rai N, Sardar A, Yadav A, Rai D, Raj A, Maji B, Verma S, Tripathi AK, Dhaniya G, Hingorani L, Mishra PR and Trivedi R (2025) Fortified Withaferin A accelerates the transition from fibrovascular to bone remodeling phase during endochondral bone formation to promote ossification. *Front. Endocrinol.* 16:1540237. doi: 10.3389/fendo.2025.1540237

Fortified Withaferin A accelerates the transition from fibrovascular to bone remodeling phase during endochondral bone formation to promote ossification

Kunal Chutani[1,2], Nikhil Rai[3], Anirban Sardar[1,2], Anupama Yadav[1], Divya Rai[1,2], Anuj Raj[1,2], Bhaskar Maji[1,2], Shikha Verma[1,2], Ashish Kumar Tripathi[1,4], Geeta Dhaniya[1,4], Lal Hingorani[5], Prabhat Ranjan Mishra[2,3] and Ritu Trivedi[1,2]*

[1]Division of Endocrinology, CSIR-Central Drug Research Institute, Lucknow, UP, India, [2]Academy of Scientific and Innovative Research (AcSIR), Ghaziabad, India, [3]Division of Pharmaceutics and Pharmacokinetics, CSIR-Central Drug Research Institute, Lucknow, UP, India, [4]Jawaharlal Nehru University, New Delhi, India, [5]Pharmanza Herbals Pvt Ltd., Anand, Gujarat, India

Introduction: This study shows that Fortified Withaferin A (FWA, 10% w/w) accelerates bone healing, advancing from the fibrovascular to bone remodeling stage within 12 days, compared to the typical 23–24-day healing time in rodents. FWA (10% w/w) outperformed parathyroid hormone (PTH) in osteoclast regulation and minimized recovery time, highlighting its potential as a therapeutic agent for bone health.

Methods: FWA (10% w/w) was administered orally at 125 mg·kg^{-1}. A transverse osteotomy model was used to assess post-natal bone regeneration. Additionally, an estrogen-deficient model was employed to evaluate the therapeutic potential of FWA (10% w/w). Bone regeneration was validated through calcein incorporation, gene expression analyses, micro-CT imaging and mechanical testing. Pharmacokinetic profiling was used to determine plasma exposure and trough concentration.

Results: FWA (10% w/w) effectively downregulated bone-resorbing genes, promoted anabolic responses, and reduced inflammation. It enhanced post-natal bone regeneration, likely via Runx-2 activation and modulation of osteogenic genes, alongside suppression of E3 ubiquitin-ligases Smurf1 and Smurf2, resulting in significantly enhanced callus formation and healing speed. Micro-CT revealed an enhanced callus area of ~95.14% within 12 days, compared to ~72.87% associated with normal healing. In the estrogen-deficient model, FWA (10% w/w) led to ~83.88% bone volume fraction at 23 days, exceeding the ~76.80% in controls and matching PTH effects. Material stiffness showed significant gains, with average Young's modulus rising from ~54 ± 1.03 MPa to ~63 ± 2.54 MPa. Pharmacokinetic profiling indicated plasma exposure at 226 ng/ml*hr and higher trough concentration at 24 hr, contributing to optimum therapeutic effectiveness.

Discussion: These results demonstrate that FWA (10% w/w) could significantly enhance bone mineralization and healing, facilitating an earlier transition from fibrovascular tissue to bone remodeling. The enhanced results, such as increased healing, better callus formation, and improved mechanical properties, indicate that FWA (10% w/w) is a potential intervention for delayed healing, especially in osteoporotic fractures.

KEYWORDS

Withaferin A, parathyroid hormone, delayed union, menopause (estrogen withdrawal), bone mineralization, Young's modulus

1 Introduction

Fractures are traumatic injuries that many times require hospitalization. In this light, fragility fractures pose a problem as they are common in postmenopausal women (experiencing estrogen withdrawal) or women who have undergone hysterectomy with bilateral oophorectomy (1), resulting in weakened bones from reduced bone density. The drop in estrogen levels significantly accelerates bone loss, leading to a condition known as osteoporosis and, thus, susceptibility to frequent fractures (2). Without sufficient estrogen, bone resorption outpaces bone formation, resulting in thinner, more fragile bones. In postmenopausal women, fragility fractures frequently occur in the spine, hip, and wrist. Literature indicates that estrogen deficiency reduces callus formation and alters the healing process, resulting in a longer overall recovery time (3), as a balanced inflammatory response is important for successful fracture healing. These fractures contribute to long-term morbidity, disability, and even mortality in women.

A non-healing fracture is generally treated surgically to restore proper anatomical alignment and maintained with rigid internal fixation (4). Using rigid compression plates ensures tight alignment, promoting intramembranous healing, where bone regenerates without forming a callus by directly differentiating mesenchymal progenitors into osteoblasts. However, most fractures heal through endochondral ossification, which involves bridging the fracture gap with cartilage produced by chondrocytes before osteoblasts form bone. Bone repair is complete when the disorganized bone is remodeled into mature lamellar bone. Bone healing is a complex and dynamic process involving coordinating multiple cell types and communication networks. It involves three distinct phases: inflammation, repair, and remodeling (5, 6). The process begins with an accumulation of immune cells at the injury site, forming a fracture hematoma that initiates inflammation and promotes angiogenesis to recruit progenitor cells from the endosteum and periosteum (7). Postmenopausal osteoporosis has been considered a chronic inflammatory disease and thus increased levels of proinflammatory cytokines (8).

Progenitor cells like mesenchymal stromal cells (MSCs) and skeletal stem cells (SSCs) are essential in fracture healing. This primarily involves an attempt to reestablish continuity between the fracture fragments wherein osteoblasts derived from mesenchymal stromal cells (MSCs) form osteoid or callus on the exposed bone surface and establish a new haversian system through intracortical remodelling (9). Within the fracture site, callus formation occurs by endochondral ossification. Chondrocytes derived from MSCs in the periosteum and endosteum undergo hypertrophy, causing the cartilage matrix to become calcified (10, 11) later, to which they undergo apoptosis and osteoblasts take over to induce bone formation. Given these complexities, the various stages of fracture healing offer opportunities for therapeutic interventions, including preclinical evaluation of pharmacological agents and the investigation of the molecular mechanisms underlying the bone repair process. Therefore, identifying potential molecules aimed at enhancing the fracture healing process in osteoporotic conditions was the objective of our study, as in osteoporotic fractures, systemic inflammatory response during healing is generally higher compared to normal fractures, thus delaying the process or even non-union.

In our lab, we have previously demonstrated and established that Withaferin A (WFA), a steroidal lactone, exhibits potent anti-obesity properties (13). This is primarily achieved by binding and inhibiting the specific catalytic β subunit of the 20S proteasome. WFA also positively impacts bone formation by promoting osteoblast proliferation and differentiation, and in osteoclasts, it reduces cell numbers by downregulating the expression of tartrate-resistant acid phosphatase. This is achieved by virtue of its role in modulating the E3 ubiquitin ligase expression.

In our current investigation, we have elucidated the correlation between fracture healing and gene expression in normal and pathophysiological conditions of estrogen loss (menopause), establishing that the inflammatory phase and transition from fibrovascular tissue to bone remodelling are notably accelerated during fracture repair. Our findings reveal that Fortified Withaferin A extract (FWA, 10% w/w) significantly mitigates systemic inflammation and downregulates bone-resorbing genes, resulting in faster bone repair compared to the prolonged healing observed in menopausal fracture recovery. Additionally, Fortified Withaferin A extract (FWA, 10% w/w) addresses the challenges associated with

the high cost of pure Withaferin A, making it a more viable option for positioning Withaferin A as a therapeutic agent.

2 Methods and materials

2.1 Animal and experimental study

All animal care and experimental procedures were conducted following approval from the Institute Animal Ethics Committee of the Central Drug Research Institute for the respective animal studies:

- SD rats (Animal ethics approval number: IAEC/2022/50/Renew-0/Dated-05/07/2022 (IAEC/2022/148/Renew-0/Dated-15/11/2022), and IAEC/2023/66/Renew-0/Dated-20/03/2023).

All the animals were housed in controlled conditions with a temperature of 24°C and 12-hour light-dark cycles. They were provided with ad libitum diet and water. At the conclusion of the study, all animals were individually weighed and sacrificed (12).

2.2 Osteotomy model

A total of 221 adult Sprague-Dawley rats were randomly assigned to three different studies.

Study 1: Dose-dependent effect of FWA enrichment on callus formation Eighty rats were divided into five groups (n=8-10 per group): Control (Fractured), PTH (20 µg, thrice a week; Positive Control), and FWA-enriched treatment groups (2.5%, 5%, and 10% at doses of 75, 125, and 250 mg/kg).

Study 2: Time-dependent effect of FWA (10% w/w) on early bone regeneration Sixty-nine rats were assigned to three groups (n=23 per group): Control, PTH, and FWA (10% w/w) at 125 $mg.kg^{-1}$. The effect of FWA on fracture healing was assessed over a time course of 1-12 days.

Study 3: Effect of FWA (10% w/w) on delayed healing in an estrogen withdrawal model Seventy-two rats were used in this study (n=24 per group) and divided into three groups: Ovx (estrogen withdrawal model), Ovx + PTH, and Ovx + FWA (10% w/w) at 125 $mg.kg^{-1}$. The study spanned 1-23 days to assess fracture healing in estrogen-deficient conditions.

After anaesthesia (Ketamine: Xylazine) in 3:1, the right hind leg was swabbed with 75% EtOH and a small skin 1 cm incision was made on the front skin of the mid-diaphysis of the femur to expose the targeted region for injury in SD rats. The surrounding muscles were cleared, and the periosteum was removed to expose the surface of the femoral bone. In order to create an injury, a drill hole was made in the anterior portion of the diaphysis, approximately 2 cm above the knee joint in SD Rats. The drill bit diameter used was 0.8 mm for rats. Upon recovery from anaesthesia, animals were housed individually with free access to food and water. Under these conditions, bone fractures heal through endochondral ossification at the centre of the fracture site, while intramembranous ossification occurs at the distal edges of the callus (13). The treatment was initiated on the following days and continued until the 12th day for the transverse osteotomy model and 23 days for the menopausal (estrogen withdrawal). At the end of the designated time period, the animals were sacrificed, and their femurs were collected to analyse bone microarchitectural parameters and dynamic histomorphometry study at the injury site (14).

2.3 Fracture site bone regeneration

Animals were given a single calcein dose of 20 $mg.kg^{-1}$ of body weight through intraperitoneal administration 24 hours before they were sacrificed. The bones were embedded in acrylic material, and 50 µm sections were cut using an ISOMET bone cutter. Images were captured under a confocal microscope with appropriate filters for enhanced visualization to analyse the intensity of calcein binding to the fracture site, indicating new mineral deposition using Image J software.

For quantifying the microarchitecture of the callus formed in the drill hole, we performed µCT analysis using a Sky Scan 1276 CT scanner (Aartselaar, Belgium). The soft tissues were meticulously cleared without disturbing the bone callus and scanned using a 70kV, 200mA X-ray source and 1mm aluminium filter with a pixel size of 21.1 µm for rats for image acquisition. The images were reconstructed with the Sky Scan N recon and CTan software (1.7.4.6 and 1.18.8.0, Sky Scan, Bruker). For each fractured femur, the fracture line was identified using Dataviewer (SkyScan), and a volume of interest (VOI) was defined by selecting 100 axial slices centered on the fracture. The outer boundary of the callus—comprising bone, cartilage, and void space—was manually outlined in the 2D tomograms to determine the total callus volume (TCV). To assess maximum cortical bone density, 100 slices of the contralateral femur at the mid-diaphyseal region were analysed. The mineralized callus volume (MCV) was segmented using a density threshold of ~35% to ~57% of the maximum cortical density. Tissues below ~35% were considered non-mineralized. The total mineralized tissue volume, normalized to callus volume (TMV/TCV, %), used a range of ~35% to ~100% of the maximum cortical density, while bone volume normalized to callus volume (BV/TCV, %) was quantified with a range of ~57% to ~100% (13, 15).

2.4 Pharmacokinetic study

In this study, a validated UHPLC-MS/MS method was used to analyse the pharmacokinetics of FWA (10%w/w), a fortified extract enriched with Withaferin A, while also containing minor amounts of Withanolide A, Withanolide B, and Withanone. The analysis was conducted following the oral administration of FWA (10%w/w) in Sprague Dawley rats (SD rats; n=6) at the dose of 75, 125 and 250 $mg.kg^{-1}$. The 125 $mg.kg^{-1}$ dose was identified as the effective therapeutic concentration based on its optimal fracture-healing response. Initially, the UHPLC-MS/MS method was validated with respect to specificity, linearity, precision, accuracy, and robustness to ensure reliable quantification of Withaferin A and other withanolides in plasma samples. The accuracy and precision

of the constituents in rat plasma samples and other validated parameters have been represented in Tables 1, 2. The inter and intraday precision and robustness are represented in Tables 3, 4, respectively. For pharmacokinetic assessment, plasma samples were analysed using PKSolver 2.0 software through non-compartmental analysis following extravascular input. The linear trapezoidal method was applied to calculate pharmacokinetic parameters such as Cmax, Tmax, AUC, and t1/2, to ensure that drug absorption, distribution, and elimination are thoroughly evaluated. The concentration of each Withanolide was measured in ng/ml units, allowing direct comparison of their pharmacokinetic behaviour and confirming that FWA (10% w/w) is enriched with Withaferin A as its primary bioactive component, with minor contributions from other withanolides (16).

2.5 RNA extraction and real-time PCR

We took the entire fracture site on the femur diaphysis and snap-frozen it in liquid nitrogen for the gene expression analysis. Frozen samples were then powdered with prechilled mortar and pestle and homogenised in 1ml Trizol RNAiso PLUS (Takara) following the manufacturer's instructions. We used 500-1000 ng of RNA to reverse transcribed into cDNA with the High-Capacity cDNA Reverse Transcription Kit (Catalogue- 4368814 Thermo Fisher). Following this, quantitative real-time PCR (qRT-PCR) was performed in triplicates using PowerUP SYBR Green Master Mix (Thermo Fisher) on a QuantStudio 3 system (Applied Biosystems, Thermo Fisher, Mississauga, ON, Canada), in accordance with the manufacturer's protocol. Gene transcript levels (as listed in Table 5) were assessed using the comparative Ct (2-ΔΔCt) method (17, 18). Primers were designed using Primer-BLAST (National Centre for Biotechnology Information [NCBI], Bethesda, MD, USA) and are listed in Table 5.

2.6 Histology and histomorphometric analysis

Bone samples were decalcified in 10% EDTA (Sigma-Aldrich) for three weeks, and the solution was changed every three days. Decalcified mice bone samples were further embedded in paraffin wax before the staining procedure. Sections were then sectioned to 7-micron thickness and stained with Safranin O/Fast green to determine cartilage and bone. The proportions of cartilage and bone were quantitated by determining the areas that stained positive for Safranin O (red, indicating proteoglycan content) and Fast Green (blue, indicating collagen), respectively. This was done through thresholding and then

TABLE 1 The linear equation, linear range, and LLOQ of the Withaferin A, Withanolide A, Withanolide B and withanone.

Withanolides	Linear equation	Range (ng/ml)	r2	LOD (ng/ml)	LOQ (ng/ml)
Withaferin-A	y =32943x-2845.1	0.49-250	0.9992	0.12	0.25
Withanolide-A	y = 7236.3x + 3114.2	0.49-250	0.9993	0.49	0.98
Withanolide-B	y =32950X-2662.2	0.49-250	0.9992	0.49	0.98
Withanone	Y=7800.9x + 104298	3.90-1000	0.9997	–	–

*r^2-correlation coefficient; LOD, Limit of Detection; LOQ, Limit of Quantitation; LLOQ, lower, limit of quantification.

TABLE 2 Accuracy and Precision of the constituents in rat plasma samples, (n = 6).

Analyte	Nominal concentration (ng/mL)	Average Area Raito (± SD)	Extraction recovery (% ± SD)	Precision (RSD, %)	Accuracy (RE, %)
Withaferin A	1.95	0.20±0.01	95.79	2.61	1.87
	15.63	1.20±0.02	100.61	1.61	15.73
	125.00	9.11±0.22	100.01	2.39	125.02
Withanolide A	1.95	0.20±0.02	90.44	7.61	1.76
	15.63	0.93±0.03	101.25	3.46	15.82
	125.00	6.62±0.27	99.91	4.06	124.88
Withanolide B	1.95	0.12±0.00	105.60	2.98	2.06
	15.63	1.12±0.02	98.73	2.06	15.43
	125.00	9.29±0.60	100.02	6.46	125.02
Withanone	1.95	0.18±0.01	98.60	2.78	1.92
	15.63	0.98±0.04	99.83	1.87	15.60
	125.00	9.38±0.38	100.51	2.37	125.63

10.3389/fendo.2025.1540237

TABLE 3 Intra and inter-day precision and accuracies of the analyte in rat plasma samples, (ng/mL).

Analyte	Concentration (ng/ml)	Intra-day 01 (n = 6)		Intra-day 02 (n = 6)		Intra-day 03 (n = 6)		Inter-day (n = 6x3)	
		Average Area Ratio	% RSD	Average Area Ratio	% RSD	Average Area Ratio	% RSD	Average Area Ratio	%RSD
Withaferin A	0.98	0.13	3.11	0.13	4.71	0.13	1.54	0.13	4.71
	1.95	0.20	2.53	0.20	2.57	0.18	7.61	0.20	2.57
	15.63	1.18	4.15	1.19	1.83	1.15	2.62	1.19	1.83
	125.00	9.38	2.60	9.02	2.82	8.86	2.39	9.02	2.82
Withanolide A	0.98	0.09	8.69	0.09	9.54	0.10	8.93	0.09	9.54
	1.95	0.17	10.12	0.18	10.55	0.17	9.47	0.18	10.55
	15.63	0.88	3.20	0.94	2.93	0.79	4.98	0.93	2.93
	125.00	6.62	2.45	6.59	4.65	5.68	2.67	6.59	4.65
Withanolide B	0.98	0.86	4.24	0.91	2.58	0.87	1.78	0.91	2.58
	1.95	0.93	3.41	0.99	3.44	0.87	3.17	0.99	3.44
	15.63	1.98	4.92	2.04	3.73	1.83	1.96	2.04	3.73
	125.00	10.47	4.35	10.43	4.38	9.45	1.91	10.43	4.38
Withanone	0.98	0.78	4.12	0.75	2.46	0.72	1.62	0.89	2.36
	1.95	0.91	2.98	0.87	3.32	0.68	3.12	0.83	3.31
	15.63	1.85	4.57	1.98	3.68	1.73	1.93	2.12	3.62
	125.00	9.92	4.28	10.26	4.27	9.56	1.89	10.29	4.18

TABLE 4 Robustness; column temperature.

Withaferin A								
Column oven: 35^{0}C			Column oven: 40^{0}C			Column oven: 45^{0}C		
Average Area Ratio	SD	%RSD	Average Area Ratio	SD	% RSD	Average Area Ratio	SD	% RSD
1.11	0.03	2.26	1.15	0.02	1.53	1.19	0.02	1.53
Withanolide A								
Column oven: 35^{0}C			Column oven: 40^{0}C			Column oven: 45^{0}C		
Average Area Ratio	SD	% RSD	Average Area Ratio	SD	% RSD	Average Area Ratio	SD	% RSD
0.64	0.03	4.35	0.76	0.02	3.19	0.73	0.02	2.81
Withanolide B								
Column oven: 35^{0}C			Column oven: 40^{0}C			Column oven: 45^{0}C		
Average Area Ratio	SD	% RSD	Average Area Ratio	SD	% RSD	Average Area Ratio	SD	% RSD
1.84	0.06	3.25	1.73	0.07	4.05	1.66	0.05	2.89
Withanone								
Average Area Ratio	SD	% RSD	Average Area Ratio	SD	% RSD	Average Area Ratio	SD	% RSD
1.62	0.04	2.98	1.53	0.05	3.98	1.46	0.03	2.35

TABLE 5 List of primers and their sequences used in the study.

Gene Symbol	Gene Name	Primer Sequence	Accession No.
β - actin	β-actin	F–CTCCCTGGAGAAGAGCTATGA R–AGGAAGGAAGGCTGGAAGA	NM_031144.3
BMP2	Bone morphogenetic protein2	F– CGGCTGCGGTCTCCTAA R–GGGAAGCAGCAACACTAGA	NM_017178.2
Sox9	SRY Box Transcription Factor 9	F–GTACCCGCATCTGCACAAC R–CTCCTCCACGAAGGGTCTCT	NM_080403.3
Col2a1	Collagen Type 2, α1 chain	F- GGATGTATGGAAGCCCTCGTC R-GTGACCCTTGACACCAGGAA	NM_001414896.1
Col1a1	Collagen Type 1, α1 chain	F- CAAGATGGTGGCCGTTACTAC R- GCTGCGGATGTTCTCAATCT	NM_053304.1
Col10a1	Collagen Type X, α1	F- ATGGCTTCACAAAGAGCGGA R- CCTACCCAAACGTGAGTCCC	NM_013140.1
Runx2	Runt related transcription factor 2	F- TGGCCTTCCTCTCTCAGTAA R- GTAAGTGAAGGTGGCTGGATAG	NM_001278483.2
Ocn	Osteocalcin	F- TGACTGCATTCTGCCTCTC R- CGGAGTCTATTCACCACCTTAC	NM_013414.1
Acp5 (Trap)	Tartrate resistant acid phosphatase 5	F– GGAACCACAGAGGCTTACAT R– CCACTCCCAAGAAAGGTCTAC	NM_001270889.1
Opn (Spp1)	Osteopontin	F– CAGCCAAGGACCAACTACAA R–TGCCAAACTCAGCCACTT	NM_012881.2
Rankl	TNF Superfamily member 11	F–ACTGTCTGGACCTCGGTGAA R–CTGCGCTCGAAAGTACAGGA	NM_057149.2
CtsK	Cathepsin K	F- TCCTCAACAGTGCAAGCGAA R- CCAGCGTCTATCAGCACAGA	NM_031560.2
Acan	Aggrecan	F- AGCCCTTGTCTGAATGGAGC R- GTTGGTTTGGACGCCACTTC	NM_022190.2
Smurf 1	SMAD specific E3 ubiquitin protein ligase 1	F - CTGAAACCCAATGGCAGAAATG R – GGGCTTCGATTCCTCTCATAAA	NM_001109598.1
Smurf 2	SMAD specific E3 ubiquitin protein ligase 2	F - CCAGACTAGCAGAGAGAAGAGT R - TAGGTCTGGAGGAGTGTGTAAG	XM_039086171.2

manually fine-tuning the region of interest, with results expressed as a percentage of the entire callus area. Tartrate-resistant acidic phosphatase (TRAP) staining was performed by immersing them in a pre-warmed TRAP staining solution mix for 30 minutes. After rinsing with distilled water, a 0.02% fast green counterstain was applied. The tissue sections were dehydrated using graded alcohols and cleared in Xylene before mounting for observation under a light microscope. Osteoclasts were identified as TRAP-positive cells with at least three nuclei (19, 20).

2.7 Mechanical testing of bone

The micro-indentation tests were performed at the fracture site in the femur diaphysis using the MACH-1 TM v500css micromechanical system (Bio momentum, Laval, Quebec, Canada). The tests were conducted under displacement control using a spherical 1mm diameter ruby tip. Force–displacement data were measured with a 1.5 N load cell and the linear stage's optical encoder (0.1 μm resolution) at a sampling rate of 200 Hz. To position the bone for indentation, the indenter was mounted using a custom fabricated adaptor attached to an XY positioning stage (Newport motion controller ESP302, linear XY stage, Newport Corporation, Irvine, California) with a micrometre (1 μm precision). The Basler camera (1.3MPX, MA732) was utilized to identify the region of interest for micro-indentation testing. All indentations were conducted at room temperature, and each sample was rehydrated with phosphate-buffered saline prior to testing (21, 22). Tissue mechanical properties, such as Young's modulus (E), Bulk modulus (K) and toughness (I), were calculated.

2.8 Statistical analysis

Data are presented as means ± standard error of the mean (SEM) unless otherwise specified, with sample sizes detailed in the figure legends. To assess genotype differences across time points in

micro-CT, gene expression analysis, osteoclast number, mechanical testing data, mineralized callus volume by total callus volume, a one-way ANOVA followed by Tukey's multiple comparisons test was conducted using GraphPad Prism 8.4.2 (GraphPad, La Jolla, CA, USA). For qualitative analysis of immunostaining data, two fields of view (FOVs) per animal and three animals per genotype were included, with representative results presented. Statistical significance was set at (***p< 0.001, **p 0.002, *p 0.033).

3 Results

3.1 Effect of different doses and strength of FWA (10% w/w) at the fracture site in healthy rats

Osteotomies were produced, generating gaps of approximately 0.8mm that were not significantly different between the Control and Treatment groups when measured by Micro-CT and the experimental design of this schematic administration of FWA (10% w/w) at different concentrations is shown in (Figure 1). Fracture calluses were examined at different doses and at different enrichment strength (2.5, 5.0, and 10.0%) in the groups for 12 days by micro-CT post-fracture to determine the effects FWA (10% w/w) on changes in callus formation and mineralization. Comparisons were made with standard of care parathyroid hormone (PTH) that is known to regulate endochondral bone repair (Figure 1). Estimation of the total callus volume (Figure 1), mineralized callus volume, total mineralized tissue volume normalized to callus volume, and total normalized bone volume show that these indices were significantly increased in 125 $mg.kg^{-1}$ dose as compared to the other doses. Peak mineralized callus volume was observed on day 12 of treatment with FWA (10% w/w) at 125 $mg.kg^{-1}$ (10% w/w) by which time ossification of the callus is observed at the fracture site (Figure 1). When this was normalized to tissue callus volume the dose of 125 $mg.kg^{-1}$ FWA (10% w/w) showed an increase in percentage of total mineralized callus tissue at compared to that of control in normal healing process (Figure 1). Data shows that the administration of FWA (10% w/w) at 125 $mg.kg^{-1}$ and 250 $mg.kg^{-1}$ resulted in the best response to callus formation that was comparable to PTH at the fracture site and evidence of new bone formation. Quantitatively, a significantly increased trabecular bone volume/tissue callus volume (BV/TCV) to ~87.76% (125 $mg.kg^{-1}$) and ~53.78% (250 $mg.kg^{-1}$) compared to the negative (control) ~30.09% and positive control (PTH) ~96.98% (Figure 1).

The calcein labelling intensity observed in newly formed callus at the drill hole site during fracture healing reveals that the most robust bone-regeneration occurred with FWA (10% w/w) at a dosage of 125 $mg.kg^{-1}$, which was found comparable to the positive control (PTH 20 µg/3 days a week alternatively) (Figures 2A, B).

The micro-CT and the calcein labelling intensity at the callus site suggest that administering FWA (10% w/w) at 125 $mg.kg^{-1}$ was the most effective dose for repairing the fracture as early as day 12. This data suggests that FWA could reduce the therapeutic window to half (day 12) compared to the normal healing process of 21-35 days. This dose and timepoint were taken up for further experiments.

3.2 Pharmacokinetic profiling of optimized FWA formulation in SD rats

Having proven the efficacy dose of FWA (10% w/w) to be 125 $mg.kg^{-1}$, we wanted to establish the pharmacokinetic profile of the FWA (10% w/w) formulation. The C_{max} of Withaferin A (WFA) was found to be 274.90± 15.41 ng/ml, which is substantially higher as compared to other markers like Withanolide A, Withanolide B, and Withanone. Similarly, the $AUC_{0\text{-}12}$ of Withaferin A was found to be 226.05± 5.66 ng/ml*h, which is nearly nine-fold higher as compared to other withanolides (Figure 3), suggesting that the FWA (10% w/w) formulation was indeed enriched with WFA as its primary bioactive component. Additionally, we assess the other withanolides present in FWA (10% w/w) that might have imparted therapeutic efficacy after *in vivo* administration. Data shows that Withanolide A, Withanolide B, and Withanone were rapidly absorbed from the gastrointestinal tract. The concentration of different withanolides; Withaferin A, Withanolide A, Withanolide B, and Withanone in the bloodstream over 12 hours following a single dose of 125 $mg.kg^{-}1$ is represented in the plasma concentration-time curve overlay graph (Figure 3). The y-axis is on a logarithmic scale, ranging from 0.1 to 300 ng/mL, and the x-axis represents time in hours. At 0 hours, the concentration of Withaferin A starts low, marking the baseline. Within the first hour, a sharp increase, peaking slightly above 100 ng/mL, indicating rapid absorption. After this peak at around 1 hour, the concentration declines noticeably, reaching about 10 ng/mL by the 4-hour mark. The decline continues slowly from 4 to 12 hours, with the concentration approaching 1 ng/mL by 12 hours, reflecting a slower elimination phase. This data conforms to the fact that Withaferin A is responsible for the improved efficacy in the rapid fracture model. These results suggest that the time required to reach maximum concentration (T_{max}) and plasma half-life ($t_{1/2}$) of Withaferin A was found to be 0.83 h and 5.94 ± 1.62 h, respectively, while for Withanolide A and B, $t_{1/2}$ were found to be 2.91 ± 0.01 h and 1.65 ± 0.04 h respectively. The data also agrees with the fact that molecules like Withaferin A having reported log P value (3.86) less than 5 and Total polar surface area (TPSA) of ~96 are well absorbed, thus showing the improved activity. These pharmacokinetic properties establish FWA (10% w/w) as a Withaferin-A enriched extract with optimized bioavailability.

3.3 Longitudinal assessment of callus formation in healthy SD rats using the effective dose of FWA (10% w/w), compared to the standard of care PTH

The impact of FWA (10% w/w) at the effective dose of 125 $mg.kg^{-}1$ was examined time-dependently over 12 days by micro-CT. This helped us determine the effects of increased levels of FWA (10% w/w) in a longitudinal fashion in callus formation and mineralization.

10.3389/fendo.2025.1540237

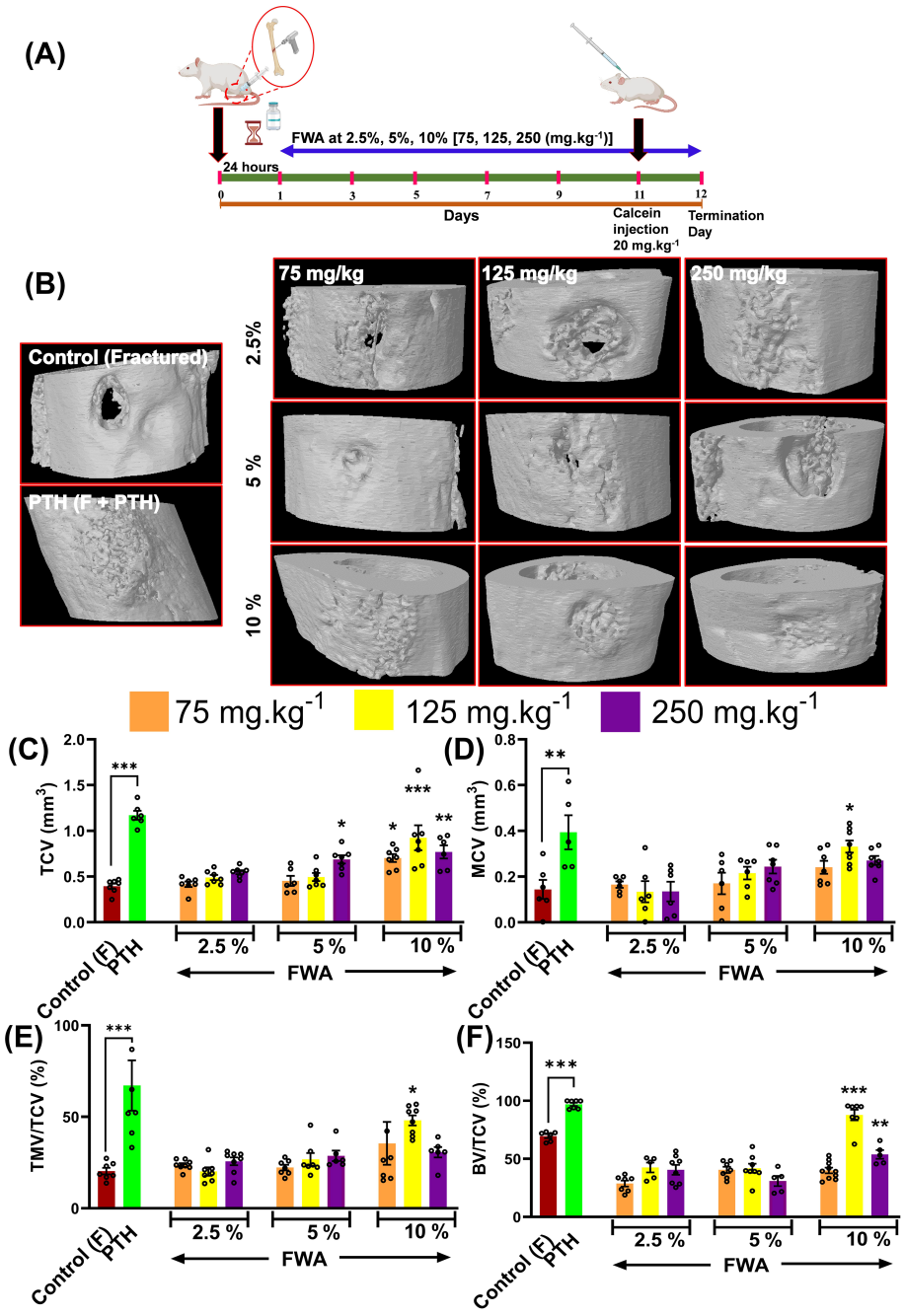

FIGURE 1
Effects of Withania somnifera enriched extract (FWA) on bone healing in a transverse osteotomy model. **(A)** In a drill hole injury model (transverse osteotomy), The experimental design depicts the timeline for administering FWA at varying concentrations (2.5%, 5%, and 10%, corresponding to 75, 125, and 250 mg.kg^{-1}). Calcein injection was carried out on day 11 to label mineralizing bone, and the SD rats were sacrificed on day 12 for analysis. **(B)** Micro-CT images of fractured femurs from different treatment groups, including controls (both untreated and treated with parathyroid hormone [PTH]) and those treated with various concentrations of FWA. The images display the progression of bone healing and callus formation at the fracture site. **(C-F)** Quantitative analysis of tissue callus volume (TCV), mineralized callus volume (MCV), total mineralized volume normalized to callus volume (TMV/TCV), and bone volume/total callus volume (BV/TCV) in the fractured femurs across different groups. The data are presented as mean ± SE (n = 6). Significant differences compared to control groups are indicated (***p< 0.001, **p 0.002, *p 0.033).

FWA (10% w/w) at 125 mg.kg^{-1} showcases a progressive enhancement in BV/TCV (%) in the duration of healing, culminating in complete restoration by day 12. A 3D μ-CT visualization elucidates the complex process of *in-vivo* bone regeneration, highlighting the efficacy of FWA (10% w/w) at 125 mg.kg^{-1} from day 1 to 12. (Figure 4). The BV/TCV significantly increased by day 6 in the control (Fractured group); however, in the FWA (10% w/w) and the PTH treatment groups, BV/TCV increased as early as day 3, reaching its peak by day 12. Femoral data analysis reveals that in the control fractured group, BV/TCV (%) increased

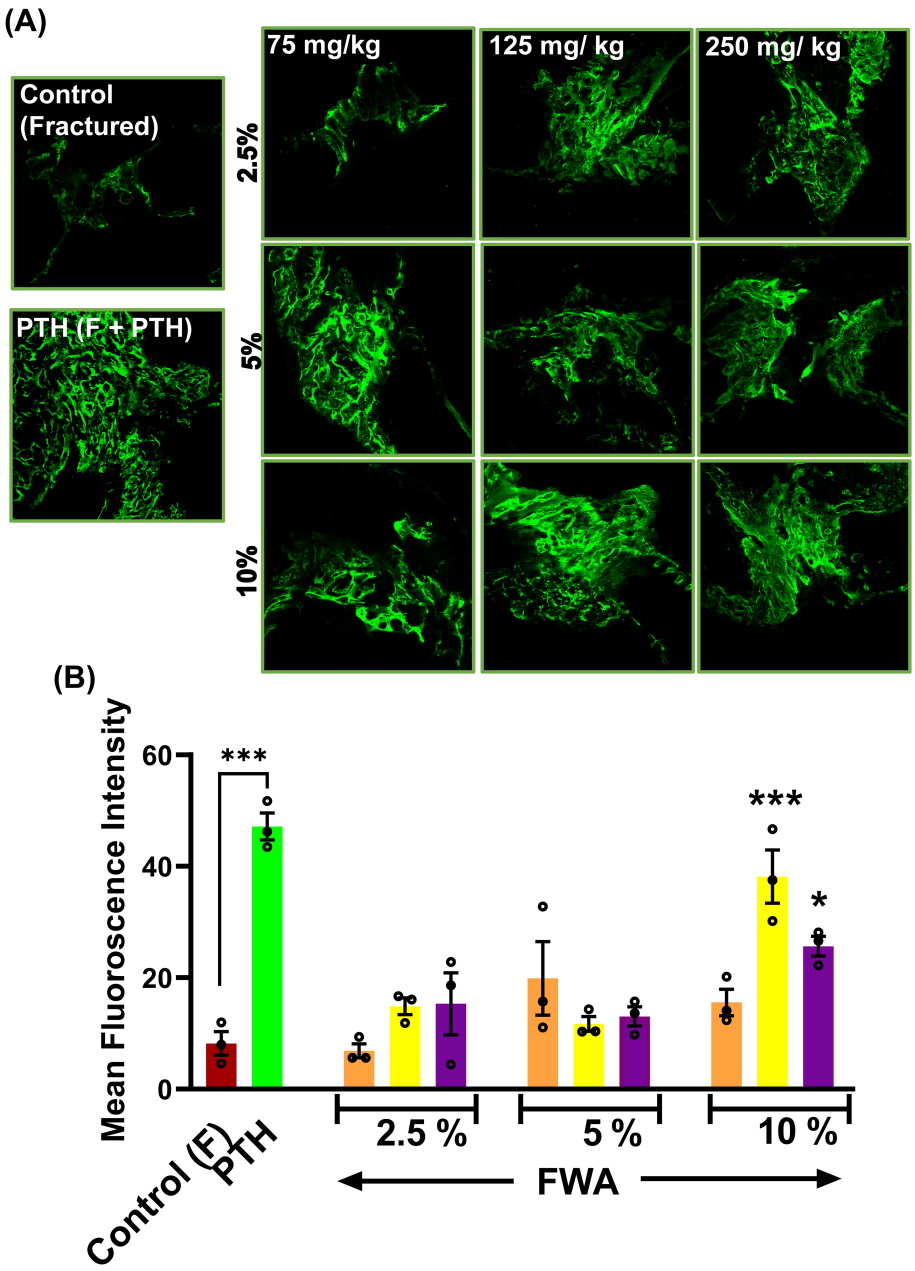

FIGURE 2
Effects of Withania somnifera enriched extract (FWA) on fracture healing and bone formation. **(A)** Fluorescence microscopy images of calcein-labeled sections from different treatment groups, illustrating new bone formation at the fracture site. Control (fractured), PTH-treated, and various doses of FWA-treated groups (2.5%, 5%, 10%) are shown for comparison. **(B)** Quantitative analysis of calcein fluorescence intensity, representing new bone formation in the different treatment groups. The data are presented as mean ± SE (n = 6). Significant differences compared to control groups are indicated (***p < 0.001, *p 0.033). This figure demonstrates the positive impact of FWA on bone formation and fracture healing, as evidenced by improved structural parameters and increased new bone formation in treated groups compared to fractured control animals.

from approximately (14.39%) on day 3 to a notable (~72.87%) by the end of day 12 (Figure 4), aligning with typical fracture healing timelines. In contrast, administering PTH and FWA (10% w/w) at 125 mg.kg^{-1} demonstrated remarkable enhancements in BV/TCV. On day 3, PTH exhibited a striking increase of approximately (34.0%) (Figure 4), while FWA (10% w/w) showed a substantial rise of approximately (25.0%) (Figure 4). By day 12, these interventions maintained their efficacy, with PTH and FWA (10% w/w) showing further increases of approximately (99.86%) and (95.0%) respectively. Figure 4 illustrates bone volume to tissue callus volume (BV/TCV %) across different time points for three groups—Control (F), PTH treatment, and FWA (10% w/w) treatment. These findings underscore the potential of PTH and FWA (10% w/w) as accelerators of fracture healing, surpassing the typical healing trajectory (23). In summary, the results suggest that, like PTH treatment, FWA (10% w/w) is equally effective in promoting bone-

10.3389/fendo.2025.1540237

(A)

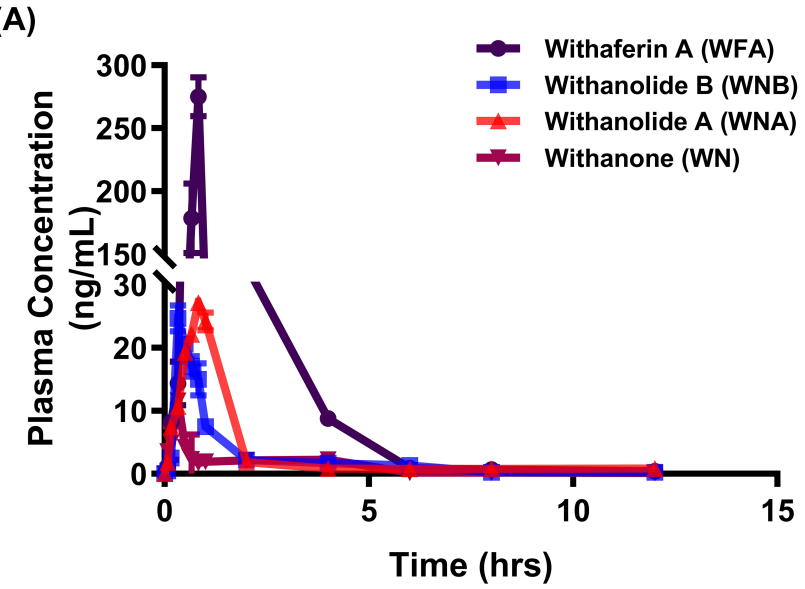

(B)

PK parameter	Unit	Markers			
		WFA	WNA	WNB	WN
Lambda_z	1/h	0.12±0.03	0.24±0.00	0.42±0.01	0.29±0.03
$t_{1/2}$	h	5.94±1.62	2.91±0.01	1.65±0.04	2.41±1.00
T_{max}	h	0.83± 0.00	0.67±0.00	0.33±0.00	0.33±0.01
C_{max}	ng/ml	274.90± 15.41	27.15±0.21	24.67±2.09	11.60±1.90
AUC_{0-12}	ng/ml*h	226.05± 5.66	24.14±0.11	28.10±0.50	14.22±0.80
AUC_{0-inf_obs}	ng/ml*h	229.66±4.39	27.29±0.36	28.63±0.56	14.78±0.55
$AUC_{0-12/0-inf\_obs}$	-	0.98± 0.00	0.88±0.01	0.98±0.00	0.96±0.10
$AUMC_{0-inf\_obs}$	ng/ml*h^2	410.22± 36.29	117.35±3.81	66.21±1.59	46.30±2.00
MRT_{0-inf_obs}	h	1.79±0.19	4.29±0.08	2.31±0.10	3.13±0.10
$Vz/F_{\_obs}$	(mg)/(ng/ml)	4.68±1.36	19.22±0.19	10.42±0.37	29.38±0.91
$Cl/F_{\_obs}$	(mg)/(ng/ml)/h	0.54±0.01	4.58±0.06	4.37±0.08	8.46±1.00

FIGURE 3
Pharmacokinetic profile of Withaferin A and related withanolides in SD rats. **(A)** Mean plasma concentration-time plots of four withanolides (WFA, WNA, WNB, and WN) after oral administration of Withania somnifera extract (FWA) at the dose of 125 $mg.kg^{-1}$ (10% w/w) in Sprague Dawley rats (Mean ± SD, n = 6). are represented in different colours: WFA (purple), WNA (red), WNB (blue), and WN (pink). The data points reflect mean concentrations ± SE (n = 6). **(B)** The table presents the pharmacokinetic (PK) parameters of WFA and related withanolides. The parameters are presented with their units and values for each Withanolide (WFA, WNA, WNB, WN) showing mean ± SE (n = 6). This figure offers a comprehensive overview of the pharmacokinetic behaviour of Withaferin A and its related compounds in SD rats, highlighting their absorption, distribution, metabolism, and elimination characteristics in the rat model.

regeneration and improving bone quality. The control group with no additional treatment exhibited minimal bone repair.

3.4 Time-dependent gene expression analysis of healing at the fracture site

Time-dependent changes in callus formation during fracture healing involve specific gene expression at each time point like, from Inflammation (Bmp-2) to Fibrovascular (Sox 9), (Col2a1, Acan, Col10a1 to the bone formation (Col1a1) to finally the remodeling period (OCN) when the bone is completely mineralized and repaired (Figure 5), our assessment at these timepoints shows that when the treatment groups were normalized with the control (F) group the Fracture (F) + PTH and F+FWA (10% w/w) group exhibited a time-specific increase, in the distinct phases of fracture repair.

Early on, periosteal cells responded to Bone Morphogenetic Protein 2 (BMP2) (Figure 5), leading to a significant ~57.0-fold increase in the PTH administered group and ~17.0-fold increase in the FWA (10% w/w) group, fostering chondrogenesis followed by osteogenesis. By *day 6*, angiogenic cells facilitated the formation of small blood vessels and fibrovascular tissue, with remarkable upregulation of genes observed in PTH and FWA (10% w/w) at

10.3389/fendo.2025.1540237

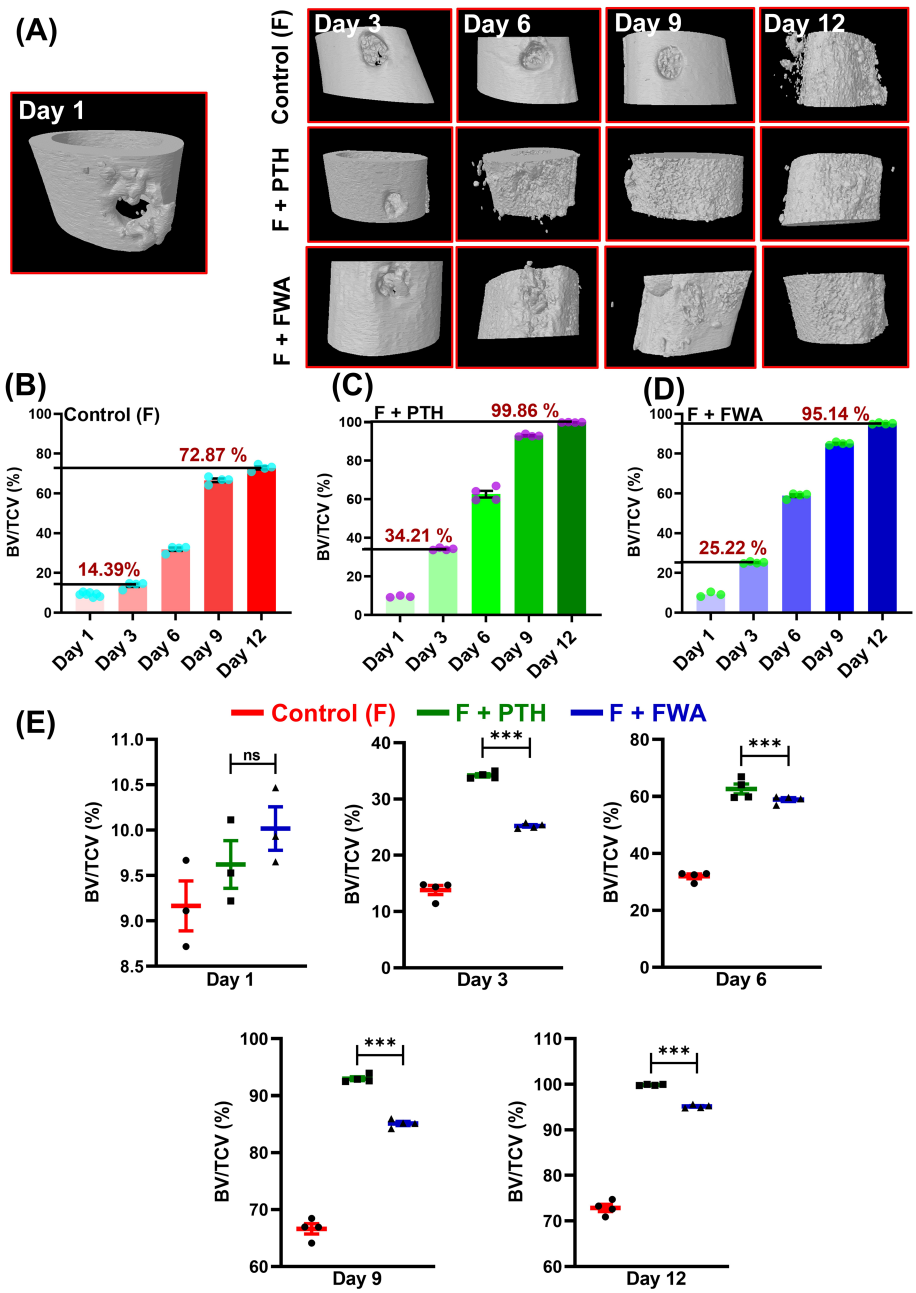

FIGURE 4
FWA promotes fracture healing in the transverse osteotomy model (Drill hole injury) in time specific manner. **(A)** 3-D representation of the bone microarchitecture as obtained from μCT analysis. **(B)** Quantitative measures of the parameter bone volume/tissue callus volume (BV/TCV, %) between control (fractured) group **(C)** PTH treatment in fractured SD rats with comparison to **(D)** FWA treatment **(E)** Values of BV/TCV, % with respect to healing are represented in time specific manner. Data are represented as mean ± SEM compared to the control group (***p < 0.001). ns, non-significant (ns p = 0.47).

125 mg.kg^{-1}. This was evident through substantial elevations in Sox9 (Figure 5) (~32.29-fold and ~22.16-fold, respectively), Aggrecan (Acan) (Figure 5) (~14.0-fold and ~8.0-fold, respectively), Col10a1 (Figure 5) (~71-fold and ~54.0-fold, respectively).

As the process progressed, markers indicative of endochondral bone formation and remodeled bone were expressed by *day 9* and *day 12* in PTH and FWA (10% w/w) at 125 mg.kg^{-1}. Notable increases were observed in Col1a1 (Figure 5) (~32.0-fold and ~26.00-fold, respectively) in Runx2 (Figure 5) (~102.0-fold and ~56.0-fold, respectively), as well as mineralization markers like Osteopontin (Opn) (Figure 5) (~15.0-fold and ~8.0-fold, respectively) and Osteocalcin (Ocn) (Figure 5) (~38.0-fold and ~23.0-fold, respectively.

The expression analysis data of the remodeling phase when the bone is completely formed showed that the PTH did not affect the osteoclast activity. As we observed, no significant changes in the

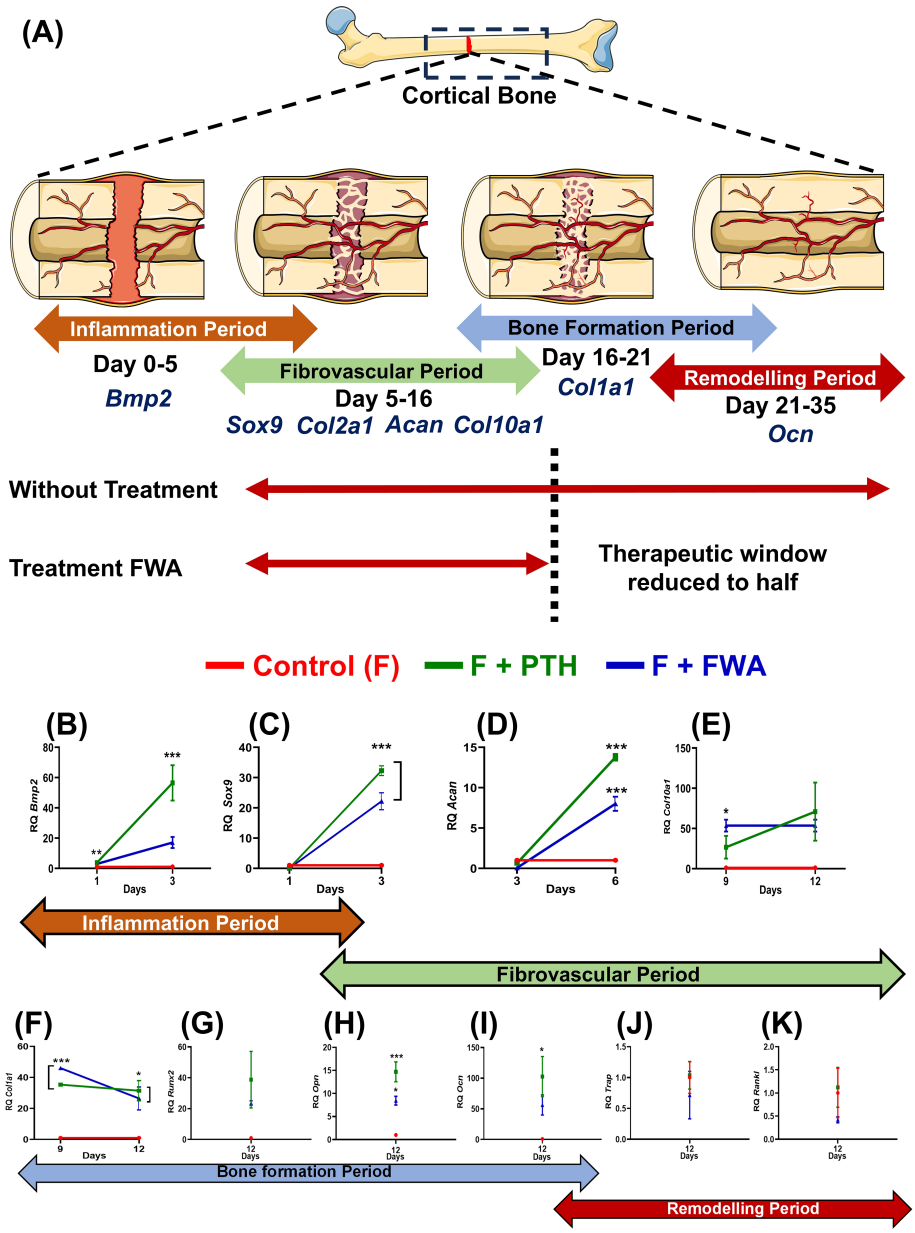

FIGURE 5
Phases of bone healing post drill hole injury in the femur diaphysis. **(A)** Schematic representation of the four phases of bone healing: Inflammation phase (Days 1-6), Fibrovascular phase (Days 3-12), Bone formation phase (Days 9-18), and Bone remodeling phase (Day 18-23). Key regulatory markers for each phase are indicated: BMP2 for inflammation, Sox9, Col2a1, ACAN, and Col1a1 for the fibrovascular period, Runx2, Col10a1, Ocn, and Opn for bone formation, and RANKL, Cathepsin K, and TRAP for remodeling. Quantitative analysis of gene expression levels over time for different treatment groups: Control (F, red), F + PTH (green), and F + FWA (blue) is shown with respect to different phases BMP2 **(B)**, Sox 9 **(C)**, Acan **(D)**, Col10a1 **(E)**, Col1a1 **(F)**, Runx2 **(G)**, Opn **(H)**, Ocn **(I)**, Trap **(J)** and Rankl **(K)**. Data are represented as mean ± SEM compared to the control group (***p< 0.001, **p 0.002, *p 0.033).

expression of the TRAP osteoclast-specific marker gene (Figure 5) (~1.0-fold), Rankl (Figure 5) (~1.0-fold, respectively). However, FWA (10% w/w) did affect the remodeling phase as we observed downregulation of osteoclast marker genes by approximately 50%, indicating a shift towards a less resorptive state, suggesting a trend towards a very normal healing process involving all the three cell types of chondrocytes forming callus and then the bone-forming cells osteoblast and bone-resorbing cells osteoclast.

3.5 Assessment of FWA (10% w/w) in estrogen withdrawal (menopause) model

As estrogen deficiency reduces callus formation and alters the healing process, resulting in a longer overall recovery time, we wanted to assess the efficacy of FWA in this pathophysiological condition. The effect of FWA (10% w/w) shows that BV/TCV (%) increased over time at the fracture site, ultimately resulting in

maximum healing by day 23, even in the context of estrogen withdrawal. The three-dimensional μ-CT visualization illustrates the *in-vivo* bone-regeneration process under the influence of FWA (10% w/w), spanning from days 1 to 23 (Figure 6). Notably, bone volume normalized to tissue callus volume fraction (BV/TCV) exhibited a gradual increase over time, peaking on day 23, showcasing the efficacy of this intervention in facilitating bone healing, particularly in scenarios of delayed fracture repair.

Quantitative analysis in the osteoporotic fracture group for BV/TCV (%) illustrates ~ 37.0% on day 12 due to a delay in the healing process, compared to the expected ~73.0% in the normal fracture group by the same time frame. By day 23, this rose to ~77.0%

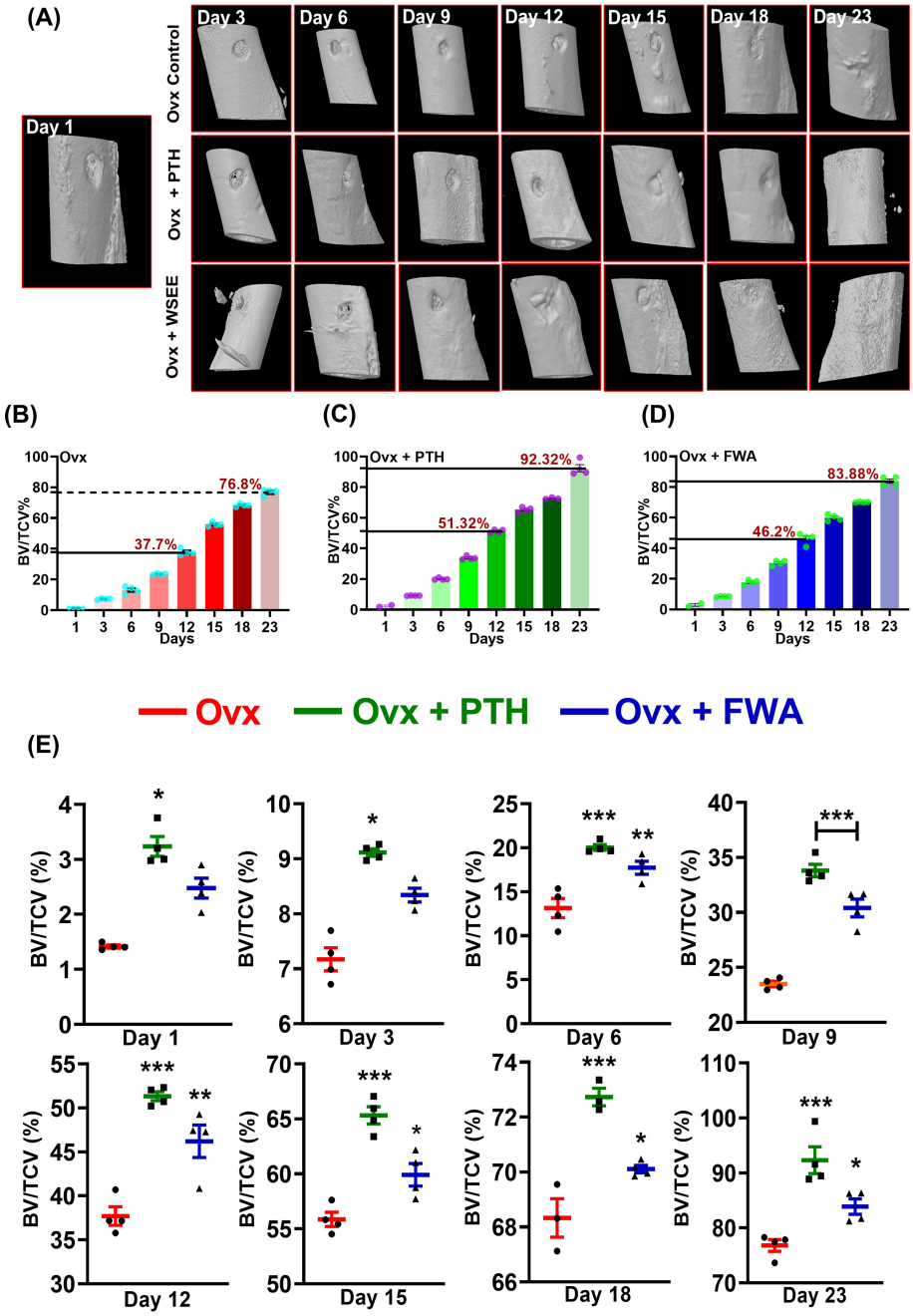

FIGURE 6
Quantitative assessment of bone regeneration in ovariectomized (Ovx) rats treated with PTH or FWA, focusing on bone volume to total callus volume (BV/TCV) measurements over time. **(A)** 3D reconstructed images from μ-CT scans showing the progression of bone healing in Ovx rats across different days (Day 3, 6, 9, and 12) for the Control (Ovx), Ovx + PTH, and Ovx + FWA treatment groups. The images illustrate the newly mineralized tissue formed at the fracture site over time. FWA treatment leads to faster and more extensive mineralization than PTH and control groups. **(B)** Quantification of μ-CT data of trabecular parameter represented in percentage of Bone volume/Tissue callus volume (% BV/TCV) in Ovx rats in comparison to different treatment with **(C)** PTH and **(D)** FWA. **(E)** Values of BV/TCV, % with respect to healing are represented in a time-specific manner. Data are represented as mean ± SEM compared to the control group (***p< 0.001, **p 0.002, *p 0.033).

(Figure 6). Contrastingly, in groups administered with PTH and FWA (10% w/w), BV/TCV (%) on day 12 showcased significant improvements, with PTH exhibiting a ~36% increase (51%) and FWA (10% w/w) showing a remarkable ~23% increase (46.0%) (Figures 6C). On day 23, BV/TCV continued to demonstrate enhancements, with PTH and FWA (10% w/w) displaying increases of approximately ~20% (92%) and ~9% (83%), respectively, compared to the prolonged 35-50 days typically required for delayed osteoporotic fracture healing processes (24). The administration of FWA (10% w/w) in the menopause (estrogen withdrawal) model showed a steady increase in BV/TCV (%) over the observed timeframe (Figure 6).

3.6 Histological and histomorphometric assessment of callus formation in estrogen withdrawal conditions

To evaluate the proportions of cartilage and bone within the fracture callus, micro-CT analysis was complemented by histological assessment of Safranin-O/Fast Green–stained callus tissue sections (Figure 7). The percentage of mineralized callus volume (MCV) relative to the total callus volume (TCV) was highest in the Ovx + PTH group, followed by the Ovx + FWA (10% w/w) group, and was lowest in the Ovx control group. This indicates that treatment with FWA (10% w/w) and PTH promoted greater mineralization of the callus compared to untreated Ovx controls (Figure 7). FWA (10% w/w) and PTH treatment showed better outcomes in reducing fracture gap width, which was measured for bone- regeneration at the fracture site when administered with FWA (10% w/w) and PTH at day 23 (Figure 7). Quantitative histomorphometry revealed a ~36% increase in mineralized cartilage volume. Safranin O staining reveals differences in cartilage content between the groups. The control group Ovx revealed mostly red-stained regions, which indicated that a higher percentage of cartilage was contained in the fracture callus. In contrast, the group Ovx + PTH showed fewer Safranin O-positive regions, indicating a process progressing towards bone formation with a reduced cartilage content. The Ovx + PTH group had the least cartilage staining, indicating more advanced healing with a higher degree of endochondral ossification and matrix remodeling, and was comparable to Ovx + FWA (10% w/w).

3.7 Modulation of osteoclast formation and activity in FWA (10% w/w) rats secures bone remodeling during the repair

Callus remodeling, which enables the conversion of cartilage to bone and remodeling of woven bone to lamellar bone, requires osteoclastic resorption. Osteoclast formation and activity were evaluated by histological examination of TRAP-stained fracture calluses 20-23 days post-fracture. This time frame coincides with the transition to the osteogenic phase of endochondral repair. FWA (10% w/w) on bone resorption was evaluated histologically by TRAP staining in bone tissue sections at 10X and 20X magnification. Figure 7 demonstrates that PTH and FWA (10% w/w) treatments significantly improve fracture healing compared to the Ovx control group.

It was interesting to observe that FWA (10% w/w) treatment of fractured groups demonstrated its ability to modulate and reduce osteoclast numbers, as evidenced by less TRAP+ve stained cells ~40% in contrast to the ovariectomized group that presented with a large number of TRAP +ve osteoclast cells, while PTH showed no effect on osteoclasts as assessed by OC NO./BS (Figure 7).

RT-qPCR analyses confirmed the decrease in osteoclastogenesis by FWA (10% w/w). Expression of several osteoclast-specific genes, including TRAP (Figure 7), RANKL (Figure 7), and Cathepsin K (Figure 7) robustly down-regulated compared with the ovariectomized group.

This means FWA (10% w/w) supports the whole cycle of bone remodeling and the process of fracture repair, and therefore, it could be a much more effective therapeutic agent that can accelerate healing.

3.8 Impact of FWA (10% w/w) on the material properties of bone formed at the fracture site

To assess if the differential healing mechanisms affect the mechanical behaviour of the healing bone, the quality of bone being formed was assessed by nano-indentation testing to assess Young's modulus (E) of the FWA (10% w/w) groups in comparison to the Ovx and PTH treated (positive control) groups. Figure 8 shows the mechanical testing setup to assess the biomechanical properties of bone specimens, especially measuring bone material properties. The graph and equation highlight Poisson's ratio calculation. Poisson's ratio (**v**) is derived from the relationship between Young's modulus (E) and shear modulus (G) using the formula.

v = (E–2G)/(2E). This provides insight into the elastic behaviour of the bone tissue under mechanical stress (Figure 8).

$$E = \sigma/\varepsilon$$

where E is the Young's modulus
σ is the ultimate stress (MPa)
ε is the strain

$$Poisson's \quad Ratio(v) = (E - 2G)/(2E)$$

$$\text{Bulk} \quad \text{Modulus(K)} = E - [3(1 - 2 \quad v)]$$

The progression of Young's modulus over time (Days 1-23) in three experimental groups under estrogen withdrawal conditions is represented in (Figure 8). FWA (10% w/w) treatment significantly improves the biomechanical properties of bone during healing in ovariectomized models, surpassing the effects of PTH. FWA (10% w/w)-treated bones exhibit superior stiffness, toughness, and overall mechanical integrity, indicating its potential as an effective therapeutic agent for enhancing bone healing and recovery, particularly under estrogen-deficient conditions (Figure 8).

10.3389/fendo.2025.1540237

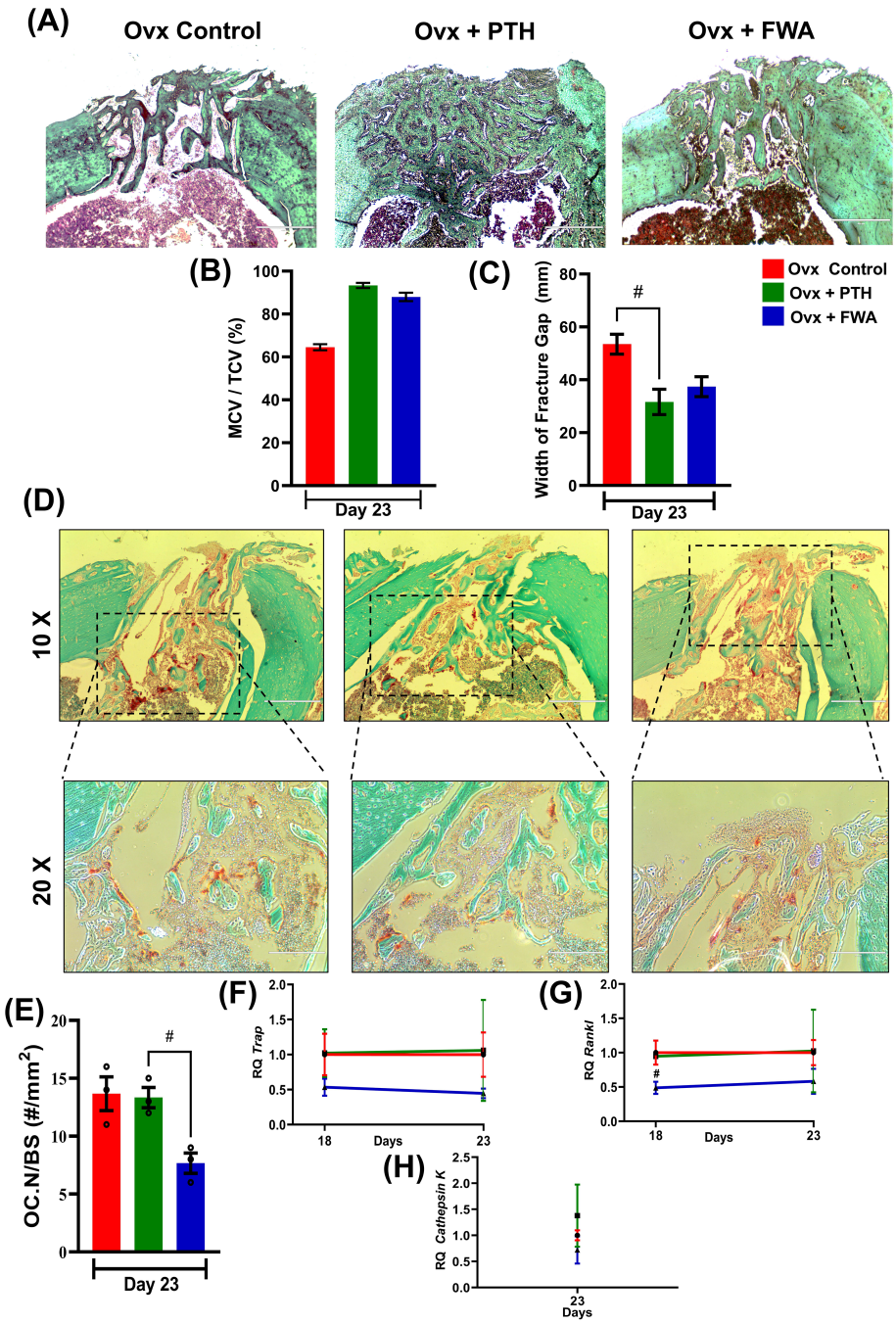

FIGURE 7
Histological and histomorphometric analysis of fracture healing in ovariectomized (Ovx) rats treated with PTH or FWA. **(A)** Representative images of fractured bone sections stained with Safranin O (to visualize cartilage) in Ovx Control, Ovx + PTH, and Ovx + FWA groups on Day 23. The images highlight differences in cartilage and bone remodeling among the groups. **(B)** Mineralized callus volume as a percentage of total callus volume (MCV/TCV): PTH and FWA treatments increased MCV/TCV compared to Ovx Control, indicating enhanced mineralization. **(C)** Quantification of the fracture gap width (mm) on Day 23. The Ovx control group exhibited the largest fracture gap, while both PTH and FWA treatments significantly reduced the fracture gap size. PTH treatment led to the smallest fracture gap, indicating superior bone regeneration. **(D)** Representative TRAP (Tartrate-resistant acid phosphatase) staining images of fracture callus sections on Day 23 from Ovx control (red), Ovx + PTH (green), and Ovx + FWA (blue) groups. The images at 10X and 20X magnification demonstrate osteoclast activity and bone resorption at the fracture site. **(E)** Quantification of osteoclast numbers per bone surface area (OC. N/BS, #/mm^2) on Day 23. The Ovx control group showed the highest osteoclast numbers, while FWA treatments significantly reduced osteoclast activity compared to Ovx control and PTH groups. The FWA group exhibited the lowest osteoclast number, suggesting enhanced inhibition of bone resorption. Quantitative analysis of gene expression levels over time for different treatment groups: Control (F, red), F + PTH (green), and F + FWA (blue) is shown with respect to different phases for TRAP **(F)** RANKL **(G)**, Cathepsin K **(H)**. Data are presented as mean ± SEM, with statistical significance ($^{\#}$p 0.033) compared to the Ovx control group. # denotes statistically significant downregulation relative to the control.

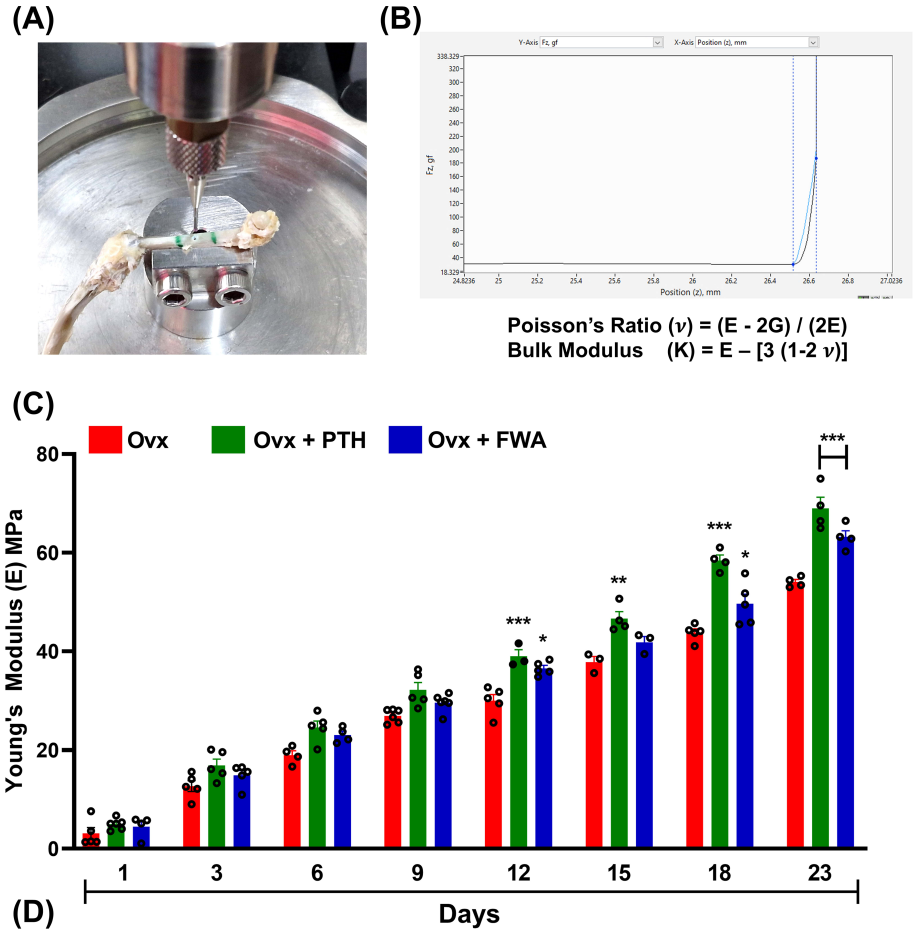

Material Properties / Parameters	Day 12			Day 23		
	Ovx	Ovx + PTH	Ovx + FWA	Ovx	Ovx + PTH	Ovx + FWA
Young Modulus (E) MPa	30.01 ± 2.78	39.00 ± 2.28	36.54 ± 1.37	54.06 ± 1.03	65.71 ± 4.44	63.19 ± 2.54
Bulk Modulus (K) MPa	28.01 ± 2.78	37.00 ± 2.28	35.25 ± 1.81	52.40 ± 0.94	68.34 ± 4.35	46.64 ± 4.32
Toughness (gf mm)	5.86 ± 0.38	10.24 ± 1.27	9.08 ± 1.28	9.65 ± 1.45	17.83 ± 5.99	14.65 ± 0.70

FIGURE 8
Biomechanical analysis of bone healing in ovariectomized (Ovx) rats treated with PTH or FWA. **(A)** Image showing the mechanical testing setup used to measure the biomechanical properties of healing tibiae, specifically Young's modulus, using Biomomentum Mach 1 v500css. **(B)** Graph and equation illustrating the calculation of Poisson's ratio (*v*) based on the relationship between Young's modulus **(E)** and shear modulus **(G)**. This provides insights into the elastic deformation behaviour of bone under applied force. **(C)** Young's modulus (E, MPa) of cortical bone from Day 1 to Day 23 post-fracture in Ovx models treated with Control (red), PTH (green), or FWA (blue). PTH and FWA treatment significantly improved Young's modulus, showing the highest mechanical stiffness across all time points, particularly from Day 12 onwards. **(D)** Table summarizing key material properties (Young's modulus, bulk modulus, and toughness) measured on Days 12 and 23. FWA-treated bones exhibited superior mechanical properties compared to the control, with higher Young's modulus, bulk modulus, and toughness, especially on Day 23, indicating enhanced fracture healing. Data are presented as mean ± SEM, with statistical significance (***p < 0.001, **p 0.002, *p 0.05) compared to the Ovx control group.

3.9 Effect of FWA (10% w/w) on gene Expression at the fracture site

Compared to the Ovx fracture group, the mRNA level increased temporally, corresponding to the stages of inflammation, endochondral bone formation and remodeling phases. During the initial stages, periosteal cells exhibited a robust response to BMP2 (Figure 9), particularly noticeable on days 1, 3, and 6. Notably, on day 3, there was a significant increase in BMP2 gene expression, approximately (~9.0-fold) for PTH and about (~5.0-fold) for FWA (10% w/w), indicating a pronounced promotion of chondrogenesis followed by osteogenesis. As angiogenic cells began forming small blood vessels and fibrovascular tissue, upregulation of genes was

observed in both PTH and FWA (10% w/w) at 125 mg.kg^{-1} by day 6. This was evidenced by notable increases in Sox9 (Figure 9) (~7.74-fold and ~9.31-fold respectively), Col2a1 (Figure 9) (~9.52-fold and ~6.22-fold respectively), and Aggrecan (Figure 9) (Acan) on day 9 (~17.20-fold and ~7.53-fold respectively), indicating progression towards endochondral bone formation. Subsequent stages involved the remodeling of bone tissue, marked by the expression of specific markers in both PTH and FWA (10% w/w) at 125 mg.kg^{-1}. Notably, Col10a1 (Figure 9) exhibited increased expression on day 9 (~4.40-fold and ~3.67-fold, respectively), followed by Col1a1 (Figure 9) on day 12 (~7.57-fold and ~12.01-fold respectively). The expression of Runx2 (Figure 9) peaked on day 18 (~15.76-fold and ~9.11-fold, respectively), while that of PTH and FWA (10% w/w) decreased the expression of SMAD-specific E3 ubiquitin-protein ligases which degrades Runx2, at day 18. We observed that Smurf 1 was decreased by ~0.2835-fold and ~0.3296-fold respectively (Figure 9) and Smurf 2 by ~0.026-fold and ~0.3240-fold respectively (Figure 9), coinciding with mineralized marker expression such as Ocn (Figure 9) on day 18 (~14.81-fold and ~8.95-fold respectively) and Opn (Figure 9) on day 23 (~24.59-fold and ~18.73-fold respectively). These findings underscore a coordinated cascade of events leading to bone formation and maturation.

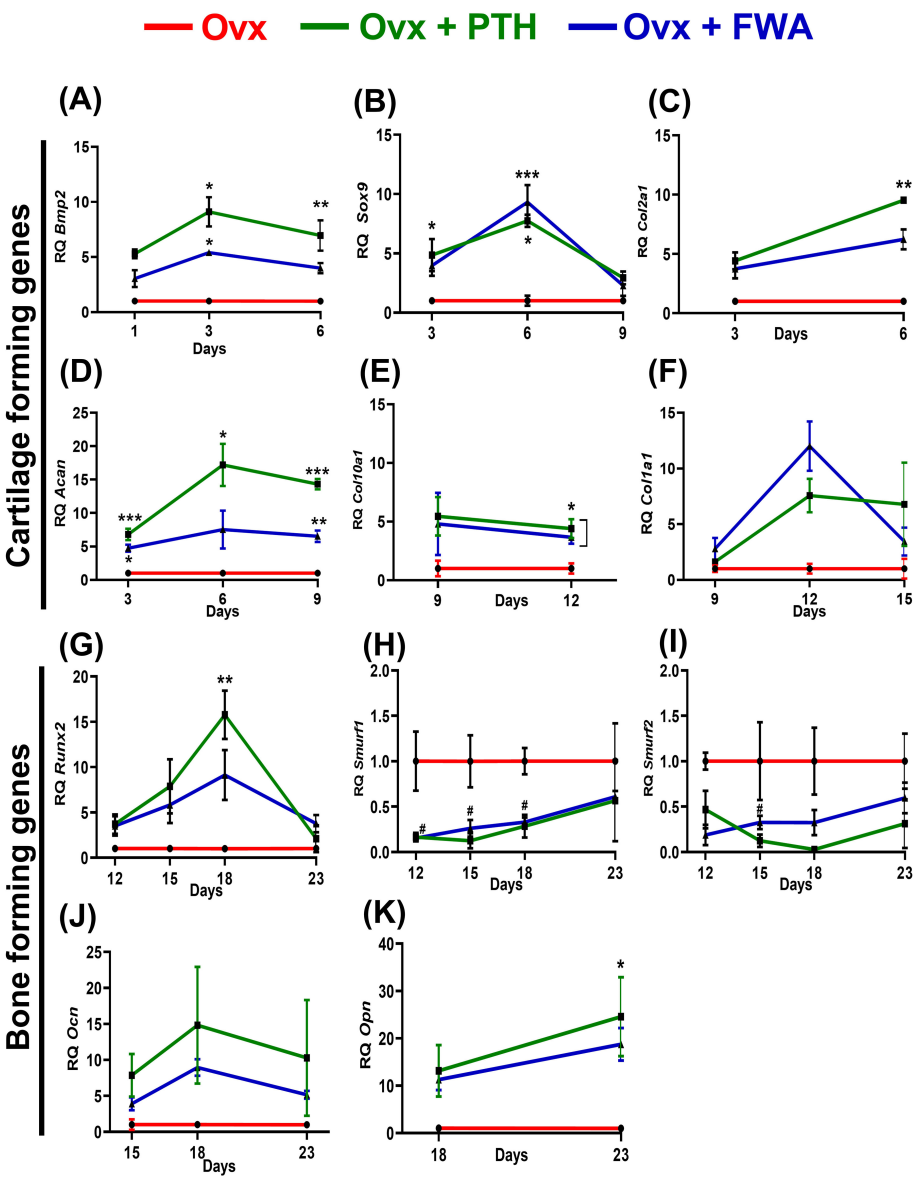

FIGURE 9
Analysis of gene expression levels in ovariectomized (Ovx) rats treated with Parathyroid Hormone (PTH) or Withania somnifera enriched extract (FWA). Quantitative analysis of gene expression levels over time for different treatment groups: Control (F, red), F + PTH (green), and F + FWA (blue) is shown with respect to different phases for BMP2 **(A)** Sox9 **(B)**, Col2a1 **(C)**, Acan **(D)**, Col1a1 **(E)**, Col10a1 **(F)**, Runx2 **(G)**, Smurf 1 **(H)**, Smurf 2 **(I)** Ocn **(J)**, Opn **(K)**. Statistical significance is denoted as follows: ***p< 0.001, **p 0.002, *p 0.033. Data are presented as mean ± SEM. ***p < 0.001, **p 0.002, *p 0.033, $^{\#}$p 0.05. Data are presented as mean ± SEM. * indicate significant upregulation compared to the control group, while # denotes statistically significant downregulation relative to the control.

4 Discussion

This study examines the effectiveness of FWA (10% w/w) at different dosages and strengths on fracture healing, including the potential of its acceleration in callus formation and mineralization at the fracture site in healthy and estrogen-cut-down (Menopausal) rats.

Our findings show that a dose of 125 $mg.kg^{-1}$ of FWA (10% w/w) enrichment consistently improved key indices of fracture healing, including total callus volume, mineralized tissue volume, and bone volume, as compared to other doses and PTH treatment.

At the fracture site, administration of FWA (10% w/w) led to a notable decrease in the activity of osteoclast marker genes, indicating reduced bone resorption. Simultaneously, there was an increase in anabolic responses, as evident by including heightened expression of osteogenic markers (25) and by downregulating the expression of E3 ubiquitin ligase genes Smurf 1 and Smurf 2 which are responsible for degradation of Runx2, a key transcription factor for bone formation phase. By keeping Smurf 1 and 2 levels significantly low, FWA (10% w/w) may have provided early bone-forming effects in different physiological models. These molecular changes facilitated endochondral ossification and bone remodeling, resulting in a remarkable increase in bone volume/tissue volume (BV/TCV %) by day 12, significantly faster than the normal healing process that takes 21-35 days for complete fracture healing in the rodents (Figure 10) (24).

The pharmacokinetic profiling of FWA (10% w/w) at 125 $mg.kg^{-1}$ confirmed an optimized formulation enriched with Withaferin A (WFA), as evidenced by its high plasma concentration (Cmax) and area under the curve (AUC). Withanolide profiling revealed rapid absorption and a prolonged half-life for WFA, suggesting it may drive FWA's (10% w/w) efficacy in fracture repair. The Tmax and extended plasma half-life of WFA indicate favourable pharmacokinetics for fracture healing applications. These properties, along with FWA's (10% w/w) favourable log P and total polar surface area, suggest an optimal balance of lipophilicity and permeability conducive to its therapeutic activity in rapid fracture models.

The effectiveness of FWA (10% w/w) was compared to Parathyroid Hormone (PTH), a well-known stimulator of bone healing (26). Animal experiments show that PTH can improve normal fracture healing (27, 28). While PTH increased Bone Volume to completion, FWA (10% w/w) was also able to achieve almost the same value (~95%). This nearly equivalent bone-regeneration by FWA (10% w/w) suggests that it could be a potent alternative for PTH, with reduced side effects. PTH, which primarily aided bone healing through bone modelling. Studies show that PTH treatment in mice delays the complete replacement of cartilage anlagen by endochondral bone during skeletal repair due to the inhibitory effect of PTH on chondrocyte maturation. However, it improves biomechanical properties by enhancing osteoblastogenesis and new bone formation (13). In contrast, FWA (10% w/w) effectively reduced osteoclast activity and promoted bone remodelling, indicating a more balanced and comprehensive approach to bone regeneration. Bone stiffness has also been shown to be significantly influenced by the degree of bone mineralization; several studies have described a direct relationship between Young's modulus, a material index of stiffness, and bone mineral density (29, 30).

In a menopausal model, which mimics delayed healing due to estrogen deficiency, FWA (10% w/w) showed significant callus mineralization over the time period, achieving significant increases in BV/TCV by day 23 and underscoring its potential to support fracture repair under osteoporotic conditions. Histological analysis confirmed greater mineralized callus volume and reduced cartilage proportions in the FWA (10% w/w) and PTH groups

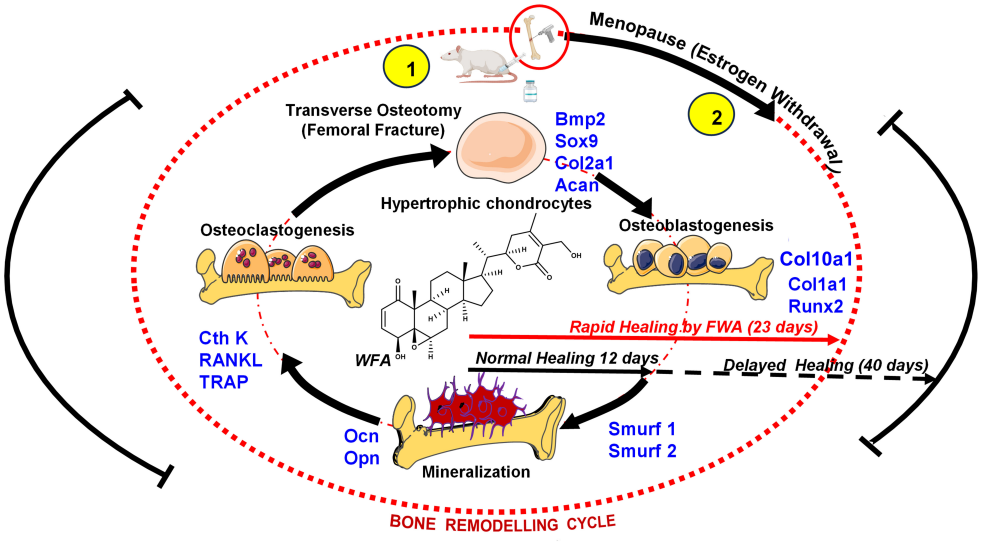

FIGURE 10
Schematic representation to show how FWA administration in rodents modulates the bone remodeling cycle at the molecular level to accelerate bone formation at the time of menopause (estrogen deficiency) and in fractures (transverse osteotomy).

compared to controls, suggesting that FWA (10% w/w) facilitates endochondral ossification. FWA (10% w/w) restored the callus area and promoted bone healing with better mechanical strength (Young's Modulus). These positive results were accomplished within 23 days, thus shortening by approximately 30% from the standard healing time to 35-50 days (31).

This study highlights the promising potential of wound-healing enriched *Withania somnifera* extract (FWA, 10%w/w) in accelerating fracture healing and improving bone regeneration in typical and estrogen-deficient (menopausal) conditions. FWA (10% w/w) has been found to show excellent improvements in callus formation and mineralization that are very effective in stimulating osteoblast activity and thereby balancing osteoclast function for effective healing. FWA (10% w/w) is a less expensive and accessible alternative with broad therapeutic potential in addressing the limitations of conventional therapies. These findings, therefore, provide a robust foundation to advance FWA (10% w/w) into clinical applications and pave the way for its use as a novel agent in bone health management.

This study highlights the efficacy of FWA (10% w/w) in promoting fracture healing; however, several areas merit further exploration to enhance its practical application. Based on the pharmacokinetics observed in this research, investigating alternative drug delivery methods with FWA (10% w/w) —such as nano formulations, or combination therapies with existing therapeutic agents—could significantly improve bioavailability and its potential.

However, it is essential for future studies with FWA (10% w/w) beyond current preclinical models that includes large-animal models for better simulate human bone physiology. Conducting clinical trials to evaluate the efficacy of FWA (10% w/w) in patients with osteoporosis or those experiencing impaired fracture healing will be vital for translating these findings into clinical practice. Addressing these aspects will further validate FWA's (10% w/w) potential as a cost-effective, safe, and effective therapeutic option for bone repair and fracture healing.

5 Conclusion

The findings summarize FWA's (10% w/w) potential to support the biological process of bone remodeling by modulating osteoclast activity, promoting osteoblast differentiation, and enhancing the mechanical integrity of healing bone. Such characteristics place FWA (10% w/w) in a lead position as a therapeutic agent to hasten fracture healing, especially in delayed bone repair.

Besides overcoming the excessive expense of pure Withaferin A, FWA (10% w/w) has several other benefits. Its enriched composition increases bioavailability and prolonged plasma concentration, corresponding to more efficient therapeutics' effects. In contrast to common anabolic drugs like Parathyroid Hormone (PTH), Which mainly include bone growth but have little impact on osteoclast regulation, FWA (10% w/w) reveals a greater therapeutic potential in enhancing osteogenesis while suppressing uncontrolled osteoclast activity, thus ensuring harmonious remodeling of bones. This is particularly evident in osteoporotic fractures, where enhanced bone resorption can result in delayed healing or non-union.

Additionally, the effectiveness of FWA (10% w/w) in inhibiting systemic inflammation offers another benefit, as chronic inflammation plays a significant role in impaired bone repair in postmenopausal osteoporosis and other skeletal diseases. Its capacity to advance the process from the fibrovascular stage towards bone remodeling sets it apart as a treatment with the potential to reduce recovery time.

Further, FWA's (10% w/w) beneficial pharmacokinetics, such as slow plasma half-life and ideal absorption rate, underpin its potential to be given orally- providing a minimally invasive alternative to injectable anabolic drugs currently employed in fracture repair. Such properties and their efficacy in estrogen-deficient states indicate that FWA (10% w/w) may be versatile therapeutic agent for generalised clinical use in managing bone metabolic disorders.

Data availability statement

The raw data supporting the conclusions of this article will be made available by the authors, without undue reservation.

Ethics statement

The animal study was approved by Institutional Animal Ethics Board (CSIR-CDRI). The study was conducted in accordance with the local legislation and institutional requirements.

Author contributions

KC: Conceptualization, Data curation, Formal analysis, Investigation, Methodology, Resources, Software, Writing – original draft, Writing – review & editing. NR: Data curation, Formal analysis, Methodology, Writing – review & editing. AS: Data curation, Formal analysis, Writing – review & editing. AY: Data curation, Formal analysis, Methodology, Writing – review & editing. DR: Data curation, Formal analysis, Writing – review & editing. AR: Data curation, Methodology, Writing – review & editing. BM: Data curation, Methodology, Writing – review & editing. SV: Data curation, Methodology, Writing – review & editing. AT: Data curation, Methodology, Writing – review & editing. GD: Data curation, Methodology, Writing – review & editing. LH: Data curation, Formal analysis, Methodology, Writing – review & editing. PM: Conceptualization, Data curation, Formal analysis, Investigation, Methodology, Writing – review & editing. RT: Conceptualization, Data curation, Formal analysis, Funding acquisition, Investigation,

Methodology, Project administration, Resources, Software, Supervision, Validation, Visualization, Writing – original draft, Writing – review & editing.

Funding

The author(s) declare that financial support was received for the research and/or publication of this article. Sanction Number: 5/258/107/2020-NMITLI dated 02-06-2021.

Acknowledgments

The authors thank the CSIR- Central Drug Research Institute (CSIR-CDRI) Director for providing necessary research facilities. Instrumentation facilities from the Biological Central Facility (BCF) and CSIR- Central Institute of Aromatic and Medicinal Plants (CSIR-CIMAP) are gratefully acknowledged for the confocal microscopy experimentations. We sincerely acknowledge Dr. Rajendra P. Patel for his help on this occasion. We also thank Geet Kumar Nagar for the histological slide's preparation from the Division of Endocrinology, CSIR-CDRI, for the technical help. We also thank Dr. Lal Hingorani (Pharmanza India Pvt. Ltd.) for providing the *Withania somnifera* enriched extract. This manuscript bears CDRI communication number 55/2025/RT. The author KC is thankful to the Indian Council of Medical Research, New Delhi; AS, AY, AT are thankful to the Council of Scientific & Industrial Research, New Delhi; DR, AR, BM, SV are grateful to the University Grants Commission, New Delhi, for the financial assistance in the form of fellowships.

Conflict of interest

Author LH was employed by Pharmanza Herbals Pvt Ltd.

The remaining authors declare that the research was conducted in the absence of any commercial or financial relationships that could be construed as a potential conflict of interest.

Generative AI statement

The author(s) declare that no Generative AI was used in the creation of this manuscript.

Publisher's note

References

1. Panevin TS, Bobkova AO, Karateev AE, Zotkin EG. Endogenous estrogen deficiency and the development of chronic musculoskeletal pain: A review. *Ter Arkh*. (2022) 94:683–8. doi: 10.26442/00403660.2022.05.201490

2. Cheng C-H, Chen L-R, Chen K-H. Osteoporosis due to hormone imbalance: an overview of the effects of estrogen deficiency and glucocorticoid overuse on bone turnover. *Int J Mol Sci*. (2022) 23:1376. doi: 10.3390/ijms23031376

3. Chen L, Shao C, Sun K, Wang J, Liu X, Zhao Y, et al. Changes in macrophage and inflammatory cytokine expressions during fracture healing in an ovariectomized mice model. *BMC Musculoskelet Disord*. (2021) 22:494. doi: 10.1186/s12891-021-04360-z

4. Beeharry MW, Ahmad B. Principles of fracture healing and fixation: A literature review. *Cureus*. (2024) 16(12):e76250. doi: 10.7759/cureus.76250

5. Steppe L, Megafu M, Tschaffon-Müller MEA, Ignatius A, Haffner-Luntzer M. Fracture healing research: Recent insights. *Bone Rep*. (2023) 19:101686. doi: 10.1016/j.bonr.2023.101686

6. Loi F, Córdova L, Pajarinen J, Lin T, Yao Z, Goodman S. Inflammation, fracture and bone repair. *Bone*. (2016) 86:119–30. doi: 10.1016/j.bone.2016.02.020

7. Bastian O, Pillay J, Alblas J, Leenen L, Koenderman L, Blokhuis T. Systemic inflammation and fracture healing. *J Leukoc Biol*. (2011) 89:669–73. doi: 10.1189/jlb.0810446

8. Malutan AM, Dan M, Nicolae C, Carmen M. Proinflammatory and anti-inflammatory cytokine changes related to menopause. *Menopausal Rev*. (2014) 3:162–8. doi: 10.5114/pm.2014.43818

9. Knight MN, Hankenson KD. Mesenchymal stem cells in bone regeneration. *Adv Wound Care (New Rochelle)*. (2013) 2:306–16. doi: 10.1089/wound.2012.0420

10. Neagu TP, Ţigliş M, Cocoloş I, Jecan CR. The relationship between periosteum and fracture healing. *Rom J Morphol Embryol*. (2016) 57:1215–20.

11. Schmidt I, Albert J, Ritthaler M, Papastavrou A, Steinmann P. Bone fracture healing within a continuum bone remodelling framework. *Comput Methods Biomech BioMed Engin*. (2022) 25:1040–50. doi: 10.1080/10255842.2021.1998465

12. Gautam J, Khedgikar V, Kushwaha P, Choudhary D, Nagar G, Dev K, et al. Formononetin, an isoflavone, activates AMP-activated protein kinase/β-catenin signalling to inhibit adipogenesis and rescues C57BL/6 mice from high-fat diet-induced obesity and bone loss. *Br J Nutr*. (2017) 117:645–61. doi: 10.1017/S0007114517000149

13. Lee KK, Changoor A, Grynpas MD, Mitchell J. Increased osteoblast GαS promotes ossification by suppressing cartilage and enhancing callus mineralization during fracture repair in mice. *JBMR Plus*. (2023) 7:e10841. doi: 10.1002/jbm4.10841

14. Sardar A, Gautam S, Sinha S, Rai D, Tripathi A, Dhaniya G, et al. Nanoparticles of naturally occurring PPAR-γ inhibitor betulinic acid ameliorates bone marrow adiposity and pathological bone loss in ovariectomized rats via Wnt/β-catenin pathway. *Life Sci*. (2022) 309:121020. doi: 10.1016/j.lfs.2022.121020

15. Sardar A, Rai D, Tripathi A, Chutani K, Sinha S, Dhaniya G, et al. FDA-approved polypeptide PTH 1–34 impedes palmitic acid-mediated osteoblasts dysfunction by promoting its differentiation and thereby improving skeletal health. *Mol Cell Endocrinol*. (2025) 597:112445. doi: 10.1016/j.mce.2024.112445

16. Modi SJ, Tiwari A, Ghule C, Pawar S, Saste G, Jagtap S, et al. Pharmacokinetic study of withanosides and withanolides from withania somnifera using ultra-high performance liquid chromatography-tandem mass spectrometry (UHPLC-MS/MS). *Molecules*. (2022) 27:1476. doi: 10.3390/molecules27051476

17. Rai D, Tripathi A, Sardar A, Pandey A, Sinha S, Chutani K, et al. A novel BMP2 secretagogue ameliorates glucocorticoid induced oxidative stress in osteoblasts by activating NRF2 dependent survival while promoting Wnt/β-catenin mediated osteogenesis. *Free Radic Biol Med*. (2022) 190:124–47. doi: 10.1016/j.freeradbiomed.2022.08.007

18. Jaiswal AK, Raj A, Kushawaha A, Maji B, Bhatt H, Verma S, et al. Design, synthesis and biological evaluation of new class of pyrazoles-dihydropyrimidinone derivatives as bone anabolic agents. *Bioorg Chem*. (2025) 157:108216. doi: 10.1016/j.bioorg.2025.108216

19. Wang C, Zhang X, Chen R, Zhu X, Lian N. EGR1 mediates METTL3/m6A/CHI3L1 to promote osteoclastogenesis in osteoporosis. *Genomics*. (2023) 115:110696. doi: 10.1016/j.ygeno.2023.110696

20. Kothari P, Dhaniya G, Sardar A, Sinha S, Girme A, Rai D, et al. A glucuronated flavone TMMG spatially targets chondrocytes to alleviate cartilage degeneration through negative regulation of IL-1β. *Biomed Pharmacother*. (2023) 163:114809. doi: 10.1016/j.biopha.2023.114809

21. Piccoli A, Cannata F, Strollo R, Pedone C, Leanza G, Russo F, et al. Sclerostin regulation, microarchitecture, and advanced glycation end-products in the bone of elderly women with type 2 diabetes. *J Bone Miner Res*. (2020) 35:2415–22. doi: 10.1002/jbmr.4153

22. Thomas PK, Sullivan LK, Dickinson GH, Davis CM, Lau AG. The effect of helium ion radiation on the material properties of bone. *Calcif Tissue Int*. (2021) 108:808–18. doi: 10.1007/s00223-021-00806-7

23. Dincel YM, Alagoz E, Arikan Y, Caglar A, Dogru S, Ortes F, et al. Biomechanical, histological, and radiological effects of different phosphodiesterase inhibitors on femoral fracture healing in rats. *J Orthop Surg (Hong Kong)*. (2018) 26:2309499018777885. doi: 10.1177/2309499018777885

24. Oliver RA, Yu Y, Yee G, Low A, Diwan A, Walsh W. Poor histological healing of a femoral fracture following 12 months of oestrogen deficiency in rats. *Osteoporos Int*. (2013) 24:2581–9. doi: 10.1007/s00198-013-2345-2

25. Husain A. Empagliflozin may be a game changer in managing pulmonary embolism: A case report. *Mymensingh Med J*. (2024) 33:311–2.

26. Zhang D, Potty A, Vyas P, Lane J. The role of recombinant PTH in human fracture healing: a systematic review. *J Orthop Trauma*. (2014) 28:57–62. doi: 10.1097/BOT.0b013e31828e13fe

27. Menger MM, Tobias A, Bauer D, Bleimehl M, Scheuer C, Menger M, et al. Parathyroid hormone stimulates bone regeneration in an atrophic non-union model in aged mice. *J Transl Med*. (2023) 21:844. doi: 10.1186/s12967-023-04661-y

28. Ellegaard M, Kringelbach T, Syberg S, Petersen S, Beck Jensen J, Brüel A, et al. The effect of PTH(1-34) on fracture healing during different loading conditions. *J Bone Mineral Res*. (2013) 28:2145–55. doi: 10.1002/jbmr.1957

29. Mulder L, Koolstra JH, den Toonder JMJ, van Eijden TMGJ. Relationship between tissue stiffness and degree of mineralization of developing trabecular bone. *J BioMed Mater Res A*. (2008) 84:508–15. doi: 10.1002/jbm.a.v84a:2

30. Morgan EF, Unnikrisnan GU, Hussein AI. Bone mechanical properties in healthy and diseased states. *Annu Rev BioMed Eng*. (2018) 20:119–43. doi: 10.1146/annurev-bioeng-062117-121139

31. Khajuria DK, Soliman M, Elfar J, Lewis G, Abraham T, Kamal F, et al. Aberrant structure of fibrillar collagen and elevated levels of advanced glycation end products typify delayed fracture healing in the diet-induced obesity mouse model. *Bone*. (2020) 137:115436. doi: 10.1016/j.bone.2020.115436

frontiers | Frontiers in Endocrinology

TYPE Original Research
PUBLISHED 08 May 2025
DOI 10.3389/fendo.2025.1535509

OPEN ACCESS

EDITED BY
Fátima Baptista,
Universidade de Lisboa, Portugal

REVIEWED BY
Hengyi Xu,
The University of Texas at Austin, United States
Wu Xujin,
The Second Affiliated Hospital of Soochow University, China

*CORRESPONDENCE
Yan Liu
liuyan95@126.com

†These authors have contributed equally to this work

RECEIVED 27 November 2024
ACCEPTED 14 April 2025
PUBLISHED 08 May 2025

CITATION
Liu H, Xiang R, Liu C, Chen Z, Shi Y, Liu Y and Liu Y (2025) Association between cardiometabolic index and bone mineral density among adolescents in the United States.
Front. Endocrinol. 16:1535509.
doi: 10.3389/fendo.2025.1535509

Association between cardiometabolic index and bone mineral density among adolescents in the United States

Haobiao Liu[1,2†], Rongqi Xiang[2†], Chenyue Liu[3†], Zhuohang Chen[4], Yuhang Shi[5], Yiting Liu[6] and Yan Liu[1*]

[1]Department of Dermatology, The Second Affiliated Hospital of Xi'an Jiaotong University, Xi'an, China, [2]Department of Occupational and Environmental Health, School of Public Health, Health Science Center, Xi'an Jiaotong University, Xi'an, China, [3]Department of Radiology, The First Affiliated Hospital of Xi'an Jiaotong University, Xi'an, China, [4]Department of Epidemiology, School of Public Health, Shanghai Institute of Infectious Disease and Biosecurity, Fudan University, Shanghai, China, [5]School of Basic Medical Sciences, Shanghai Jiaotong University, Shanghai, China, [6]Faculty of Medicine, Dentistry and Health Sciences, Melbourne School of Population and Global Health, The University of Melbourne, Melbourne, VIC, Australia

Objectives: The cardiometabolic index (CMI) serves as a comprehensive metric for evaluating cardiometabolic health, and is correlated with several health outcomes. However, research examining the relationship between CMI and bone mineral density (BMD), particularly in adolescent populations, remains limited and warrants further investigation.

Methods: The weighted multiple linear regression analysis was conducted to elucidate the association between CMI and BMD.

Results: Our study ultimately included 1,514 participants. After adjusting for pertinent covariates, we observed that per-unit increases in the CMI corresponded with reductions in BMD by 0.052 g/cm^2 for femoral neck (β=-0.052, 95% CI: -0.087 to -0.018) and 0.048 g/cm^2 for lumbar spine (L1-L4) (β=-0.048, 95% CI: -0.085 to -0.011). In quartile analyses, individuals in the highest quartile displayed significantly reduced BMD at the femoral neck (β=-0.036, 95% CI: -0.064 to -0.007) and lumbar spine (L1-L4) (β=-0.041, 95% CI: -0.070 to -0.011) compared to those in the lowest quartile (P<0.05). No statistical significance was detected between CMI and BMD at the total femur, trochanter, and intertrochanter sites. Furthermore, stratified analyses indicated no significant interactions involving age, sex, or race in relation to CMI and BMD.

Conclusions: In the adolescent population, CMI is inversely related to BMD. These findings highlight a potential link between cardiometabolic health and bone health. Future longitudinal investigations are warranted to determine causal relationships and underlying mechanisms.

KEYWORDS

cardiometabolic index, bone mineral density, adolescents, population-based study, NHANES

1 Introduction

Skeletal health during adolescence plays a crucial role in lifelong well-being. This period marks a critical window for the rapid accrual of bone mineral density (BMD), which largely determines the peak BMD achieved in adulthood and its maintenance over time. Peak BMD has a significant correlation with the risk of developing osteoporosis and experiencing fractures in later life, as fluctuations in BMD can increase the susceptibility to fragility fractures and other bone-related diseases (1). Therefore, understanding the factors influencing BMD during adolescence is of paramount clinical importance for preventing osteoporosis and promoting optimal skeletal health.

In recent years, the potential relationship between cardiometabolic health indicators and bone health has gained significant attention, particularly in pediatric and adolescent populations. The cardiometabolic index (CMI) is a composite marker that integrates both lipid profiles and central obesity to assess cardiometabolic risk. CMI is calculated as triglyceride (TG) to high-density lipoprotein cholesterol (HDL-C) ratio multiplied by waist-to-height ratio (WHtR). This index has been widely used to evaluate metabolic dysfunction and cardiovascular disease risk. However, its relationship with bone health remains underexplored. Given that dysregulated lipid metabolism and obesity-related inflammation are known to influence bone metabolism, CMI may serve as a valuable indicator for assessing the relationship between cardiometabolic health and BMD.

Lipid metabolism plays a key role in skeletal health. For instance, elevated TG levels have been linked to lower BMD in older adults, revealing an inverse association between lipid profiles and BMD (2). Lipidomics profiling also indicates significant alterations in lipid composition among individuals with low BMD compared to those with normal BMD (3). Additionally, a Mendelian randomization study supports the causal relationship between lipid metabolites and bone health (4). Furthermore, obesity, a known risk factor for cardiovascular diseases, is closely associated with changes in bone quality. Studies have indicated that excessive adipose tissue may secrete adipokines such as leptin and adiponectin, which can influence bone metabolism and remodeling (5). The accumulation of visceral fat during early life negatively impacts bone health, consequently elevating the risk of osteopenia and osteoporosis in adults and the elderly (6).

Although the relationship between cardiometabolic health and conditions such as depression (7), non-alcoholic fatty liver disease (8), and chronic obstructive pulmonary disease (9) has been explored, there is a scarcity of research focusing on its association with BMD, particularly in adolescent populations. Adolescence is not only a pivotal period for BMD accrual but also a time of significant physiological changes in the cardiometabolic system, necessitating further investigation in this unique cohort. During this developmental stage, bone metabolism is particularly sensitive to nutritional, hormonal, and cardiometabolic factors. Understanding the influence of cardiometabolic health on BMD during adolescence will provide valuable insights into the early prevention of chronic conditions such as osteoporosis, cardiovascular diseases, and metabolic syndrome. Moreover, elucidating the link between CMI and BMD may help determine whether CMI can serve as a potential indicator for skeletal health assessment in adolescents.

Against this backdrop, the present study aims to evaluate the association between CMI and BMD in adolescents, addressing an existing gap in the literature and providing new insights into the potential role of CMI as an alternative indicator for skeletal health.

2 Materials and methods

2.1 Study design and population

Information was extracted from the NHANES spanning from 2005 to 2010, which involved 4,865 participants within the age range of 12 to 19. Following this, individuals without BMD information (n=711), those lacking complete CMI data or presenting abnormal values (n=36), and participants with missing covariate information (n=158) were excluded from the analysis. Ultimately, this resulted in the inclusion of 1,514 participants in the study (Supplementary Figure S1).

2.2 Evaluation of CMI

CMI was derived from anthropometric and biochemical measurements, specifically height, waist circumference (WC), TG, and HDL-C. TG and HDL-C were measured using an enzymatic method on a Roche Modular P Chemistry Analyzer (Roche Diagnostics, Indianapolis, IN, USA). Quality control procedures followed the guidelines of the National Center for Health Statistics. Initially, the WHtR was computed as the ratio of WC to height. Subsequently, CMI was calculated by multiplying the WHtR by the ratio of TG to HDL-C, as shown in the formula below.

$$\mathrm{CMI} = (\mathrm{TG}/\mathrm{HDL} - \mathrm{C}) \times \mathrm{WHtR}$$

2.3 Inspection of BMD

In this study, the primary outcome measures were total femur BMD, femoral neck BMD, trochanter BMD, intertrochanter BMD, and lumbar spine (L1-L4) BMD. The femur and spine scans were acquired with a Hologic QDR-4500A dual-energy X-ray absorptiometry (DXA) scanner (Hologic, Inc., Bedford, MA, USA), using software version Discovery v12.4. Typically, lumbar spine BMD was derived from a dedicated lumbar spine scan (vertebrae L1-L4) using DXA. The quality control and calibration procedures were performed using a standardized phantom provided by the manufacturer. For a comprehensive description of the procedures utilized, please consult the Body Composition Procedures Manual (10).

2.4 Covariate assessment

All factors considered and adjusted for at present research were gathered in accordance with existing literature (11, 12). These factors encompassed age, sex, race, poverty income ratio (PIR), body mass index (BMI), levels of physical activity, serum biochemistry indicators (total calcium, phosphorus, and total protein), as well as systolic blood pressure, diastolic blood pressure, and glycohemoglobin. See Supplementary Table S1 for a complete definition and categorization of covariates. Additional information regarding covariates is available on the website (13).

2.5 Statistical analysis

Continuous variables were reported as weighted mean values along with their standard errors, whereas categorical variables were presented as unweighted counts along with corresponding weighted percentages. All statistical analyses conducted in this research utilized R software (version 4.2.2), ensuring adherence to NHANES sampling protocols as outlined in the analysis guidelines (13). To compare baseline characteristics across CMI quartiles, we used weighted ANOVA for continuous variables and weighted Rao-Scott chi-square tests for categorical variables. When significant overall differences were detected, we conducted *post-hoc* pairwise comparisons using Bonferroni-corrected methods. To investigate the relationship between CMI and BMD, we developed three distinct linear regression models based on specific criteria for variable selection. Model 1 was adjusted solely for BMI, as it is closely related to weight and health status and has been shown to significantly influence BMD. Model 2 further accounted for age, sex, and race, which are known to have significant associations with BMD and can impact CMI expression across diverse populations. Finally, Model 3 included additional adjustments for PIR, physical activity, serum biochemical indicators, systolic blood pressure, diastolic blood pressure, and glycohemoglobin. These variables were selected based on biological plausibility and previous research findings. We reported the coefficient of determination (R^2) for the weighted regression model to assess the proportion of variance in BMD explained by the independent variables. To compare CMI with traditional lipid indicators, including HDL-C, low-density lipoprotein cholesterol (LDL-C), LDL-C and HDL-C ratio, and total cholesterol (TC), we conducted additional multiple linear regression analyses, where each indicator was separately included in the model with the same set of covariates. The absolute values of standardized β coefficients were compared across models to evaluate their relative associations with BMD. Subgroup and interaction analyses were performed according to age, sex, and race. Furthermore, sensitivity analysis was further performed to test the robustness of this association. We additionally adjusted other covariates such as alanine aminotransferase, aspartate aminotransferase, alkaline phosphatase, blood urea nitrogen, and uric acid, and re-analysis the results using unweighted data. Statistical significance was set as $P<0.05$.

3 Result

3.1 Basic characteristics of the study population

The present study included a total of 1,514 adolescents aged 12 to 19 years. The weighted characteristics of participants were compared at different CMI levels, and the results are detailed in Table 1.

The mean age of all individuals was 15.49 (± 2.21) years, with 53.35% being males and 63.02% identified as non-Hispanic White. Notable disparities in age, race, PIR, BMI, phosphorus, systolic blood pressure, total femur BMD, femoral neck BMD, trochanter BMD, intertrochanter BMD, and lumbar spine (L1-L4) BMD were observed among the different CMI groups ($P<0.05$). The higher group had both an older mean age and a greater proportion of non-Hispanic White individuals in contrast to the lower group. Furthermore, the Q4 group had elevated BMI and systolic blood pressure values, as well as higher BMD levels for the total femur, femoral neck, trochanter, intertrochanter, and lumbar spine (L1-L4) when compared to the Q1 group, whereas the Q1 group exhibited higher PIR and phosphorus levels ($P<0.05$). *Post-hoc* analyses revealed that significant differences in BMD were primarily found between Q1 and Q4 across all sites, and between Q1 and Q3 in the other four sites, except for the total femur.

3.2 Association between CMI and BMD among adolescents

Weighted linear regression models were adopted to elucidate the correlation between CMI and BMD among adolescents. In Model 1, adjustment of BMI, we found that each unit increase in CMI was significantly associated with decreased BMD at all measured sites ($P<0.05$). Model 2, which included additional adjustments for age, sex, and race, reaffirmed the existence of a statistically significant correlation ($P<0.05$). When we extended our analysis in Model 3 to include adjustments for PIR, physical activity, total calcium, phosphorus, total protein, systolic blood pressure, diastolic blood pressure, and glycohemoglobin, we observed that per-unit increases in the CMI corresponded with reductions in BMD by 0.052 g/cm^2 for femoral neck (β=-0.052, 95% CI: -0.087 to -0.018) and 0.048 g/cm^2 for lumbar spine (L1-L4) (β=-0.048, 95% CI: -0.085 to -0.011). The weighted regression models explained 39.87% (R^2 = 0.3987) of the variance in femoral neck BMD and 51.42% (R^2 = 0.5142) in lumbar spine (L1-L4) BMD. For further details, please see Table 2.

When converting the CMI into a categorical variable, a negative correlation with BMD was also observed (Table 2). When the analysis was restricted to the adjustment for BMI only (Model 1), a notable association was observed between the Q4 group and lower BMD at all sites in comparison with the Q1 group. Upon further adjustment for age, sex, and race (Model 2), these associations remained statistically significant, while also demonstrating that the Q2 and Q3 groups exhibited significant associations with lower

10.3389/fendo.2025.1535509

TABLE 1 Weighted characteristics of participants based on cardiometabolic index quartiles.

Characteristic	Cardiometabolic index					*P* value
	Total	Q1	Q2	Q3	Q4	
Age, years	15.49 (2.21)	14.94 (2.06)[b,c]	15.36 (2.28)[d]	15.96 (2.08)[b,d]	15.72 (2.30)[c]	<0.001
Sex						0.706
Male	841 (53.35)	231 (52.04)	206 (51.28)	180 (52.90)	224 (57.21)	
Female	673 (46.65)	179 (47.96)	165 (48.72)	164 (47.10)	165 (42.79)	
Race						<0.001
Non-Hispanic White	463 (63.02)	91 (51.58)[a,b,c]	112 (61.53)[a,d,e]	126 (71.33)[b,d,f]	134 (67.67)[c,e,f]	
Non-Hispanic Black	400 (13.83)	171 (24.11)[a,b,c]	98 (13.97)[a,d,e]	81 (10.55)[b,d,f]	50 (6.60)[c,e,f]	
Hispanic	571 (16.56)	122 (14.11)[a,c]	133 (15.67)[a,d,e]	122 (13.84)[d,f]	194 (22.69)[c,e,f]	
Other	80 (6.60)	26 (10.21)[a,b,c]	28 (8.83)[a,d,e]	15 (4.28)[b,d,f]	11 (3.04)[c,e,f]	
Poverty income ratio						0.010
<1.3	614 (27.11)	162 (25.33)[b,c]	139 (24.47)[e]	131 (22.90)[b,f]	182 (35.81)[c,e,f]	
1.3-3.5	548 (35.07)	140 (33.28)[a,b,c]	143 (35.32)[a]	123 (35.34)[b]	142 (36.36)[c]	
>3.5	352 (37.82)	108 (41.39)[c]	89 (40.21)[e]	90 (41.75)[f]	65 (27.82)[c,e,f]	
Physical activity						0.458
Low	466 (28.24)	112 (25.37)	107 (26.48)	111 (26.87)	136 (34.30)	
Medium	204 (12.89)	58 (14.24)	46 (10.76)	56 (14.83)	44 (11.71)	
High	844 (58.87)	240 (60.39)	218 (62.77)	177 (58.30)	209 (53.99)	
Body mass index, Kg/m^2	23.12 (5.25)	20.34 (2.83)[a,b,c]	22.09 (4.53)[a,d,e]	23.44 (4.52)[b,d,f]	26.64 (6.35)[c,e,f]	<0.001
Total calcium, mg/dL	9.66 (0.30)	9.66 (0.29)	9.65 (0.29)	9.64 (0.30)	9.68 (0.32)	0.409
Phosphorus, mg/dL	4.38 (0.67)	4.43 (0.61)[b]	4.48 (0.63)	4.23 (0.70)[b]	4.39 (0.72)	0.001
Total protein, g/dL	7.19 (0.41)	7.21 (0.41)	7.19 (0.41)	7.13 (0.43)	7.22 (0.39)	0.238
Systolic blood pressure, mmHg	109.23 (9.92)	108.35 (9.93)[c]	107.39 (9.74)[d,e]	109.73 (9.12)[d]	111.47 (10.41)[c,e]	<0.001
Diastolic blood pressure, mmHg	59.96 (10.35)	59.89 (9.70)	59.51 (10.45)	59.59 (10.74)	60.86 (10.47)	0.425
Glycohemoglobin, %	5.18 (0.51)	5.20 (0.58)	5.15 (0.29)	5.16 (0.36)	5.20 (0.70)	0.618
Total femur BMD, g/cm^2	0.983 (0.161)	0.958 (0.155)[c]	0.967 (0.167)	0.999 (0.146)	1.010 (0.168)[c]	0.003
Femoral neck BMD, g/cm^2	0.906 (0.151)	0.878 (0.146)[b,c]	0.898 (0.160)	0.920 (0.136)[b]	0.928 (0.155)[c]	0.002
Trochanter BMD, g/cm^2	0.772 (0.139)	0.755 (0.135)[b,c]	0.761 (0.143)	0.786 (0.130)[b]	0.787 (0.147)[c]	0.010
Intertrochanter BMD, g/cm^2	1.126 (0.186)	1.096 (0.180)[b,c]	1.105 (0.193)	1.145 (0.170)[b]	1.159 (0.193)[c]	0.002
Lumbar spine (L1-L4) BMD, g/cm^2	0.945 (0.159)	0.928 (0.154)[b,c]	0.929 (0.169)	0.960 (0.147)[b]	0.963 (0.161)[c]	0.024
Triglyceride, mmol/L	0.912 (0.448)	0.514 (0.129)[a,b,c]	0.718 (0.148)[a,d,e]	0.963 (0.206)[b,d,f]	1.460 (0.474)[c,e,f]	<0.001
HDL-C, mmol/L	1.396 (0.311)	1.661 (0.311)[a,b,c]	1.463 (0.246)[a,d,e]	1.318 (0.221)[b,d,f]	1.140 (0.191)[c,e,f]	<0.001
Waist-to-height ratio	0.482 (0.077)	0.439 (0.040)[a,b,c]	0.467 (0.063)[a,d,e]	0.484 (0.064)[b,d,f]	0.539 (0.092)[c,e,f]	<0.001
Cardiometabolic index	0.351 (0.246)	0.137 (0.032)[a,b,c]	0.227 (0.026)[a,d,e]	0.350 (0.044)[b,d,f]	0.694 (0.248)[c,e,f]	<0.001

The numbers of participants in each category are unweighted observed frequencies, while means, standard errors, and percentages are population-weighted. The *post-hoc* pairwise comparisons between quartiles with statistically significant differences are indicated using the following markers: [a]for the comparison between Q1 and Q2, [b]for the comparison between Q1 and Q3, [c]for the comparison between Q1 and Q4, [d]for the comparison between Q2 and Q3, [e]for the comparison between Q2 and Q4, [f]for the comparison between Q3 and Q4. BMD, bone mineral density; HDL-C, high-density lipoprotein cholesterol.

10.3389/fendo.2025.1535509

TABLE 2 Association between cardiometabolic index and bone mineral density.

Variable	Model 1 β (95% CI)	Model 2 β (95% CI)	Model 3 β (95% CI)
Total femur BMD			
Continuous variable	**-0.061 (-0.104, -0.019)****	**-0.054 (-0.094, -0.015)****	-0.035 (-0.076, 0.005)
Categorical variable			
Q1	Reference	Reference	Reference
Q2	-0.018 (-0.047, 0.011)	-0.018 (-0.045, 0.009)	-0.012 (-0.038, 0.013)
Q3	-0.007 (-0.033, 0.019)	-0.018 (-0.043, 0.007)	-0.016 (-0.041, 0.009)
Q4	**-0.044 (-0.077, -0.010)***	**-0.039 (-0.071, -0.008)***	-0.027 (-0.060, 0.006)
Femoral neck BMD			
Continuous variable	**-0.072 (-0.107, -0.037)*****	**-0.066 (-0.099, -0.034)*****	**-0.052 (-0.087, -0.018)****
Categorical variable			
Q1	Reference	Reference	Reference
Q2	-0.008 (-0.036, 0.020)	-0.008 (-0.035, 0.019)	-0.003 (-0.028, 0.022)
Q3	-0.008 (-0.033, 0.016)	-0.016 (-0.040, 0.008)	-0.015 (-0.041, 0.011)
Q4	**-0.049 (-0.077, -0.020)****	**-0.045 (-0.071, -0.019)****	**-0.036 (-0.064, -0.007)***
Trochanter BMD			
Continuous variable	**-0.055 (-0.092, -0.017)****	**-0.053 (-0.089, -0.016)****	-0.033 (-0.070, 0.004)
Categorical variable			
Q1	Reference	Reference	Reference
Q2	-0.013 (-0.041, 0.015)	-0.013 (-0.039, 0.014)	-0.008 (-0.033, 0.016)
Q3	-0.003 (-0.024, 0.018)	-0.011 (-0.031, 0.010)	-0.010 (-0.030, 0.011)
Q4	**-0.036 (-0.066, -0.007)***	**-0.035 (-0.062, -0.008)***	-0.023 (-0.051, 0.005)
Intertrochanter BMD			
Continuous variable	**-0.065 (-0.115, -0.015)***	**-0.053 (-0.099, -0.008)***	-0.031 (-0.078, 0.015)
Categorical variable			
Q1	Reference	Reference	Reference
Q2	-0.022 (-0.056, 0.011)	-0.022 (-0.053, 0.008)	-0.015 (-0.044, 0.013)
Q3	-0.008 (-0.039, 0.024)	-0.021 (-0.051, 0.008)	-0.018 (-0.047, 0.011)
Q4	**-0.048 (-0.087, -0.008)***	**-0.040 (-0.078, -0.003)***	-0.025 (-0.064, 0.014)
Lumbar spine (L1-L4) BMD			
Continuous variable	**-0.083 (-0.118, -0.047)*****	**-0.058 (-0.091, -0.026)*****	**-0.048 (-0.085, -0.011)***
Categorical variable			
Q1	Reference	Reference	Reference
Q2	-0.028 (-0.057, 0.001)	**-0.028 (-0.053, -0.003)***	-0.018 (-0.043, 0.006)
Q3	-0.018 (-0.040, 0.005)	**-0.032 (-0.050, -0.014)****	**-0.028 (-0.048, -0.008)****
Q4	**-0.066 (-0.096, -0.036)*****	**-0.052 (-0.075, -0.028)*****	**-0.041 (-0.070, -0.011)****

Model 1, adjusted for BMI; Model 2, adjusted for BMI, age, sex, and race; Model 3, adjusted for BMI, age, sex, race, poverty income ratio, physical activity, total calcium, phosphorus, total protein, systolic blood pressure, diastolic blood pressure, and glycohemoglobin. Results in bold indicate statistical significance. BMI, body mass index; CI, confidence interval; BMD, bone mineral density. Cardiometabolic index quartiles, Q1,<0.184; Q2, 0.184-0.280; Q3, 0.281-0.430; Q4, >0.430. * P<0.05; ** P<0.01; *** P<0.001.

lumbar spine (L1-L4) BMD. Further adjustments in Model 3 revealed a reduction of lower levels of BMD at all sites, but only a significant correlation of the CMI with femoral neck BMD (Q4, β=-0.036, 95% CI: -0.064 to -0.007) and lumbar spine (L1-L4) BMD (Q3, β=-0.028, 95% CI: -0.048 to -0.008, and Q4, β=-0.041, 95% CI: -0.070 to -0.011). Notably, the relationship with lumbar spine (L1-L4) BMD intensified as CMI levels increased, highlighting a potential gradient effect of the CMI on BMD.

3.3 Comparison of CMI with traditional lipid indicators

Compared with traditional lipid indicators (HDL-C, LDL-C, LDL-C/HDL-C, and TC), CMI demonstrated a stronger negative association with femoral neck and lumbar spine (L1-L4) BMD, as indicated by larger absolute β values (Supplementary Table S2). In total femur and trochanter BMD, CMI had the largest absolute β value among all lipid indicators, although it did not reach statistical significance, whereas some traditional lipid variables (LDL-C, LDL-C/HDL-C, and TC) were statistically significant. For intertrochanter BMD, CMI had the second-largest effect size but was not statistically significant, while certain traditional indicators (HDL-C, LDL-C, and TC) were significant. These results suggest that CMI may capture metabolic variations relevant to bone health, potentially more comprehensively than individual lipid indicators in specific skeletal sites.

3.4 Subgroup and sensitivity analysis

The stratified analysis results were displayed in Table 3, indicating that no significant interactions involving age, sex, or race in relation to CMI and BMD.

Furthermore, sensitivity analyses demonstrated that these negative correlations remained robust even after adjusting for variables such as alanine aminotransferase, aspartate aminotransferase, alkaline phosphatase, blood urea nitrogen, and uric acid (Supplementary Table S3) or when the data were re-evaluated using unweighted methods (Supplementary Table S4).

4 Discussion

This study represents the investigation into the relationship between CMI and BMD. Utilizing data from the NHANES spanning 2005 to 2010, the research examined this association among the 12-19-year adolescent population. The findings indicated a correlation between CMI and reduced BMD. Furthermore, the analyses demonstrated that this relationship was consistent across various subgroups and remained unaffected by other confounding factors.

The relationship between obesity and bone health has garnered considerable attention and debate among scholars, yet controversy remains (14, 15). BMI is often used to evaluate obesity's influence on BMD. Some studies show an inverted U-shaped association between BMI and BMD (16, 17). While other evidence indicates a negative correlation between BMI and BMD, suggesting that obesity may adversely affect bone health (18). Obesity is not just about weight gain; it includes fat accumulation and distribution. Individuals who are obese but have a normal BMI yet a high body fat percentage face a higher risk of lower BMD (19). We hypothesize that adipose tissue significantly influences the relationship between obesity and BMD.

Researchers have developed new indexes to examine the relationship between obesity and BMD by considering the impact of adipose tissue. The weight-adjusted waist index standardizes waist circumference and body weight, reflecting the level of central obesity and abdominal fat accumulation in obese individuals (20, 21). Similarly, the body roundness index and abdominal obesity index were used to assess the effects of central obesity and visceral fat on BMD (22, 23). The results of these studies align with the present findings, suggesting a link between obesity and fat accumulation and decreased BMD. However, additional research is needed to clarify the potential relationship between quantitative adiposity, dyslipidemia, and BMD. In this paper, we introduce the CMI index to more comprehensively evaluate the effects of obesity and lipids on BMD. The CMI, which reflects both fat distribution and lipid levels, presents a novel lens through which to examine these relationships. CMI can serve as a potential indicator for evaluating the impact of metabolic disorders on BMD, as it reflects cardiac metabolic burden.

The comparison with traditional lipid indicators suggests that CMI may be a more robust indicator of BMD, particularly at the femoral neck and lumbar spine (L1-L4), where it exhibited a stronger negative association than traditional variables. This aligns with previous findings that link metabolic dysregulation to bone health. However, in some skeletal sites (e.g., total femur and intertrochanter), certain traditional lipid markers showed significant associations, while CMI did not reach statistical significance. This may be attributed to differences in bone composition, metabolic activity, and potential confounding effects. Future studies should explore its potential utility alongside traditional lipid markers to better understand metabolic influences on bone health.

Multiple mechanisms may elucidate the impact of CMI on BMD. Obesity is frequently associated with systemic inflammation, triggering the release of pro-inflammatory factors and initiating inflammatory responses that can significantly contribute to decreased BMD (24, 25). Chronic low-grade inflammation associated with obesity may serve as a key mediator in the relationship between cardiometabolic health and bone metabolism. Adipose tissue secretes pro-inflammatory cytokines, such as tumor necrosis factor-alpha and interleukin-6, which can stimulate osteoclast activity and bone resorption while inhibiting osteoblast function. Furthermore, adipokines such as leptin and adiponectin have been implicated in bone remodeling and may partly explain the inverse association between CMI and BMD observed in this study (5). Gut dysbiosis, common in obese individuals, can further influence BMD (26). Moreover, vitamin

TABLE 3 Stratified analyses of the association between cardiometabolic index and bone mineral density.

Characteristic	Total femur BMD		Femoral neck BMD		Trochanter BMD		Intertrochanter BMD		Lumbar spine (L1-L4) BMD	
	β (95% CI)	$P_{interaction}$	β (95% CI)	$P_{interaction}$	β (95% CI)	$P_{interaction}$	β (95% CI)	$P_{interaction}$	β (95% CI)	$P_{interaction}$
Age		0.935		0.896		0.888		0.989		0.505
12–15 years	-0.029 (-0.076, 0.017)		-0.045 (-0.084, -0.006)		-0.030 (-0.073, 0.013)		-0.018 (-0.074, 0.039)		-0.066 (-0.121, -0.010)	
16–19 years	-0.031 (-0.084, 0.022)		-0.055 (-0.101, -0.009)		-0.028 (-0.081, 0.025)		-0.029 (-0.093, 0.035)		-0.017 (-0.072, 0.038)	
Sex		0.710		0.837		0.930		0.487		0.914
Male	-0.061 (-0.110, -0.011)		-0.080 (-0.126, -0.035)		-0.061 (-0.106, -0.015)		-0.056 (-0.113, 0.002)		-0.062 (-0.102, -0.022)	
Female	-0.032 (-0.098, 0.035)		-0.038 (-0.090, 0.014)		-0.023 (-0.085, 0.039)		-0.034 (-0.112, 0.044)		-0.048 (-0.112, 0.015)	
Race		0.372		0.509		0.424		0.365		0.182
Non-Hispanic White	-0.023 (-0.075, 0.029)		-0.047 (-0.092, -0.003)		-0.027 (-0.074, 0.020)		-0.008 (-0.071, 0.054)		-0.033 (-0.080, 0.015)	
Non-Hispanic Black	-0.061 (-0.173, 0.050)		-0.072 (-0.156, 0.011)		-0.051 (-0.153, 0.050)		-0.068 (-0.192, 0.056)		-0.086 (-0.194, 0.021)	
Hispanic	-0.060 (-0.103, -0.018)		-0.052 (-0.092, -0.012)		-0.049 (-0.093, -0.004)		-0.079 (-0.123, -0.035)		-0.096 (-0.143, -0.050)	
Other	-0.122 (-0.503, 0.258)		-0.125 (-0.489, 0.239)		0.015 (-0.323, 0.353)		-0.179 (-0.567, 0.208)		-0.107 (-0.382, 0.167)	

The models were adjusted for BMI, age, sex, race, poverty income ratio, physical activity, total calcium, phosphorus, total protein, systolic blood pressure, diastolic blood pressure, and glycohemoglobin, except for the corresponding stratification variable. CI, confidence interval; BMD, bone mineral density.

10.3389/fendo.2025.1535509

D, crucial for maintaining BMD, is often found at lower levels in obese individuals due to sequestration in adipose tissue, potentially diminishing bone strength. Reduced growth hormone production in obese individuals may also contribute to lower BMD (27). Furthermore, obese individuals typically produce less growth hormone, which may contribute to lower BMD (28). Obesity-related oxidative stress can further reduce BMD by disrupting bone homeostasis and enhancing bone resorption (29–31). Additionally, dysregulated lipid metabolism also significantly impacts bone homeostasis, contributing to low BMD. Dyslipidemia-induced oxidative stress and inflammation promote increased osteoclast activity and bone resorption (32). Specifically, elevated cholesterol levels modulate the function of bone-resident osteoblasts and osteoclasts, accelerating bone deterioration (33). Furthermore, reduced HDL levels are linked to the development of an inflammatory microenvironment, impairing osteoblast differentiation and function. Perturbations in HDL metabolic pathways also favor adipoblastic differentiation while inhibiting osteoblastic differentiation, potentially through the modification of specific bone-related chemokines and signaling cascades (34). Collectively, these mechanisms may contribute to the observed negative association between CMI and BMD.

This is despite recent articles exploring the association between CMI and BMD, which have reached conflicting conclusions about CMI's effect on femoral versus vertebral BMD (35, 36). We are still dedicated to utilizing CMI to investigate how childhood and adolescent obesity affects BMD. The two existing studies on CMI and BMI involved adult subjects, but there is a significant age difference among the participants, which may explain the contrasting findings. BMD and bone health are vital for the growth and development of young people, yet research on the effects of obesity during these stages is limited and inconsistent. Our study indicates that elevated lipid levels and obesity correlate with lower BMD and poorer bone health, highlighting the need to address metabolic disorders in children and adolescents. Notably, the seemingly paradoxical finding that BMD in the Q4 group was higher than in the Q1 group despite an overall negative correlation between CMI and BMD may be attributed to BMI confounding. Higher BMI is associated with both increased CMI and greater mechanical loading on bones, which may partially mask the negative metabolic effects of CMI on bone density.

Of course, there is no denying that this article has some shortcomings. As a cross-sectional investigation, it does not provide conclusive evidence for the causal association of CMI and BMD, thereby necessitating further studies to establish such links. Additionally, the geographic, demographic, and ethnographic constraints of this study may impact the generalizability of its findings. Another limitation of this study is the potential for measurement error in key variables (such as BMD and biochemical markers) due to variations in calibration or operator technique, despite the implementation of standardized protocols, and future studies should aim to improve the accuracy of these measurements. While the results offer valuable insights, these limitations must be considered when deciphering the significance of the research.

5 Conclusion

Utilizing data from the NHANES, we identified a robust negative association between CMI and BMD. Notably, this relationship remained unaffected by other confounding factors. These findings suggest that CMI may be a relevant factor associated with bone health in adolescents. Further research, particularly longitudinal studies, is needed to clarify potential underlying mechanisms.

Data availability statement

The raw data supporting the conclusions of this article will be made available by the authors, without undue reservation.

Ethics statement

This research is based on an analysis of publicly available data from NHANES, obtained with approval from the Ethics Review Board of the National Center for Health Statistics (https://www.cdc.gov/nchs/nhanes/irba98.htm). Since the NHANES public use datasets do not include any personally identifiable information, the requirement for ethical review and approval was waived for this study. All procedures were performed in compliance with the World Medical Association Declaration of Helsinki. All participants provided informed consent prior to their involvement in the study. The studies were conducted in accordance with the local legislation and institutional requirements. Written informed consent for participation in this study was provided by the participants' legal guardians/next of kin.

Author contributions

HL: Conceptualization, Formal analysis, Methodology, Supervision, Visualization, Writing – original draft. RX: Data curation, Validation, Writing – original draft. CL: Data curation, Validation, Writing – review & editing. ZC: Methodology, Writing – review & editing. YS: Data curation, Writing – review & editing. YiL: Data curation, Writing – review & editing. YaL: Writing – review & editing.

Funding

The author(s) declare that no financial support was received for the research and/or publication of this article.

Conflict of interest

The authors declare that the research was conducted in the absence of any commercial or financial relationships that could be construed as a potential conflict of interest.

Generative AI statement

The author(s) declare that no Generative AI was used in the creation of this manuscript.

Publisher's note

Supplementary material

The Supplementary Material for this article can be found online at: https://www.frontiersin.org/articles/10.3389/fendo.2025.1535509/full#supplementary-material

References

1. Farr JN, Khosla S. Skeletal changes through the lifespan–from growth to senescence. *Nat Rev Endocrinol*. (2015) 11:513–21. doi: 10.1038/nrendo.2015.89

2. Kim J, Ha J, Jeong C, Lee J, Lim Y, Jo K, et al. Bone mineral density and lipid profiles in older adults: a nationwide cross-sectional study. *Osteoporos Int*. (2023) 34:119–28. doi: 10.1007/s00198-022-06571-z

3. Aleidi SM, Al-Ansari MM, Alnehmi EA, Malkawi AK, Alodaib A, Alshaker M, et al. Lipidomics profiling of patients with low bone mineral density (LBMD). *Int J Mol Sci*. (2022) 23:12017. doi: 10.3390/ijms231912017

4. Wu M, Du Y, Zhang C, Li Z, Li Q, Qi E, et al. Mendelian randomization study of lipid metabolites reveals causal associations with heel bone mineral density. *Nutrients*. (2023) 15:4160. doi: 10.3390/nu15194160

5. Kirk B, Feehan J, Lombardi G, Duque G. Muscle, bone, and fat crosstalk: the biological role of myokines, osteokines, and adipokines. *Curr Osteoporos Rep*. (2020) 18:388–400. doi: 10.1007/s11914-020-00599-y

6. Lopes KG, Rodrigues EL, da Silva Lopes MR, do Nascimento VA, Pott A, Guimarães R de CA, et al. Adiposity metabolic consequences for adolescent bone health. *Nutrients*. (2022) 14:3260. doi: 10.3390/nu14163260

7. Zhou X, Tao X-L, Zhang L, Yang Q-K, Li Z-J, Dai L, et al. Association between cardiometabolic index and depression: National Health and Nutrition Examination Survey (NHANES) 2011-2014. *J Affect Disord*. (2024) 351:939–47. doi: 10.1016/j.jad.2024.02.024

8. Yan L, Hu X, Wu S, Cui C, Zhao S. Association between the cardiometabolic index and NAFLD and fibrosis. *Sci Rep*. (2024) 14:13194. doi: 10.1038/s41598-024-64034-3

9. Wang L, Liu X, Du Z, Tian J, Zhang L, Yang L. Cardiometabolic Index and chronic obstructive pulmonary disease: A population-based cross-sectional study. *Heart Lung*. (2024) 68:342–9. doi: 10.1016/j.hrtlng.2024.09.002

10. CDC. *Body Composition Procedures Manual* . Available online at: https://www.cdc.gov/nchs/nhanes/index.htm (Accessed October 5, 2024).

11. Liu H, Bao M, Liu M, Deng F, Wen X, Wan P, et al. The association between serum copper and bone mineral density among adolescents aged 12 to 19 in the United States. *Nutrients*. (2024) 16:453. doi: 10.3390/nu16030453

12. Li T, Xie Y, Wang L, Huang G, Cheng Y, Hou D, et al. The association between lead exposure and bone mineral density in childhood and adolescence: results from NHANES 1999–2006 and 2011-2018. *Nutrients*. (2022) 14:1523. doi: 10.3390/nu14071523

13. NCHS. *About the National Health and Nutrition Examination Survey* . Available online at: https://www.cdc.gov/nchs/nhanes/about_nhanes.htm (Accessed October 5, 2024).

14. Sukumar D, Schlussel Y, Riedt CS, Gordon C, Stahl T, Shapses SA. Obesity alters cortical and trabecular bone density and geometry in women. *Osteoporos Int*. (2011) 22:635–45. doi: 10.1007/s00198-010-1305-3

15. Rinonapoli G, Pace V, Ruggiero C, Ceccarini P, Bisaccia M, Meccariello L, et al. Obesity and bone: A complex relationship. *Int J Mol Sci*. (2021) 22:13662. doi: 10.3390/ijms222413662

16. Li Y. Association between obesity and bone mineral density in middle-aged adults. *J Orthop Surg Res*. (2022) 17:268. doi: 10.1186/s13018-022-03161-x

17. Lee J, Yoon I, Cha H, Kim H-J, Ryu O-H. Inverted U-shaped relationship between obesity parameters and bone mineral density in korean adolescents. *J Clin Med*. (2023) 12:5869. doi: 10.3390/jcm12185869

18. Asomaning K, Bertone-Johnson ER, Nasca PC, Hooven F, Pekow PS. The association between body mass index and osteoporosis in patients referred for a bone mineral density examination. *J Womens Health (Larchmt)*. (2006) 15:1028–34. doi: 10.1089/jwh.2006.15.1028

19. Yoon H, Sung E, Kang J-H, Kim C-H, Shin H, Yoo E, et al. Association between body fat and bone mineral density in Korean adults: a cohort study. *Sci Rep*. (2023) 13:17462. doi: 10.1038/s41598-023-44537-1

20. Wang X, Yang S, He G, Xie L. The association between weight-adjusted-waist index and total bone mineral density in adolescents: NHANES 2011-2018. *Front Endocrinol (Lausanne)*. (2023) 14:1191501. doi: 10.3389/fendo.2023.1191501

21. Guo M, Lei Y, Liu X, Li X, Xu Y, Zheng D. The relationship between weight-adjusted-waist index and total bone mineral density in adults aged 20-59. *Front Endocrinol (Lausanne)*. (2023) 14:1281396. doi: 10.3389/fendo.2023.1281396

22. Lin R, Tao Y, Li C, Li F, Li Z, Hong X, et al. Central obesity may affect bone development in adolescents: association between abdominal obesity index ABSI and adolescent bone mineral density. *BMC Endocr Disord*. (2024) 24:81. doi: 10.1186/s12902-024-01600-w

23. Yang P, Li D, Li X, Tan Z, Wang H, Niu X, et al. High-density lipoprotein cholesterol levels is negatively associated with intertrochanter bone mineral density in adults aged 50 years and older. *Front Endocrinol (Lausanne)*. (2023) 14:1109427. doi: 10.3389/fendo.2023.1109427

24. Yamauchi T, Kamon J, Waki H, Terauchi Y, Kubota N, Hara K, et al. The fat-derived hormone adiponectin reverses insulin resistance associated with both lipoatrophy and obesity. *Nat Med*. (2001) 7:941–6. doi: 10.1038/90984

25. Guo YX, Wang AQ, Gao X, Na J, Zhe W, Zeng Y, et al. Obesity is positively associated with depression in older adults: role of systemic inflammation. *BioMed Environ Sci*. (2023) 36:481–9. doi: 10.3967/bes2023.059

26. Wang N, Ma S, Fu L. Gut microbiota dysbiosis as one cause of osteoporosis by impairing intestinal barrier function. *Calcif Tissue Int*. (2022) 110:225–35. doi: 10.1007/s00223-021-00911-7

27. Walsh JS, Bowles S, Evans AL. Vitamin D in obesity. *Curr Opin Endocrinol Diabetes Obes*. (2017) 24:389–94. doi: 10.1097/MED.0000000000000371

28. Hjelholt A, Høgild M, Bak AM, Arlien-Søborg MC, Bæk A, Jessen N, et al. Growth hormone and obesity. *Endocrinol Metab Clin North Am*. (2020) 49:239–50. doi: 10.1016/j.ecl.2020.02.009

29. Čagalová A, Tichá Ľ, Gaál Kovalčíková A, Šebeková K, Podracká Ľ. Bone mineral density and oxidative stress in adolescent girls with anorexia nervosa. *Eur J Pediatr*. (2022) 181:311–21. doi: 10.1007/s00431-021-04199-5

30. Tao Y-A, Long L, Gu J-X, Wang P-Y, Li X, Li X-L, et al. Associations of oxidative balance score with lumbar spine osteopenia in 20–40 years adults: NHANES 2011-2018. *Eur Spine J*. (2024) 33:3343–51. doi: 10.1007/s00586-024-08424-1

31. Li K, Huang K, Lu Q, Geng W, Jiang D, Guo A. TRIM16 mitigates impaired osteogenic differentiation and antioxidant response in D-galactose-induced senescent osteoblasts. *Eur J Pharmacol*. (2024) 979:176849. doi: 10.1016/j.ejphar.2024.176849

32. Anagnostis P, Florentin M, Livadas S, Lambrinoudaki I, Goulis DG. Bone health in patients with dyslipidemias: an underestimated aspect. *Int J Mol Sci*. (2022) 23:1639. doi: 10.3390/ijms23031639

33. Mandal CC. High cholesterol deteriorates bone health: new insights into molecular mechanisms. *Front Endocrinol (Lausanne)*. (2015) 6:165. doi: 10.3389/fendo.2015.00165

34. Papachristou NI, Blair HC, Kypreos KE, Papachristou DJ. High-density lipoprotein (HDL) metabolism and bone mass. *J Endocrinol*. (2017) 233:R95–R107. doi: 10.1530/JOE-16-0657

35. Liu H, Dong H, Zhou Y, Jin M, Hao H, Yuan Y, et al. Nonlinear relationship between cardiometabolic index and bone mineral density in U.S. adults: the mediating role of percent body fat. *Sci Rep*. (2024) 14:22449. doi: 10.1038/s41598-024-73427-3

36. Wu X, Jin X, Xu W, She C, Li L, Mao Y. Cardiometabolic index is associated with increased bone mineral density: a population-based cross-sectional study. *Front Public Health*. (2024) 12:1403450. doi: 10.3389/fpubh.2024.1403450

frontiers | Frontiers in Endocrinology

TYPE Original Research
PUBLISHED 23 May 2025
DOI 10.3389/fendo.2025.1587985

OPEN ACCESS

EDITED BY
Federico Baronio,
IRCCS AOU S.Orsola-Malpighi, Italy

REVIEWED BY
Amir Mohammad Malvandi,
Ospedale Galeazzi S.p.A, Italy
Wenjie Zhou,
Sichuan University, China

*CORRESPONDENCE
Berta Magallares
bmagallares@santpau.cat
Helena Codes-Méndez
hcodes@santpau.cat

RECEIVED 05 March 2025
ACCEPTED 28 April 2025
PUBLISHED 23 May 2025

CITATION
Magallares B, Cerdá D, Betancourt J, Fraga G, Park H, Codes-Méndez H, Quesada-Masachs E, López-Corbeto M, Torrent M, Marín A, Herrera S, Gich I, Boronat S, Casademont J, Corominas H and Malouf J (2025) Risk factors associated with low bone mineral density and childhood osteoporosis in a population undergoing skeletal growth: a cross-sectional analytic study. *Front. Endocrinol.* 16:1587985. doi: 10.3389/fendo.2025.1587985

Risk factors associated with low bone mineral density and childhood osteoporosis in a population undergoing skeletal growth: a cross-sectional analytic study

Berta Magallares[1,2,3]*, Dacia Cerdá[4], Jocelyn Betancourt[3,5], Gloria Fraga[3,5], HyeSang Park[1,3], Helena Codes-Méndez[1,3]*, Estefanía Quesada-Masachs[2,6], Mireia López-Corbeto[6], Montserrat Torrent[5], Ana Marín[7], Silvia Herrera[3,7], Ignasi Gich[3,8,9], Susana Boronat[3,5], Jordi Casademont[3,7,10], Héctor Corominas[1,3] and Jorge Malouf[7]

[1]Department of Rheumatology, Hospital de la Santa Creu i Sant Pau, Barcelona, Spain, [2]Department of Rheumatology, Universitari Dexeus-Grupo Quirón Salud Hospital, Barcelona, Spain, [3]Institut de Recerca Sant Pau (IR SANT PAU), Barcelona, Spain, [4]Department of Rheumatology, Hospital Sant Joan Despí Moisès Broggi, Barcelona, Spain, [5]Department of Pediatrics, Hospital de la Santa Creu i Sant Pau, Barcelona, Spain, [6]Department of Pediatric Rheumatology, Vall d'Hebrón Barcelona Hospital Campus, Barcelona, Spain, [7]Department of Mineral Metabolism Unit - Internal Medicine, Hospital de la Santa Creu i Sant Pau, Barcelona, Spain, [8]Centro de Investigación Biomédica en Red de Enfermedades Raras (CIBERER), Madrid, Spain, [9]Department of Clinical Epidemiology and Public Health, Hospital de la Santa Creu i Sant Pau, Barcelona, Spain, [10]Department of Internal Medicine, Hospital de la Santa Creu i Sant Pau, Barcelona, Spain

Background: Early identification of risk factors for low bone mass for chronological age (LBMca) and childhood osteoporosis (cOP) in patients undergoing skeletal growth is essential to mitigate long-term skeletal complications. cOP is diagnosed when LBMca (BMD Z-score ≤2) is accompanied by a clinically significant fracture history, or when vertebral fragility fractures are present.

Methods: Patients under 21 years of age with at least one risk factor for LBMca (malabsorption syndrome, chronic inflammatory diseases, hematological diseases, endocrinopathies, drugs that affect bone metabolism, or insufficient calcium intake) were included. Data on fractures history and physical activity levels were collected. Spine and whole-body dual-energy x-ray absorptiometry (DXA) and vertebral morphometry were performed. Age-adjusted linear regression analysis evaluated associations between bone mineral density (BMD) and risk factors.

Results: A total of 103 patients were included (mean age 9.8 years; 52.4% female), and 96.1% had more than two risk factors. The prevalence of LBMca was 10.5% and the prevalence of cOP was 4.8%. Vertebral BMD was positively associated with male sex. Whole body BMD was negatively associated with sedentary lifestyle and fracture history. Total body less head BMD showed negative

associations with current steroid treatment, sedentary lifestyle, and history of fractures.

Conclusions: Pediatric populations at risk of LBMca or cOP often have multiple risk factors, notably modifying ones such as physical inactivity. Up to 10.5% of children with risk factors present LBMca and 4.8% have an undiagnosed or unknown cOP. Longitudinal studies are warranted to understand the long-term impact of the identified risk factors, including age, sex, sedentary lifestyle, ethnicity and vitamin D status, on bone health.

KEYWORDS

low bone mass for chronological age, childhood osteoporosis, bone fragility, bone mineral density, DXA (dual-energy x-ray absorptiometry)

1 Introduction

Currently, osteoporosis is a prevalent condition that may cause fractures due to bone fragility (1). Although these fractures mainly occur in individuals older than 50, the causes are often present during bone development at early ages (2). Reaching an adequate peak bone mass during adolescence is essential to prevent osteoporosis at older ages due to the effects of hormonal deficiencies and other factors associated with aging such as sarcopenia (3, 4).

Despite its clinical significance, Childhood Osteoporosis (cOP) remains frequently underdiagnosed in everyday pediatric practice. Its subtle presentation, lack of standardized screening protocols, and limited awareness among healthcare providers often delay recognition. As a result, many children at risk -particularly those with chronic conditions or on prolonged exposure to bone-impacting medications- may go unnoticed until fractures occur.

At present, the impact each osteoporosis-related risk factor has on bone development and their prevalence are unknown. Additionally, the short-term and long-term consequences of the risk factors present during childhood are unknown. The currently accepted primary risk factors for developing low bone mass for chronological age (LBMca) include insufficient calcium and vitamin D intake (5), sedentary lifestyle (5, 6) diseases that cause chronic inflammation (7), hypercalciuria (5, 6) and malabsorptive diseases (8). Drugs that affect bone metabolism, such as glucocorticoids or immunosuppressants, are also described as common causes of secondary osteoporosis (6, 9, 10).

In addition to the aforementioned risk factors, related conditions such as sarcopenia, a component of malnutrition, can adversely impact overall bone health and physical function by reducing skeletal muscle mass and muscle function, highlighting the importance of early detection and management through assessments of muscle mass, strength, and physical performance (11, 12).

The early detection of these risk factors may allow for better control of LBMca and treatment of cOP at early ages. Adherence to treatment is vital for effectively managing these conditions (13), as it helps prevent complications such as fractures and enhances overall patient care.

Since most of our knowledge regarding LBMca and Bone mineral density (BMD) was ascertained from adult populations, the objective of this study is to determine the risk factors for LBMca and BMD, and to describe the prevalence of risk factors for LBMca in a cohort of patients undergoing skeletal growth.

2 Materials and methods

We conducted a cross-sectional ambispective analytic study. Eligible patients were consecutively recruited from our Pediatric Rheumatology Outpatient Clinic between January 2018 and December 2020. Patients and/or their legal guardians gave their informed consent prior to recruitment. The study obtained approval from the institutional ethics committee of Hospital Sant Pau (IIBSP-FRA-2016-11). The study was conducted in accordance with the Helsinki Declaration.

2.1 Study population

Inclusion criteria were patients under 21 years of age who presented with at least one of the following risk factors: malabsorption syndrome, chronic inflammatory diseases, hematological diseases, endocrinopathies, treatment with drugs that affect bone metabolism (glucocorticosteroids or immunosuppressant drugs), or insufficient calcium intake. Patients who had previously received any anti-osteoporotic drugs were excluded.

Patients were classified as LBMca and cOP according to the International Society for Clinical Densitometry 2013 Pediatric Position Development Conference (14). The study was approved by the ethics committee at our hospital (IIBSP-FRA-2016-11).

Informed consent was obtained from all patients and/or their legal guardians prior to recruitment.

2.2 Data collection and study variables

Electronic medical records from the hospital were used for data collection. All patients attended a baseline visit for a clinical interview and physical examination. Demographic and clinical variables were collected during the clinical interview. The patients who fulfilled the inclusion criteria underwent a dual-energy x-ray absorptiometry (DXA) and blood test. The following demographic and clinical variables were collected: age, sex, weight, height, disease history, history of previous fractures and current and past medication. Average calcium intake (milligrams/day) was calculated with the INDICAD 2001 study test (15), a validated, non-invasive questionnaire assessing dietary calcium consumption. Although we acknowledge potential recall bias inherent to dietary questionnaires, this method was selected for its feasibility and established use in routine clinical practice, allowing for consistent data collection across a wide age range. Physical activity was measured by the PAQ-A (Physical Activity Questionnaire for Adolescents) for patients older than 12. For patients younger than 12, the PAQ-C (Physical Activity Questionnaire for Children) was used. Both questionnaires were validated in the Spanish population (16, 17). Scores ranged from 1 (very low level of physical activity) to 5 (high level of physical activity). Data on physical activity were not collected for children under three years of age since the questionnaires are not validated for this age range.

Fasting laboratory parameters collected were calcemia, phosphatemia, OH-25-vitamin D concentration (determined by liquid chromatography coupled with tandem mass spectrometry), and calciuria from 6-hour urine collection. Outlier results from the 6-hour urine test were double-checked with a 24-hour calciuria test.

The following data were obtained by DXA: total body BMD, total body less head BMD, BMD at vertebrae L1-L4, and total body and vertebrae L1-L4 Z-score. Height adjustment for vertebral and total body Z-score values was performed for all cases by means of the formulas published by Zemel et al. (18). Densitometric determinations were obtained using an Hologic Discovery densitometer scanner (Hologic Discovery, Inc., Bedford, MA, USA) equipped with TBS iNsight® software (Medimaps Group, Mérignac, France), and calibrated for pediatric use. All DXA scans were performed within one week of the clinical evaluation to ensure consistency between clinical and densitometric data.

The presence or absence of vertebral fractures was analyzed with vertebral morphometry by applying Genant's semi-quantitative scale (19, 20).

2.3 Statistical analysis

Statistical analyses were performed with the IBM-SPSS (V26.0) software package. Quantitative variables are presented as mean (standard deviation). Categorical variables are presented as absolute frequencies and percentages. The relationship between categorical variables was assessed with contingency tables and the Chi square test, or Fisher's exact test. The T-test was used to evaluate quantitative variables in comparison to a two-grouped categorical data analysis, and an analysis of variance was used in the case of more than two groups. The Mann–Whitney U test was used for non-normally distributed ordinal or quantitative variables in the case of two groups, and the Kruskal–Wallis test was used for more than two groups. Pearson's linear correlation coefficient was used to correlate two quantitative variables. Spearman's correlation coefficient was calculated when one of these variables or both were ordinal or showed a non-normal distribution in the Shapiro-Wilk test. Multivariable regression analyses were conducted adjusting for age and sex. However, due to the limited sample size and heterogeneity of the sample, a sensitivity analysis could not be performed. Potential cofounding factors were evaluated in the univariate analysis, stratified by risk factors. 95% confidence intervals were calculated for clinically relevant results. For all cases, the type I error level was 5% ($\alpha = 0.05$) and a bilateral approximation was used.

An empirical sample size calculation was conducted based on an expected prevalence of LBM between 10% and 20%, with the inclusion of at least two key covariates (age and sex). Following the rule of one predictor per ten outcome events for multivariable analysis, a target sample size of approximately 100 participants was estimated. A *post-hoc* power calculation was then performed using the observed data. Assuming a small-to-medium effect size ($f^2 = 0.10$), two predictors (age and sedentary lifestyle), $\alpha = 0.05$, and a desired power of 0.80, the required sample size was estimated at 100 participants. Our final cohort of 103 meets this threshold, providing an actual power of 0.803 and supporting the strength and stability of the planned analyses.

3 Results

3.1 Baseline characteristics and prevalence of the risk factors

A total of 103 patients were included for analysis, with a variety of comorbid diseases reflecting the diverse clinical backgrounds of the study population. The baseline characteristics of the population and the risk factors for LBMca are summarized in Table 1. Mean age was 9.8 years (SD ±4.7, range 2-20). The comorbidities included malabsorption syndromes and food allergies (mostly cow's milk protein allergy and celiac disease, but also multiple food allergies, eosinophilic esophagitis, Chron's disease, and short bowel syndrome), juvenile idiopathic arthritis (JIA) with its various subtypes (oligoarticular, polyarticular, enthesitis-related, psoriatic arthritis, and systemic JIA), nephropathies (including nephrotic syndrome, renal tubular acidosis, and chronic renal failure), hematological diseases (such as lymphoma, acute lymphoblastic leukemia, and graft-versus-host disease), systemic autoimmune diseases (including vasculitis, systemic lupus erythematosus, autoimmune hepatitis, and eosinophilic fasciitis), and

10.3389/fendo.2025.1587985

autoinflammatory diseases (such as ADA2 deficiency, familial Mediterranean fever, and PFAPA syndrome).

No patients were diagnosed with hypogonadism, delayed developmental milestones, or non-ambulatory conditions that could affect bone mass acquisition. This is important to note, as mechanical load related to gravity is essential for normal bone development, as is age (21).

At some timepoint, 40 patients (38.8% of the sample) had received systemic corticosteroid treatment, and 20 (19.4%) were receiving it at the time of recruitment. The mean daily doses and accumulated doses of prednisone in patients in current use were 6.9 mg/day (range 1.125 mg – 40 mg) and 8605 mg (median of 8283 mg), respectively. The mean accumulated dose of prednisone in patients with a prior use of corticosteroids was 4853 mg (median 2305 mg).

Data regarding daily calcium intake and daily recommended amounts (DRA) (22) are summarized in Table 2. Daily average calcium intake in diet was 696 mg. A decrease in adherence to calcium DRA was observed in accordance with age increase (p= 0.035). Median physical activity in each age group measured by PAQ was: 3.19 (IQ 25-75%:0.57) out of a maximum of 5 in school age subjects (4–9 years), 2.8 (IQ 25-75%:0.95) in adolescents (10-17years) and 2.45 (IQ 25-75%:1.67) in young adults.

For 100% of the cohort, calcemia was normal with an average of 2.49 (0.75) mmol/L. For 86% of the cohort, phosphatemia levels were normal with a mean of 1.57 (0.21) mmol/L, while 14% of patients presented elevated levels of serum phosphorus with a mean of 1.84 (0.16) nmol/L. The mean level of serum calcidiol was 66.82 (33.65) nmol/L. Calcidiol concentration was normal (≥ 30 nmol/L) [17] for 88% of measurements and deficient for 12%, with an average of 22.8 (3.9) nmol/L.

6-hour urine calciuria was obtained for 94% of the cohort. The concentration of calcium in urine was reduced (<1.6mmol/L) in 37.1% of the cohort (according to our local reference values), normal in 58.8% of the cohort, and high (> 5.3 mmol/L) in 4.1%, with a mean calciuria of 2.86 (1.1) mmol/L, 0.86 (0.4) nmol/L, and 7.65 (1.8) nmol/L, respectively.

TABLE 1 Baseline characteristics.

Variable	n (%)
Sex, female	54 (52.4)
Age (years; range)	
Early childhood (2-3)	9 (8.7)
Childhood (4-9)	33 (32)
Adolescence (10-17)	55 (53.4)
Young adulthood (18-20)	6 (5.8)
Ethnicity	
Caucasian	82 (79.6)
Other	21 (20.38)
Anthropometric characteristics	
Height ≤ 3rd and 97th percentile	7 (6.8) and 5 (4.9)
Weight ≤ 3rd and 97th percentile	9 (8.7) and 9 (8.7)
Number of Fractures (n) by patient	
None	85 (82.5)
1 fracture; long bone or vertebral	12 (11.7); 8
2 fractures; long bone or vertebral	4 (3.9); 4
≥3 fractures; long bone or vertebral	2 (1.9); 6
Comorbid disease	**99 (96.1)**
Malabsorption/food allergies	47 (46.6)
Juvenile idiopathic arthritis	18 (17.5)
Nephropathies	18 (17.5)
Hematological diseases	7 (6.8)
SARDs and autoinflammatory diseases	11 (10.67)
Endocrinopathies (pituitary hypoplasia)	1 (1)
Osteoporosis inducing medication	
Prior use of corticosteroid	40 (28.8)
Current use of corticosteroid	20 (19.4)
Other IS or chemotherapy	23 (22.33)
Other risk factors	
Insufficient dietary calcium intake	87 (84.5)
Sedentary lifestyle (PAQ<2)	14 (13.6)
History of long bone or vertebral fractures	13 (12.6)
Hypovitaminosis D in blood (<30nmol/L)	12 (11.7)
Hypercalciuria in 24-hour urine	4 (3.9)
N° Risk Factors	
1 risk factor	4 (3.9)
2 risk factors	40 (38.8)
3 risk factors	32 (31.1)
4 risk factors	15 (14.6)
5 risk factors	12 (11.7)

(Continued)

TABLE 1 Continued

SARDs, systemic autoimmune rheumatic diseases; IS, immunosuppressants.

3.2 Comparison of risk factors between patient groups

While statistically significant differences were observed when comparing the number of risk factors among the different comorbid disease groups (p<0.001), these findings should be interpreted cautiously due to small sample sizes. Patients with hematologic

10.3389/fendo.2025.1587985

TABLE 2 Daily mean calcium intake.

Age Group	DRA* (mg/day)	Mean Intake (mg/day)	SD	Range: min- max (mg/d)	% Meeting DRA
Pre-school (2-3y)	700	823	263	513-1346	44.4%
School (4-9y)	1000	655	233	254 - 1186	24.2%
Adolescent (10-17y)	1300	695	329	99 - 1925	10.9%
Young adult (18-20y)	1100	725	156	555 - 985	0%

DRA, daily recommended amount; SD, standard deviation.

diseases presented the highest number of risk factors (5.4 ± 1.64), followed by those with systemic autoimmune diseases (3.75 ± 0.95), while patients with digestive diseases had the lowest number of risk factors (2.29 ± 0.7). A similar consideration applies to the observed proportion of fractures (57.1%) and sedentary behavior (71.4%) in the hematologic group.

When comparing risk factors between age groups, higher proportions of immunosuppressant treatment (43.6%, p=0.016) and lower daily calcium intake (p=0.035) were found in adolescents, followed by young adults. In addition, the number of risk factors increased with age (1.6 in pre-school children, 3.4 in adolescents, and 3.2 in young adults) (p<0.001). Sedentary lifestyle was most frequent among young adults (33.3%, p=0.017).

3.3 Densitometric results of the population

Tables 3 and 4 show BMD values for the major body regions of interest by sex and the mean BMD for each comorbid disease. A higher age-adjusted vertebral BMD was observed in females (p=0.005), but it was not observed in total body BMD or in total body less head BMD (p=0.762 and p=0.902, respectively).

Table 5 shows the proportion of LBMca in each comorbid disease group according to non-adjusted and height adjusted vertebral and total body Z-score.

Figure 1 shows the classification flow of the 103 patients included in the study according to their BMD Z-scores and fracture history. Of the total cohort, 11 patients met the criteria for LBMca, defined as a BMD Z-score ≤ -2. Among these, 5 patients also presented a clinically significant fracture history, thus fulfilling the criteria for cOP.

Vertebral morphometry was performed on 95 children: five patients showed vertebral fractures, of whom four were asymptomatic. Table 6 provides detailed information about the vertebral fractures identified through morphometry in these patients, including fracture types and associated diagnoses.

3.4 Association of clinical risk factors and BMD value

The correlation between clinical risk factors and BMD was assessed. A statistically significant relationship between vertebral BMD and age (p<0.001), sex (p<0.001), presence of hypovitaminosis D (p<0.001), time since diagnosis (p<0.001) and Latin American ethnicity (p<0.001) was found with a combined correlation coefficient of 0.73. This indicates that these risk factors accounted for 73% of the observed variability in vertebral BMD.

There was also a statistically significant relationship between total body BMD and age (p<0.001), time since diagnosis (p<0.001) and sedentary behaviors (p<0.001), with a combined correlation coefficient of 0.81 (p<0.001) and a statistically significant relationship between total body BMD less head and age (p<0.001), time since diagnosis (p<0.001), level of physical activity (p<0.001), and Latin American ethnicity (p=0.031). In this context, Latin American ethnicity may reflect underlying sociocultural, environmental, or genetic factors that were not directly measured in this study.

There was a statistically significant positive correlation between the number of risk factors and BMD in the three major regions of interest, but this relationship lost statistical significance when stratified by age.

TABLE 3 BMD values of major body regions of interest by sex.

Sex	Bone Mineral Density				
	Total Body	Total Body Less Head	Vertebral	Femur (Total)	Femoral Neck
Female					
Mean (SD)	0.83 (0.16)	0.71 (0.16)	0.69 (0.18)	0.74 (0.16)	0.69 (0.15)
Range	0.54 – 1.17	0.41 – 1.01	0.39 – 1.06	0.44 – 1.17	0.40 – 10.30
Male					
Mean (SD)	0.79 (0.16)	0.66 (0.18)	0.59 (0.16)	0.74 (0.17)	0.68 (0.14)
Range	0.53 – 1.12	0.39 - 1	0.36 – 0.99	0.46 – 1.06	0.38 – 0.94

BMD, bone mineral density.

10.3389/fendo.2025.1587985

TABLE 4 Age-adjusted BMD of major body regions of interest by comorbid disease.

Comorbid disease	Bone Mineral Density		
	Vertebral Mean (SD)	Total Body Mean (SD)	Total Body Less Head Mean (SD)
Juvenile idiopathic arthritis (JIA)	0.70 (0.16)	0.86 (0.13)	0.73 (0.12)
Autoinflammatory diseases	0.76 (0.30)	0.94 (0.24)	0.78 (0.23)
Vasculitis	0.74 (0.17)	0.91 (0.14)	0.80 (0.14)
Connective tissue diseases	0.83 (0.23)	0.93 (0.18)	0.82 (0.17)
Malabsorption/ food allergies	0.66 (0.17)	0.84 (0.14)	0.72 (0.14)
Hematologic diseases	0.69 (0.16)	0.84 (0.16)	0.76 (0.15)
Endocrinopathy	0.68 (0.13)	0.87 (0.11)	0.71 (0.19)

Results from subgroup analyses are exploratory. Limited sample sizes within diagnostic groups may affect the precision and generalizability of prevalence estimates.
BMD, bone mineral density; SD, standard deviation.

A stepwise backward elimination of variables was performed to select the best predictive linear regression model. Finally, a linear regression test adjusted by age was performed to evaluate the association of risk factors and BMD values in different regions (Table 7). Vertebral BMD had a positive adjusted association with male sex and hypovitaminosis D. Whole body BMD had a negative adjusted association with a sedentary lifestyle and a history of fracture. Total body less head BMD had a negative adjusted association with current steroid treatment, a sedentary lifestyle, and a history of fracture.

4 Discussion

The objective of this study was to identify patients at risk of presenting LBMca based on their risk factors, describe this population, and assess the prevalence of LBMca and cOP. Additionally, the study aimed to investigate the impact of each risk factor on BMD. Our findings offer novel insights into the prevalence and influence of various risk factors on BMD within a growing population at risk of LBMca in a real-world setting.

4.1 Risk factors in our population

The patients included in the study were initially identified based on having one risk factor for developing LBMca. Upon further evaluation, we found that more than one-third of these patients had two or more risk factors. Notably, over one-quarter had at least four risk factors, which had previously gone unnoticed. This finding underscores the need for greater vigilance in identifying and monitoring risk factors to prevent them from being overlooked.

A higher number of risk factors was observed in patients with hematologic diseases, which could be expected given their frequent comorbidities. Additionally, the number of risk factors increased with age. However, these subgroup patterns are preliminary and should be viewed as hypothesis-generating, since subgroup sample sizes were small, particularly in the hematologic subgroup (n=7). To our knowledge, no other published studies of similar cohorts have described this observation, and further research is needed to validate these findings.

The most prevalent risk factor in this study was low calcium intake, which was found in 84.5% of the total cohort. Previous studies had observed a decrease in calcium intake in young, healthy individuals who were completing the transition to adulthood (23). A high percentage of inadequate calcium intake favors the presence of additional risk factors.

TABLE 5 Proportion of LBMca by diagnosis groups before and after height adjustment.

Comorbid disease	Low Bone Mass for chronological age			
	Vertebral Z-score (%)	Vertebral Adjusted Z-score (%)	Total Body Z-score (%)	Total Body Adjusted Z-score (%)
Juvenile idiopathic arthritis (JIA)	11.1	5.6	11.8	0
Autoinflammatory diseases	0	0	0	0
Vasculitis	0	0	25	0
Connective tissue diseases	0	0	0	0
Malabsorption/food allergies	9.1	7.1	7	9.8
Hematologic diseases	28.6	33.3	50	60
Nephropathies	0	0	5.6	0
Total	8.2	6.4	10.5	7.7

Results from subgroup analyses are exploratory. Limited sample sizes within diagnostic groups may affect the precision and generalizability of prevalence estimates.
LBMca, low bone mass for chronological age (Z-score ≤ -2SD); Adjusted Z-score: height-adjusted Z-score.

10.3389/fendo.2025.1587985

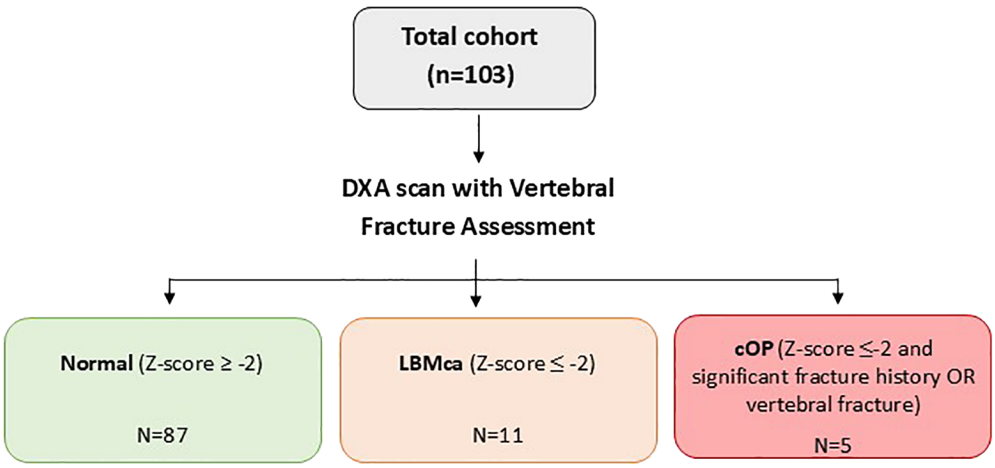

FIGURE 1
Flowchart study of population classification according to bone mineral density and fracture history. DXA, dual-energy x-ray absorptiometry; LBMca, Low Bone Mass for chronological age; cOP, Childhood Osteoporosis.

The relatively low fracture history (13/103) despite the prevalence of risk factors is not due to under-reporting, as our methodology included thorough examination of clinical histories for both personal and familial fracture incidents. Our approach was strengthened by implementing DXA morphometry assessment specifically to identify vertebral fractures that might otherwise go undetected. This proactive screening revealed a higher prevalence of asymptomatic vertebral fractures that initially anticipated, underscoring the importance of systematic radiological assessment in this population beyond reliance on reported symptoms or clinical history alone.

4.2 Diagnosis groups and BMD differences

When assessing whether there were differences in BMD according to the diagnosis group, it was observed that hematologic diseases along with digestive diseases and nephropathies were the groups with the lowest BMD. Although prior literature supports decreased BMD in relation to these conditions (24–30), our results are not conclusive due to small sample sizes within each subgroup. Nephrotic syndrome is one of the most widely studied diseases (29, 31, 32), and prior evidence illustrates that up to 25% of affected children present Z-scores lower than expected when compared to an average population one year after diagnosis (33).

In our study, hematologic diseases showed the highest proportion of LBMca (60%), followed by Juvenile Idiopathic Arthritis (JIA) and digestive diseases. While these trends are consistent with prior studies, they should be interpreted as exploratory given the limited subgroup sizes and thus require confirmation in larger, prospective cohorts.

4.3 Impact of risk factors on BMD

We observed that the main risk factors related to BMD were age and sedentary lifestyle, which accounted for 81.9% of the variability

TABLE 6 Vertebral fractures by morphometry.

N° Fractures	Fracture Type	Gender	Age (years)	Diagnosis	Other Fractures	LBMca
5	4 wedge (2 mild, 2 moderate) 1 severe biconcave	Female	13	Lymphoma	No	No
1	T7 mild wedge	Female	15	Polyartheritis Nodosa	No	No
1	T7 mild wedge	Male	11	Juvenile Idiopathic Arthritis	Yes	Yes
1	T8 moderate wedge	Female	11	Acute Lymphoblastic Leukemia + Hypopituitarism	Yes	Yes
1	T7 mild biconcave	Female	11	Cow's Milk Protein Allergy	No	No

LBMca, Low Bone Mass for chronological age.

in total body BMD. For total body less head BMD, these two factors, along with Latin American ethnicity, likely serving as a proxy for broader unmeasured sociocultural, environmental, or genetic factors, explained 82.5% of the variability. Regarding vertebral BMD, a sedentary lifestyle was not found to be associated with variability in BMD. However, hypovitaminosis D, along with age, sex, and ethnicity, were found to be statistically significant related factors. The positive association between hypovitaminosis D and vertebral BMD may be influenced by several factors, including seasonal fluctuations in sunlight exposure (34, 35), the patient's ethnicity (36), genetic polymorphisms (34, 35, 37), underlying diseases (35), vitamin D supplementation history, and other potential confounders (37). In particular, ethnic differences in vitamin D metabolism and seasonal variations in solar exposure could contribute to variability in vitamin D levels.

Moreover, prior studies, including ours, have described lower vitamin D concentrations in individuals with higher body weight (36). In the pediatric population, weight gain is often related to a higher BMD (38–40), a trend also described in our sample. Therefore, the relationship between Vitamin D and body weight may exert a further confounding effect in the interpretation of hypovitaminosis D and its effects on BMD, particularly in a growing population experiencing both weight gain and increasing BMD over time.

Additionally, disease severity in children with chronic diseases could play a critical role in both vitamin D metabolism and BMD. Similarly, vitamin D supplementation may modify the observed association between hypovitaminosis D and BMD, as those receiving supplementation could exhibit different bone health outcomes. Given these considerations, we interpret the positive association between hypovitaminosis and vertebral BMD with caution. Further sensitivity analyses, including adjustments for these potential confounders, are warranted to validate this finding. The complexity of the relationship between vitamin D, weight, and BMD in pediatric populations underscores the need for additional studies to clarify these associations.

Interestingly, whole body less head BMD had a negative adjusted association with current steroid treatment, but vertebral BMD did not, even though trabecular bone would be expected to be more sensitive to glucocorticoids. Previous histomorphometric studies describe that the use of corticosteroids in the pediatric population is associated with a decrease in trabecular thickness and the thickness of the osteoid material, together with an increase in the space between trabeculae, but these children are also reported as presenting heterogeneous and hypermineralized mineralization (41). The authors postulate that this heterogeneous hypermineralization, may partially explain why whole body less head may be more sensitive for evaluating the bone effects of glucocorticoids, since the evaluated area is larger and probably less sensitive to heterogeneity in mineralization.

It can be deduced from these data that sedentary lifestyle is the modifiable risk factor with the greatest impact on BMD in pediatric age. However, due to the cross-sectional design of this study, causality cannot be inferred, thus longitudinal cohort studies are needed to better understand temporal associations. In this study, a link between a decrease in the level of physical activity and increasing age was observed, and this observation has also been described in a comparable healthy population (17, 42). This decrease in the level of physical activity is a growing concern, and is also important in both healthy adolescents and adolescents suffering from chronic diseases, especially because of the well-known benefits of physical activity for both groups (43–48). In this respect, there are studies in which a lower level of physical activity is described in children and adolescents with JIA despite an adequate management of the disease (49). The same lower level was observed in children suffering from hematologic diseases 10 months after receiving their last treatment (50), as well as in children with chronic nephropathies (51), and in children with systemic autoimmune diseases (52), among others. Our study found a lower level of physical activity in children with hematologic diseases, followed by nephropathies, vasculitis, and autoinflammatory diseases.

There was no statistically significant association between the number of risk factors and total body, total body less head, and vertebral BMD measurements stratified by age. However, there was a clear trend of patients with a higher number of risk factors presenting a lower BMD. Although this study did not find a statistically significant relationship between any risk factors, or a combination of them, and LBMca, the authors believe it is important to consider them when evaluating children at risk of fractures.

A major limitation of our study is the inability to calculate Z-scores for the Total Body Less Head projections due to technical constraints of outdated DXA software, which undermines the standardization and comparability of these measurements. To mitigate this issue, we prioritized the use of raw BMD values alongside the available Z-scores, enhancing transparency and emphasizing their role in preserving the interpretability of our findings. While we believe the raw BMD values offer valuable clinical insights, they may not be as easily interpretable as Z-scores. These limitations should be taken into account when interpreting our findings, and further research with updated DXA software and standardized protocols is warranted to validate and expand upon our results.

The study's cross-sectional design also represents a limitation, as it restricts our ability to draw causal inferences. Although we observed associations between sedentary lifestyle, hematological diseases, and BMD, these findings should be interpreted with caution. Further longitudinal studies are necessary to establish the temporal relationship between clinical risk factors and the development of LBMca or cOP over time. Moreover, the relatively small sample size (n=103) limits the statistical power of subgroup analyses. As such, all subgroup findings should be interpreted as exploratory.

Regarding data collection, another limitation concerns potential measurement bias in dietary calcium intake and physical activity levels. While the INDICAD questionnaire to estimate calcium intake is practical, it remains subject to recall bias inherent in

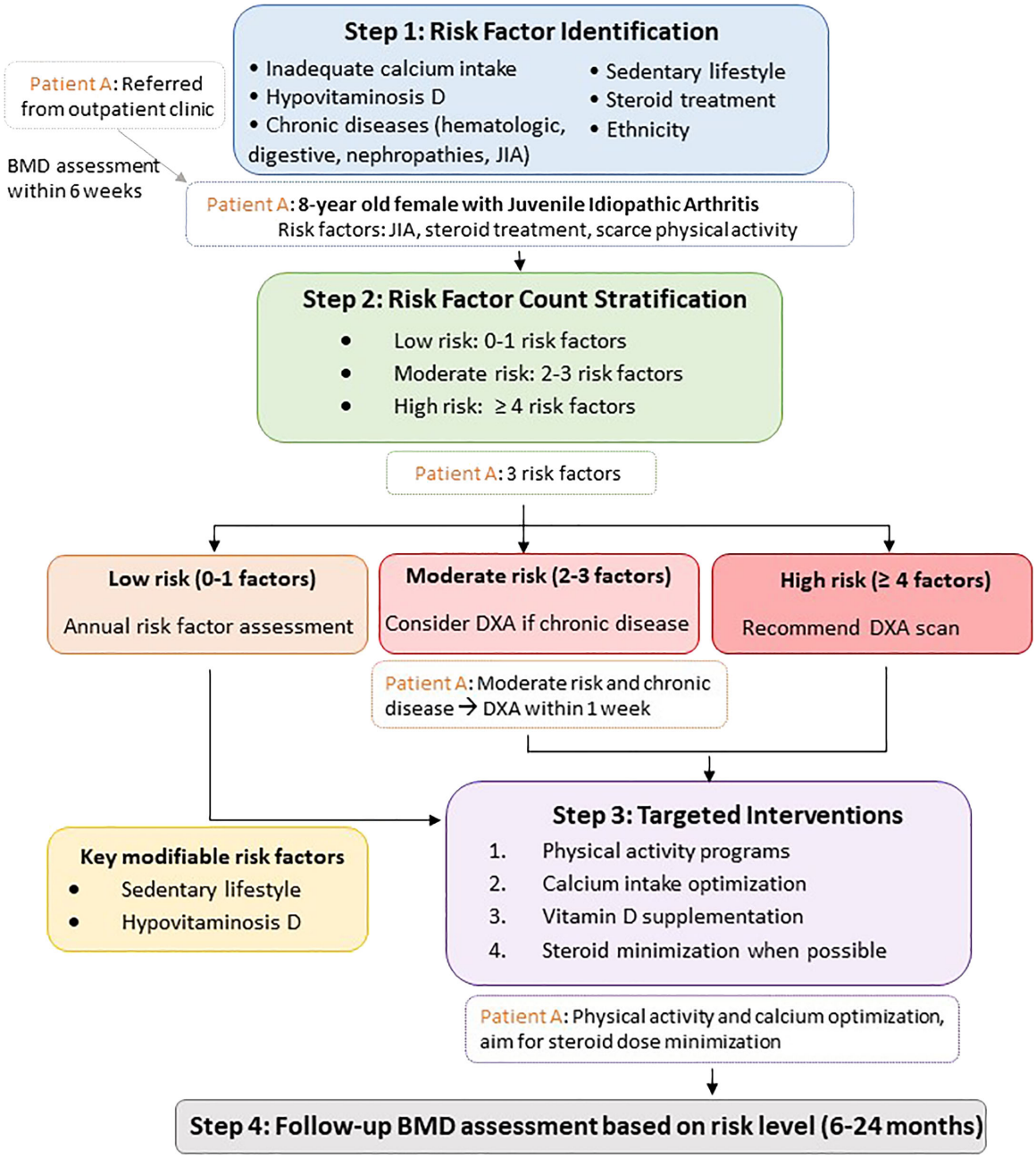

FIGURE 2
Screening Algorithm for Pediatric LBMca Risk. *A representative patient pathway has been added to illustrate the clinical decision process. LBMca, Low Bone Mass for chronological age; BMD, Bone Mineral Density; JIA, juvenile idiopathic arthritis; cOP, Childhood Osteoporosis.

self-reported dietary assessments. Likewise, physical activity questionnaires are not validated for children under three years of age, leading to incomplete data from this subgroup.

Despite these limitations, our study offers valuable insights. To our knowledge, this is the first study to investigate the prevalence and relevance contribution of each risk factor on BMD in a real setting of a pediatric growing population at risk of LBMca. While the current data provide an important foundation, future research should aim for larger, longitudinal designs.

Based on our findings regarding risk factor prevalence and their impact on BMD, we propose a screening algorithm for patients at risk of LBMca (Figure 2). This algorithm emphasizes the identification of risk factors and provides a structured approach to risk stratification and monitoring. The role of modifiable factors, especially physical activity, is further emphasized as a key public health message. Implementation of such a screening protocol in clinical practice could facilitate timely intervention in pediatric populations with chronic diseases, potentially preventing long-term bone health complications. While our cross-sectional data cannot establish causality, this screening framework offers a practical application that could inform clinical guidelines for pediatric bone health assessment.

10.3389/fendo.2025.1587985

TABLE 7 Best predictive regression model adjusted by age.

Variable	Age-adjusted regression Coefficient (95%CI)							
	Vertebral BMD	p	Total Body BMD	p	Total Body Less Head BMD	p	Trabecular Bone Score (TBS)	p
Sex (male)	+0.059 (0.041, 0.159)	**0.00**	+0.10 (0.041, 0.159)	0.51	+0.004 (-0.055, 0.063)	0.81	-34.04 (-63.44, -4.64)	0.08
Calcium intake under DRA	+0.037 (-0.022, 0.096)	0.22	+0.041 (-0.018, 0.100)	0.07	+0.004 (-0.055, 0.063)	0.06	-41.62 (-71.02, -12.22)	0.19
Comorbid disease	-0.043 (-0.102, 0.016)	0.67	+0.026 (-0.033, 0.085)	0.74	-0.038 (-0.097, 0.021)	0.64	-21.16 (-50.56, 8.24)	0.81
>1 comorbid disease	+0.046 (-0.013, 0.105)	0.33	+0.047 (-0.012, 0.106)	0.23	+0.043 (-0.016, 0.102)	0.3	-6.87 (-36.27, 22.53)	0.87
IS treatment	+0.009 (-0.050, 0.068)	0.68	-0.017 (-0.076, 0.042)	0.31	-0.02 (-0.079, 0.039)	0.26	-18.89 (-48.29, 10.51)	0.35
Steroid treatment	-0.016 (-0.075, 0.043)	0.53	-0.033 (-0.092, 0.026)	0.09	-0.047 (-0.106, 0.012)	**0.02**	-25.16 (-54.56, 4.24)	0.29
Previous steroid treatment	+0.05 (0.009, 0.109)	0.06	+0.039 (-0.020, 0.098)	0.05	+0.039 (-0.020, 0.098)	0.07	+3.10 (-26.30, 32.50)	0.90
Accumulated steroid doses	-<0.001 (-0.059, 0.059)	0.74	-0.000 (-0.059, 0.059)	0.73	-<0.001 (-0.059, 0.059)	0.72	-0.003 (-29.43, 29.42)	0.25
Duration of steroid treatment	+<0.001 (-0.059, 0.059)	0.57	+0.000 (-0.059, 0.059)	0.66	+<0.001 (-0.059, 0.059)	0.90	+0.19 (-29.21, 29.59)	0.66
Hypovitaminosis D	+0.083 (0.004, 0.162)	**0.03**	+0.049 (-0.010, 0.108)	0.09	+0.054 (-0.005, 0.113)	0.08	+13.91 (-15.49, 43.31)	0.67
Sedentary lifestyle	-0.052 (-0.111, 0.007)	0.09	-0.083 (-0.142,-0.024)	**0.00**	-0.091 (-0.150,-0.032)	**0.00**	-34.1 (-63.50, -4.70)	0.22
Fracture history	-0.060 (-0.119,-0.001)	0.05	-0.048 (-0.107, 0.011)	**0.04**	-0.055 (-0.114, 0.004)	**0.03**	-25.87 (-55.27, 3.53)	0.34
Hypercalciuria	-0.005 (-0.064, 0.054)	0.94	+<0.001 (-0.059, 0.059)	1.00	+0.034 (-0.025, 0.093)	0.48	+17.49 (-11.91, 46.89)	0.74
Proteinuria	+0.016 (-0.043, 0.075)	0.56	+0.023 (-0.036, 0.082)	0.27	+0.032 (-0.027, 0.091)	0.14	-23.18 (-52.58, 6.22)	0.37
Calcium supplement intake	-0.068 (-0.127,-0.009)	0.05	-0.046 (-0.105, 0.013)	0.08	0.038 (-0.021, 0.097)	0.17	-27.17 (-56.57, 2.23)	0.40
Vit D supplement intake	+0.009 (-0.050, 0.068)	0.76	-0.007 (-0.066, 0.052)	0.73	-0.001 (-0.060, 0.058)	0.95	+0.73 (-28.67, 30.13)	0.98
Caucasian	+0.014 (-0.045, 0.073)	0.60	+0.034 (-0.025, 0.093)	0.8	+0.036 (-0.023, 0.095)	0.08	+54.53 (25.13, 83.93)	0.02
Latin American	-0.047 (-0.106, 0.012)	0.17	-0.040 (-0.099, 0.019)	0.12	-0.067 (-0.126,-0.008)	0.01	-92.51 (-121.91, -63.11)	0.01

BMD, Bone Mineral Density; IS, immunosuppressant.
Emphases (bold text) are used for "p-values" reaching statistical significance.

5 Conclusions

In our cohort, LBMca and cOP prevalence in children with risk factors was up to 10.5% and 4.85%, respectively. Children at risk of LBMca/cOP typically presented with two or more risk factors identified, including age, sex, sedentary lifestyle, ethnicity, and hypovitaminosis D. While associations between these factors and bone health were observed, causality remains uncertain due to the cross-sectional nature of the study. Our findings support integrating routine DXA morphometry screening into clinical pathways for pediatric rheumatology and endocrinology, especially for at-risk children, as this revealed asymptomatic vertebral fractures that would have otherwise gone undetected. To fully understand the impact of these factors on the development of bone health and their potential long-term consequences, larger prospective studies are required.

Data availability statement

The original contributions presented in the study are included in the article. Further inquiries can be directed to the corresponding authors.

Ethics statement

The studies involving humans were approved by Institutional Ethics Committee of Hospital de la Santa Creu I Sant Pau, Barcelona, Spain (IIBSP-FRA-2016-11). The studies were conducted in accordance with the local legislation and institutional requirements. Written informed consent for participation in this study was provided by the participants' legal guardians/next of kin.

Author contributions

BM: Conceptualization, Formal Analysis, Methodology, Project administration, Validation, Writing – original draft, Writing – review & editing. DC: Writing – review & editing. JB: Methodology, Writing – review & editing. GF: Methodology, Writing – review & editing. HP: Methodology, Writing – review & editing. HC-M: Methodology, Project administration, Validation, Visualization, Writing – review & editing. EQ: Methodology, Writing – review & editing. ML: Methodology, Writing – review & editing. MT: Writing – review & editing. AM: Investigation, Writing – review & editing. SH: Investigation, Writing – review & editing. IG: Software, Writing – review & editing. SB: Writing – review & editing. JC: Writing – review & editing. HC: Writing – review & editing. JM: Conceptualization, Methodology, Project administration, Writing – review & editing.

Funding

The author(s) declare that no financial support was received for the research and/or publication of this article.

Acknowledgments

We wish to thank the Spanish Society of Rheumatology (SER) Investigation Unit for their methodological support.

Conflict of interest

The authors declare that the research was conducted in the absence of any commercial or financial relationships that could be construed as a potential conflict of interest.

Generative AI statement

The author(s) declare that no Generative AI was used in the creation of this manuscript.

Publisher's note

References

1. Klibanski A, Adams-Campbell L, Bassford T, Blair SN, Boden SD, Dickersin K, et al. Osteoporosis prevention, diagnosis, and therapy. NIH consensus statement. *Journal of the American Medical Association (JAMA)*. (2000) 17:1–45. doi: 10.1001/jama.285.6.785

2. Pitukcheewanont P, Austin J, Chen P, Punyasavatsut N. Bone health in children and adolescents: risk factors for low bone density. *Pediatr Endocrinol Rev: PER*. (2013) 10:318–35.

3. Cooper C, Westlake S, Harvey N, Javaid K, Dennison E, Hanson M. Review: developmental origins of osteoporotic fracture. *Osteoporosis Int*. (2006) 17:337–47. doi: 10.1007/s00198-005-2039-5

4. Zhu X, Zheng H. Factors influencing peak bone mass gain. *Front Med*. (2021) 15:53–69. doi: 10.1007/s11684-020-0748-y

5. S B. Osteoporosis infantil. *Protoc Diagn Ter Pediatr*. (2014) 1:197–201.

6. Makitie O. Causes, mechanisms and management of paediatric osteoporosis. *Nat Rev Rheumatol*. (2013) 9:465–75. doi: 10.1038/nrrheum.2013.45

7. Galindo Zavala R, Núñez Cuadros E, Martín Pedraz L, Díaz-Cordovés Rego G, Sierra Salinas C, Urda Cardona A. Baja densidad mineral ósea en artritis idiopática juvenil: prevalencia y factores relacionados. *Anales Pediatría*. (2017) 87:218–25. doi: 10.1016/j.anpedi.2016.12.005

8. Reumatología S. *Manual de Enfermedades Óseas*. (2010). *Editorial médica Panamericana S.A. España*. 512 p.

9. Bianchi ML, Cimaz R, Galbiati E, Corona F, Cherubini R, Bardare M. Bone mass change during methotrexate treatment in patients with juvenile rheumatoid arthritis. *Osteoporosis Int*. (1999) 10:20–5. doi: 10.1007/s001980050189

10. Borusiak P, Langer T, Heruth M, Karenfort M, Bettendorf U, Jenke AC. Antiepileptic drugs and bone metabolism in children: data from 128 patients. *J Child Neurol*. (2013) 28:176–83. doi: 10.1177/0883073812443005

11. Ooi PH, Thompson-Hodgetts S, Pritchard-Wiart L, Gilmour SM, Mager DR. Pediatric sarcopenia: A paradigm in the overall definition of malnutrition in children? *JPEN J Parenteral Enteral Nutr*. (2020) 44:407–18. doi: 10.1002/jpen.1681

12. Buccheri E, Dell'Aquila D, Russo M, Chiaramonte R, Musumeci G, Vecchio M. Can artificial intelligence simplify the screening of muscle mass loss? *Heliyon*. (2023) 9:e16323. doi: 10.1016/j.heliyon.2023.e16323

13. Mangano GRA, Avola M, Blatti C, Caldaci A, Sapienza M, Chiaramonte R, et al. Non-adherence to anti-osteoporosis medication: factors influencing and strategies to overcome it. A narrative review. *J Clin Med*. (2022) 12. doi: 10.3390/jcm12010014

14. Gordon CM, Leonard MB, Zemel BS. 2013 Pediatric Position Development Conference: executive summary and reflections. *J Clin Densitom: Off J Int Soc Clin Densitom*. (2014) 17:219–24. doi: 10.1016/j.jocd.2014.01.007

15. Orozco P, Vilert Garrofa E, Zwart Salmeron M. *Evaluación de la ingesta de calcio en la población adulta de España. Estudio INDICAD* Vol. 13. España: Revista Española de Enfermedades Metabólicas Óseas (REEMO) (2004) p. 117–21.

16. Kowalski KC, Crocker PR, Donen RM. *The physical activity questionnaire for older children (PAQ-C) and adolescents (PAQ-A) manual*. Saskatoon. Canada: College of KInesiology University of Saskatchewan. (2004), 11–5.

17. Martínez-Gómez D, Martínez-de-Haro V, Pozo T, Welk GJ, Villagra A, Calle ME, et al. Fiabilidad y validez del cuestionario de actividad física PAQ-A en adolescentes españoles. *Rev Española Salud Pública*. (2009) 83:427–39.

18. Zemel BS, Leonard MB, Kelly A, Lappe JM, Gilsanz V, Oberfield S, et al. Height adjustment in assessing dual energy x-ray absorptiometry measurements of bone mass and density in children. *J Clin Endocrinol Metab*. (2010) 95:1265–73. doi: 10.1210/jc.2009-2057

19. Zeytinoglu M, Jain RK, Vokes TJ. Vertebral fracture assessment: Enhancing the diagnosis, prevention, and treatment of osteoporosis. *Bone*. (2017) 104:54–65. doi: 10.1016/j.bone.2017.03.004

20. Alqahtani FF, Offiah AC. Diagnosis of osteoporotic vertebral fractures in children. *Pediatr Radiol*. (2018) 49(3):283–96. doi: 10.1007/s00247-018-4279-5

21. Di Marcello F, Di Donato G, d'Angelo DM, Breda L, Chiarelli F. Bone health in children with rheumatic disorders: focus on molecular mechanisms, diagnosis, and management. *Int J Mol Sci*. (2022) 23. doi: 10.3390/ijms23105725

22. Martinez Suarez V, Moreno Villares JM, Dalmau Serra J. Recommended intake of calcium and vitamin D: positioning of the Nutrition Committee of the AEP. *Anales Pediatria (Barcelona Spain: 2003)*. (2012) 77:57.e1–8.

23. Larson NI, Neumark-Sztainer D, Harnack L, Wall M, Story M, Eisenberg ME. Calcium and dairy intake: Longitudinal trends during the transition to young adulthood and correlates of calcium intake. *J Nutr Educ Behav*. (2009) 41:254–60. doi: 10.1016/j.jneb.2008.05.001

24. Wong SC, Catto-Smith AG, Zacharin M. Pathological fractures in paediatric patients with inflammatory bowel disease. *Eur J Pediatr*. (2014) 173:141–51. doi: 10.1007/s00431-013-2174-5

25. Rayar MS, Nayiager T, Webber CE, Barr RD, Athale UH. Predictors of bony morbidity in children with acute lymphoblastic leukemia. *Pediatr Blood Cancer*. (2012) 59:77–82. doi: 10.1002/pbc.24040

26. Nakavachara P, Petchkul J, Jeerawongpanich K, Kiattisakthavee P, Manpayak T, Netsakulnee P, et al. Prevalence of low bone mass among adolescents with nontransfusion-dependent hemoglobin E/beta-thalassemia and its relationship with anemia severity. *Pediatr Blood Cancer*. (2018) 65. doi: 10.1002/pbc.26744

27. Petryk A, Polgreen LE, Barnum JL, Zhang L, Hodges JS, Baker KS, et al. Bone mineral density in children with fanconi anemia after hematopoietic cell transplantation. *Biol Blood Marrow Transpl: J Am Soc Blood Marrow Transpl*. (2015) 21:894–9. doi: 10.1016/j.bbmt.2015.01.002

28. Schundeln MM, Goretzki SC, Hauffa PK, Wieland R, Bauer J, Baeder L, et al. Impairment of bone health in pediatric patients with hemolytic anemia. *PloS One*. (2014) 9:e108400. doi: 10.1371/journal.pone.0108400

29. Hajizadeh N, Mehrkash M, Fahimi D, Qorbani M, Shafa N. Association of bone mineral density with biochemical markers of bone turnover in hemodialysis children. *J Renal Injury Prevent*. (2016) 5:174–8. doi: 10.15171/jrip.2016.37

30. Kärnsund S, Lo B, Bendtsen F, Holm J, Burisch J. Systematic review of the prevalence and development of osteoporosis or low bone mineral density and its risk factors in patients with inflammatory bowel disease. *World J Gastroenterol*. (2020) 26:5362–74. doi: 10.3748/wjg.v26.i35.5362

31. Moon RJ, Gilbert RD, Page A, Murphy L, Taylor P, Cooper C, et al. Children with nephrotic syndrome have greater bone area but similar volumetric bone mineral density to healthy controls. *Bone*. (2014) 58:108–13. doi: 10.1016/j.bone.2013.10.012

32. Hahn D, Hodson EM, Craig JC. Interventions for metabolic bone disease in children with chronic kidney disease. *Cochrane Database Syst Rev*. (2015) 2015: Cd008327. doi: 10.1002/14651858.CD008327.pub2

33. Phan V, Blydt-Hansen T, Feber J, Alos N, Arora S, Atkinson S, et al. Skeletal findings in the first 12 months following initiation of glucocorticoid therapy for pediatric nephrotic syndrome. *Osteoporosis Int*. (2014) 25:627–37. doi: 10.1007/s00198-013-2466-7

34. Ferrari D, Lombardi G, Banfi G. Concerning the vitamin D reference range: pre-analytical and analytical variability of vitamin D measurement. *Biochem Medica*. (2017) 27:030501. doi: 10.11613/BM.2017.030501

35. Doyon A, Schmiedchen B, Sander A, Bayazit A, Duzova A, Canpolat N, et al. Genetic, environmental, and disease-associated correlates of vitamin D status in children with CKD. *Clin J Am Soc Nephrol: CJASN*. (2016) 11:1145–53. doi: 10.2215/CJN.10210915

36. Rajan S, Weishaar T, Keller B. Weight and skin colour as predictors of vitamin D status: results of an epidemiological investigation using nationally representative data. *Public Health Nutr*. (2017) 20:1857–64. doi: 10.1017/S1368980016000173

37. Moon RJ, Harvey NC, Cooper C, D'Angelo S, Curtis EM, Crozier SR, et al. Response to antenatal cholecalciferol supplementation is associated with common vitamin D-related genetic variants. *J Clin Endocrinol Metab*. (2017) 102:2941–9. doi: 10.1210/jc.2017-00682

38. Wetzsteon RJ, Petit MA, Macdonald HM, Hughes JM, Beck TJ, McKay HA. Bone structure and volumetric BMD in overweight children: a longitudinal study. *J Bone Mineral Res: Off J Am Soc Bone Mineral Res*. (2008) 23:1946–53. doi: 10.1359/jbmr.080810

39. Silva CC, Goldberg TB, Teixeira AS, Dalmas JC. Bone mineralization in Brazilian adolescents: the years of maximum bone mass incorporation. *Archivos Latinoamericanos Nutricion*. (2007) 57:118–24.

40. del Rio L, Carrascosa A, Pons F, Gusinye M, Yeste D, Domenech FM. Bone mineral density of the lumbar spine in white Mediterranean Spanish children and adolescents: changes related to age, sex, and puberty. *Pediatr Res*. (1994) 35:362–6. doi: 10.1203/00006450-199403000-00018

41. Harrington J, Holmyard D, Silverman E, Sochett E, Grynpas M. Bone histomorphometric changes in children with rheumatic disorders on chronic glucocorticoids. *Pediatr Rheumatol Online J*. (2016) 14:58. doi: 10.1186/s12969-016-0119-z

42. Proia P, Amato A, Drid P, Korovljev D, Vasto S, Baldassano S. The impact of diet and physical activity on bone health in children and adolescents. *Front Endocrinol*. (2021) 12:704647. doi: 10.3389/fendo.2021.704647

43. Marker AM, Steele RG, Noser AE. Physical activity and health-related quality of life in children and adolescents: A systematic review and meta-analysis. *Health Psychol: Off J Division Health Psychol Am psychol Association*. (2018) 37:893–903. doi: 10.1037/hea0000653

44. Aguilar Jurado MA, Gil Madrona P, Ortega Dato JF, Rodriguez Blanco OF. Improvement of students' physical condition and health after a physical activity breaks program. *Rev Esp Salud Publica*. (2018) 92.

45. Mousikou M, Kyriakou A, Skordis N. Stress and growth in children and adolescents. *Horm Res Paediatr*. (2023) 96:25–33. doi: 10.1159/000521074

46. Fintini D, Cianfarani S, Cofini M, Andreoletti A, Ubertini GM, Cappa M, et al. The bones of children with obesity. *Front Endocrinol (Lausanne)*. (2020) 11:200. doi: 10.3389/fendo.2020.00200

47. Zürcher SJ, Jung R, Monnerat S, Schindera C, Eser P, Meier C, et al. High impact physical activity and bone health of lower extremities in childhood cancer survivors: A cross-sectional study of SURfit. *Int J Cancer*. (2020) 147:1845–54. doi: 10.1002/ijc.32963

48. Cannalire G, Biasucci G, Bertolini L, Patianna V, Petraroli M, Pilloni S, et al. Osteoporosis and bone fragility in children: diagnostic and treatment strategies. *J Clin Med*. (2024) 13:4951. doi: 10.3390/jcm13164951

49. Bohr AH, Nielsen S, Muller K, Karup Pedersen F, Andersen LB. Reduced physical activity in children and adolescents with Juvenile Idiopathic Arthritis despite satisfactory control of inflammation. *Pediatr Rheumatol Online J*. (2015) 13:57. doi: 10.1186/s12969-015-0053-5

50. Bianco A, Patti A, Thomas E, Palma R, Maggio MC, Paoli A, et al. Evaluation of fitness levels of children with a diagnosis of acute leukemia and lymphoma after completion of chemotherapy and autologous hematopoietic stem cell transplantation. *Cancer Med*. (2014) 3:385–9. doi: 10.1002/cam4.2014.3.issue-2

51. Clark EM, Ness AR, Bishop NJ, Tobias JH. Association between bone mass and fractures in children: a prospective cohort study. *J Bone Mineral Res: Off J Am Soc Bone Mineral Res*. (2006) 21:1489–95. doi: 10.1359/jbmr.060601

52. Houghton KM, Tucker LB, Potts JE, McKenzie DC. Fitness, fatigue, disease activity, and quality of life in pediatric lupus. *Arthritis Rheum*. (2008) 59:537–45. doi: 10.1002/art.23534

frontiers | Frontiers in Endocrinology

TYPE Original Research
PUBLISHED 30 June 2025
DOI 10.3389/fendo.2025.1620573

OPEN ACCESS

EDITED BY
Federico Baronio,
Dpt Hospital of Woman and Child, Italy

REVIEWED BY
Giorgio Radetti,
Ospedale di Bolzano, Italy
Sadettin Ciftci,
Selçuk University, Türkiye

*CORRESPONDENCE
Leigh Gabel
Leigh.gabel@ucalgary.ca

RECEIVED 29 April 2025
ACCEPTED 30 May 2025
PUBLISHED 30 June 2025

CITATION
Hodgson E, Condliffe EG and Gabel L (2025) Smaller and thinner long bones in children and adolescents with cerebral palsy and other neuromotor impairments. *Front. Endocrinol.* 16:1620573. doi: 10.3389/fendo.2025.1620573

Smaller and thinner long bones in children and adolescents with cerebral palsy and other neuromotor impairments

Erin Hodgson[1,2,3,4], Elizabeth G. Condliffe[1,2,4,5,6] and Leigh Gabel[1,2,3,4]*

[1]Department of Biomedical Engineering, University of Calgary, Calgary, AB, Canada, [2]Faculty of Kinesiology, University of Calgary, Calgary, AB, Canada, [3]McCaig Institute for Bone and Joint Health, University of Calgary, Calgary, AB, Canada, [4]Alberta Children's Hospital Research Institute, University of Calgary, Calgary, AB, Canada, [5]Departments of Clinical Neurosciences and Pediatrics, University of Calgary, Calgary, AB, Canada, [6]Hotchkiss Brain Institute, University of Calgary, Calgary, AB, Canada

Introduction/Background: Compromised bone and muscle health is a significant concern for children and youth with cerebral palsy (CP) and other non-progressive neuromotor impairments. Weak bones increase the incidence of fragility fractures and predispose individuals to lifelong problems, such as osteoporosis.

Objectives: This study quantified bone and muscle health in children and adolescents with CP and other neuromotor impairments across all five gross motor function classification system (GMFCS) levels.

Methods: Peripheral quantitative computed tomography (pQCT) scans of both tibiae were acquired at the 3%, 38%, and 66% of tibia length in 22 children and adolescents (4–17 years old) diagnosed with CP and "CP-like" neurodevelopmental conditions causing motor impairment. Age-, sex-, and ethnicity-matched Z-scores were generated in reference to a normative typically developing population for total bone mineral content (BMC), trabecular and cortical bone mineral density (Tb.BMD, Ct.BMD), cortical BMC (Ct.BMC), cortical area (Ct.Ar), cortical thickness (Ct.Th), periosteal and endosteal circumference, cortical section modulus (Z), and muscle cross-sectional area (MCSA).

Results: Tibial total BMC, Tb.BMD, Ct.BMC, Ct.Th, Ct.Ar, periosteal circumference, Z, and MCSA were significantly lower in children with CP and CP-like conditions compared to typically developing peers (median Z-scores ranged from -2.66 to -1.09; $p = 0.019$ to <0.001) and showed greater deficits in children and adolescents with lower levels of motor function than those with higher functional abilities (GMFCS I-II *vs* III-V; $p = 0.042$ to <0.001). Endosteal circumference was not different from zero ($p = 0.756$) but was smaller in children and adolescents with lower levels of motor function ($p = 0.042$). Ct.BMD did not differ compared to typically developing youth ($p = 0.202$) or between functional abilities ($p = 0.168$).

Conclusions: Results reveal that bone and muscle size, total and cortical content, and trabecular density are impaired in children with CP and CP-like conditions;

however, cortical mineralization is not impaired. Therefore, the heightened risk of fragility fractures in children and adolescents with CP and CP-like conditions is likely due to smaller and thinner bone structure. Future investigation into bone microarchitecture is warranted.

KEYWORDS

cerebral palsy, bone health, muscle health, neuromotor impairments, children, adolescents, pQCT

1 Introduction

Weight-bearing physical activity is essential for the development of bone and muscle (1, 2). Bones are particularly responsive to stimuli during childhood and adolescence because they accrue bone minerals rapidly, providing a "window of opportunity" to maximize gains from physical activity and mechanical loading (3, 4). Children with cerebral palsy (CP) and similar neuromotor impairments have reduced weight-bearing physical activity and are weaker than their typically developing peers (5, 6). Compromised bone strength significantly increases the incidence of fragility fractures in the lower limbs of individuals with CP (7–10), with an increasing incidence with age (10, 11). Further, the incidence of fragility fractures is significantly greater in those who experience more severe motor function limitations (12), and there remains a high risk of fragility fractures across all functional abilities throughout life (10). Fragility fractures cause immobilization and pain and predispose to osteoporosis, such that adults with CP have a 6–7 times greater risk of osteoporosis than individuals without CP (13, 14). Investigating the impacts of neuromotor impairments and the severity of functional limitations on bone structure during growth is crucial to understanding the factors contributing to lifelong elevated risk of fractures that cause further losses of functional abilities (15).

Individuals with CP are a heterogenous population in terms of the etiology underlying the non-progressive disturbance to brain development causing limitations in movement and posture (e.g. cerebral malformation and stroke) and the severity of the resultant functional limitations (16). Some individuals with CP walk with little to no visible impairment, whereas others have very limited voluntary movement and are unable to stand, sit, or propel a wheelchair without support. To accommodate the variability in abilities, youth with CP are classified based on their degree of motor function on the Gross Motor Function Classification System (GMFCS), with the above abilities corresponding to GMFCS levels I and V, respectively (17). As functional abilities differ across the GMFCS spectrum, so does the impact on musculoskeletal health (13, 14). Therefore, understanding bone and muscle health in childhood and adolescence across the entire spectrum is essential to help healthcare providers and clinicians select appropriate interventions to improve bone and muscle health.

While CP is the most prevalent severe childhood motor disability (18), many other conditions, such as rare genetic disorders, have similar clinical presentations impairing mobility. Most of what is known about bone and muscle development in children with neuromotor impairments comes from studies that used dual X-ray absorptiometry (DXA) to measure two-dimensional areal bone mineral density (BMD). Although the clinical gold standard, DXA cannot differentiate between cortical and trabecular bone, and outcomes are influenced by body size such that areal BMD is systematically underestimated in smaller children (19, 20). On the other hand, peripheral quantitative computed tomography (pQCT) is a three-dimensional imaging modality that assesses volumetric BMD. pQCT can also differentiate between trabecular and cortical bone and image muscle.

Few studies have examined bone and muscle health across a wide range of functional abilities. Further, the current diagnostic approach to CP leads to many uncertainties (21), resulting in gaps in knowledge about the comprehensive assessment of bone health in youth with neuromotor impairments. Therefore, this study aimed to quantify lower limb bone density, geometry, strength, and muscle cross-sectional area and density in youth with CP and other neuromotor impairments across all five GMFCS levels. We hypothesized that youth with CP have significantly impaired bone and muscle health compared to typically developing peers and that those with greater functional limitations will have greater deficits.

2 Materials and methods

2.1 Study design

This cross-sectional study invited participants from a pair of ongoing clinical trials (NCT05473676; NCT05731609) to participate. We decided to include all participants from either parent study regardless of their underlying diagnosis as they all had non-progressive neurodevelopmental conditions that impact their mobility and physical activity levels without primary impairments in bone development. The first (robotic walking) study included participants at least four years of age, unable to walk independently due to a non-progressive childhood-onset

neurological impairment, who were able to fit a Trexo robotic gait trainer (<150 lbs and roughly <5'6") and able to participate in the intensive training and assessments without medical conditions that would preclude weight-bearing or physical activity. All participants in this first parent study were GMFCS III-V. This study included participants with genetic neurodevelopmental conditions that do not align with the current definition of CP (16) (e.g. due to hypotonia being the primary motor impairment or involvement of the spinal cord). Due to the extremely rare nature of these genetic conditions and the potential that revealing the diagnosis may identify participants, the diagnosis cannot be shared and will hereafter be referred to as "CP-like". Their bone imaging was acquired from January 2023 to June 2024. The second (power training) study included participants 8–18 years old, with CP, who were able to exert a maximum voluntary motor effort and follow directions in English who did not have an acute injury or surgery. All participants in this second parent study were GMFCS I-IV. Their bone imaging was acquired between September 2023 and June 2024.

Written informed consent was obtained from the parents or guardians of all participants, and written assent was obtained from participants. The study designs were approved by the University of Calgary Conjoint Health Research Ethics Board, REB21–1166 and REB22-1701.

2.2 Anthropometry

Tibia length was assessed to the nearest 0.1 cm as the distance from the medial malleolus to the tibial plateau, as described previously (22). All measurements were duplicated unless differences were >0.4 cm, where a third measurement was obtained (22). The mean of two measurements or median of three were used to calculate tibia length. Participants' age, biological sex, diagnosis, GMFCS classification, and ethnicity were reported by parents or caregivers in questionnaires. GMFCS classification was determined by the GMFCS Family Report measure (23) following Palisano and Colleagues' definition where those classified as level I could ambulate independently, GMFCS level III can ambulate with a handheld mobility device in some settings, and those GMFCS level V are transported in a manual wheelchair (17). In the first trial, height and weight were either reported by caregivers or through chart review. Heights were not available for all participants and were highly variable due to the severity of functional impairments. In the second community-based trial, participants' height and weight were measured using standard techniques. Height and body mass index (BMI) Z-scores were calculated from the WHO Child Growth Standards (24).

2.3 Bone and muscle imaging

One of two trained operators scanned participants' tibiae using the pQCT XCT 3000 scanner (*Stratec Medical, Pforzheim, Germany*) (25). All participants underwent pre-screening to identify previous relevant fracture/surgery history, confirm there was no implanted metal in the lower limbs, no medical devices that could be impacted by the CT scanner, no contrast imaging administered within five days of the appointment, and no chance of pregnancy. If possible, both tibiae were scanned. If there was a previous fracture or implanted metal in one distal lower limb, only the contralateral limb was scanned.

Daily single-slice quality control and monthly multi-slice quality control were performed on a hydroxyapatite calibration phantom. A two-dimensional scout view was acquired to landmark the growth plates for each participant. A reference line was placed at the most proximal end of the most distal growth plate (26) to ensure the growth plate was not scanned. From this line, scans were acquired at the 3%, 38%, and 66% sites proximal from the reference line to assess trabecular, cortical, and muscle measures, respectively. All participants were scanned using the manufacturer's protocol of 2.4 mm slice at 400 µm, tube voltage of 46 kV DC and current of <0.3 mA. The scout view duration was ~80 seconds, and the slice duration was ~100 seconds (30 mm/sec). The effective dose for this protocol was less than 3 µSV per series of scans. The total scan measurement time was ~8 minutes. In the instance of motion artifact, scans were repeated once. *In vivo* precision at the sites used in this study is excellent (<2% CV) (27).

A single researcher analyzed all scans and evaluated all scans for motion artifacts using a scale from 1 (no motion) to 5 (substantial motion) (28). All scans with a grade of 3 or below were analyzed (software version 6.20); scans graded as 4 were reviewed by a second researcher to confirm grading and exclusion. Analysis included one leg per participant. In participants with bilateral impairments, the limb with the best quality scan was used. In participants with unilateral impairments, the scan of the impaired limb was included in the analysis if possible. In recognition that physiological differences are present in the side not noted to have motor impairments in people with unilateral CP, the less impaired limb was included in the analysis if it was the only scan available.

The region of interest was manually selected for each scan. In each scan, a density threshold differentiated between cortical and trabecular bone, muscle, fat, and other *in vivo* tissues. The 3% total bone mineral content (BMC) and trabecular BMD (Tb.BMD) measurements were calculated using a threshold of 180 mg/cm^3 and a cortical threshold of 480 mg/cm^3, with peel mode and contour mode "1" and a trabecular area of 45%. For the 38% slice measurements, cortical measures including cortical BMD (Ct.BMD), cortical BMC (Ct.BMC), cortical area (Ct.Ar), cortical thickness (Ct.Th) and endosteal and periosteal circumference were analyzed with a threshold of 710 mg/cm^3, with peel mode and contour mode "1", and a trabecular area of 45%. Strength measures, including section modulus (Z) and polar stress-strain index (SSI_p), were calculated with a threshold of 480 mg/cm^3. In brief, Z represents a measure of bone strength by taking into account bone size, while SSI_p is a density-weighted measure that considers bone size and material composition to provide estimates of bending strength (29). The muscle measurements, muscle cross-sectional area (MCSA) and density were calculated with a threshold of 280 mg/cm^3 with contour mode "1", peel mode "2", and smoothing

filter F0305. Muscle separation from subcutaneous fat utilized a threshold-based edge detection with a threshold of 40 mg/cm^3 with contour mode "3", peel mode "1", and smoothing filter F030505; a manual ROI was drawn around the muscle (30). To determine MCSA, bone area was subtracted from total bone and muscle area combined. Muscle density was calculated by dividing total muscle mass by MCSA. Measurements by slice at the 3% site include total BMC (mg/mm) and Tb.BMD (mg/cm^3); at the 38% slice include Ct.BMD (mg/cm^3), Ct.BMC (mg/mm), Ct.Th (mm), Ct.Ar (mm^2), endosteal circumference and periosteal circumference (mm), Z (mm^3) and SSI_p (mm^3); and at the 66% slice include MCSA (mm^2) and muscle density (mg/cm^3). All values (excluding SSI_p and muscle density) were converted to age-, sex-, and ethnicity-matched Z-scores from a normative population (31). All participants were matched to "White" normative data unless they identified as "Black" to align with reference data.

2.4 Positioning in the scanner

Positioning children with neuromotor impairments in the scanner can be challenging (32). The presence of metal in the legs and the short stature of younger participants made acquiring scans on both legs or at the 66% slice (muscle assessment) particularly difficult (66% slice not acquired in 7 participants). Further, as involuntary movement is common in individuals with CP and CP-like conditions, having participants sit stationary for the ~8-minute scan proved difficult. We adopted several modifications over the first months to increase the success of imaging. For example, the use of adapted seating, a Special Tomato Soft-Touch Sitter (*Bergeron Health Care, Dolgeville New York*), aided in positioning children and youth comfortably by adding a slight recline to better align their legs with the scanner and avoid stretching the frequently spastic hamstrings (Figure 1). Further, dimming the lights in the room, having a movie/show on a device that was fixed and out of reach, holding a stuffed animal, and placing stickers on the wall to look at helped participants remain calm and still for the scan duration. Lastly, before the appointment, we sent families a video of what to expect during the appointment, including the sounds the machine makes to reduce anxiety.

FIGURE 1
Participant positioned in the pQCT scanner.

2.5 Statistical analysis

Data were assessed for normality through exploratory histograms and boxplots. The median and interquartile range as well as mean and standard deviations are reported for continuous variables and percent for categorical variables. One-sided Wilcoxon sign rank tests determined whether Z-scores were significantly different from zero (expected Z-scores for typically developing peers). Mann-Whitney tests determined whether variables differed between those with lower functional abilities (GMFCS III-V) compared to those with greater functional abilities (GMFCS I-II), with significance set at $p<0.05$.

3 Results

Twenty-six participants aged 4–17 years consented to bone imaging. Twenty-three participants were diagnosed with CP, and three participants were diagnosed with other non-progressive neuromotor impairments (CP-like). Twenty-two participants had valid scans from at least one impaired leg and were included in the analysis; twenty were diagnosed with CP, and two were diagnosed with CP-like conditions. Participant characteristics are described in Table 1. Amongst those with a diagnosis of CP, 75% had bilateral impairments, and both participants with CP-like conditions had bilateral impairments. All participants with CP had spasticity (GMFCS I-V, n=15); four had a mixed motor impairment (e.g. spastic and either dyskinetic (GMFCS IV, n=3) or ataxic motor impairment (GMFCS II, n=1); one had dystonic spasticity (GMFCS II, n=1). Both CP-like participants had neurodevelopmental disorders causing hypotonia (GMFCS IV, n=2) and like participants with CP, neither had a metabolic or other disorder associated with primary impairments in bone.

3.1 Participant characteristics

Participants included all five GMFCS levels (I:23%; II:32%; III:14%; IV:27%; V:4%). Most participants were biologically male (77%), and 65% identified as White, 14% Black, 9% Indigenous, 4% Arab, 4% Latin American, and 4% Mixed population groups. Height and BMI Z-scores ranged from -3.09 to 2.33 and were not statistically different from zero (p=0.071 and p=0.926, respectively). Tibia length Z-scores ranged from -5.49 to 1.64 (median: -1.05), were significantly different from zero (p=0.019), and were lower in those with greater functional limitations (p=0.015).

3.2 pQCT imaging

Of one hundred forty-eight scans acquired from 26 participants, 47 scans from GMFCS II-IV were excluded due to excessive motion

TABLE 1 Overview of participant characteristics. Mean (+/- SD) and median (Interquartile range), unless otherwise indicated.

	Variable (n=22)	Mean (+/- SD)	Median (IQR)
Population	Age (Years)	11.8 (3.6)	12.2 (9.2, 14.8)
	Sex (M:F)	17:5	
	*Height (cm)	145.7 (22.0)	144.0 (130.4, 167.0)
	*Height Z-score	-0.78 (1.46)	-0.69 (-1.94, 0.76)
	*Weight (kg)	38.7 (20.4)	31.2 (22.6, 56.7)
	*BMI (kg/m^2)	19.3 (5.2)	16.8 (16.2, 23.7)
	*BMI Z-score	0.03 (1.25)	0.05 (-0.71, 0.88)
	GMFCS Level (I/II/III/IV/V)	5:7:3:6:1	
	Motor Impairment Type (Spastic/Mixed-Spastic-Dyskinetic/ Mixed-Spastic-Ataxic/Spastic-Dystonic/Hypotonia)	15:3:1:1:2	
	Tibia Length (mm)	320 (70)	315 (269, 385)
3%Slice	Total BMC (mg/mm)	187.1 (108.5)	158.4 (101.9, 277.4)
	Tb.BMD (mg/cm^3)	178.3 (48.4)	179.7 (141.0, 213.3)
38%Slice	Ct.BMC (mg/mm)	178.2 (81.2)	175.4 (103.6, 235.2)
	Ct.BMD (mg/cm^3)	1100.7 (60.4)	1096.1 (1077.2, 1129.3)
	Ct.Th (mm)	3.5 (0.9)	3.5 (2.7, 4.1)
	Ct.Ar (mm^2)	161.4 (78.2)	155.5 (94.4, 211.5)
	Periosteal Circumference (mm)	55.0 (14.2)	54.1 (41.4, 65.3)
	Endosteal Circumference (mm)	33.2 (9.7)	32.9 (25.4, 37.9)
	Z (mm^3)	849 (599)	702 (327, 1215)
	SSI_p (mm^3)	1104 (768)	884 (432, 1524)
66%Slice	MCSA (mm^2)	3633 (1638)	3587 (2574, 4467)
	Muscle Density (mg/cm^3)	76.4 (3.8)	77.4 (74.2, 79.1)

The 3, 38, and 66% slices included n=20, n=20, and n=17 participants, respectively. *n=17 for height and BMI, n=22 for weight.

artifact (grade of >3). Four participants GMFCS levels III (n=1) and IV (n=3) had all scans excluded (i.e. no valid scans at any site for either leg). Out of all scans acquired, 68% were used in this analysis. Amongst those GMFCS levels I-II, 75%, 85%, and 92% of scans were of acceptable quality for the 3%, 38%, and 66% slices, respectively. GMFCS levels III-V had lower quality scans, with 45%, 48%, and 71% of scans of acceptable quality at the 3%, 38%, and 66% slices, respectively.

3.3 Bone outcomes

3.3.1 Trabecular bone

Total BMC and Tb.BMD Z-scores ranged from -7.15 to 1.43 (median: -2.36) and -5.94 to 0.52 (median: -2.66), respectively. Both total BMC and Tb.BMD were significantly different from zero (Figure 2; p<0.001, for both). Total BMC Z-scores were significantly lower in youth with CP and CP-like conditions with greater functional limitations (GMFCS I-II *vs.* III-V; p<0.001). A trend for lower Tb.BMD was observed in those with greater functional limitations (p=0.076).

3.3.2 Cortical bone and bone strength

Ct.BMC and Ct.Th Z-scores ranged from -7.47 to -0.16 (median: -2.25) and -5.20 to -0.01 (median: -2.55), respectively, and were significantly different from zero (Figure 3; p<0.001). Children and adolescents with greater motor function limitations had lower Ct.BMC (GMFCS I-II *vs.* III-V; p=0.002) and Ct.Th (p=0.004) compared with those with greater functional abilities. Ct.Ar and periosteal circumference Z-scores ranged from -8.58 to 0.17 (median -2.33) and -7.06 to 1.55 (median: -1.09), respectively, were significantly different from zero (p<0.001; Figure 3), and significantly lower in those with greater functional limitations (p<0.001 and p=0.002, respectively). Endosteal circumference Z-scores ranged from -4.23 to 3.07 (median: -0.07) and did not differ compared to typically developing peers (p=0.756). However, endosteal circumference was significantly lower in those with greater functional limitations (p=0.042). Ct.BMD Z-scores ranged

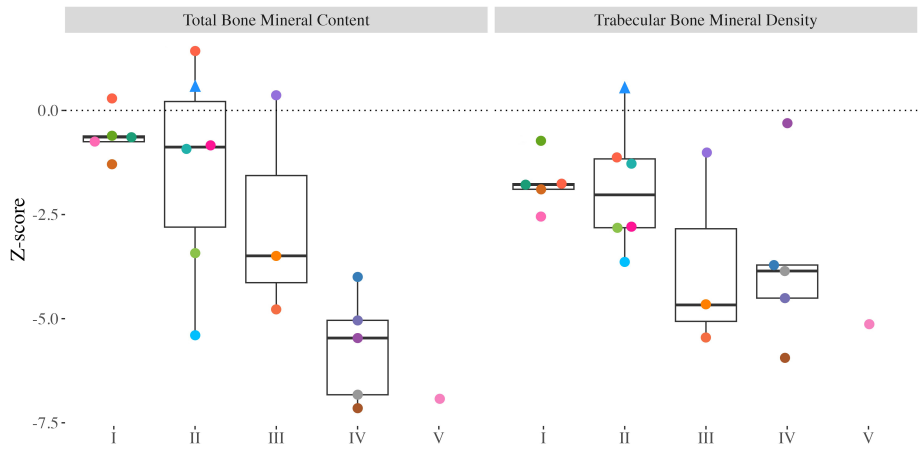

FIGURE 2
Distal tibia Z-scores from all participants with valid scans at the 3% slice. Individual dots represent a unique participant, colours correspond to the same participants across Figures 2-4. Triangles indicate the less impaired leg is included in the analysis (n=1). Bone mineral content (BMC) and trabecular bone mineral density (Tb.BMD).

from -2.21 to 5.71 (median: 0.45), were not significantly different from zero (p=0.202), and did not differ between children and adolescents of varying functional abilities (p=0.168). The Z Z-scores ranged from -13.00 to 0.90 (median: -2.14), were significantly lower than typically developing peers (p<0.001), and were significantly lower in those with greater functional limitations (p<0.001). SSI_p ranged between 206 to 2947 mm^3 (median: 884) and were significantly lower in children and adolescents with greater functional limitations (p=0.002).

3.3.3 Muscle outcomes

MCSA Z-scores ranged from -7.12 to 0.78 (median: -2.73), were significantly different from zero (Figure 4; p<0.001), and were significantly lower in children and adolescents with greater functional limitations (GMFCS I-II *vs.* III-V; p=0.003). Muscle density did not differ between children and adolescents with varying functional abilities (p=0.676).

4 Discussion

This study quantifies bone and muscle health at the tibia in youth with CP and CP-like conditions using pQCT and reveals significant deficits compared to age-, sex-, and ethnicity-matched normative data. Across all GMFCS levels, children with CP and CP-like conditions exhibit significantly lower tibial bone and muscle measures, including total and cortical BMC, cortical size, strength and MCSA, with deficits correlating with functional limitations. Our findings support the notion that elevated lower-limb fracture risk in children and adolescents living with CP can be partially attributed to their slender, thinner, long bone structure. As bone strength in bending is proportional to bone area (bending strength is equal to the cube of the bone's diameter) (33), smaller-diameter bones that are thinner and have lower mineral content are less able to resist fracture (32–36).

Since bones adapt to mechanical loads, ambulation is essential for bone development, stimulating bone accrual and mineralization (1, 2, 37). The deficits we observed in bone mineral content, size, and strength were exacerbated in children and adolescents who experience lower levels of motor function. The early onset of limited loading experienced by individuals with CP and CP-like conditions is likely an important factor contributing to their lower total and cortical bone mineral content (38) accrual. Our findings regarding lower total and cortical bone content align with previous work demonstrating lower values compared to typically developing peers and larger deficits with greater functional limitations (34). In our cohort, Tb.BMD at the distal tibia was significantly lower than that of a typically developing population and, although not statistically significant, showed a trend consistent with previous literature suggesting declines with increasing functional limitations (35). The significantly lower trabecular BMD may suggest that youth with CP and CP-like conditions have impaired trabecular mineralization or fewer and thinner trabeculae (34).

In contrast to other cortical measures, cortical BMD did not differ from a typically developing population or across diagnosis severity. Our finding of average cortical BMD for age aligns with earlier reports showing no differences from typically developing peers (32). Cortical BMD results were unique because there was no association with functional abilities, which likely reflects the proportional relationship between lower cortical content and smaller bone area. Previous studies using DXA indicated impaired mineralization in children with CP who are unable to ambulate independently (39). For example, distal femur DXA scans revealed that absolute areal BMD increased slower than expected for typically developing peers (39). However, previous findings of impaired mineralization (39) may be explained by the fact that DXA systematically underestimates areal BMD in smaller bodies (20), as in this population, and cannot separate trabecular and cortical bone compartments. Future research utilizing high-resolution modalities such as HR-pQCT may provide better

10.3389/fendo.2025.1620573

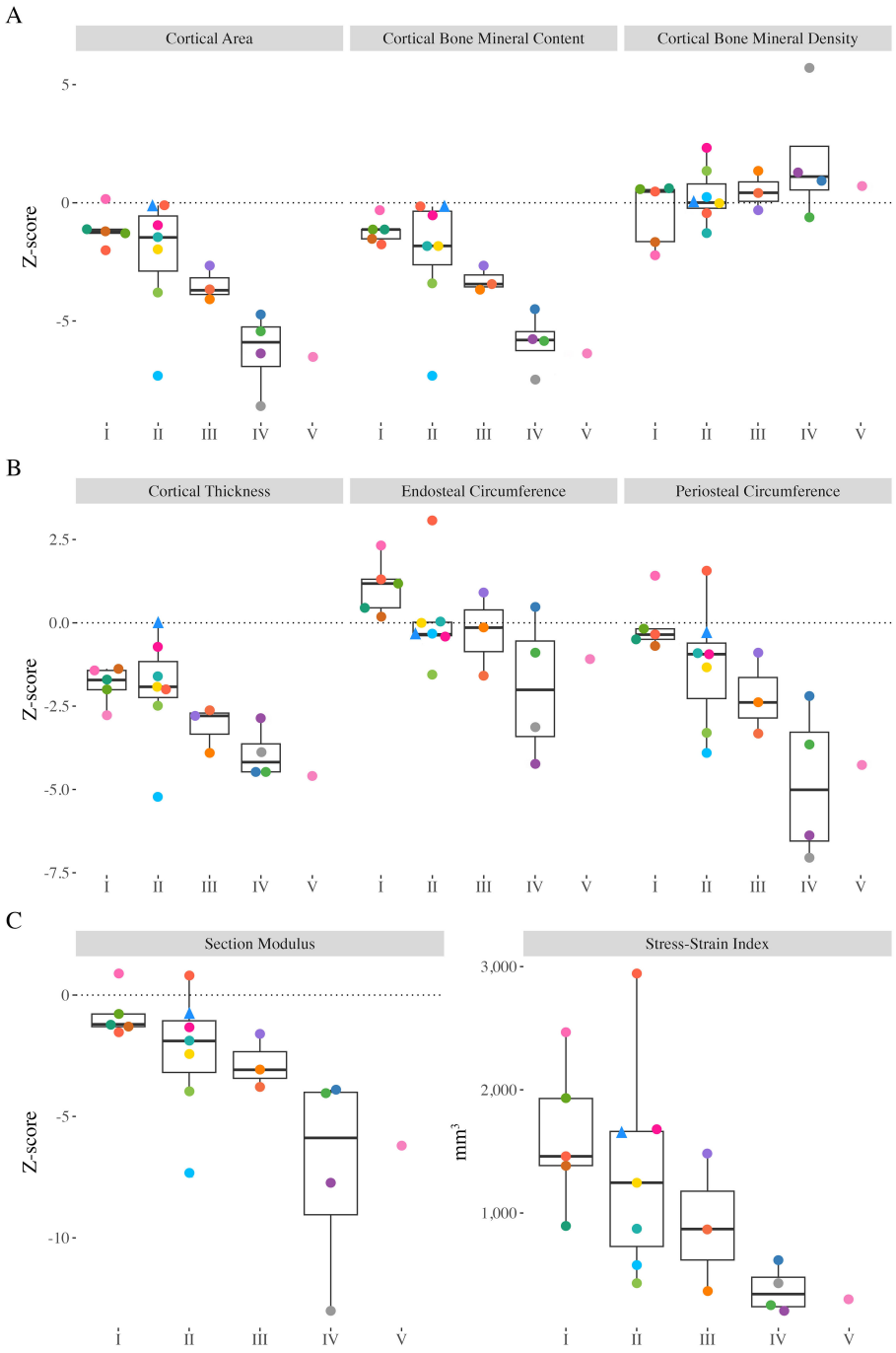

FIGURE 3
Distal tibia Z-scores from all participants with valid scans at the 38% slice. Individual dots represent a unique participant, colours correspond to the same participants across Figures 2-4. Triangles indicate the less impaired leg is included in the analysis (n=1). **(A)** Cortical area (Ct.Ar), cortical bone mineral content (Ct.BMC), cortical bone mineral density (Ct.BMD). **(B)** Cortical thickness (Ct.Th), endosteal circumference, periosteal circumference. **(C)** Section modulus (Z) and polar stress-strain index (SSI_p).

insights into trabecular and cortical microarchitecture, including cortical porosity and trabecular separation, that contribute to BMD measurements and enhance our understanding of bone strength in children and youth with CP and CP-like conditions.

Children with CP and CP-like conditions who experience limited ambulation and loading have greater skeletal fragility (10, 35, 36, 40, 41). Given the importance of loading for periosteal expansion, it was not surprising that we observed more substantial deficits in periosteal expansion and cortical area in youth with greater functional limitations. The smaller periosteal circumference observed in our cohort aligns with previous literature (32) and may be attributed to the early onset of limited loading, which impairs periosteal expansion regardless of GMFCS classification (5, 6). A previous study using MRI highlighted that ambulation is essential

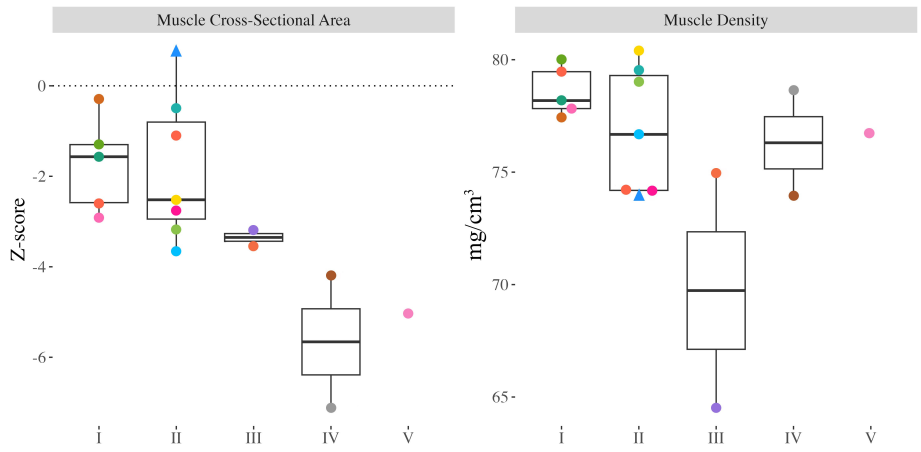

FIGURE 4
Proximal tibia muscle cross-sectional area (MCSA) Z-scores and muscle density from all participants with valid scans at the 66% slice. Individual dots represent a unique participant, colours correspond to the same participants across Figures 2-4. Triangles indicate the less impaired leg is included in the analysis (n=1).

for endosteal and periosteal expansion at the femoral shaft in children classified as GMFCS III-V (5). Although we did not observe lower endosteal circumferences in youth classified as GMFCS I-V compared to a typically developing population, we found that children and adolescents who experience lower levels of motor function had smaller endosteal circumferences. Our observations suggest that endosteal circumference at the tibial shaft is not compromised in individuals with greater functional abilities and that even partial loading may positively influence endocortical bone modelling. Collectively, reduced cortical bone content and size contributed to significantly lower bone strength in children and adolescents with CP and CP-like conditions. Deficits in tibial bone strength were evident across all GMFCS levels and increased with increasing functional limitations. Our finding that section modulus (Z) was 48% lower than expected compared to a normative population aligns with previous research (6) and corroborates greater deficits in strength with increasing functional limitations. Although we speculate that reduced ambulation may be the primary cause of lower bone strength in youth with CP and CP-like conditions, we acknowledge that other factors, such as gait abnormalities that are common in this population (42) as well as nutritional deficiencies due to feeding difficulties (7), may also contribute to reduced bone size and strength. Altered gait would simultaneously change the loading experienced by bones (43) and subsequently affect adaptive responses. Similarly, inadequate nutrition would limit growth, reducing bone size and strength (39). The interplay of limited loading and gait abnormalities resulting in compromised bone size and strength in children with CP and CP-like conditions likely explains their higher incidence of lower limb fragility fractures (6).

To better understand how bone development differs in children with CP and CP-like conditions, the influence of muscle should also be considered. Muscle size can be used as a proxy for the internal muscle strains exerted on bones (36, 44). We found that children with CP and CP-like conditions who experience lower levels of motor function exhibited significantly smaller MCSA (approximately 49% lower than normative data), corroborating similar findings from previous studies (45, 46). Substantially lower MCSA likely reflects a lack of loading and contributes to our observed deficits in bone accrual and strength. We also assessed muscle density, a proxy for muscle fat content (29). We expected to find greater fatty infiltration (lower muscle density) in children and adolescents who experience lower levels of motor function since fatty infiltration is inversely related to physical activity levels (6, 29, 47); however, we did not see differences in muscle density across GMFCS levels (6, 36). As there are no reference values for muscle density, we could not assess whether muscle density differed compared to a typically developing population.

5 Limitations

We note several limitations of our study. Although current results are compared to a normative population of typically developing youth matched for age, sex, and ethnicity, our small sample of children and adolescents with CP may not be representative of the general population of youth living with CP. We included the scan from the less impaired leg of one participant with unilateral CP due to a metal implant in the more impaired leg. This may have underestimated the impact on musculoskeletal outcomes. Further, because we improved our methods incrementally and started with participants with higher GMFCS levels, these participants may be underrepresented. We did not assess other factors that can impact bone development in participants, including vitamin D or calcium levels, which were previously found to be lower in children with CP and CP-like conditions and impact bone (48, 49), anticonvulsant use (48), hormone status (2), or nutritional status (7). We included two participants with CP-like conditions; however, their hypotonia may have influenced bone accrual differently than those with CP. Further, the available normative data were for White and Black youth;

therefore, we could not adjust for other ethnicities and Z-scores may not accurately account for ethnic differences in bone strength (50). Future work would benefit from a more representative normative data set as well as exploration into biomarkers of bone turnover in youth with CP and CP-like conditions. Finally, a higher resolution modality in future, such as HR-pQCT, would provide valuable information regarding trabecular microarchitecture.

6 Conclusions

This study highlights significant deficits in bone and muscle health in youth with CP and CP-like conditions, especially in youth with lower functional abilities. Smaller and thinner bones may make children and adolescents with CP and CP-like conditions more susceptible to fragility fractures in the lower limbs. Despite lower bone mineral content and limited periosteal expansion, cortical bone mineralization was not impaired in youth with CP and CP-like conditions. Knowing these substantial deficits, interventions that improve bone and muscle strength are warranted to reduce fragility fractures and lifelong comorbidities for youth with CP and CP-like conditions.

Data availability statement

Some of the data that support the findings of this study are openly available in Bone Bank: A Bone Health Database for Children with Cerebral Palsy and Neuromotor Impairments at https://doi.org/10.5683/SP3/VLV4YC. Due to the nature of the research and participant privacy, some supporting data is only available upon request with research ethics board approval.

Ethics statement

The studies involving humans were approved by the University of Calgary Conjoint Health Research Ethics Board. The studies were conducted in accordance with the local legislation and institutional requirements. Written informed consent for participation in this study was provided by the participants' legal guardians/next of kin. Written informed consent was obtained from the minor(s)' legal guardian/next of kin for the publication of any potentially identifiable images or data included in this article.

Author contributions

EH: Writing – original draft, Validation, Investigation, Formal analysis, Methodology, Visualization. EGC: Project administration, Writing – review & editing, Funding acquisition, Supervision, Conceptualization. LG: Funding acquisition, Writing – review & editing, Project administration, Supervision, Conceptualization, Methodology.

Funding

The author(s) declare that financial support was received for the research and/or publication of this article. This work was supported by grants to LG and EGC from the Hotchkiss Brain Institute's Robertson Fund for Cerebral Palsy Research, RT752968, to EGC from the Alberta Children's Hospital Vi Riddell Centre for Children's Pain and Rehabilitation and to EGC and LG from the University of Calgary's Vice President Research Catalyst Fund and Alberta Health Services, Maternal Neonatal Children and Youth Strategic Clinical Network's Health Innovations Fund 3.0.

Acknowledgments

We would like to thank the participants and their families for their participation in this research. We further acknowledge those who have contributed in various forms, including our patient partners, the Pediatric Onset of Neuromotor Impairments Lab (PONI Lab)'s patient engagement group as well as members of the PONI Lab, the Centre for Mobility and Joint Health (MOJO), and the Movement and Musculoskeletal Health Lab (MyMSK Lab).

Conflict of interest

The authors declare that the research was conducted in the absence of any commercial or financial relationships that could be construed as a potential conflict of interest.

Generative AI statement

The author(s) declare that no Generative AI was used in the creation of this manuscript.

Publisher's note

References

1. Frost HM. Bone "mass" and the "mechanostat": A proposal. *Anatomical Rec.* (1987) 219:1–9. doi: 10.1002/ar.1092190104

2. Ward KA, Caulton JM, Mughal MZ. Perspective: Cerebral palsy as a model of bone development in the absence of postnatal mechanical factors. *J Musculoskelet Neuronal Interact* (2006) 6:154–9

3. Gabel L, Macdonald HM, Nettlefold L, McKay HA. Physical activity, sedentary time, and bone strength from childhood to early adulthood: A mixed longitudinal HR-pQCT study. *J Bone Mineral Res.* (2017) 32:1525–36. doi: 10.1002/jbmr.3115

4. Hart NM, Nimphius S, Rantalainen T, Ireland A, Siafarikas A, Newton RU. Mechanical basis of bone strength: influence of bone material, bone structure and muscle action. *J Musculoskelet Neuronal Interact* (2017) 17:114–39.

5. Modlesky CM, Kanoff SA, Johnson DL, Subramanian P, Miller F. Evaluation of the femoral midshaft in children with cerebral palsy using magnetic resonance imaging. *Osteoporosis Int.* (2009) 20:609–15. doi: 10.1007/s00198-008-0718-8

6. Whitney DG, Singh H, Miller F, Barbe MF, Slade JM, Pohlig RT, et al. Cortical bone deficit and fat infiltration of bone marrow and skeletal muscle in ambulatory children with mild spastic cerebral palsy. *Bone.* (2017) 94:90–7. doi: 10.1016/j.bone.2016.10.005

7. Henderson RC, Lark RK, Gurka MJ, Worley G, Fung EB, Conaway M, et al. Bone density and metabolism in children and adolescents with moderate to severe cerebral palsy. *Pediatrics.* (2002) 110:e5–5. doi: 10.1542/peds.110.1.e5

8. Damcott M, Blochlinger S, Foulds R. Effects of passive versus dynamic loading interventions on bone health in children who are nonambulatory. *Pediatr Phys Ther.* (2013) 25:248–55. doi: 10.1097/PEP.0b013e318299127d

9. Whitney DG, Hurvitz EA, Caird MS. Bone marrow fat physiology in relation to skeletal metabolism and cardiometabolic disease risk in children with cerebral palsy. *Am J Phys Med Rehabil.* (2018) 97:911–9. doi: 10.1097/PHM.0000000000000981

10. Whitney DG, Hurvitz EA, Caird MS. Critical periods of bone health across the lifespan for individuals with cerebral palsy: Informing clinical guidelines for fracture prevention and monitoring. *Bone.* (2021) 150:1–8. doi: 10.1016/j.bone.2021.116009

11. Stevenson RD, Conaway M, Barrington JW, Cuthill SL, Worley G, Henderson RC. Fracture rate in children with cerebral palsy. *Pediatr Rehabil.* (2006) 9:396–403. doi: 10.1080/13638490600668061

12. Uddenfeldt Wort U, Nordmark E, Wagner P, Düppe H, Westbom L. Fractures in children with cerebral palsy: a total population study. *Dev Med Child Neurol.* (2013) 55:821–6. doi: 10.1111/dmcn.12178

13. Whitney D, Hurvitz E, Ryan J, Devlin M, Caird M, French Z, et al. Noncommunicable disease and multimorbidity in young adults with cerebral palsy. *Clin Epidemiol.* (2018) 10:511–9. doi: 10.2147/CLEP.S159405

14. O'Connell NE, Smith KJ, Peterson MD, Ryan N, Liverani S, Anokye N, et al. Incidence of osteoarthritis, osteoporosis and inflammatory musculoskeletal diseases in adults with cerebral palsy: A population-based cohort study. *Bone.* (2019) 125:30–5. doi: 10.1016/j.bone.2019.05.007

15. Hanna SE, Rosenbaum PL, Bartlett DJ, Palisano RJ, Walter SD, Avery L, et al. Stability and decline in gross motor function among children and youth with cerebral palsy aged 2 to 21 years. *Dev Med Child Neurol.* (2009) 51:295–302. doi: 10.1111/j.1469-8749.2008.03196.x

16. Rosenbaum P, Paneth N, Leviton A, Goldstein M, Bax M. A report: the definition and classification of cerebral palsy April 2006. *Dev Med Child Neurol.* (2007) 49:8–14. doi: 10.1111/j.1469-8749.2007.tb12610.x

17. Palisano RJ, Rosenbaum P, Bartlett D, Livingston MH. Content validity of the expanded and revised Gross Motor Function Classification System. *Dev Med Child Neurol.* (2008) 50:744–50. doi: 10.1111/j.1469-8749.2008.03089.x

18. Amankwah N, Oskoui M, Garner R, Bancej C, Manuel DG, Wall R, et al. Cerebral palsy in Canada 2011-2031: results of a microsimulation modelling study of epidemiological and cost impacts. *Health Promotion Chronic Dis Prev Canada.* (2020) 40:25–37. doi: 10.24095/hpcdp.40.2.01

19. Noble JJ, Fry N, Lewis AP, Charles-Edwards GD, Keevil SF, Gough M, et al. Bone strength is related to muscle volume in ambulant individuals with bilateral spastic cerebral palsy. *Bone.* (2014) 66:251–5. doi: 10.1016/j.bone.2014.06.028

20. Ward LM, Konji VN. Advances in the bone health assessment of children. *Endocrinol Metab Clinics North America.* (2020) 49:613–36. doi: 10.1016/j.ecl.2020.07.005

21. Aravamuthan BR, Fehlings DL, Novak I, Gross P, Alyasiry N, Tilton AH, et al. Uncertainties regarding cerebral palsy diagnosis: opportunities to clarify the consensus definition. *Neurol Clin Pract.* (2024) 14:e200353. doi: 10.1212/CPJ.0000000000200353

22. Gabel L, Mckay HA, Nettlefold L, Race D, Macdonald HM. Bone architecture and strength in the growing skeleton: the role of sedentary time. *Med Sci Sports Exercise.* (2015) 47:363–72. doi: 10.1249/MSS.0000000000000418

23. Morris C, Galuppi BE, Rosenbaum PL. Reliability of family report for the Gross Motor Function Classification System. *Dev Med Child Neurol.* (2004) 46:455–60. doi: 10.1111/j.1469-8749.2004.tb00505.x

24. Chaput JP, Willumsen J, Bull F, Chou R, Ekelund U, Firth J, et al. 2020 WHO guidelines on physical activity and sedentary behaviour for children and adolescents aged 5–17 years: summary of the evidence. *Int J Behav Nutr Phys Activity.* (2020) 17:141. doi: 10.1186/s12966-020-01037-z

25. *'XCT 3000 manual; Software version 6.20.* Durlacher Str., BE, Germany: Stratec Medizintechnik (2017) p. 1–96.

26. Duff WRD, Björkman KM, Kawalilak CE, Kehrig AM, Wiebe S, Kontulainen S. Precision of pQCT-measured total, trabecular and cortical bone area, content, density and estimated bone strength in children. *J Musculoskelet Neuronal Interact* (2017) 17:59–68.

27. Gabel L, Nettlefold L, Brasher PM, Moore SA, Ahamed Y, Macdonald HM, et al. Reexamining the surfaces of bone in boys and girls during adolescent growth: A 12-year mixed longitudinal pQCT study. *J Bone Mineral Res.* (2015) 30:2158–67. doi: 10.1002/jbmr.2570

28. Wong AKO. A comparison of peripheral imaging technologies for bone and muscle quantification: a technical review of image acquisition. *J Musculoskelet Neuronal Interact* (2016) 16:265–82.

29. Farr JN, Funk JL, Chen Z, Lisse JR, Blew RM, Lee VR, et al. Skeletal muscle fat content is inversely associated with bone strength in young girls. *J Bone Mineral Res.* (2011) 26:2217–25. doi: 10.1002/jbmr.414

30. Wong AKO, Hummel K, Moore C, Beattie KA, Shaker S, Craven BC, et al. Improving reliability of pQCT-derived muscle area and density measures using a watershed algorithm for muscle and fat segmentation. *J Clin Densitometry.* (2015) 18:93–101. doi: 10.1016/j.jocd.2014.04.124

31. Leonard MB, Elmi A, Mostoufi-Moab S, Shults J, Burnham JM, Thayu M, et al. Effects of sex, race, and puberty on cortical bone and the functional muscle bone unit in children, adolescents, and young adults. *J Clin Endocrinol Metab.* (2010) 95:1681–9. doi: 10.1210/jc.2009-1913

32. Binkley T, Johnson J, Vogel L, Kecskemethy H, Henderson R, Specker B. Bone measurements by peripheral quantitative computed tomography (pQCT) in children with cerebral palsy. *J Pediatr.* (2005) 147:791–6. doi: 10.1016/j.jpeds.2005.07.014

33. Rauch F. Bone accrual in children: adding substance to surfaces. *Pediatrics.* (2007) 119:S137–40. doi: 10.1542/peds.2006-2023E

34. Modlesky CM, Subramanian P, Miller F. Underdeveloped trabecular bone microarchitecture is detected in children with cerebral palsy using high-resolution magnetic resonance imaging. *Osteoporosis Int.* (2008) 19:169–76. doi: 10.1007/s00198-007-0433-x

35. Wren TA, Lee DC, Kay RM, Dorey FJ, Gilsanz V. Bone density and size in ambulatory children with cerebral palsy: Bone Density and Size in CP. *Dev Med Child Neurol.* (2011) 53:137–41. doi: 10.1111/j.1469-8749.2010.03852.x

36. Modlesky CM, Zhang C. Complicated muscle-bone interactions in children with cerebral palsy. *Curr Osteoporosis Rep.* (2020) 18:47–56. doi: 10.1007/s11914-020-00561-y

37. Schoenau E, Neu CM, Rauch F, Manz F. The Development of Bone Strength at the Proximal Radius during Childhood and Adolescence. *Journal of Clinical Endocrinology & Metabolism* (2001) 86:613–8. doi: 10.1210/jcem.86.2.7186

38. Mughal MZ. Fractures in children with cerebral palsy. *Curr Osteoporosis Rep.* (2014) 12:313–8. doi: 10.1007/s11914-014-0224-1

39. Henderson RC, Kairalla JA, Barrington JW, Abbas A, Stevenson RD. Longitudinal changes in bone density in children and adolescents with moderate to severe cerebral palsy. *J Pediatr.* (2005) 146:769–75. doi: 10.1016/j.jpeds.2005.02.024

40. Peterson MD, Zhang P, Haapala HJ, Wang SC, Hurvitz EA. Greater adipose tissue distribution and diminished spinal musculoskeletal density in adults with cerebral palsy. *Arch Phys Med Rehabil.* (2015) 96:1828–33. doi: 10.1016/j.apmr.2015.06.007

41. Sadowska M, Sarecka-Hujar B, Kopyta I. Cerebral palsy: current opinions on definition, epidemiology, risk factors, classification and treatment options. *Neuropsychiatr Dis Treat.* (2020) 16:1505–18. doi: 10.2147/NDT.S235165

42. Meyns P, Van Gestel L, Bar-On L, Goudriaan M, Wambacq H, Aertbeliën E, et al. Children with spastic cerebral palsy experience difficulties adjusting their gait pattern to weight added to the waist, while typically developing children do not. *Front Hum Neurosci.* (2016) 10:657. doi: 10.3389/fnhum.2016.00657

43. Steele KM, DeMers MS, Schwartz MH, Delp SL. Compressive tibiofemoral force during crouch gait. *Gait Posture.* (2012) 35:556–60. doi: 10.1016/j.gaitpost.2011.11.023

44. Robling AG. Is bone's response to mechanical signals dominated by muscle forces? *Med Sci Sports Exercise.* (2009) 41:2044–9. doi: 10.1249/MSS.0b013e3181a8c702

45. Moreau NG, Teefey SA, Damiano DL. *In vivo* muscle architecture and size of the rectus femoris and vastus lateralis in children and adolescents with cerebral palsy. *Dev Med Child Neurol.* (2009) 51:800–6. doi: 10.1111/j.1469-8749.2009.03307.x

46. Sahrmann AS, Stott NS, Besier TF, Fernandez JW, Handsfield GG. Soleus muscle weakness in cerebral palsy: Muscle architecture revealed with Diffusion Tensor Imaging. *PloS One.* (2019) 14:e0205944. doi: 10.1371/journal.pone.0205944

47. Johnson DL, Miller F, Subramanian P, Modlesky CM. Adipose tissue infiltration of skeletal muscle in children with cerebral palsy. *J Pediatr*. (2009) 154:715–20. doi: 10.1016/j.jpeds.2008.10.046

48. Ozel S, Switzer L, Macintosh A, Fehlings D. Informing evidence-based clinical practice guidelines for children with cerebral palsy at risk of osteoporosis: an update. *Dev Med Child Neurol*. (2016) 58:918–23. doi: 10.1111/dmcn.13196

49. Alenazi KA, Alanezi AA. Prevalence of vitamin D deficiency in children with cerebral palsy: A meta-analysis. *Pediatr Neurol*. (2024) 159:56–61. doi: 10.1016/j.pediatrneurol.2024.03.021

50. Wetzsteon RJ, Hughes JM, Kaufman BC, Vazquez G, Stoffregen TA, Stovitz SD, et al. Ethnic differences in bone geometry and strength are apparent in childhood. *Bone*. (2009) 44:970–5. doi: 10.1016/j.bone.2009.01.006

frontiers | Frontiers in Endocrinology

TYPE Original Research
PUBLISHED 02 July 2025
DOI 10.3389/fendo.2025.1599437

OPEN ACCESS

EDITED BY
Federico Baronio,
Dpt Hospital of Woman and Child, Italy

REVIEWED BY
Cecilia Motta,
Sapienza University of Rome, Italy
Zengzheng Li,
The First People's Hospital of Yunnan Province, China
Koushik Handattu,
Manipal Academy of Higher Education, India
Muhammad Abul Hasanat,
Bangabandhu Sheikh Mujib Medical University (BSMMU), Bangladesh

*CORRESPONDENCE
Yongrong Lai
laiyongrong@263.net
Yuzhen Liang
liangyuzhen26@163.com

RECEIVED 25 March 2025
ACCEPTED 16 June 2025
PUBLISHED 02 July 2025

CITATION
Zhang W, Liu R, He S, Huang J, Wu L, Huang C, Liang Y and Lai Y (2025) Risk factors of low bone mass in young patients with transfusion-dependent beta-thalassemia. *Front. Endocrinol.* 16:1599437. doi: 10.3389/fendo.2025.1599437

Risk factors of low bone mass in young patients with transfusion-dependent beta-thalassemia

Wei Zhang[1,2], Rongrong Liu[3,4,5], Siping He[1], Jihua Huang[1], Liting Wu[1], Cuifeng Huang[2], Yuzhen Liang[1]* and Yongrong Lai[3,4,5]*

[1]Department of Endocrinology, The Second Affiliated Hospital of Guangxi Medical University, Nanning, China, [2]Guangxi Medical University, Nanning, China, [3]Department of Hematology, The First Affiliated Hospital of Guangxi Medical University, Nanning, China, [4]National Health Commission (NHC) Key Laboratory of Thalassemia Medicine, Nanning, China, [5]Guangxi Key Laboratory of Thalassemia Research, Nanning, China

Objective: To determine the prevalence of low bone mass and associated risk factors among children and adolescents suffering from transfusion-dependent beta-thalassemia (TDT).

Methods: In this study, a total of 389 children and adolescents with TDT (236 males and 153 females), treated between January 2015 and December 2024 in the Department of Hematology at the First Affiliated Hospital of Guangxi Medical University, were selected. Subjects were categorized into those with normal bone mass and those with low bone mass based on bone mineral density assessments. Comparative analyses of various indicators between these two groups were performed.

Results: The overall prevalence of low bone mass in TDT patients aged 2–19 years without height-adjusted bone mineral density(BMD)correction was 31.6%, with a prevalence of 33.4% in the 5-19-year subgroup. Multivariate analysis identified age (OR = 1.149, 95% CI 1.052–1.256, P < 0.05), IGF-1 levels < -2 SD (OR = 1.832, 95% CI 1.095–3.067, P < 0.05), and hypogonadism (OR = 2.990, 95% CI 1.087–8.229, P < 0.05) as independent risk factors for low bone mass. After applying height-adjusted BMD correction to the 5-19-year subgroup, the prevalence of low bone mass decreased to 15.8%. In this subgroup, multivariate analysis revealed age (OR = 1.137, 95% CI: 1.034–1.251, P < 0.05), normal BMI (OR = 0.383, 95% CI: 0.158–0.976, P < 0.05), and albumin (ALB) levels (OR = 0.866, 95% CI: 0.783–0.953, P < 0.05) as independent predictors of low bone mass.

Conclusion: This study reveals a high prevalence of low bone mass in children and adolescents with TDT. Without height-adjusted BMD correction, the overall prevalence was 31.6% (33.4% in the 5-19-year subgroup), which significantly decreased to 15.8% in the 5-19-year subgroup after height-adjusted correction, highlighting that traditional BMD assessments may overestimate risk due to unaccounted short stature. Multivariate analysis demonstrated that advancing age consistently remained an independent risk factor (pre-correction OR=1.149; post-correction OR=1.137). The corrected model further identified normal BMI (OR=0.383) and ALB (OR=0.866) as protective factors, while IGF-1 levels < -2 SD

(OR=1.832) and hypogonadism (OR=2.990) emerged as significant risks in the uncorrected model. Clinical management should prioritize height-adjusted BMD evaluation and integrated interventions targeting growth hormone axis function, gonadal status, and nutritional indicators to optimize bone health in TDT patients.

KEYWORDS

transfusion-dependent beta-thalassemia, low bone mass, pediatric and adolescents, bone mineral density, height-adjusted

1 Introduction

Transfusion-Dependent beta -Thalassemia (TDT) is a serious hereditary hemolytic disease caused by defects in the beta-globin genes. It requires long-term blood transfusions and regular iron-chelation therapy to sustain life and is one of the global social public health concerns highlighted by the World Health Organization (WHO) (1). With advancements in standardized transfusion protocols, iron chelation therapy, and hematopoietic stem cell transplantation, the life expectancy of TDT patients has significantly improved. However, this progress has been accompanied by an increased incidence of skeletal complications, particularly osteoporosis and low bone mass (LBM), which have emerged as critical clinical concerns (2–4). Research indicates that 10%-50% of pediatric and adolescent TDT patients develop osteoporosis—significantly exceeding rates in healthy peers—with 20%-40% suffering pathological fractures, severely compromising quality of life and long-term outcomes (5–8). LBM, a precursor to osteoporosis, is especially prevalent in TDT children, characterized by bone mineral density (BMD) below age- and sex-matched norms without meeting osteoporosis diagnostic criteria (9). Adolescence represents a crucial window for bone mass accrual, and failure to intervene early in LBM may lead to progressive bone loss, eventually resulting in osteoporosis and pathological fractures (10).

In our study, we used dual-energy X-ray absorptiometry (DXA) to determine BMD in the lumbar region (L1-L4) for assessing bone mass in TDT children and adolescents. This method was chosen due to the lumbar spine's high trabecular bone content, optimal for detecting bone mass changes. In pediatric bone density assessment, DXA surpasses QCT (quantitative computed tomography) with its minimal radiation exposure, high standardization, operational simplicity, and cost-effectiveness (9).

The pathogenesis of LBM in TDT children involves multifaceted mechanisms, including genetic predisposition, age and sex factors, anemia severity, disease progression, extramedullary hematopoiesis, iron overload, chelating therapy types/side effects, endocrine dysfunction, growth retardation, hepatic/renal impairment, calcium-phosphorus imbalance, vitamin D deficiency, malnutrition, and physical inactivity (8, 11–14). Current screening and management strategies for LBM in TDT patients remain inadequate, particularly lacking systematic interventions during adolescence—the critical period for bone mass accumulation. Existing studies show ongoing controversies regarding key determinants of LBM, underscoring the urgent need for new research to identify critical risk factors for LBM in TDT children and adolescents. Such investigations could provide theoretical foundations for clinical interventions during this reversible phase, ultimately reducing long-term skeletal complications.

Thalassemia is a prevalent medical condition in Guangxi, China. With a carrier rate of 6.66% for beta-thalassemia genes among the population of Guangxi, it ranks as the province with the highest prevalence in China, thus designating it as a high-incidence region for the disease (15). Unfortunately, comprehensive research on bone mass reduction among Chinese children and adolescents with TDT is currently sparse. Situated within the First Affiliated Hospital of Guangxi Medical University, the Department of Hematology is recognized as a leading national center for hematopoietic stem cell transplantation in the treatment of thalassemia in China. The department has been dedicated to performing hematopoietic stem cell transplantation procedures for TDT patients. This study seeks to investigate BMD and associated influencing factors in pediatric and adolescent patients with TDT scheduled for hematopoietic stem cell transplantation at the Department. The objective is to elucidate the incidence of low bone mass among Chinese children and adolescents afflicted with TDT, pinpoint the predictors of diminished bone density, and assist in the timely recognition of individuals at elevated risk for osteoporosis.

2 Methods

2.1 Study design

This was a single-center, cross-sectional, retrospective study that used data obtained from the Department of Hematology at the First Affiliated Hospital of Guangxi Medical University. The study has been reviewed and received approval from the Medical Ethics Committee of the First Affiliated Hospital of Guangxi Medical University, under approval number: 2024-S1000-01.

2.2 Study population

We selected 389 pediatric and adolescent patients diagnosed with TDT who underwent BMD assessments within the Department of Hematology at the First Affiliated Hospital of Guangxi Medical University between January 2015 and December 2024; all were candidates for hematopoietic stem cell transplantation. Participants were categorized into two cohorts based on BMD assessments: the normal bone mass cohort and the low bone mass cohort. Inclusion criteria included patients diagnosed with Thalassemia major, either through hemoglobin electrophoresis, DNA analysis, or clinical evidence of transfusion dependence, aligning with diagnostic standards set by established guidelines (as documented in discharge or initial outpatient records) and who had undergone a BMD test; patients were less than 20 years of age. Exclusion Criteria: Patients with other known diseases that affect bone quantity; patients on long-term glucocorticoid therapy or other medications that impact bone metabolism; and those with incomplete personal and medical records.

Each patient underwent dual-energy X-ray absorptiometry (DXA; Hologic Horizon-A, Hologic Inc. USA), focusing on the lumbar spine (L1-L4) for bone mineral density assessments. The mean bone mineral density values and related Z-scores were meticulously recorded and subsequently diagnosed. The primary clinical data collected include: Demographic information: age, gender, height, weight, and history of splenectomy. Laboratory parameters included hemoglobin (Hb), albumin (ALB), alkaline phosphatase (ALP), creatinine (Cr), total cholesterol (TC), triglycerides (TG), low-density lipoprotein cholesterol (LDLC), high-density lipoprotein cholesterol (HDLC), calcium (Ca), phosphorus (P), parathyroid hormone (PTH), 25-hydroxyvitamin D [25(OH)D], fasting plasma glucose (FPG), fasting insulin (FINS), serum ferritin (SF), insulin-like growth factor-1 (IGF-1), testosterone (T), estradiol (E2), thyroid hormones (free triiodothyronine [FT3], free thyroxine [FT4], thyroid-stimulating hormone [TSH]), osteocalcin (OC), liver iron concentration (LIC), cardiac MRI T2* (a measure of myocardial iron deposition), type of iron chelator, and lumbar spine bone mineral density (BMD) values with corresponding Z-scores. Height and weight were expressed as SD scores and percentiles, while BMI was presented as percentiles (referencing Chinese growth and development reference norms for children and adolescents). Calculation of BMI= weight (Kg)/height squared (m^2).

2.3 Definition

Height: Short Stature: height percentile <3%, Normal: height percentile 3-97%, Tall Stature: >97% (16).

Weight: Underweight: weight percentile <3%, Normal: weight percentile 3-97%, Obesity: >97% (16).

BMI: Thinness: BMI percentile <3%, Normal: BMI percentile 3-85%, Overweight: BMI percentile 85-97%, Obesity: BMI percentile >97% (16).

Low BMD: Characterized by a Z-score of -2.0 or lower at the lumbar spine, as assessed via DXA. In contrast, Normal BMD is denoted by a Z-score greater than -2.0 at the same skeletal site (17).

Hypogonadism (18):Females ≥ 13 years old and males ≥ 14 years old exhibit prepubertal and/or per pubertal progression levels of sex steroids(serum testosterone levels in males < 3.5 nmol/L, serum estradiol levels in females < 50 ng/L).

IGF-1 < -2SD: Using the IGF-1 levels of the general Chinese population of the same sex and age as the reference (19).

Hypothyroidism is characterized by elevated TSH levels beyond the upper limit of the reference range and diminished free T4 levels below the lower limit of the reference range.

Subclinical hypothyroidism is defined by elevated TSH levels surpassing the upper limit of the reference range, in conjunction with free T4 levels that fall within the normal range.

Vitamin D deficiency: Serum levels of 25-hydroxyvitamin D (25 (OH)D) are below 50 nmol/L.

Iron overload: Serum ferritin levels are categorized as follows: mild (< 1000 ng/ml), moderate (1000–2500 ng/ml), and severe (> 2500 ng/ml).

2.4 Statistical analysis

Data analysis was conducted utilizing Excel and SPSS 27.0 (IBM) software. In instances of normally distributed continuous data, results were presented as the mean ± standard deviation, with intergroup comparisons carried out using the independent samples t-test. For continuous data that were not normally distributed, results were depicted as the median (M) along with the interquartile range (P25-P75), and intergroup comparisons were executed using the Mann-Whitney U test. Categorical variables were presented in terms of frequency counts and percentages, and were analyzed using either the chi-square test or Fisher's exact test. Variables that reached a significance level of $P < 0.05$ in the univariate analysis were subsequently incorporated into a binary logistic regression model to determine the independent risk factors associated with reduced bone density in the pediatric and adolescent population with TDT. Statistical significance was defined as a P value of less than 0.05.

3 Results

3.1 Study population

In the group of 389 enrolled patients, ages spanned from 2 to 19 years, with an average age of 8 ± 3years. The cohort comprised 236 males and 153 females. Low bone mass prevalence was 31.6% overall, slightly lower in males at 30.9% compared to females at 32.7%, with no statistically significant discrepancy noted. Among those with low bone mass, ages varied from a minimum of 3 years to a maximum of 19 years. The prevalence of low bone mass was observed to rise with increasing age. Furthermore, 282 patients (72.5%) exhibited severe iron overload, defined by ferritin levels

above 2500 ng/ml, with an average serum ferritin concentration of 3760.620 ng/ml (IQR: 2360.320 to 5502.850 ng/ml). The prevalence of LIC (Liver Iron Concentration) is overall 88.7%, while that for CID (Cardiac Iron Deposition, measured by Cardiac MRI T2*) is 22.4%. The prevalence of chelation therapy usage is as follows: DFO 10.0%, DFP 9.8%, DFX 25.7%, and combined iron chelation 41.3%, with 13.1% not using any or with usage being unknown. A history of splenectomy is present in 12.3% of patients. The prevalence of vitamin D deficiency is 39.1% (152 patients) overall, reaching 36.0% (85 of 236 patients) in males and 43.8% (67 of 153 patients) in females. The prevalence of hypothyroidism is 0.5% (2 of 389 patients), with subclinical hypothyroidism affecting 6.9% (27 of 389 patients) of the population. IGF-1<-2SD is identified in 50.1% (195 of 389 patients) of individuals, with 54.7% (129 of 236 patients) prevalence in males and 43.1% (66 0f 153 patients) in females. Among patients over the age of 13, hypogonadism is prevalent in 70.6% (36 of 51 patients), occurring in 74.2% (23 of 31 patients) of males and 65.0% (13 of 20 patients) of females. Upon comparative analysis of the two groups, the low bone mass group was observed to have higher mean age, lower SDs values for height and weight, increased proportions of short stature and low body weight, elevated TG levels, higher prevalence of hypogonadism and IGF-1<-2SD, alongside significantly reduced BMD and Z-scores at the lumbar spine. No statistically significant differences were observed in other parameters. For detailed results, refer to Table 1.

The study population spanned an age range from 2 to 19 years old. Consistent with growth and developmental principles (20), participants were categorized into two age groups: Group 1 included pre-pubertal individuals aged 2–11 years, while Group 2 comprised adolescents aged 12–19 years. Group 1 had an average age of 7 years, while Group 2's average age was 13. In comparing Group 2 to Group 1, the following characteristics were noted in Group 2: reduced height and weight SDs, an elevated percentage of patients exhibiting low body weight, an increased prevalence of patients with hypogonadism and IGF-1<-2SD, a higher proportion of patients with low bone mass, notably elevated SF concentrations and enhanced CID, a greater incidence of splenectomy, elevated lumbar spine BMD values despite significantly reduced corresponding Z-scores, lower Hb levels, elevated TG and diminished HDLC, increased FPG and INS levels, and diminished 25(OH)D levels (Table 2).

3.2 Univariate analysis

Given that BMI is a standardized measure calculated from height and weight, we opted to include BMI in the analysis while excluding height and weight to mitigate multicollinearity among independent variables. Univariate analysis revealed statistically significant differences (P<0.05) in Age, ALP, TG, P, the proportion of individuals with Overweight BMI (85-97%), Hypogonadism and IGF-1<-2SD (Supplementary Material). The correlation analysis revealed no significant associations among the seven variables(r<0.5). (Supplementary Material). In multivariable logistic regression analysis, with low bone mass as the dependent variable, Age, ALP, TG, P, BMI, Hypogonadism and IGF-1<-2SD were included as independent variables to investigate their associations with the outcome.

3.3 Multivariate logistic regression analysis

Following a comprehensive multivariate logistic regression analysis of seven key variables, we identified Age (OR =1.138, 95% CI 1.041-1.248, P < 0.05), IGF-1<-2SD (OR =1.962, 95% CI1.163-3.321, P < 0.05) and Hypogonadism (OR =2.951, 95% CI1.085-8.444, P < 0.05) as independent risk factors for low bone mass in the pediatric and adolescent population with TDT, as outlined in Figure 1.

3.4 Subgroup analysis

In the 5–19-year patient subgroup, we applied a pediatric bone density calculator (https://zscore.research.chop.edu/calcpedbonedens.php) to perform height-adjusted BMD correction.

TABLE 1 Baseline characteristics.

Variable	Total (n=389)	Normal BMD (n=266)	Low BMD (n=123)	P
Age [IQR, years]	8.00[5.00,11.00]	7.00[5.00,10.00]	10.00[8.00,13.00]	<0.001
SF [IQR, ng/ml]	3760.62 [2360.32,5502.85]	3675.50[2356.74,5179.27]	4053.00[2402.51,6541.92]	0.177
Height SDs [IQR, cm]	-1.00[-2.00,-1.00]	-1.00[-2.00,0.00]	-2.00[-2.00,-1.00]	<0.001
Weight SDs [IQR, Kg]	-1.000[-2.000,0.000]	-1.000[-1.000,0.000]	-2.000[-2.000,-1.000]	<0.001
Hb (± SD, g/L)	102.48 ± 16.93	102.44 ± 16.73	102.57 ± 17.36	0.945
ALB (± SD, g/L)	42.61 ± 3.19	42.56 ± 2.96	42.74 ± 3.63	0.634
ALP [IQR,U/L]	218.00[176.00,271.00]	215.00[173.00,260.00]	226.00[182.00,308.00]	0.087

(Continued)

TABLE 1 Continued

Variable	Total (n=389)	Normal BMD (n=266)	Low BMD (n=123)	P
Cr [IQR, umol/L]	28.00[24.00,32.00]	28.00[24.00,32.00]	28.00[24.00,32.00]	0.777
TCHO [IQR, mmol/L]	2.94[2.57,3.32]	2.94[2.56,3.30]	2.95[2.58,3.47]	0.627
TG [IQR, mmol/L]	1.08[0.84,1.45]	1.04[0.80,1.39]	1.19[0.91,1.86]	0.002
HDLC [IQR, mmol/L]	0.88[0.74,1.02]	0.89[0.75,1.04]	0.83[0.71,1.01]	0.140
LDLC [IQR, mmol/L]	1.53[1.28,1.85]	1.52[1.24,1.80]	1.56[1.37,1.87]	0.123
Ca [IQR, mmol/L]	2.33[2.26,2.40]	2.33[2.26,2.39]	2.34[2.24,2.41]	0.813
P [IQR, mmol/L]	1.67[1.46,1.81]	1.68[1.51,1.81]	1.66[1.40,1.79]	0.129
FPG [IQR, mmol/L]	4.69[4.35,5.07]	4.69[4.36,5.06]	4.70[4.33,5.16]	0.847
FINS [IQR, pmol/L]	43.06[29.01,63.91]	42.39[29.,58.50]	46.19[27.17,67.63]	0.406
25 (OH)D[IQR, nmol/L]	54.60[44.00,68.40]	56.10[44.50,68.63]	50.50[42.27,67.50]	0.097
PTH [IQR, pg/ml]	28.25[21.28,38.92]	28.42[21.09,38.73]	28.02[21.28,39.90]	0.968
Lumbar Z-score [IQR, SD]	-1.50[-2.20, -0.90]	-1.10[-1.50, -0.60]	-2.50[-3.20, -2.20]	<0.001
BMD [IQR, g/cm2]	0.48[0.43,0.54]	0.49[0.45,0.54]	0.45[0.40,0.54]	<0.001
Lumbar BMD Z score adjusted for height (5–19 year) [IQR, SD] (n=335)	-0.79[-1.40,-0.16]	-0.61[-1.13,0.06]	-2.22[-2.67,-2.02]	<0.001
Gender,n(%)				
Male	236 (60.67)	163 (61.28)	73 (59.35)	0.717
Female	153 (39.33)	103 (38.58)	50 (40.98)	
Hypogonadism, n(%)				
No	353 (90.75)	258 (96.99)	95 (77.24)	<0.001
Yes	36 (9.26)	8 (3.01)	28 (22.76)	
Chelator usage, n(%)				
DFO	39 (10.03)	26 (9.77)	13 (10.57)	0.198
DFP	38 (9.77)	27 (10.15)	11 (8.94)	
DFX	100 (25.71)	75 (28.20)	25 (20.33)	
Combined drugs	161 (41.39)	100 (37.59)	61 (49.59)	
Unused or Unclear	51 (13.11)	38 (14.29)	13 (10.57)	
IGF-1<-2SD, n(%)				
No	194 (49.87)	155 (58.27)	39 (31.71)	<0.001
Yes	195 (50.13)	111 (41.73)	84 (68.29)	
Splenectomy, n(%)				
No	341 (87.66)	237 (89.10)	104 (84.55)	0.205
Yes	48 (12.34)	29 (10.90)	19 (15.45)	
LIC (mg Fe/g dw),n(%)				
No	44 (11.31)	26 (9.77)	18 (14.63)	0.159
Yes	345 (88.69)	240 (90.23)	105 (85.37)	
Cardiac MRI T2* (ms), n(%)				
No	302 (77.64)	206 (77.44)	96 (78.05)	0.894
Yes	87 (22.37)	60 (22.56)	27 (21.95)	

(Continued)

10.3389/fendo.2025.1599437

TABLE 1 Continued

Variable	Total (n=389)	Normal BMD (n=266)	Low BMD (n=123)	P
Thyroid Function, n(%)				
Normal	360 (92.55)	246 (92.48)	114 (92.68)	0.944
Abnormal	29 (7.46)	20 (7.52)	9 (7.32)	
OC, n(%)				
Normal	81 (20.82)	54 (20.30)	27 (21.95)	0.709
Abnormal	308 (79.18)	212 (79.70)	96 (78.05)	
Height n(%)				
Short Stature	126 (32.39)	59 (22.18)	67 (54.47)	<0.001
Normal	259 (66.58)	203 (76.32)	56 (45.53)	
Tall Stature	4 (1.03)	4 (1.50)	0 (0.00)	
Weight n(%)				
Underweight	86 (22.11)	33 (12.41)	53 (43.09)	<0.001
Normal	302 (77.64)	232 (87.22)	70 (56.91)	
Obesity	1 (0.26)	1 (0.38)	0 (0.00)	
BMI n(%)				
Thinness	30 (7.71)	17 (6.39)	13 (10.57)	0.045
Normal	334 (85.86)	227 (85.34)	107 (86.99)	
Overweight	19 (4.88)	18 (6.77)	1 (0.81)	
Obesity	6 (1.54)	4 (1.50)	2 (1.63)	

In the subgroup of Lumbar BMD Z score adjusted for height (5–19 years) (n = 335), Normal BMD = 282, Low BMD = 53 annotations: Abnormal thyroid function includes hypothyroidism and subclinical hypothyroidism; Abnormal osteocalcin levels include both elevated and reduced values.

After correction, the prevalence of low bone mass in this age group decreased from 33.4% to 15.8%. In this subgroup, univariate and multivariate logistic regression analyses revealed that Age, normal BMI, and ALB levels were independent predictors of low bone mass. Specifically, Age was identified as a risk factor (OR = 1.137, 95% CI: 1.034–1.251, $P < 0.05$), while normal BMI (OR = 0.383, 95% CI: 0.158–0.976, $P < 0.05$) and ALB levels (OR = 0.866, 95% CI: 0.783–0.953, $P < 0.05$) were protective factors (Table 3).

4 Discussion

Thalassemia-related bone disease is a prevalent complication among patients with Thalassemia major. Distinct from prior research that primarily considered adult patient populations with TDT, our study shifts its focus to pediatric and adolescent patients affected by TDT, investigating the prevalence and determinants of low bone mass within this youthful demographic.

Low bone mass, a condition with reduced bone mineral density but not classified as osteoporosis, has pivotal clinical impacts. It increases fracture risk due to weakened bones, signals impending osteoporosis, necessitating intervention to prevent further bone loss, and offers a window to assess skeletal health, enabling early identification and management of bone issues. For LBM patients, personalized treatment can mitigate bone mass loss. Essentially, the core clinical significance of LBM lies in its value as an "intervention window"—early detection and intervention can delay or halt progression to osteoporosis, reduce fracture risk, and enhance patients' long-term quality of life (10).

Our study demonstrates that the overall prevalence of low bone mass in children and adolescents with TDT is 31.6%, with the prevalence in the 5–19-year subgroup decreasing to 15.8% after height-adjusted BMD correction. Previous studies reported a prevalence of low bone mass in TDT patients ranging from 40% to 50% (8, 21). he lower prevalence observed in our cohort may be attributed to potential explanations:1) the relatively younger age of our patient cohort, 2)traditional BMD assessments may overestimate prevalence due to the lack of height-adjusted correction. However, even after height correction, the prevalence of low bone mass in TDT patients remains higher than that in the general population, indicating that TDT patients are vulnerable to bone disease from childhood. These findings underscore the critical need for implementing early BMD screening and timely therapeutic interventions in this population to mitigate long-term skeletal complications.

In this cross-sectional study of children and adolescents diagnosed with TDT, we identified that without height-adjusted

10.3389/fendo.2025.1599437

TABLE 2 Comparison of patient characteristics between different age groups.

Variable	Total (n=389)	Group1 (n=313)	Group2 (n=76)	P
Gender n (%)				
Male	236 (60.668)	187 (59.744)	49 (64.474)	0.449
Female	153 (39.332)	126 (40.256)	27 (35.526)	
BMI n (%)				
Thinness	30 (7.71)	19 (6.07)	11 (14.47)	0.031
Normal	334 (85.86)	270 (86.26)	64 (84.21)	
Overweight	19 (4.88)	18 (5.75)	1 (1.32)	
Obesity	6 (1.54)	6 (1.92)	0 (0.00)	
Hypogonadism n (%)				
No	353 (90.746)	313 (100.000)	40 (52.632)	<0.001
Yes	36 (9.254)	0 (0.000)	36 (47.368)	
Ironchelators n (%)				
DFO	39 (10.026)	30 (9.585)	9 (11.842)	0.169
DFP	38 (9.769)	30 (9.585)	8 (10.526)	
DFX	100 (25.707)	87 (27.796)	13 (17.105)	
Combined drugs	161 (41.388)	122 (38.978)	39 (51.316)	
Unused or Unclear	51 (13.111)	44 (14.058)	7 (9.211)	
IGF-1<-2SD n (%)				
No	194 (49.871)	185 (59.105)	9 (11.842)	<0.001
Yes	195 (50.129)	128 (40.895)	67 (88.158)	
LBM n (%)				
No	266 (68.380)	236 (75.399)	30 (39.474)	<0.001
Yes	123 (31.620)	77 (24.601)	46 (60.526)	
Splenectomy n (%)				
No	341 (87.661)	287 (91.693)	54 (71.053)	<0.001
Yes	48 (12.339)	26 (8.307)	22 (28.947)	
LIC,n (%)				
No	44 (11.311)	35 (11.182)	9 (11.842)	0.871
Yes	345 (88.689)	278 (88.818)	67 (88.158)	
CardiacMRIT2* n (%)				
No	302 (77.635)	251 (80.192)	51 (67.105)	0.014
Yes	87 (22.365)	62 (19.808)	25 (32.895)	
Thyroidfunction n (%)				
Normal	360 (92.545)	289 (92.332)	71 (93.421)	0.746
Abnormal	29 (7.455)	24 (7.668)	5 (6.579)	
Osteocalcin n (%)				
Normal	81 (20.823)	66 (21.086)	15 (19.737)	0.795
Abnormal	308 (79.177)	247 (78.914)	61 (80.263)	

(Continued)

10.3389/fendo.2025.1599437

TABLE 2 Continued

Variable	Total (n=389)	Group1 (n=313)	Group2 (n=76)	P
Osteocalcin n (%)				
Age median [IQR]	8.000 [5.000,11.000]	7.000 [5.000,9.000]	13.000 [12.000,15.000]	<0.001
Height SDs median [IQR]	-1.000 [-2.000,-1.000]	-1.000 [-2.000,0.000]	-2.000 [-3.000,-2.000]	<0.001
Weight SDs median [IQR]	-1.000 [-2.000,0.000]	-1.000 [-1.000,0.000]	-2.000 [-3.000,-1.000]	<0.001
Z median [IQR]	-1.500 [-2.200,-0.900]	-1.400 [-1.900,-0.800]	-2.300 [-3.200,-1.300]	<0.001
SF median [IQR]	3760.620 [2360.320,5502.850]	3473.960 [2334.200,5100.690]	5543.400 [3044.110,7993.910]	<0.001
Hb mean (± SD)	102.481 ± 16.932	103.377 ± 16.835	98.791 ± 16.831	0.034
Alb mean (± SD)	42.614 ± 3.188	42.527 ± 3.193	42.975 ± 3.144	0.273
ALP median [IQR]	218.000 [176.000,271.000]	217.000 [176.000,271.000]	220.000 [176.000,269.000]	0.774
Cr median [IQR]	28.000 [24.000,32.000]	28.000 [24.000,31.000]	30.000 [24.000,36.000]	0.052
TCHO median [IQR]	2.940 [2.570,3.320]	2.970 [2.600,3.350]	2.879 [2.540,3.170]	0.13
TG median [IQR]	1.080 [0.840,1.450]	1.020 [0.790,1.330]	1.390 [1.106,2.090]	<0.001
HDLC median [IQR]	0.880 [0.740,1.020]	0.890 [0.750,1.050]	0.809 [0.700,0.930]	0.002
LDLC median [IQR]	1.530 [1.280,1.850]	1.540 [1.300,1.860]	1.520 [1.270,1.690]	0.472
Ca median [IQR]	2.330 [2.260,2.400]	2.340 [2.270,2.400]	2.310 [2.230,2.390]	0.107
P median [IQR]	1.670 [1.460,1.810]	1.660 [1.480,1.796]	1.690 [1.450,1.880]	0.411
FPG median [IQR]	4.690 [4.350,5.070]	4.660 [4.320,5.020]	4.920 [4.560,5.370]	<0.001
INS median [IQR]	43.060 [29.010,63.905]	40.260 [26.340,56.290]	66.820 [41.540,95.010]	<0.001
25 (OH)D,median [IQR]	54.600 [44.000,68.400]	56.200 [45.200,69.100]	47.900 [37.600,57.100]	<0.001
PTH median [IQR]	28.250 [21.280,38.920]	28.160 [21.460,37.850]	31.090 [19.970,41.010]	0.643
BMDL1L4 median [IQR]	0.480 [0.431,0.539]	0.462 [0.425,0.508]	0.586 [0.535,0.654]	<0.001

BMD correction, age (OR = 1.138, 95% CI 1.041–1.248, P 0.05), IGF-1<-2SD (OR = 1.962, 95% CI 1.163–3.321, P 0.05), and hypogonadism (OR = 2.951, 95% CI 1.085–8.444, P 0.05) were significant independent risk factors associated with low bone mass.

Our research identified that advancing age serves as a significant independent risk factor for low bone mass in pediatric and adolescent patients with TDT, corroborating the findings from numerous studies (3, 10, 22, 23). In alignment with the developmental trend of human bone density, there exists an accumulation and increase phase prior to the age of 20, characterized by swift skeletal growth and osteoblastic activity that exceeds osteoclastic activity. Consequently, bone mass

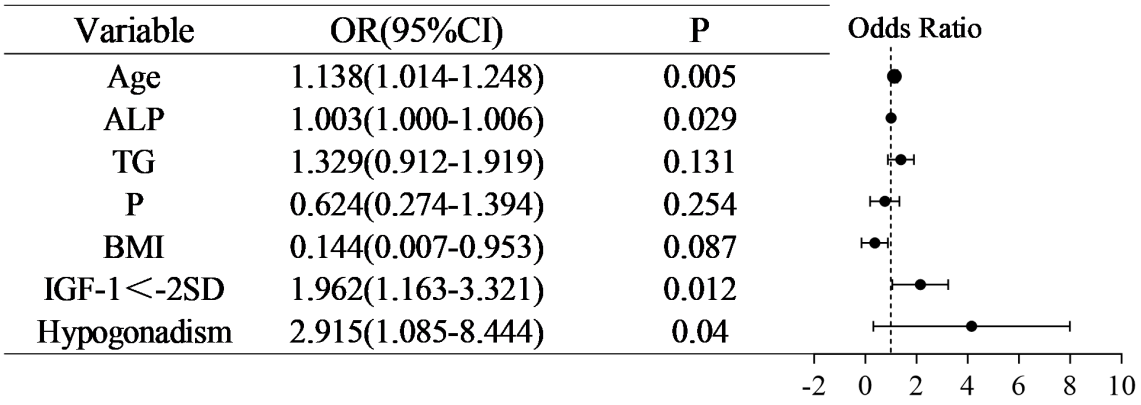

FIGURE 1
Forest plot for multivariate regression analysis of the entire group.

10.3389/fendo.2025.1599437

TABLE 3 Multivariate logistic regression analysis in the 5–19 years subgroup.

Variable	P	OR	95%CI
ALB	0.004	0.866	0.783 - 0.953
ALP	0.071	1.003	1.000 - 1.006
P	0.117	0.443	0.158 - 1.212
Age	0.008	1.137	1.034 - 1.251
BMI	0.037	0.383	0.158 - 0.976

TDT, transfusion-dependent beta-thalassemia; BMD, Bone mineral density; DXA, dual-energy X-ray absorptiometry; Hb, Hemoglobin; ALB, Albumin; ALP, Serum Alkaline Phosphatase; Cr, Creatinine; TC, Total Cholesterol; TG, Triglycerides; LDLC, Low-Density Lipoprotein Cholesterol; HDLC, High-Density Lipoprotein Cholesterol; Ca, Serum Calcium; P, Serum Phosphorus; PTH, Parathyroid Hormone; [25(OH)D],25-Hydroxy Vitamin D; FPG, Fasting Plasma Glucose; FINS, Fasting Insulin Levels; SF, Serum Ferritin; IGF-1,Insulin-like Growth Factor 1; T, Testosterone; E2,Estradiol; OC, Osteocalcin; LIC, Liver Iron Concentration; CID, Cardiac Iron Deposition (measured by Cardiac MRI T2*); BMI, Body Mass Index; DFO, Deferoxamine; DFP, Deferiprone; DFX, Deferasirox; GH, Growth hormone; IGF-1,Insulin-like growth factor 1; IGF-BP3, Insulin-like Growth Factor Binding Protein 3.

progressively accumulates (24). Over a quarter of one's peak bone mass is rapidly accrued during adolescence, and by age 18, an individual has usually reached 90% of their maximum bone mass (25), which is a critical time for the accumulation of peak bone mass. Participants in our study ranged in age from 2 to 19 years, with an average age of 8 ± 3 years, coinciding with the critical period for peak bone mass accumulation. With increasing age, patients exhibited a rising trend in bone density, yet their respective Z-scores declined. This suggests that the patients' bone density increase was markedly inferior to the normative values for a comparable demographic. This outcome aligns with previously reported studies (21, 23). With advancing age in TDT patients, there is a progressive accumulation of skeletal risks. The burden of accumulated iron significantly exacerbates the impairment of osteoblast function. Persistent anemia results in bone marrow expansion and cortical thinning. Additionally, the cumulative effects of long-term complications associated with transfusions, including endocrine dysfunction, further complicate the clinical picture. Adolescence represents a pivotal period for substantial bone mass accretion. If impaired by the aforementioned factors, it can result in a substantial decrease in peak bone mass and heighten the risk of osteoporosis in later life (23). Hence, prioritizing the detection and prevention measures among high-risk individuals for osteoporosis during the formative years in children and adolescents with TDT is crucial for enhancing peak bone mass achievement in adulthood and mitigating the risk of osteoporosis later in life.

Hypogonadism represents one of the prevalent endocrine disorders observed in individuals affected by TDT, with estimated prevalence varying between 20% and 77.5% (26). In our study, we found a high prevalence of hypogonadism at 70.6%among patients aged 13 and older, with male patients having a prevalence of 74.2% and female patients at 65.0%.Our research demonstrated a significant correlation between hypogonadism and low bone mass, aligning with prior studies conducted on patients with TDT (8, 10, 22, 27). Sex steroid hormones, namely estrogen and testosterone, are crucial for maintaining the equilibrium of bone remodeling processes. Iron accumulation may result in decreased levels of sex hormones, either by directly damaging gonadal cells or by inhibiting the function of the hypothalamic-pituitary-gonadal axis. Consequently, this disruption affects the estrogen/androgen-regulated pathways crucial for bone metabolism (28), resulting in diminished osteoblast function and augmented bone resorption by osteoclasts (29, 30). Prior research has predominantly concentrated on adults, our research establishes a link in children and adolescents, suggesting that gonadal dysfunction could intervene in early skeletal development, severely impacting the attainment of peak bone mass, and substantially elevating the risk of osteoporosis in adulthood (31). Consequently, there is a pressing need to enhance scrutiny over gonadal function and to implement timely hormone replacement therapy for adolescent patients.

In our investigation, the incidence of IGF-1<-2SD reached 50.1%, with males exhibiting a higher incidence at 54.7% compared to females at 43.1%. In 2022, a study by Gong Chunxiu et al. delineated the standard levels and trends of IGF-1 in Chinese children and adolescents, spanning the age range of 1 to 19 years (19):Serum IGF-1 levels increase with age in both genders, displaying a notable surge in boys around 12–13 years of age, peaking around 15 years of age. In girls, a similar surge is observed at 10–11 years of age, with levels peaking between 12 and 13 years of age. In our study, boys aged 15 exhibited the highest IGF-1 levels at 272.00 ng/ml, which is within the range of -1 to -2 SD below the mean for the general population. The average IGF-1 level among these boys was 141.64 ng/ml, which is significantly lower than the average for the normal population, at 411.50 ng/ml. For girls, at age 12, the highest IGF-1 level reached 285.00 ng/ml, situating between -1 and -2 SD from the norm, with an average of 167.89 ng/ml. This average is considerably below the typical average for the normal population, which stands at 442.00 ng/ml. At age 13, girls' IGF-1 levels peaked at 257.00 ng/ml, which is below -2SD from the mean of the normal population, and the average was 158.03 ng/ml. This average value is substantially below the average for the normal population of 456.00 ng/ml. These findings suggest that children and adolescents diagnosed with TDT exhibit markedly decreased growth hormone levels when compared to their unaffected peers within the same racial, age, and gender groups. Studies have revealed that the GH/IGF-1 axis is pivotal for regulating bone hyperplasia across prepubertal, pubertal, and postpubertal developmental phases. This axis is also essential for modulating peak bone density and bone mass acquisition during pubertal development (8). In individuals with thalassemia, it has been shown that bone mineral density is correlated with the blood levels of IGF-1 and IGFBP-3 (32). GH facilitates chondrocyte proliferation and the mineralization of bone matrix by enhancing liver production of IGF-1. However, iron overload-induced toxicity in the anterior pituitary may result in reduced GH secretion, leading to osteoporosis and demineralization in TDT patients (33). These alterations contribute significantly to the degradation of bone mineralization. Notably, compared to adults, the detrimental effects of markedly decreased growth hormone levels on bone density are more pronounced in children and adolescents.

Iron overload is widely regarded as a primary cause of reduced bone mass in patients with TDT (34), however, several previous studies have failed to demonstrate a substantial correlation between elevated serum ferritin levels and decreased bone mass (3, 21, 34). In this study, we presented the measurement results for LIC and CID. We also compared the serum ferritin levels, LIC, and CID across the two groups. However, no significant correlation was observed between these independent variables and low bone mass. Possible reasons for the observed discrepancies may include: 1) The study population consisted of children and adolescents, whereas long-term effects of iron overload are potentially more evident in adults. 2) The variability in iron chelation therapy, such as differences in drug selection and patient adherence, could confound the relationship between iron burden and bone metabolism. 3) Administration of iron chelators may mitigate some of the direct toxic effects of iron accumulation on bone, underscoring the critical need for uniform iron chelation therapies. Moreover, aligning with Nakavachara P et al.'s findings, this study likewise failed to detect any substantial influence of hemoglobin and vitamin D levels on osteoporosis or reduced bone mineral density (35).

In the 5–19-year patient subgroup, the significant reduction in the prevalence of low bone mass after height-adjusted correction highlights the critical role of stature in BMD assessment for this age group. Univariate and multivariate logistic regression analyses demonstrated that advancing age was an independent risk factor for low bone mass, with increasing age correlating with elevated risk —a finding consistent with the uncorrected model. In the height-adjusted model, normal BMI and higher ALB levels emerged as protective factors. Normal BMI may reflect adequate nutritional status and optimal levels of bone-modulating factors secreted by adipose tissue, while ALB, as a marker of nutritional health, likely supports skeletal integrity through its role in maintaining metabolic homeostasis. Although IGF-1<-2SD and hypogonadism did not retain significance in the height-adjusted model, their high-risk associations in the uncorrected model suggest that growth hormone axis dysfunction and gonadal hormone deficiency remain potential underlying drivers of bone loss in TDT patients. These findings underscore the need to integrate endocrine and nutritional evaluations alongside height-adjusted BMD assessments to comprehensively address multifactorial bone health challenges in this population.

Our study compared two groups divided by developmental stages (Group 1: pre-pubertal, 2–11 years; Group 2: pubertal and adolescent, 12–19 years) and found that children and adolescents with TDT exhibited significant age-related deteriorations, including impaired growth parameters, increased malnutrition, worsening anemia and iron overload, glucose and lipid metabolism disorders, compromised secretion of sex hormones and growth hormone, and reduced vitamin D levels. These findings indicate that pubertal and adolescent patients face more severe challenges, such as growth retardation, hypogonadism, growth hormone deficiency, skeletal abnormalities, iron overload, and metabolic dysregulation. This underscores the necessity for dynamic monitoring and intervention targeting growth, development, and metabolic parameters during adolescence, alongside multisystem comprehensive interventions, to improve long-term outcomes and quality of life.

This study's clinical significance is underscored by its identification of independent risk factors for low bone mass in TDT patients, spanning from childhood through adolescence, within a large-sample, retrospective framework. This finding furnishes a theoretical underpinning for the management of bone health. However, several inherent limitations are associated with the study. Firstly, due to its cross-sectional design, this study cannot establish causality and necessitates longitudinal studies to confirm the dynamic effects of risk factors. Secondly, the inclusion of cases solely from one center cannot be overlooked; it introduces potential bias and reduces the study's statistical power. Thirdly, this study failed to account for height-related BMD across the entire patient cohort and did not conduct assessments for vertebral fractures (VFs).

5 Conclusion

Our study revealed that the prevalence of low bone mass in TDT children and adolescents decreased after height-adjusted correction, underscoring the critical role of stature adjustment in BMD assessment. Multivariate analysis consistently identified advancing age as an independent risk factor for low bone mass, normal BMI and ALB as protective factors, while IGF-1 levels < -2 SD and hypogonadism demonstrated significant risk associations in the uncorrected model. Based on these findings, we advocate that clinical management of TDT pediatric and adolescent patients should prioritize height-adjusted BMD evaluation and implement comprehensive interventions targeting growth hormone axis function, gonadal status, and nutritional indicators to optimize bone health outcomes.

Data availability statement

The data analyzed in this study is subject to the following licenses/restrictions: The data that support the findings of this study are available from the corresponding author upon reasonable request. Requests to access these datasets should be directed to Yongrong Lai, laiyongrong@263.net.

Ethics statement

The studies involving humans were approved by The Medical Ethics Committee of the First Affiliated Hospital of Guangxi Medical University. The studies were conducted in accordance with the local legislation and institutional requirements. The ethics committee/institutional review board waived the requirement of written informed consent for participation from the participants or the participants' legal guardians/next of kin because This study has significant scientific and social value. It is a

retrospective study that involves only the analysis of existing medical data. The participants will not face any additional physical or psychological risks due to the study itself. The data used in the study have been de-identified, thus protecting the privacy of the participants.

Author contributions

WZ: Visualization, Writing – original draft, Methodology, Software, Writing – review & editing. RL: Writing – review & editing, Conceptualization, Resources, Formal Analysis, Data curation. SH: Investigation, Writing – review & editing, Methodology, Data curation. Jh: Writing – review & editing, Conceptualization, Formal Analysis. LW: Writing – review & editing, Methodology, Conceptualization. CH: Data curation, Writing – review & editing. YLia: Conceptualization, Supervision, Methodology, Writing – review & editing, Formal Analysis. YLai: Resources, Writing – review & editing, Project administration, Supervision.

Funding

The author(s) declare that financial support was received for the research and/or publication of this article. This research was financially backed by the Open Project of NHC Key Laboratory of Thalassemia Medicine under project number GJWJWDP202402.

Conflict of interest

The authors declare that the research was conducted in the absence of any commercial or financial relationships that could be construed as a potential conflict of interest.

Generative AI statement

The author(s) declare that no Generative AI was used in the creation of this manuscript.

Publisher's note

All claims expressed in this article are solely those of the authors and do not necessarily represent those of their affiliated organizations, or those of the publisher, the editors and the reviewers. Any product that may be evaluated in this article, or claim that may be made by its manufacturer, is not guaranteed or endorsed by the publisher.

Supplementary material

The Supplementary Material for this article can be found online at: https://www.frontiersin.org/articles/10.3389/fendo.2025.1599437/full#supplementary-material

References

1. Red Blood Cell Diseases (Anemia) Group CSoH. Chinese Medical Association. Chinese guideline for diagnosis and treatment of transfusion dependent β-thalassemia (2022). *Chin J Hematol.* (2022) 43:889–96. doi: 10.3760/cma.j.issn.0253-2727.2022.11.002

2. Shamoon RP, Yassin AK, Omar N, Saeed MD, Akram R, Othman NN. Magnitude of bone disease in transfusion-dependent and non-transfusion-dependent β-thalassemia patients. *Cureus.* (2024) 16:e56012. doi: 10.7759/cureus.56012

3. Bordbar M, Bozorgi H, Saki F, Haghpanah S, Karimi M, Bazrafshan A, et al. Prevalence of endocrine disorders and their associated factors in transfusion-dependent thalassemia patients: a historical cohort study in Southern Iran. *J Endocrinol Invest.* (2019) 42:1467–76. doi: 10.1007/s40618-019-01072-z

4. Taher AT, Musallam KM, Cappellini MD. β-thalassemias. *N Engl J Med.* (2021) 384:727–43. doi: 10.1056/NEJMra2021838

5. Shamshirsaz AA, Bekheirnia MR, Kamgar M, Pakbaz Z, Tabatabaie SM, Bouzari N, et al. Bone mineral density in Iranian adolescents and young adults with beta-thalassemia major. *Pediatr Hematol Oncol.* (2007) 24:469–79. doi: 10.1080/08880010701533702

6. Udeze C, Ly NF, Ingleby FC, Fleming SD, Conner SC, Howard J, et al. Clinical burden and healthcare resource utilization associated with managing transfusion-dependent β-thalassemia in England. *Clin Ther.* (2025) 47:37–43. doi: 10.1016/j.clinthera.2024.09.024

7. Al-Agha AE, Bawahab NS, Nagadi SA, Alghamdi SA, Felemban DA, Milyani AA. Endocrinopathies complicating transfusion-dependent hemoglobinopathy. *Saudi Med J.* (2020) 41:138–43. doi: 10.15537/smj.2020.2.24845

8. De Sanctis V, Soliman AT, Elsedfy H, Yassin M, Canatan D, Kilinc Y, et al. Osteoporosis in thalassemia major: an update and the I-CET 2013 recommendations for surveillance and treatment. *Pediatr Endocrinol Rev.* (2013) 11:167–80.

9. Crabtree NJ, Arabi A, Bachrach LK, Fewtrell M, El-Hajj Fuleihan G, Kecskemethy HH, et al. Dual-energy X-ray absorptiometry interpretation and reporting in children and adolescents: the revised 2013 ISCD Pediatric Official Positions. *J Clin Densitom.* (2014) 17:225–42. doi: 10.1016/j.jocd.2014.01.003

10. Vogiatzi MG, Macklin EA, Fung EB, Cheung AM, Vichinsky E, Olivieri N, et al. Bone disease in thalassemia: a frequent and still unresolved problem. *J Bone Miner Res.* (2009) 24:543–57. doi: 10.1359/jbmr.080505

11. Di Paola A, Marrapodi MM, Di Martino M, Giliberti G, Di Feo G, Rana D, et al. Bone health impairment in patients with hemoglobinopathies: from biological bases to new possible therapeutic strategies. *Int J Mol Sci.* (2024) 25(5):2902. doi: 10.3390/ijms25052902

12. De Sanctis V, Soliman AT, Elsefdy H, Soliman N, Bedair E, Fiscina B, et al. Bone disease in β thalassemia patients: past, present and future perspectives. *Metabolism.* (2018) 80:66–79. doi: 10.1016/j.metabol.2017.09.012

13. Evangelidis P, Venou TM, Fani B, Vlachaki E, Gavriilaki E. Endocrinopathies in hemoglobinopathies: what is the role of iron? *Int J Mol Sci.* (2023) 24(22):16263. doi: 10.3390/ijms242216263

14. Bain B. 2021 Guidelines for the management of transfusion dependent thalassaemia (TDT). *Br J Haematology.* (2023) 200:532. doi: 10.1111/bjh.18567

15. Writing Group for Practice Guidelines for Diagnosis and Treatment of Genetic Diseases MGBoCMA. Clinical practice guidelines for β-thalassemia. *Chin J Med Genet.* (2020) 37:243–51. doi: 10.3760/cma.j.issn.1003-9406.2020.03.004

16. Li H, Ji CY, Zong XN, Zhang YQ. Height and weight standardized growth charts for Chinese children and adolescents aged 0 to 18 years. *Chin J Pediatrics.* (2009) 47:487–92.

17. Rauch F, Plotkin H, DiMeglio L, Engelbert RH, Henderson RC, Munns C, et al. Fracture prediction and the definition of osteoporosis in children and adolescents: the ISCD 2007 Pediatric Official Positions. *J Clin Densitom.* (2008) 11:22–8. doi: 10.1016/j.jocd.2007.12.003

18. Association PEGaMGoCMD, Association AHaMPCoCMD, the Subspecialty Group of Endocrinological HaMD, the Society of Pediatrics and Chinese Medical Association. Expert consensus on diagnosis and treatment of hypogonadotropic hypogonadism in children. *Chin J Pediatr.* (2023) 61:484–90. doi: 10.3760/cma.j.cn112140-20221208-01034

19. Cao B, Peng Y, Song W, Peng X, Hu L, Liu Z, et al. Pediatric continuous reference intervals of serum insulin-like growth factor 1 levels in a healthy chinese children population - based on PRINCE study. *Endocr Pract*. (2022) 28:696–702. doi: 10.1016/j.eprac.2022.04.004

20. Parent AS, Teilmann G, Juul A, Skakkebaek NE, Toppari J, Bourguignon JP. The timing of normal puberty and the age limits of sexual precocity: variations around the world, secular trends, and changes after migration. *Endocr Rev*. (2003) 24:668–93. doi: 10.1210/er.2002-0019

21. Mohseni F, Mohajeri-Tehrani MR, Larijani B, Hamidi Z. Relation between BMD and biochemical, transfusion and endocrinological parameters in pediatric thalassemic patients. *Arch Osteoporos*. (2014) 9:174. doi: 10.1007/s11657-014-0174-3

22. Vichinsky EP. The morbidity of bone disease in thalassemia. *Ann N Y Acad Sci*. (1998) 850:344–8. doi: 10.1111/j.1749-6632.1998.tb10491.x

23. Vogiatzi MG, Autio KA, Mait JE, Schneider R, Lesser M, Giardina PJ. Low bone mineral density in adolescents with beta-thalassemia. *Ann N Y Acad Sci*. (2005) 1054:462–6. doi: 10.1196/annals.1345.063

24. Golden NH, Abrams SA. Optimizing bone health in children and adolescents. *Pediatrics*. (2014) 134:e1229–43. doi: 10.1542/peds.2014-2173

25. Stagi S, Cavalli L, Iurato C, Seminara S, Brandi ML, de Martino M. Bone metabolism in children and adolescents: main characteristics of the determinants of peak bone mass. *Clin cases Miner Bone Metab*. (2013) 10:172–9.

26. Venou TM, Barmpageorgopoulou F, Peppa M, Vlachaki E. Endocrinopathies in beta thalassemia: a narrative review. *Hormones (Athens)*. (2024) 23:205–16. doi: 10.1007/s42000-023-00515-w

27. Gaudio A, Morabito N, Catalano A, Rapisarda R, Xourafa A, Lasco A. Pathogenesis of thalassemia major-associated osteoporosis: A review with insights from clinical experience. *J Clin Res Pediatr Endocrinol*. (2019) 11:110–7. doi: 10.4274/jcrpe.galenos.2018.2018.0074

28. Zhuannan J, Liyang L. Research progress in hypogonadism of patients with β-thalassemia major. *Int J Pediatrics*. (2019) 46:424–6. doi: 10.3760/cma.j.issn.1673-4408.2019.06.010

29. Thavonlun S, Houngngam N, Kingpetch K, Numkarunarunrote N, Santisitthanon P, Buranasupkajorn P, et al. Association of osteoporosis and sarcopenia with fracture risk in transfusion-dependent thalassemia. *Sci Rep*. (2023) 13:16413. doi: 10.1038/s41598-023-43633-6

30. Ananvutisombat N, Tantiworawit A, Punnachet T, Hantrakun N, Piriyakhuntorn P, Rattanathammethee T, et al. Prevalence and risk factors predisposing low bone mineral density in patients with thalassemia. *Front Endocrinol (Lausanne)*. (2024) 15:1393865. doi: 10.3389/fendo.2024.1393865

31. Carsote M, Vasiliu C, Trandafir AI, Albu SE, Dumitrascu MC, Popa A, et al. New entity-thalassemic endocrine disease: major beta-thalassemia and endocrine involvement. *Diagnostics (Basel)*. (2022) 12(8):1921. doi: 10.3390/diagnostics12081921

32. Lasco A, Morabito N, Gaudio A, Crisafulli A, Meo A, Denuzzo G, et al. Osteoporosis and beta-thalassemia major: role of the IGF-I/IGFBP-III axis. *J Endocrinol Invest*. (2002) 25:338–44. doi: 10.1007/BF03344015

33. Soliman AT, De Sanctis V, Elalaily R, Yassin M. Insulin-like growth factor- I and factors affecting it in thalassemia major. *Indian J Endocrinol Metab*. (2015) 19:245–51. doi: 10.4103/2230-8210.131750

34. Dede AD, Trovas G, Chronopoulos E, Triantafyllopoulos IK, Dontas I, Papaioannou N, et al. Thalassemia-associated osteoporosis: a systematic review on treatment and brief overview of the disease. *Osteoporos Int*. (2016) 27:3409–25. doi: 10.1007/s00198-016-3719-z

35. Nakavachara P, Weerakulwattana P, Pooliam J, Viprakasit V. Bone mineral density in primarily preadolescent children with hemoglobin E/β-thalassemia with different severities and transfusion requirements. *Pediatr Blood Cancer*. (2022) 69: e29789. doi: 10.1002/pbc.29789

frontiers | Frontiers in Endocrinology

TYPE Systematic Review
PUBLISHED 30 July 2025
DOI 10.3389/fendo.2025.1585552

OPEN ACCESS

EDITED BY
Federico Baronio,
Dpt Hospital of Woman and Child, Italy

REVIEWED BY
Fulvio Tartara,
University Hospital of Parma, Italy
Mustafa Hızal,
Abant Izzet Baysal University, Türkiye

*CORRESPONDENCE
Feng Zheng
hydgk2011@163.com
Xuewen Kang
ery_kangxw@lzu.edu.cn

†These authors have contributed equally to this work

RECEIVED 28 February 2025
ACCEPTED 10 July 2025
PUBLISHED 30 July 2025

CITATION
Cao Z, Zhang M, Jia J, Zhang G, Li L, Yang Z, Zheng F and Kang X (2025) Incidence and risk factors for modic changes in the lumbar spine: a systematic review and meta-analysis. *Front. Endocrinol.* 16:1585552. doi: 10.3389/fendo.2025.1585552

Incidence and risk factors for modic changes in the lumbar spine: a systematic review and meta-analysis

Zhenyu Cao[1,2,3†], Mingtao Zhang[1,2†], Jingwen Jia[1,2], Guangzhi Zhang[1,2], Lei Li[1,2], Zhili Yang[1,2], Feng Zheng[3*] and Xuewen Kang[1,2*]

[1]Department of Orthopaedics, Lanzhou University Second Hospital, Lanzhou, Gansu, China, [2]Orthopaedics Key Laboratory of Gansu Province, Lanzhou, Gansu, China, [3]Department of Orthopaedics, Qinghai Provincial People's Hospital, Xining, Qinghai, China

Background: Modic changes refer to bone marrow alterations beneath vertebral endplates and are potentially linked to infection, trauma, disc degeneration, scoliosis, and other pathological conditions. Systematic evaluations of their incidence and associated risk factors in the lumbar spine are lacking. This study aimed to analyze and evaluate the incidence and risk factors of Modic changes in lumbar spine disorders.

Methods: A comprehensive systematic review was conducted using Web of Science, PubMed, Cochrane Library, and Embase databases. Eligible studies reported the incidence and associated risk factors of Modic changes in the lumbar spine. Data were extracted and systematically analyzed from the selected studies, and meta-analyses were conducted employing random or fixed effects models.

Results: Twenty-five studies were included in the meta-analysis. The overall incidence of Modic changes was 35%. Six risk factors were identified and quantitatively assessed. Strong evidence supported the association of endplate changes (OR=3.56; 95% CI=2.00 to 6.32; p<0.0001); moderate evidence supported the association of age (OR=4.01; 95% CI=1.37 to 6.65; p=0.003), disc degeneration (OR=8.54; 95% CI=1.98 to 36.73; p=0.004), and lumbar lordosis angle (OR=-4.14; 95% CI=-6.79 to -1.49; p=0.002); minor evidence supported the association of spondylolisthesis (OR=2.00; 95% CI=1.12 to 3.58; p=0.02) and physical labor (OR=1.81; 95% CI=1.08 to 3.04; p=0.03) with the occurrence of Modic changes in the lumbar spine. No significant associations were found to support body mass index, sex, disc herniation, smoking, distributional segmentation, or sacral slope angle as risk factors for Modic changes in the lumbar spine.

Conclusion: Modic changes occur in 35% of lumbar spine cases, with advanced age, disc degeneration, endplate changes, spondylolisthesis, reduced anterior lumbar lordosis angles, and participation in physical labor identified as associated risk factors.

KEYWORDS

modic change, lumbar spine, lower back pain, meta-analysis, incidence, risk factor

1 Introduction

Lower back pain is a prevalent symptom of spinal disorders, often caused by various underlying conditions and associated with a certain disability rate. Severe disabling pain significantly impairs the long-term quality of life for patients and imposes a substantial burden on global economic development (1–4). The etiology of lower back pain is highly complex, involving factors such as lumbar disc degeneration, lumbar disc herniation, lumbar muscle strain, and lumbar spondylolisthesis (2, 5–8). Furthermore, Modic changes are thought to be strongly associated with lower back pain (9–11).

In 1987, De Roos reported Modic-like changes using nuclear magnetic resonance (NMR) imaging of the lumbar spine (12). Modic changes refer to alterations in the bony tissue beneath the vertebral endplates, which can be differentiated and confirmed via magnetic resonance imaging (MRI) (13). Modic changes are classified into three distinct types based on NMR manifestations: Type I is characterized by edema and inflammatory changes in the bone beneath the endplate; Type II is marked by fatty infiltration and degenerative changes; Type III is distinguished by sclerotic alterations in the local bone beneath the endplate (14–17). Modic changes are significantly associated with severe disc herniation, disc degeneration, and chronic lower back pain (12, 17–19). Nevertheless, their pathogenesis remains complex, and their etiology is yet to be fully elucidated. This may be related to compromised defensive properties, such as the structural integrity of the vertebral endplates, along with other contributing factors (20).

Numerous studies have investigated risk factors associated with Modic changes. Li et al. (21) demonstrated that factors such as disc degeneration, spondylolisthesis, and disc height may be linked to Modic changes. Some studies have suggested that obesity and elevated body mass index (BMI) may be associated with Modic changes (22), while others have found no such relationship (23). Furthermore, whether smoking, lumbar disc herniation, and lumbar segmental distribution are associated with the occurrence and progression of Modic remains controversial. To date, no meta-analysis has been conducted on the incidence and associated risk factors of Modic changes in the lumbar spine. Comprehensive analyses are crucial for confirming these factors, as they are essential for the early diagnosis and management of degenerative spinal conditions. Therefore, this systematic review and meta-analysis aimed to determine the incidence and risk factors of Modic changes in patients with lumbar spinal disorders.

Abbreviations: CI, confidence interval; OR, odds ratio; MRI, magnetic resonance imaging.

2 Methods

This systematic review and meta-analysis adhered to the guidelines outlined in the Preferred Reporting Items for Systematic Reviews and Meta-Analyses (PRISMA) statement (24) and AMSTAR (Assessing the Methodological Quality of Systematic Reviews) Guidelines (25).

2.1 Literature search strategies

A comprehensive search of all relevant English-language publications available as of May 10, 2024, was conducted across the PubMed, Embase, Web of Science, and Cochrane Library databases, in consultation with independent information technology experts. The search strategy (Table 1) utilized the following search terms: disc degeneration, lumbar spine, lower back pain, Modic changes, incidence, and risk factors. Titles and abstracts were screened to identify potentially relevant articles, and full-text publications and reference lists were obtained for further in-depth analysis based on the inclusion criteria.

2.2 Inclusion and exclusion criteria

Studies that met the following inclusion criteria were included for review: (1) Patients of all ages suffering from low back pain due to degenerative lumbar spine conditions (including lumbar disc herniation, lumbar spondylolisthesis, and degenerative lumbar lateral herniation, among other degenerative lumbar spine conditions), treated surgically or non-surgically; (2) Healthy participants; (3) Modic changes beneath the vertebral endplates confirmed by MRI; and (4) Publications in English language. Studies were excluded based on the following: (1) Pregnancy, traumatic fracture, spinal infection or tuberculosis, spinal

TABLE 1 Search strategy keywords.

Concept	Keywords used in the strategy
Intervertebral disc degeneration	("lumbar spine*") OR ("lumbar vertebra*") OR ("Intervertebral Disk Degeneration*") OR ("Intervertebral Disc Degeneration*") OR ("intervertebral disk*") OR ("intervertebral disc*") OR ("disc herniat*") OR ("disk herniat*") OR ("disc disease*") OR ("disk disease*") OR ("low back pain")OR ("Lumbago")OR ("Low Back Ache")OR ("Low Backache")OR ("Postural Low Back Pain")OR ("Recurrent Low Back Pain")OR ("Mechanical Low Back Pain")
Modic change	"Modic change" OR "Modic changes"
Risk	Risk* OR factor* OR prevalen* OR predict*OR Social Risk Factor* OR Health Correlates* OR incidence* OR "odds ratio"* OR "Relative odds"* OR "frequency"OR "morbidity"OR "epidemiology"OR "Social Epidemiology"OR "Cross-Product Ratios"OR "surveillance"OR "occurrence"OR "outbreaks"OR "endemics"

*Indicates truncation of search term.

deformity, malignancy, radiotherapy, recent use of antibiotics or corticosteroids, and psychological or psychiatric disorders; (2) Meta-analyses, case reports, reviews, technical notes, or abstracts only; and (3) Missing clinical data.

2.3 Quality assessment

Two independent reviewers used the Newcastle-Ottawa Scale (NOS) as a tool to assess the quality of the included studies, which were evaluated based on patient selection, group comparability, and the identification of outcomes of interest. Study quality was rated on a scale of 0 to 9, with low (1–3), medium (4–6), and high (7–9) ratings. Any discrepancy between the reviewers was resolved through consensus following discussion.

2.4 Data extraction

Two independent reviewers screened all titles and abstracts, selecting relevant articles for full-text review. Data were extracted from all eligible studies that met the inclusion criteria, including information on authorship, publication date, country of origin, patient type, sample size per factor, incidence of Modic changes, study design, and level of evidence. In cases where data were missing or unavailable, the corresponding authors were contacted. If the authors were unable to provide the necessary data, the study was excluded from the analysis.

2.5 Statistical analysis

Meta-analysis was performed on studies investigating the incidence of Modic changes in the lumbar spine and the associated risk factors. Statistical analyses and graphical representations were generated using Review Manager software (RevMan) version 5.4. Studies reporting odds ratios (ORs) were included in the meta-analysis. Heterogeneity was assessed using the I^2 statistic, with slight statistical heterogeneity defined as $I^2 < 50\%$. Data were analyzed using a fixed-effects model, or a random-effects model if $I^2 \geq 50\%$. The estimated incidence was calculated as a combined proportion with a 95% confidence interval (CI).

3 Results

3.1 Search results

The study initially retrieved a total of 1,126 articles for review. Most of the articles were excluded based on the predefined inclusion criteria. Titles and abstracts were screened, and 86 potentially relevant papers were selected for further assessment (Figure 1). Ultimately, 25 studies met the inclusion criteria.

3.2 Characteristics of included studies

The 25 studies that met the inclusion criteria encompassed 10,440 individuals, including patients with low back pain and healthy participants aged 10–89 years. Of these studies, 4 were prospective, 16 were retrospective, and 8 were cross-sectional in design. Nineteen studies were conducted in Asia (twelve in China (9, 20, 21, 23, 26–33), five in Turkey (22, 34–37), one in India (38), one in Japan (39)), four in Europe (two in Denmark (40, 41), one in Switzerland (42), one in the Netherlands (43)), and two in the Americas (all in the U.S.A (44, 45).). The mean quality score obtained from the included studies based on the NOS criteria was 6.84 ± 0.80. According to the level of evidence ratings, seven studies were classified as level II, nine as level III, and nine as level IV (Table 2). According to the GRADE criteria, seven risk factors received high-level recommendations, whereas five were classified as moderate. The overall incidence of Modic changes in the lumbar spine across the studies was 35%, with 12 identified and quantified risk factors. The characteristics of the studies and patient demographics are presented in Table 2.

3.3 Incidence of modic changes

This meta-analysis pooled data from 25 studies, encompassing a total of 10,440 patients and healthy participants. The overall incidence of Modic changes in the lumbar spine was 35% (95% CI = 0.28 to 0.42; Z = 9.38; $p < 0.00001$; $I^2 = 99\%$) (Figure 2).

3.4 Risk factors

Seventeen risk factors were identified, of which 12 were quantitatively analyzed based on the 25 studies included in the review. The risk factors identified in more than three studies

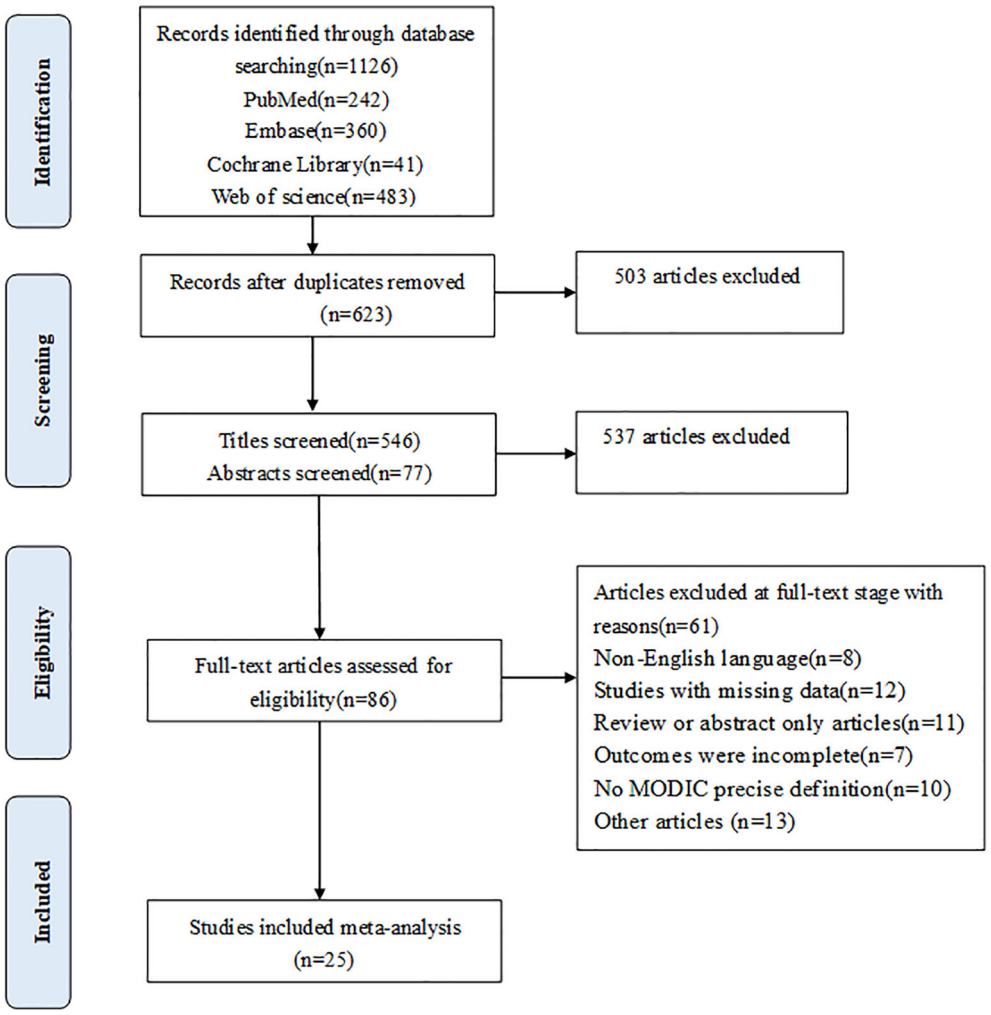

FIGURE 1
Search result.

included sex, age, smoking, BMI, disc degeneration, lumbar disc herniation, endplate changes, anterior lumbar lordosis angle, sacral angle, spondylolisthesis, segmental distribution, and physical labor.

3.5 Patient-related factors

3.5.1 Age

A total of 14 studies (9, 21, 23, 26, 29, 30, 33, 34, 36–38, 42, 44, 45) reported an association between age and the occurrence of Modic changes (Figure 3). The meta-analysis demonstrated that older patients were more likely to develop Modic changes than younger patients (OR = 4.01; 95% CI: 1.37 to 6.65; Z = 2.98; p = 0.003; I^2 = 96%; Figure 3). Based on the reviewed studies, we found moderate evidence suggesting older age as an important risk factor for Modic changes in the lumbar spine.

3.5.2 Physical labor

Three studies (32, 33, 41) reported correlations between physical labor and the occurrence of Modic changes (Figure 4). Analysis of the pooled data indicated that patients who engaged in physical labor were more likely to develop Modic changes. The meta-analysis revealed that Modic changes occurred in 15.43% of patients who engaged in physical labor and in 15.16% of patients who did not (OR = 1.81; 95% CI: 1.08 to 3.04; Z = 2.23; p = 0.03; I^2 = 70%; Figure 4). Therefore, we found minor evidence suggesting that engagement in physical labor is a risk factor for the development of Modic changes.

3.5.3 Sex, BMI, and smoking

Sixteen studies (20–23, 26, 27, 30, 32, 33, 37, 38, 40, 42–45) demonstrated a correlation between sex and Modic changes, indicating that sex was not significantly associated with the occurrence of Modic changes (OR = 0.91; 95% CI = 0.80 to 1.04; Z = 1.38; p = 0.17; I^2 = 48%; Figure 5). Additionally, nine studies (9, 21, 23, 30, 34, 36, 42, 44, 45) investigated the relationship between BMI and Modic changes, and no significant correlation was found (OR = 1.07; 95% CI = -0.38 to 2.51; Z = 1.45; p = 0.15; I^2 = 95%; Figure 6). Four studies (27, 32, 40, 44) confirmed no significant correlation between smoking and the presence of Modic changes

TABLE 2 The characteristics of the studies and patient demographics.

Lead author (Year)	Location	Age (mean±sd)	Gender (male%)	No. of total patient	No. of Modic change	Type of patient	Method	Study design	Level of evidence	NOS
Khaled Aboushaala (2024)	USA	56.9±15.7	58.1%	50	13	Symptomatic intervertebral disc degeneration or lumbar disc herniation	Modic and no modic analyse	Prospective Cross-sectional	IV	7
Guang-qing Li (2024)	China	NR	33.7%	719	150	Spondylolisthesis	Modic and no modic analyse	Retrospective	IV	6
İlter Demirhan (2023)	Turkey	NR	NR	90	45	Low back pain	Modic and no modic analyse	Prospective	III	8
Beixing Wei (2023)	China	NR	44.0%	500	126	Low back pain	Modic and no modic analyse	Retrospective	III	6
Yang Xiao (2023)	China	NR	39.0%	954	66	Lumbar degenerative diseases	Modic and no modic analyse	Retrospective	IV	6
Peter M. Udby (2024)	Denmark	NR	50.2%	620	290	Disc herniation	Modic and no modic analyse	Retrospective Cross-sectional	II	8
G. Michael Mallow (2022)	USA	16.5±2.4	46.9%	207	29	Low back pain	Modic and no modic analyse	Retrospective	IV	6
Emel Ece Özcan-Eksi (2021)	Turkey	NR	33.8%	151	56	Low back pain	Modic and no modic analyse	Retrospective	III	7
Emel Ece Ozcan-Eksi (2021)	Turkey	36.33±6.9	45.9%	527	132	Low back pain	Modic and no modic analyse	Retrospective Cross-sectional	III	6
Xiaoping Mu (2020)	China	NR	52.0%	1019	138	Low back pain	Modic and no modic analyse	Retrospective	III	6
Murat S.akir Eksi (2019)	Turkey	61.27±13.74	50.0%	3999	33	Low back pain	Modic and no modic analyse	Cross-sectional	IV	8
Ibrahim Burak Atci (2020)	Turkey	NR	60.9%	141	61	Low back pain	Modic and no modic analyse	Retrospective	IV	8
Stefan Dudli (2020)	Switzerland	NR	51.9%	54	21	Low back pain	Modic and no modic analyse	Cross-sectional	II	7
Peter van der Wurff (2019)	Netherlands	NR	90.2%	286	60	Low back pain	Modic and no modic analyse	Retrospective	II	7
Mindong Lan (2019)	China	NR	NR	277	62	Low back pain	Modic and no modic analyse	Retrospective	IV	7
Lunhao Chen (2018)	China	53.6±14.9	41.6%	442	209	Participant	Modic and no modic analyse	Cross-sectional	II	6

(Continued)

10.3389/fendo.2025.1585552

TABLE 2 Continued

Lead author (Year)	Location	Age (mean±sd)	Gender (male%)	No. of total patient	No. of Modic change	Type of patient	Method	Study design	Level of evidence	NOS
Runsheng Guo (2018)	China	54.31±13.9	52.6%	293	NA	Hospitalised patients	Modic and no modic analyse	Retrospective	III	8
Long Xiao (2017)	China	NR	58.3%	345	120	Low back pain	Modic and no modic analyse	Retrospective	II	6
Chao Han (2017)	China	NR	47.1%	230	47	Low back pain	Modic and no modic analyse	Retrospective	IV	7
Rishi Mugesh Kanna (2017)	India	36.7±10.8	56.2%	809	107	Spine patients	Modic and no modic analyse	Prospective	III	8
Florence P.S. Mok (2016)	China	40.4±10.9	NR	2449	141	Participant	Modic and no modic analyse	Cross-sectional	III	6
Juhani H. Ma'aitta (2016)	China	52.9±6.5	37.2%	1546	282	Participant	Modic and no modic analyse	Cross-sectional	IV	6
Tetsuo Hayashi (2015)	Japan	44.6±12.2	59.3%	450	129	Low back pain	Modic and no modic analyse	Retrospective	II	7
Hai-Long Wu (2012)	China	NR	39.2%	209	92	DLS patients	Modic and no modic analyse	Retrospective	II	7
Tue Secher Jensen (2010)	Denmark	NR	47%	412	200	Low back pain	Modic and no modic analyse	Prospective	III	7

10.3389/fendo.2025.1585552

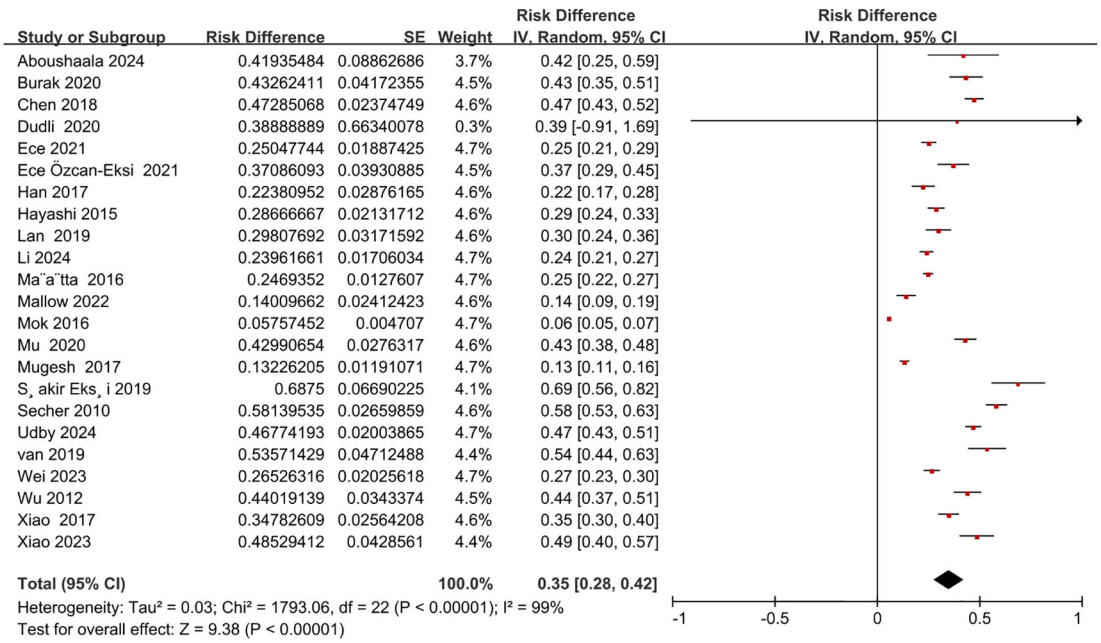

FIGURE 2
The overall incidence of Modic changes.

(OR = 1.15; 95% CI = 0.67 to 1.99; Z = 0.50; p = 0.62; I^2 = 52%; Figure 7). Consequently, this meta-analysis confirmed that sex, body mass index, and smoking were not significant risk factors for Modic changes in the lumbar spine.

3.6 Imaging-related factors

3.6.1 Degenerative discs

Three studies (27, 30, 39) reported an association between disc degeneration and Modic changes (Figure 8). The pooled data analysis indicated a correlation between the presence of disc degeneration and the occurrence of Modic changes in patients. The meta-analysis revealed that Modic changes occurred in 26.95% of patients with disc degeneration and 4.25% of patients without disc degeneration (OR = 8.54; 95% CI: 1.98 to 36.73; Z = 2.88; p = 0.004; I^2 = 98%; Figure 8). Consequently, this analysis provides moderate evidence that disc degeneration is an important risk factor for Modic changes in the lumbar spine.

3.6.2 Endplate changes

Three studies (20, 41, 45) reported an association between endplate changes and Modic changes (Figure 9). The pooled data analysis indicated a correlation between endplate changes and the occurrence of Modic changes in patients. The meta-analysis revealed that 19.84% of patients with endplate alterations

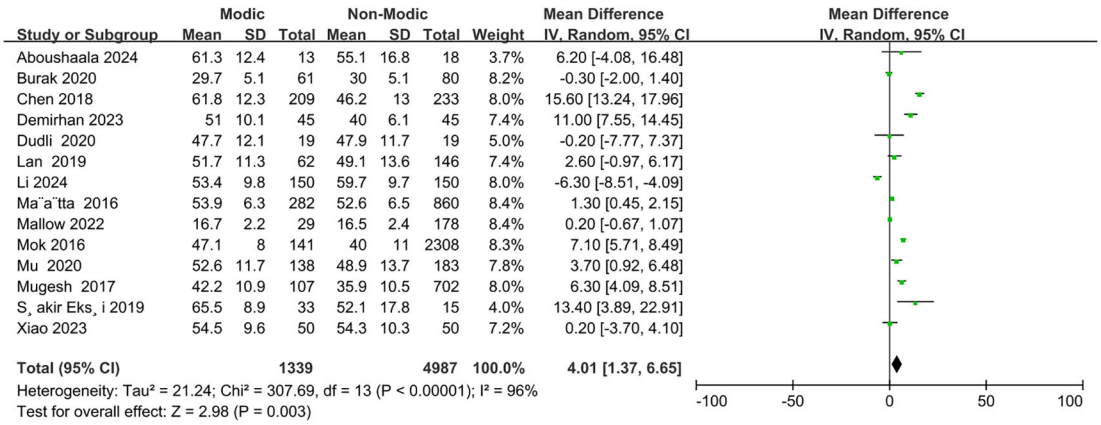

FIGURE 3
Age as a risk factor.

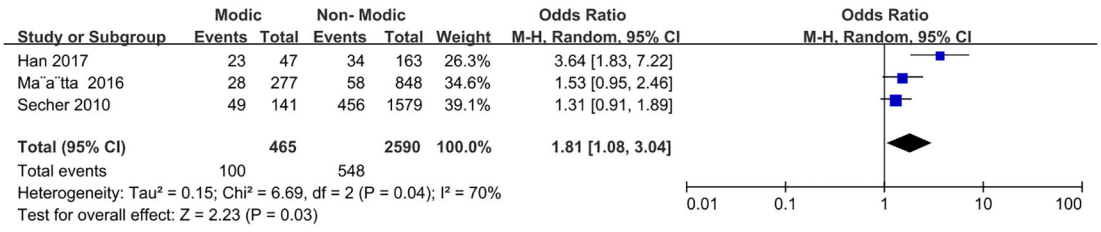

FIGURE 4
Physical labor as a risk factor.

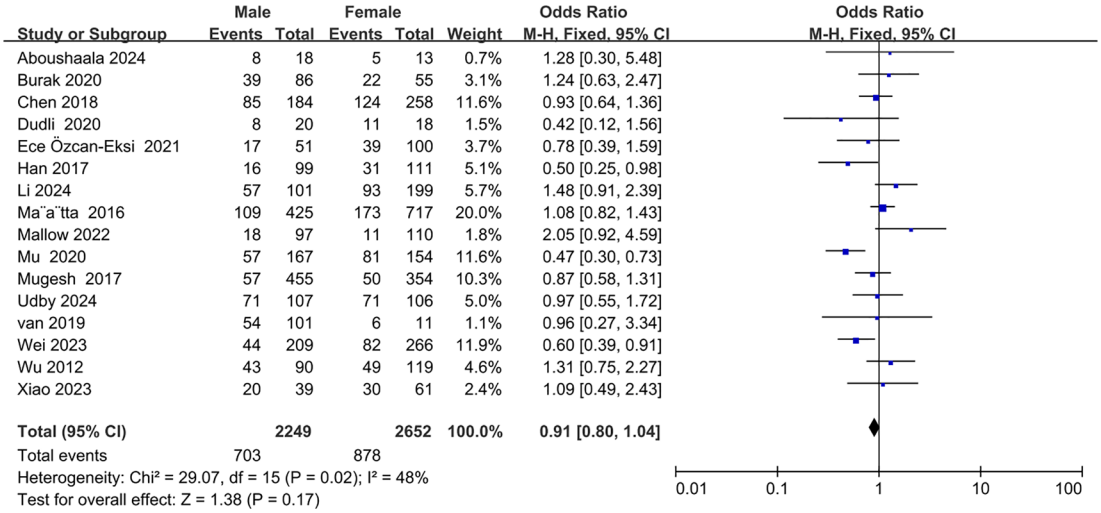

FIGURE 5
Gender as a risk factor.

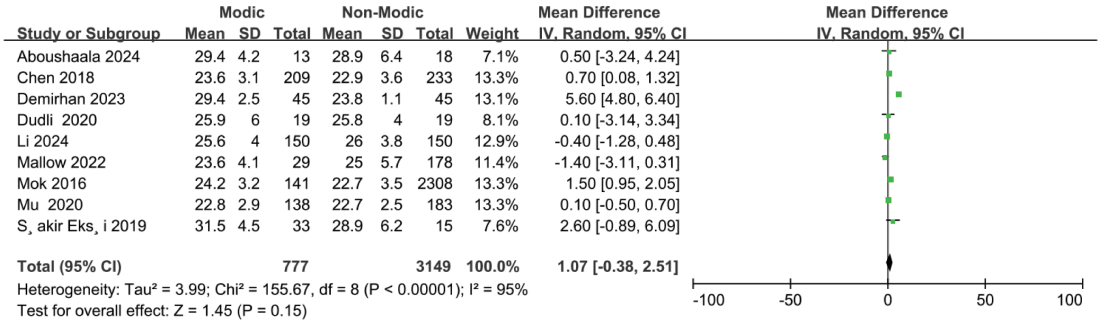

FIGURE 6
Body mass index (BMI) as a risk factor.

developed Modic changes, compared to 7.08% of those without endplate alterations (OR = 3.56; 95% CI = 2.00 to 6.32; Z = 4.32; p < 0.0001; I^2 = 64%; Figure 9). Consequently, this analysis provides compelling evidence that endplate changes represent a key risk factor for Modic changes in the lumbar spine.

3.6.3 Lumbar lordosis angle

Three studies (21, 23, 29) reported an association between lumbar lordosis and Modic changes (Figure 10). The pooled data analysis indicated that patients with smaller anterior lumbar lordosis angles were more likely to exhibit Modic changes. The

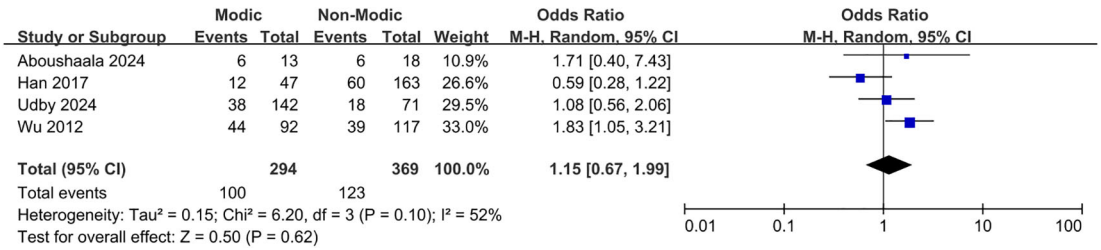

FIGURE 7
Smoking as a risk factor.

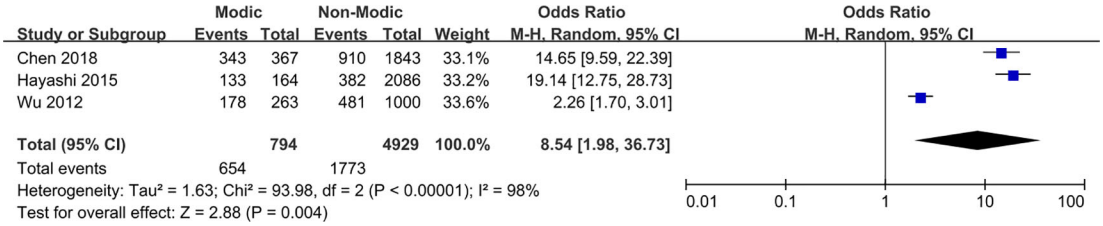

FIGURE 8
Disc degeneration as a risk factor.

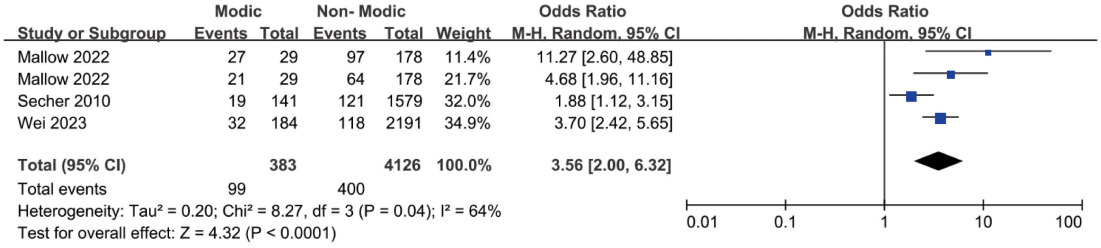

FIGURE 9
Endplate changes as a risk factor.

meta-analysis revealed that patients with smaller anterior lumbar lordosis angles were more likely to develop Modic changes, while those with larger anterior lumbar lordosis angles were less likely to do so (OR = -4.14; 95% CI = -6.79 to -1.49; Z = 3.06; p = 0.002; I^2 = 62%; Figure 10). Based on these results, we found moderate evidence suggesting that a reduced anterior lumbar lordosis angle appears to be an important risk factor for Modic changes in the lumbar spine.

3.6.4 Spondylolisthesis

Three studies (26, 44, 45) reported an association between spondylolisthesis and Modic changes (Figure 11). Pooled data analysis indicated that patients with spondylolisthesis were more likely to develop Modic changes, while the meta-analysis revealed that Modic changes occurred in 48.28% of patients with spondylolisthesis and 19.92% of those without spondylolisthesis (OR = 2.00; 95% CI = 1.12 to 3.58; Z = 2.33; p = 0.02; I^2 = 0%; Figure 11). Therefore, we found minor evidence suggesting that spondylolisthesis is a risk factor for Modic changes in the lumbar spine.

3.6.5 Lumbar disc herniation, segmental distribution, and sacral slope angle

Four studies (20, 26, 41, 45) investigated the correlation between lumbar disc herniation and Modic changes, indicating that lumbar disc herniation was not significantly associated with the presence of Modic changes (OR = 1.18; 95% CI = 0.57 to 2.44; Z = 0.45; p = 0.65; I^2 = 83%; Figure 12). Additionally, four studies (20, 22, 31, 35) reported no significant associations between segmental distribution and Modic alterations (OR = 0.83; 95% CI = 0.60 to 1.15; Z = 1.11; p = 0.27; I^2 = 63%; Figure 13). Furthermore, three studies (21, 23, 29) confirmed that the size of the sacral slope angle was not significantly

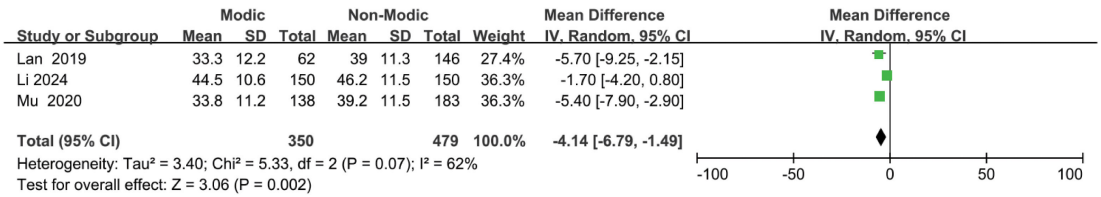

FIGURE 10
Lumbar lordosis angle as a risk factor.

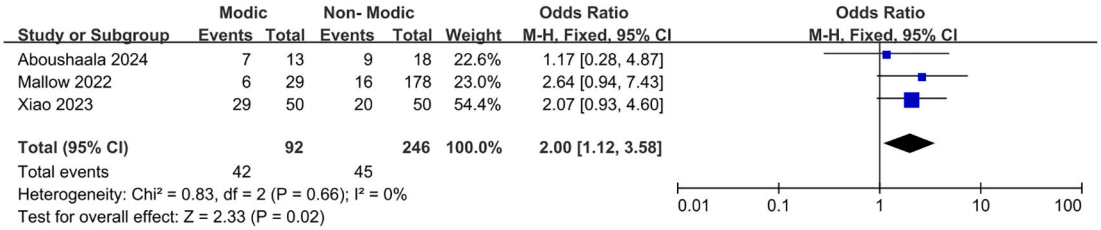

FIGURE 11
Spondylolisthesis as a risk factor.

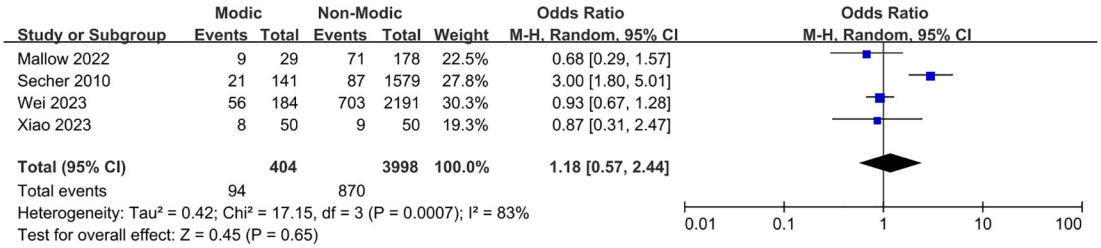

FIGURE 12
Lumbar disc herniation as a risk factor.

associated with the presence of Modic alterations (OR = -2.25; 95% CI = -5.72 to 1.21; Z = 1.28; p = 0.20; I^2 = 88%; Figure 14). Therefore, this meta-analysis found no substantial evidence to confirm that lumbar disc herniation, segmental distribution, or sacral slope angle are significant risk factors for the development of Modic changes in the lumbar spine.

4 Discussion

This systematic review and meta-analysis yielded three key findings. First, the analysis determined a 35% incidence of Modic changes in the lumbar spine based on data from X studies. Second, strong evidence suggests that the risk factors associated with the development of Modic changes in the lumbar spine include advanced age, lumbar disc degeneration, endplate changes, spondylolisthesis, reduced anterior lumbar lordosis angles, and participation in physical labor. Third, no evidence was found linking sex, BMI, smoking, lumbar disc herniation, segmental distribution, or sacral angle to Modic changes in the lumbar spine.

Lower back pain associated with Modic changes, characterized by abnormal alterations in the vertebral endplates and sub-endplates, has garnered significant research attention. These changes appear as abnormal signals in the endplates on MRI. Modic changes can induce disabling lower back pain (46, 47). The present study demonstrated an incidence rate of 35% for Modic changes, higher than that in the general population, possibly due to the broader population range included in this study. However, since De Roos et al.'s initial study (12), research on its pathogenesis and risk factors has remained controversial. This meta-analysis provides robust evidence demonstrating an association between Modic changes and various factors, including age, disc degeneration, endplate changes, spondylolisthesis, the anterior lumbar lordosis angle, and physical labor.

The 14 studies included in this meta-analysis indicated that patients with Modic changes were generally older, consistent with

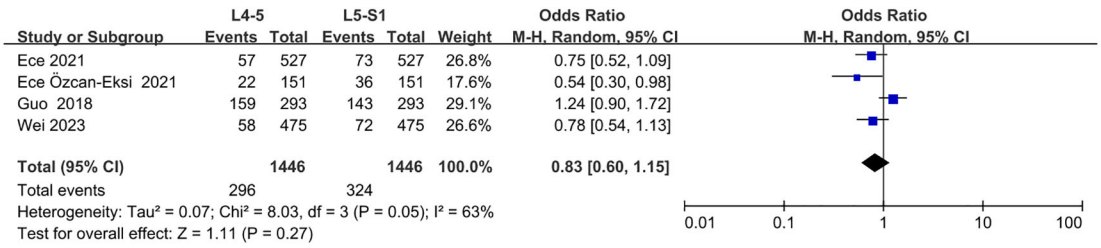

FIGURE 13
Segmental distribution as a risk factor.

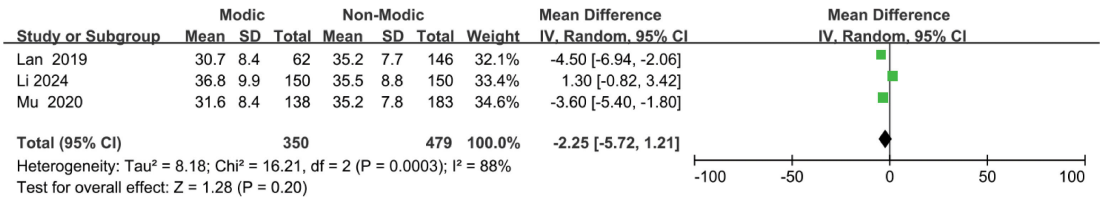

FIGURE 14
Sacral slope angle as a risk factor.

most previous findings (9, 23, 30, 33, 36). However, Li et al. (21) reported that in patients with lumbar spondylolisthesis, Modic changes were more prevalent in younger individuals (mean age, 53.44 ± 9.80 years; n = 150) than in older individuals (mean age, 59.68 ± 9.66 years; n = 150). Mallow et al. (45) reported that Modic changes were present in a subset of adolescents (Modic group: 16.7 ± 2.2 years, n = 29; non-Modic group: 16.5 ± 2.4 years, n = 178). A focus on Modic changes in younger patients may hold significant potential for advancing our understanding of its pathogenesis and providing treatment strategies. Additionally, some researchers have reported no significant relationship between age and the development of Modic changes (26, 29, 42, 44). Definitive evidence from this meta-analysis suggests that older patients are more prone to Modic changes, which may be linked to the development of disc degeneration, spondylolisthesis, reduced vertebral stability, spinal stenosis, and osteoporosis; however, the specific causes and mechanisms underlying these associations remain unclear.

Studies consistently report that disc degeneration has the potential to trigger Modic changes. Eksi et al. (35) investigated the relationship between severe disc degeneration and Modic changes, concluding that this association is particularly strong in the lower lumbar region, with Modic changes detected in 88–90% of cases involving disc degeneration in this area. Wu et al. (27) identified disc degeneration as a risk factor for Modic changes, suggesting that patients with disc degeneration (27.0% [178/659]) are more likely to develop Modic changes than those without disc degeneration (14.1% [85/604]). Jensen et al. (41) found a strong correlation between disc degeneration and new-onset Modic changes, suggesting that disc degeneration may be a potential predictor for Modic alterations. The current meta-analysis of three studies found strong evidence of a significant correlation between disc degeneration and Modic changes, with a higher incidence of Modic changes in patients with disc degeneration (26.95% [654/2427]) than in those without (4.25% [140/3296]). This may be related to changes in angular motion, translational motion, and disc height in degenerated discs. However, the exact mechanism remains unclear, warranting further research to confirm this association.

Endplate changes included Schmorl's nodes and endplate damage. The current meta-analysis, comprising three studies, demonstrated a higher incidence of Modic changes in patients with endplate changes (19.84% [99/499]) than in those without (7.08% [284/4010]). Jensen et al. (41) concluded that endplate changes were strongly associated with Modic changes, as indicated by a higher incidence of Modic changes in patients with endplate changes (13.57% [19/140]) than in those without (7.72% [122/1580]), suggesting that endplate changes could serve as a potential predictor. Similar findings were reported by Wei et al. (20), in which the incidence of Modic changes was higher in patients with endplate changes (21.33% [32/150]) than in those without endplate changes (6.83% [152/2225]). Mallow et al. (45) found a strong correlation between endplate changes and the presence of Modic changes, with the incidence of Modic changes being higher in patients with endplate changes (endplate damage, 21.8% [27/124]; Schmorl's nodes, 24.71% [21/85]) than in those without endplate changes (endplate damage, 2.4% [2/83]; Schmorl's nodes, 6.56% [8/122]). These studies suggest that the association between endplate changes and Modic changes is becoming increasingly evident. This association may be due to endplate

changes that cause microstructural alterations in the disc and microfractures in the endplate, potentially leading to bacterial invasion. However, the specific mechanisms through which endplate changes influence Modic changes remain unclear and require further investigation.

Spondylolisthesis, physical labor, and anterior lumbar lordosis angles warrant attention. Wei et al. (20) found a strong correlation between lumbar spondylolisthesis and the occurrence of Modic changes, with a higher incidence in patients with spondylolisthesis (32.7% [32/98]) than in those without (6.7% [152/2277]); most Modic changes were characterized as Modic type II. Hayashi et al. (39) demonstrated that the incidence of Modic changes in patients with a spondylolisthesis degree greater than 0.8 mm (10.9% [119/1082]) was higher than in those with a spondylolisthesis degree less than or equal to 0.8 mm (3.85% [45/1168]), providing strong evidence of the correlation between spondylolisthesis severity and Modic changes. In study, Modic type II was identified as the most prevalent form of Modic change, and Modic change was more common in patients with spondylolisthesis (45). This is hypothesized to be associated with bone marrow changes and the disease's developmental stage (48). Han et al. (32) concluded that the incidence of Modic changes was higher in patients who engaged in heavier physical labor (40.4% [23/57]) than in those who engaged in lighter physical labor (15.7% [24/153]). Additionally, Modic type III changes were more prevalent in patients who performed more rigorous physical labor, suggesting that physical labor can be considered a risk factor (32). This may be related to microinjuries of the vertebral endplates and fatigue degeneration caused by heavy physical labor, consistent with the findings of previous studies (49, 50). The anterior lumbar lordosis angle is a distinctive angle that has evolved in humans to maintain an upright posture (51). Xia et al. (52) concluded that the frequency of Modic changes was negatively correlated with the anterior lumbar lordosis angle, potentially owing to axial decompression of the vertebral body and alterations in endplate shear. However, Li et al. (21) found no significant correlation between Modic changes and the anterior lumbar lordosis angle. This meta-analysis demonstrated that spondylolisthesis, physical labor, and the anterior lumbar lordosis angle are strongly associated with Modic changes. Patients with spondylolisthesis exhibited a higher incidence of Modic changes (48.28% [42/87]) than those without spondylolisthesis (19.92% [50/251]). Similarly, individuals who engaged in physical labor had a higher incidence of Modic alterations (15.43% [100/648]) than those who did not engage in physical labor (15.16% [365/2407]). Additionally, patients with smaller anterior lumbar lordosis angles were more likely to exhibit Modic changes. These factors can be considered risk factors for Modic changes.

This review and meta-analysis had some limitations. Although 25 studies were included, their overall methodological quality was moderate, and the inclusion of lower-quality studies may have influenced the results. Subtype-specific analyses of Modic changes (Types I–III) were not conducted due to the insufficient data available from the included studies. Furthermore, significant heterogeneity was observed, indicating considerable inter-study variability. Future research should prioritize high-quality studies and employ more advanced methodologies.

5 Conclusion

The objective of this systematic review and meta-analysis was to determine the incidence and associated risk factors of Modic changes in the lumbar spine. The findings suggest an approximate incidence of 35%, with risk factors including advanced age, disc degeneration, endplate changes, spondylolisthesis, reduced anterior lumbar lordosis angles, and participation in physical labor.

Data availability statement

The raw data supporting the conclusions of this article will be made available by the authors, without undue reservation.

Author contributions

ZC: Formal Analysis, Software, Writing – original draft, Writing – review & editing. MZ: Writing – review & editing. JJ: Data curation, Formal Analysis, Writing – review & editing. GZ: Methodology, Software, Writing – review & editing. LL: Project administration, Supervision, Writing – review & editing. ZY: Software, Formal Analysis, Writing – review & editing. FZ: Conceptualization, Visualization, Writing – review & editing. XK: Conceptualization, Investigation, Visualization, Writing – review & editing.

Funding

The author(s) declare that financial support was received for the research and/or publication of this article. This work was supported by the National Natural Science Foundation of China (Grant No. 82272536), the Natural Science Foundation of Gansu province (Grant No. 24JRRA380), and the Qinghai Province "Kunlun Talents -High-end Innovation and Entrepreneurship Talents" Project in 2022 (QHKLYC-GDCXCY-2022-058).

Acknowledgments

We would like to thank Editage (www.editage.cn) for English language editing.

Conflict of interest

The authors declare that the research was conducted in the absence of any commercial or financial relationships that could be construed as a potential conflict of interest.

Generative AI statement

The author(s) declare that no Generative AI was used in the creation of this manuscript.

Publisher's note

References

1. Hartvigsen J, Hancock MJ, Kongsted A, Louw Q, Ferreira ML, Genevay S, et al. What low back pain is and why we need to pay attention. *Lancet*. (2018) 391:2356–67. doi: 10.1016/S0140-6736(18)30480-X

2. Knezevic NN, Candido KD, Vlaeyen JWS, Van Zundert J, Cohen SP. Low back pain. *Lancet*. (2021) 398:78–92. doi: 10.1016/S0140-6736(21)00733-9

3. Massaad E, Mitchell TS, Duerr E, Kiapour A, Cha TD, Coumans JC, et al. Disparities in surgical intervention and health-related quality of life among racial/ethnic groups with degenerative lumbar spondylolisthesis. *Neurosurgery*. (2024) 95:576–83. doi: 10.1227/neu.0000000000002925

4. Rahyussalim AJ, Zufar MLL, Kurniawati T. Significance of the association between disc degeneration changes on imaging and low back pain: A review article. *Asian Spine J*. (2020) 14:245–57. doi: 10.31616/asj.2019.0046

5. Wang Y, Zhang C, Cheng J, Yan T, He Q, Huang D, et al. Cutting-edge biomaterials in intervertebral disc degeneration tissue engineering. *Pharmaceutics*. (2024) 16(8):979. doi: 10.3390/pharmaceutics16080979

6. Liu Z, Qiao F, Liu D, Kong X, Liu K, Gu H, et al. Periplocin targets LRP4 to regulate metabolic homeostasis and anti-inflammation for the treatment of IVDD. *Phytomedicine*. (2025) 143:156885. doi: 10.1016/j.phymed.2025.156885

7. Lu Z, Zheng Z. Integrated analysis of single-cell and bulk RNA sequencing data identifies the characteristics of ferroptosis in lumbar disc herniation. *Funct Integr Genomics*. (2023) 23:289. doi: 10.1007/s10142-023-01216-8

8. Cholewicki J, Lee AS, Popovich JM Jr, Mysliwiec LW, Winkelpleck MD, Flood JN, et al. Degenerative spondylolisthesis is related to multiparity and hysterectomies in older women. *Spine (Phila Pa 1976)*. (2017) 42:1643–7. doi: 10.1097/BRS.0000000000002178

9. Mok FP, Samartzis D, Karppinen J, Fong DY, Luk KD, Cheung KM. Modic changes of the lumbar spine: prevalence, risk factors, and association with disc degeneration and low back pain in a large-scale population-based cohort. *Spine J*. (2016) 16:32–41. doi: 10.1016/j.spinee.2015.09.060

10. Kawabata S, Nagai S, Ito K, Takeda H, Ikeda D, Kawano Y, et al. Intradiscal administration of autologous platelet-rich plasma in patients with Modic type 1 associated low back pain: A prospective pilot study. *JOR Spine*. (2024) 7:e1320. doi: 10.1002/jsp2.1320

11. Crump KB, Alminnawi A, Bermudez-Lekerika P, Compte R, Gualdi F, McSweeney T, et al. Cartilaginous endplates: A comprehensive review on a neglected structure in intervertebral disc research. *JOR Spine*. (2023) 6:e1294. doi: 10.1002/jsp2.1294

12. de Roos A, Kressel H, Spritzer C, Dalinka M. MR imaging of marrow changes adjacent to end plates in degenerative lumbar disk disease. *AJR Am J Roentgenol*. (1987) 149:531–4. doi: 10.2214/ajr.149.3.531

13. Modic MT, Steinberg PM, Ross JS, Masaryk TJ, Carter JR. Degenerative disk disease: assessment of changes in vertebral body marrow with MR imaging. *Radiology*. (1988) 166:193–9. doi: 10.1148/radiology.166.1.3336678

14. Samartzis D, Mok FPS, Karppinen J, Fong DYT, Luk KDK, Cheung KMC. Classification of Schmorl's nodes of the lumbar spine and association with disc degeneration: a large-scale population-based MRI study. *Osteoarthritis Cartilage*. (2016) 24:1753–60. doi: 10.1016/j.joca.2016.04.020

15. Dudli S, Fields AJ, Samartzis D, Karppinen J, Lotz JC. Pathobiology of modic changes. *Eur Spine J*. (2016) 25:3723–34. doi: 10.1007/s00586-016-4459-7

16. Modic MT, Masaryk TJ, Ross JS, Carter JR. Imaging of degenerative disk disease. *Radiology*. (1988) 168:177–86. doi: 10.1148/radiology.168.1.3289089

17. Kuisma M, Karppinen J, Niinimäki J, Ojala R, Haapea M, Heliövaara M, et al. Modic changes in endplates of lumbar vertebral bodies: prevalence and association with low back and sciatic pain among middle-aged male workers. *Spine (Phila Pa 1976)*. (2007) 32:1116–22. doi: 10.1097/01.brs.0000261561.12944.ff

18. Rajasekaran S, Ramachandran K, K SS, Kanna RM, Shetty AP. From modic to disc endplate bone marrow complex - the natural course and clinical implication of vertebral endplate changes. *Global Spine J*. (2025) 15:196–209. doi: 10.1177/21925682241271440

19. Chen Y, Bao J, Yan Q, Wu C, Yang H, Zou J. Distribution of Modic changes in patients with low back pain and its related factors. *Eur J Med Res*. (2019) 24:34. doi: 10.1186/s40001-019-0393-6

20. Wei B, Wu H. Study of the distribution of lumbar modic changes in patients with low back pain and correlation with lumbar degeneration diseases. *J Pain Res*. (2023) 16:3725–33. doi: 10.2147/JPR.S430792

21. Li GQ, Kang X, Li W, Pei SS. Study and analysis of the correlation between lumbar spondylolisthesis and Modic changes. *Front Surg*. (2024) 11:1296275. doi: 10.3389/fsurg.2024.1296275

22. Özcan-Ekşi EE, Turgut VU, Küçüksüleymanoğlu D, Ekşi M. Obesity could be associated with poor paraspinal muscle quality at upper lumbar levels and degenerated spine at lower lumbar levels: Is this a domino effect? *J Clin Neurosci*. (2021) 94:120–7. doi: 10.1016/j.jocn.2021.10.005

23. Mu X, Peng W, Yu C, Xiong J, Wei J, Ou Y, et al. Modic changes of the lumbar spine-their association with the lumbar sagittal parameters: A retrospective imaging study. *J Orthop Surg Res*. (2020) 15:220. doi: 10.1186/s13018-020-01745-z

24. Page MJ, McKenzie JE, Bossuyt PM, Boutron I, Hoffmann TC, Mulrow CD, et al. The PRISMA 2020 statement: An updated guideline for reporting systematic reviews. *Int J Surg*. (2021) 88:105906. doi: 10.1016/j.ijsu.2021.105906

25. Shea BJ, Reeves BC, Wells G, Thuku M, Hamel C, Moran J, et al. AMSTAR 2: a critical appraisal tool for systematic reviews that include randomised or non-randomised studies of healthcare interventions, or both. *Bmj*. (2017) 358:j4008. doi: 10.1136/bmj.j4008

26. Xiao Y, Xiu P, Yang X, Wang L, Li T, Gong Q, et al. Does preoperative modic changes influence the short-term fusion rate of single level transforaminal lumbar interbody fusion?-a matched-pair case control study. *Orthop Surg*. (2023) 15:2309–17. doi: 10.1111/os.13795

27. Wu HL, Ding WY, Shen Y, Zhang YZ, Guo JK, Sun YP, et al. Prevalence of vertebral endplate modic changes in degenerative lumbar scoliosis and its associated factors analysis. *Spine (Phila Pa 1976)*. (2012) 37:1958–64. doi: 10.1097/BRS.0b013e31825bfb85

28. Xiao L, Ni C, Shi J, Wang Z, Wang S, Zhang J, et al. Analysis of correlation between vertebral endplate change and lumbar disc degeneration. *Med Sci Monit*. (2017) 23:4932–8. doi: 10.12659/MSM.904315

29. Lan M, Ou Y, Wang C, Wei W, Lu X, Wei J, et al. Patients with Modic type 2 change have a severe radiographic representation in the process of lumbar degeneration: a retrospective imaging study. *J Orthop Surg Res*. (2019) 14:298. doi: 10.1186/s13018-019-1355-y

30. Chen L, Hu X, Zhang J, Battié MC, Lin X, Wang Y. Modic changes in the lumbar spine are common aging-related degenerative findings that parallel with disk degeneration. *Clin Spine Surg*. (2018) 31:312–7. doi: 10.1097/BSD.0000000000000662

31. Guo R, Yang X, Zhong Y, Lai Q, Gao T, Lai F, et al. Correlations between Modic change and degeneration in 3-joint complex of the lower lumbar spine: A retrospective study. *Med (Baltimore)*. (2018) 97:e12496. doi: 10.1097/MD.0000000000012496

32. Han C, Kuang MJ, Ma JX, Ma XL. Prevalence of Modic changes in the lumbar vertebrae and their associations with workload, smoking and weight in northern China. *Sci Rep*. (2017) 7:46341. doi: 10.1038/srep46341

33. Määttä JH, Karppinen J, Paananen M, Bow C, Luk KDK, Cheung KMC, et al. Refined phenotyping of modic changes: imaging biomarkers of prolonged severe low back pain and disability. *Med (Baltimore)*. (2016) 95:e3495. doi: 10.1097/MD.0000000000003495

34. Demirhan İ, Oner E, Yuksel Z, Yuksel M, Belge Kurutas E, et al. Raftlin and 8-iso-prostaglandin F2α levels and gene network analysis in patients with Modic changes. *Eur Spine J*. (2023) 32:2368–76. doi: 10.1007/s00586-023-07757-7

35. Özcan-Ekşi EE, Yayla A, Orhun Ö, Turgut VU, Arslan HN, Ekşi M, et al. Is the distribution pattern of modic changes in vertebral end-plates associated with the severity of intervertebral disc degeneration?: A cross-sectional analysis of 527 caucasians. *World Neurosurg*. (2021) 150:e298–304. doi: 10.1016/j.wneu.2021.02.128

36. Ekşi M, Kara M, Özcan-Ekşi EE, Aytar MH, Güngör A, Özgen S, et al. Is diabetes mellitus a risk factor for modic changes?: A novel model to understand the association between intervertebral disc degeneration and end-plate changes. *J Orthop Sci*. (2020) 25:571–5. doi: 10.1016/j.jos.2019.09.005

37. Atci IB, Yilmaz H, Samanci MY, Atci AG, Karagoz Y, et al. The prevalence of lumbar paraspinal muscle fatty degeneration in patients with modic type I and I/II end plate changes. *Asian Spine J*. (2020) 14:185–91. doi: 10.31616/asj.2018.0333

38. Kanna RM, Shanmuganathan R, Rajagopalan VR, Natesan S, Muthuraja R, Cheung KMC, et al. Prevalence, patterns, and genetic association analysis of modic vertebral endplate changes. *Asian Spine J*. (2017) 11:594–600. doi: 10.4184/asj.2017.11.4.594

39. Hayashi T, Daubs MD, Suzuki A, Scott TP, Phan KH, Ruangchainikom M, et al. Motion characteristics and related factors of Modic changes in the lumbar spine. *J Neurosurg Spine*. (2015) 22:511–7. doi: 10.3171/2014.10.SPINE14496

40. Udby PM, Modic M, Elmose S, Carreon LY, Andersen M, Karppinen J, et al. The clinical significance of the modic changes grading score. *Global Spine J*. (2024) 14:796–803. doi: 10.1177/21925682221123012

41. Jensen TS, Kjaer P, Korsholm L, Bendix T, Sorensen JS, Manniche C, et al. Predictors of new vertebral endplate signal (Modic) changes in the general population. *Eur Spine J*. (2010) 19:129–35. doi: 10.1007/s00586-009-1184-5

42. Dudli S, Ballatori A, Bay-Jensen AC, McCormick ZL, O'Neill CW, Demir-Deviren S, et al. Serum biomarkers for connective tissue and basement membrane remodeling are associated with vertebral endplate bone marrow lesions as seen on MRI (Modic changes). *Int J Mol Sci*. (2020) 21. doi: 10.3390/ijms21113791

43. van der Wurff P, Vredeveld T, van de Graaf C, Jensen RK, Jensen TS. Exploratory study for clinical signs of MODIC changes in patients with low-back pain in the Netherlands armed forces. *Chiropr Man Therap*. (2019) 27:5. doi: 10.1186/s12998-018-0229-4

44. Aboushaala K, Chee AV, Toro SJ, Vucicevic R, Yuh C, Dourdourekas J, et al. Discovery of circulating blood biomarkers in patients with and without Modic changes of the lumbar spine: a preliminary analysis. *Eur Spine J*. (2024) 33:1398–406. doi: 10.1007/s00586-024-08192-y

45. Mallow GM, Zepeda D, Kuzel TG, Barajas JN, Aboushaala K, Nolte MT, et al. ISSLS PRIZE in Clinical Science 2022: Epidemiology, risk factors and clinical impact of juvenile Modic changes in paediatric patients with low back pain. *Eur Spine J*. (2022) 31:1069–79. doi: 10.1007/s00586-022-07125-x

46. Munir S, Freidin MB, Rade M, Määttä J, Livshits G, Williams FMK. Endplate defect is heritable, associated with low back pain and triggers intervertebral disc degeneration: A longitudinal study from twinsUK. *Spine (Phila Pa 1976)*. (2018) 43:1496–501. doi: 10.1097/BRS.0000000000002721

47. Määttä JH, Wadge S, MacGregor A, Karppinen J, Williams FM. ISSLS prize winner: vertebral endplate (Modic) change is an independent risk factor for episodes of severe and disabling low back pain. *Spine (Phila Pa 1976)*. (2015) 40:1187–93. doi: 10.1097/BRS.0000000000000937

48. Ohtori S, Yamashita M, Yamauchi K, Inoue G, Koshi T, Suzuki M, et al. Change in Modic type 1 and 2 signals after posterolateral fusion surgery. *Spine (Phila Pa 1976)*. (2010) 35:1231–5. doi: 10.1097/BRS.0b013e3181bde562

49. Leboeuf-Yde C, Kjaer P, Bendix T, Manniche C. Self-reported hard physical work combined with heavy smoking or overweight may result in so-called Modic changes. *BMC Musculoskelet Disord*. (2008) 9:5. doi: 10.1186/1471-2474-9-5

50. Albert HB, Kjaer P, Jensen TS, Sorensen JS, Bendix T, Manniche C. Modic changes, possible causes and relation to low back pain. *Med Hypotheses*. (2008) 70:361–8. doi: 10.1016/j.mehy.2007.05.014

51. Lee CH, Chung CK, Jang JS, Kim SM, Chin DK, Lee JK. 'Lumbar degenerative kyphosis' Is not byword for degenerative sagittal imbalance: time to replace a misconception. *J Korean Neurosurg Soc*. (2017) 60:125–9. doi: 10.3340/jkns.2016.0607.001

52. Xia W, Liu C, Duan S, Xu S, Wang K, Zhu Z, et al. The influence of spinal-pelvic parameters on the prevalence of endplate Modic changes in degenerative thoracolumbar/lumbar kyphosis patients. *PloS One*. (2018) 13:e0197470. doi: 10.1371/journal.pone.0197470

frontiers | Frontiers in Endocrinology

TYPE Original Research
PUBLISHED 14 August 2025
DOI 10.3389/fendo.2025.1602551

OPEN ACCESS

EDITED BY
Federico Baronio,
Dpt Hospital of Woman and Child, Italy

REVIEWED BY
Francisco André Da Cruz Ferreira,
University of Porto, Portugal
João Pinheiro,
University of Algarve, Portugal

*CORRESPONDENCE
Ricardo R. Agostinete
ricardo.agostinete@unesp.br
Romulo Araújo Fernandes
romulo.a.fernandes@unesp.br

RECEIVED 29 March 2025
ACCEPTED 26 June 2025
PUBLISHED 14 August 2025
CORRECTED 11 September 2025

CITATION
Agostinete RR, Narciso PH, Coelho-e-Silva MJ, Bielemann RM, Gobbo LA, Turi-Lynch BC, Fernandes RA and Vlachopoulos D (2025) Inflammatory markers as potential mediators on the negative association between training load and bone mineral density in adolescent competitive swimmers: ABCD-growth study. *Front. Endocrinol.* 16:1602551. doi: 10.3389/fendo.2025.1602551

Inflammatory markers as potential mediators on the negative association between training load and bone mineral density in adolescent competitive swimmers: ABCD-growth study

Ricardo R. Agostinete[1]*, Pedro H. Narciso[1], Manuel João Coelho-e-Silva[2], Renata M. Bielemann[3], Luis Alberto Gobbo[4], Bruna Camilo Turi-Lynch[5], Romulo Araújo Fernandes[1]* and Dimitris Vlachopoulos[6]

[1]Laboratory of Investigation in Exercise (LIVE), Department of Physical Education, Sao Paulo State University (UNESP), Presidente Prudente, Brazil, [2]CIDAF (UID/DTP/04213/2016), Faculty of Sport Sciences and Physical Education, University of Coimbra, Coimbra, Portugal, [3]Post-Graduate Program in Nutrition and Foods, Federal University of Pelotas, Pelotas, Brazil. Post-Graduate Program in Epidemiology, Federal University of Pelotas, Pelotas, Brazil, [4]Skeletal Muscle Assessment Laboratory (LABSIM), Department of Physical Education, School of Technology and Sciences, São Paulo State University (UNESP), Presidente Prudente, Brazil, [5]Department of Physical Education and Exercise Science, Lander University, Greenwood, SC, United States, [6]Children's Health and Exercise Research Centre, Sport and Health Sciences, University of Exeter, Exeter, United Kingdom

Introduction: Competitive swimming during adolescence has been linked to poor bone development, potentially influenced by training load, inflammation, hormones, and bone markers. However, this influence has been poorly investigated in the literature.

Objective: To compare whether competitive adolescent swimmers present differences in inflammatory, immunological, anabolic, and bone markers compared with non-sport group and to analyse whether inflammatory variables mediate the association between training load and areal bone mineral density (aBMD) in the swimmers group.

Methods: This cross-sectional study included 61 adolescents (20 females, 15.4 ±2.3 years), of which 30 were adolescent swimmers and 31 did not participate in sports (non-sports group). The daily training load was obtained by multiplying the perceived exertion score by the training volume of the swimmers. Lean soft tissue, fat mass and aBMD were estimated from whole-body scans using dual-energy X-ray absorptiometry and peak height velocity considering stature and body mass. Blood samples were collected to assess bone markers (calcium, 25-hydroxy vitamin D, C-terminal telopeptide, and osteocalcin), growth hormones, insulin-like growth factor 1 (IGF-1), lymphocytes, leukocytes, and inflammatory markers (interleukin-6 [IL-6] and C-reactive protein [CRP]). Statistical analyses applied a significance level at $p<0.05$.

Results: Besides lower values in BMD (expect in upper limbs), swimmers had higher calcium (10.0 ± 0.30 vs 9.7 ± 0.44, p=0.007), vitamin D (42.6 ± 10.4 vs 24.2 ± 5.9, p<0.001), and IGF-1 (397.2 ± 115.1 vs 220.3± 73.9, p<0.001) concentrations than their non-sports peers. The mediation analysis found no indirect associations between training load and aBMD through inflammatory markers. Nevertheless, training load was directly and negatively associated with aBMD in the lower limbs (β=-0.1533, 95%CI:-0.2875, -0.0191) and total body less head (β=-0.0978, 95%CI:-0.1880, -0.0076) through IL-6 and directly and negatively associated with aBMD at all sites through CRP.

Conclusion: The swimming and non-sports groups did not show differences in bone, inflammatory, or immunological markers. In contrast, swimmers had higher concentrations of IGF-1, calcium, and 25-hydroxy vitamin D. Although the training load was negatively associated with aBMD, inflammatory markers (IL-6 and CRP) did not mediate this association. Reinforcing the hypothesis that swimmers have lower aBMD due to the hypogravitational environment.

KEYWORDS

youth, athletes, bone health, cytokines, hormones

1 Introduction

The literature shows that sports with different mechanical impacts can distinctly affect the bone mineral density (BMD) (1). Sports with a higher mechanical impact and muscle activity, i.e. basketball and gymnastic, seem to be more effective for areal bone mineral density (aBMD) accrual (2), mainly during adolescence, when most of the bone mass observed in adulthood is accumulated (3). In addition, sports without a mechanical impact, such as swimming, are not beneficial for bone health, even with high muscle activity (4). Recent studies have shown that swimming can similarly or negatively affect the bone health of adolescents, even when compared to adolescents not engaged in sports, as observed in lower limbs and whole-body aBMD (4, 5).

Therefore, it is important to understand whether other factors, such as inflammation, could explain the negative association between training load and aBMD, in addition to hypogravity. Evidence indicates that the training load and previous sports practice time are negatively correlated with aBMD in adolescent swimmers (6, 7). Furthermore, training with very high physical effort (e.g., ~74% VO_{2max} or >64% VO_{2max}) may favour the increased circulation of immunological variables (8, 9), cytokines, and proteins related to the inflammatory response, such as interleukin-6 (IL-6), interleukin-1 (IL-1), tumour necrosis factor alpha (TNF-α), and C-reactive protein (CRP) (10). However, an intense bout of exercise in adolescents can lead to an acute reduction of anabolic markers such as insulin-like growth factor 1 (IGF-1) immediately after exercise (11), which is important for bone growth (12). Among the pro-inflammatory markers, IL-6 cytokine deserves special attention due to its increased expression on the activator of nuclear factor-kB ligand (RANKL), an essential protein for osteoclastogenesis (bone resorption) (13, 14). The increase in this process resultant of osteoclast activity may reduce bone mass accrual, resulting in decreased BMD. Additionally, evidence indicates that IL-6 leads to the increased production of CRP (15), which is a marker of inflammation in clinical practice (16).

However, to our knowledge, no studies have analysed whether, in fact, a competitive swimming training routine can cause changes in inflammatory, immunological, anabolic, and bone markers in adolescents compared with a non-sports group. Furthermore, whether inflammatory markers mediate the negative association between training load and BMD in swimmers has not yet been analysed. We hypothesized that adolescent competitive swimmers exhibit differences in physiological markers compared to controls, with inflammatory markers potentially mediating the negative association between training load and BMD. Thus, this cross-sectional study firstly aimed to compare whether competitive adolescent swimmers present differences in inflammatory, immunological, anabolic, and bone markers compared to adolescents who do not perform organised sports. Secondly, we analyzed whether inflammatory variables mediate the association between training load and aBMD in adolescent swimmers.

2 Methods

2.1 Study design

This was a cross-sectional study, and the data were collected as part of ongoing research, titled "Analysis of Behaviors of Children

During Growth: ABCD-Growth Study". The data from this study were collected as part of investigations by the Laboratory of InVestigation in Exercise (LIVE) conducted in Presidente Prudente, São Paulo, Brazil, from 2017 to 2018. The ABCD Growth Study aims to identify the impact of physical activity and sports participation on health variables, including bone tissue. This study was approved by the Ethical Research Committee of the São Paulo State University-UNESP (process number: 02891112.6.0000.5402).

2.2 Sample

The sports group comprised adolescents from a swimming team classified in Tier 2: Trained/Developmental, from Participant Classification Framework proposed by McKay et al. (2022) (17). While adolescents not engaged in organised sports were invited to join the non-sports group. To participate in the study, the adolescents were required to provide informed consent signed by their parents or guardians in according with the Declaration of Helsinki.

For adolescents who participated in sports, the following inclusion criteria were adopted: i) previous involvement for at least six months in the current sport (in the present study sample, the minium period of engagement observed in swimming was 24 months), ii) signed written consent form, iii) absence of clinical or metabolic disorders (previously diagnosed), iv) no regular use of medications that may affect the development and growth of the adolescent, and v) age of 10–19 years. For the adolescents in the non-sports group, the following criteria were applied: i) no regular participation in sports, ii) signed written consent, iii) absence of clinical or metabolic disorders (previously diagnosed), iv) no regular use of medications, and iv) age of 10–19 years.

The sample size was estimated based on the study by Agostinete et al. (6), using a correlation (two tailed bivariate correlation) coefficient of R=0.563 between the training load and lower limb aBMD, an alpha error of 0.05, a statistical power of 80%. The minimum estimated sample size was 22 participants, which was calculated using G*Power software. Thus, the final sample comprised 61 adolescents (41 males and 20 females) divided into two groups: 30 adolescent swimmers (21 males and 9 females) and 31 adolescents in the non-sports group (20 males and 11 females).

2.3 Outcomes

Height was measured using a fixed stadiometer (accurate to 0.1 cm; Sanny model, American Medical Do Brazil Ltda, Brazil), and body mass was measured using an electronic scale (accurate to 0.1 kg; Filizola PL 150 model; Filizzola Ltda, Brazil).

Biological maturation was estimated by the maturity offset (MO) using mathematical models based on anthropometric measures (18) for males = -7.999994+ [0.0036124 * (Age * Stature)] and females = -7.709133+ [0.0036124 * (Age * Stature)]. Thus, peak height velocity (PHV), the period of age where the fastest growth is seen, is given by the difference between chronological age and maturity offset (PHV = chronological age – MO).

To assess the whole-body aBMD (g/cm^2), lean soft tissue (kg), and fat mass (kg and %), dual-energy x-ray absorptiometry (DXA) scanning (models Lunar DPX-NT and Lunar Prodigy advance; General Electric Healthcare, Little Chalfont, Buckinghamshire, UK) was performed at the university laboratory in a temperature-controlled room using GE Medical System Lunar software. Each day, a trained researcher performed the scans and tested the scanner quality before the first examination. The scans were performed using a standardised protocol, with the participants remaining in the supine position and wearing light clothing without shoes. Regional BMD analysis according to the definitions of the regions of interest (ROIs), including the upper limbs, lower limbs, spine, and whole body (less the head), occurred offline after the scans were performed, as previously described (19).

Blood samples were collected by a certified nurse. Adolescents were instructed to refrain from exercise training on the day previous to blood collection. After an overnight fast, venous blood was collected from the antecubital vein in vacuum collection tubes with anticoagulant separating gel. Blood collection was carried out in a private laboratory, where it was also analyzed, and all the quality control standards adopted by the Brazilian Health Ministry were followed. Bone turnover markers, such as calcium, 25-hydroxy vitamin D, C-terminal telopeptide (CTX), osteocalcin, growth hormone, insulin, and IGF-1, were analysed using an electrochemiluminescence kit (Roche), Cobas e170, and Modular Analytics E170 equipment (chemiluminescence assay kit [VITROS] with the VITROS® XT 7600 equipment). Lymphocytes (CD3+, CD4+, and CD8+ cells) and leukocytes were analysed by flow cytometry using a Beckman Coulter kit and the Aquios-Beckman Coulter equipment. Finally, IL-6 and CRP levels were analysed using a Siemens kit and Immulite 2000 XPI equipment (Siemens Healthcare GmbH, Erlanger-Germany). Due to the sensitivity of the kit used, IL-6 values <1.5 were defined as 1.4 for the statistical analyses.

The training load was measured in the swimming group. The adolescents reported the intensity using the rating of perceived exertion proposed by Borg in 1982 and adapted by Foster (20) and the volume of training sessions (in hours and minutes) during the entire month (considering the days of training) prior to data collection. This method has been applied previously in studies involving adolescent swimmers, (6) and the daily training load was obtained by multiplying the rating of the perceived exertion score by the training volume (in minutes). The sum of the daily training loads was used to obtain the monthly training load used in this study.

2.4 Statistical analysis

Descriptive statistics included means, standard deviations, and confidence intervals (95% CIs). A generalized estimating equation (GEE) was used to compare variables between groups by applying linear or gamma scale responses, when appropriate, and

10.3389/fendo.2025.1602551

considering poshoc of Bonferroni. All comparisions were performed in SPSS (version 24.0). Since the adjusted GEE analysis do not provide standard deviations (SD), these values were calculated using the following formula: $SD = SEM\ x\sqrt{n}$ (21), where SEM was obtained from stardard error (std. error). In sequence, it was calculated the SD pooled applying the formula: $SD_{pooled} = \sqrt{(n_1 - 1)SD_1^2 + \frac{(n_2-1)SD_2^2}{n_1+n_2-2}}$. Lastly, the cohen's d effect sizes were calculated following the equation: $d = \frac{mean_1 - mean_2}{SD_{pooled}}$. The magnitude of effect size was calculated considering the following cut-off points: trivial ≤ 0.20, small = 0.20–0.59, moderate = 0.60–1.19, large =1.20–1.99, and very large ≥ 2.00 (22). Mediation analyses were performed using the model proposed by Valeri and Vanderweele (23) and applying the "med4way" command in Stata (version 14.0) and the theorical model is presented in Figure 1. This method decomposed the total association between training load and aBMD into direct (i.e., the direct effect of training load on aBMD through pathways not related to inflammatory markers) and pure indirect (i.e. the effect of training load on aBMD mediated by inflammatory markers) effects. In addition, we analysed the reference (i.e. the effect of training load on aBMD due to interactions with inflammatory markers) and mediated (i.e. the effect of training load on aBMD due to both mediation by and interaction with inflammatory markers) interactions. All mediation analyses were adjusted for chronological age and APHV. For all analyses, the significance level was set at p<0.05.

3 Results

The characteristics of the participants are shown in Table 1. Swimmers and control groups presented similar values for all anthropometric, maturational, and body composition variables in crude comparisons, except for body mass (p=0.022), fat mass in kilograms (p=0.004), and fat mass percentage (p=0.040). Table 2 presents the adjusted comparisons of aBMD, bone markers, and hormone/inflammatory variables between the swimmers and the control group. Swimmers showed lower aBMD in the lower limbs (p=0.011, d=0.59, small effect size), spine (p<0.001, d=1.09, moderate effect size), and total body less the head (TBLH; p<0.001, d=0.80, moderate effect size) than the control group. Regarding the bone markers, swimmers had higher calcium (p=0.002, d=0.74, moderate effect size) and vitamin D (p<0.001, d=2.18, very large effect size) concentrations. The same pattern was observed for hormonal variables such as IGF-1 (p<0.001, d=1.84, large effect size).

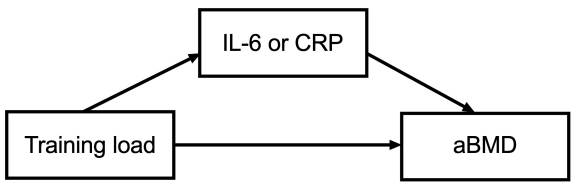

FIGURE 1
Theoretical framework of the mediation model. Independent variable: training load; dependent variable: areal bone mineral density (aBMD); mediator variables: inflammatory markers (IL-6 or CRP). Confounders: chronological age and APHV.

TABLE 1 Descriptive characteristics of the participants stratified by swimming participation (n=61).

Independent variables	Swimming group (n= 30)	Control group (n=31)	GEE
	Mean (SD)	Mean (SD)	P-value
General information			
Sex (Male/Female)	21/9	20/11	–
Chronological age (years)	15.0 (2.5)	15.9 (2.1)	0.132
MO (years)	1.5 (2.1)	2.3 (1.8)	0.547
Age at PHV (years)	13.5 (1.0)	13.6 (0.9)	0.699
Body mass (kg)	55.1 (11.9)	62.3 (13.3)	**0.022**
Stature (cm)	165.0 (10.4)	167.7 (10.3)	0.295
Lean soft tissue (kg)	42.7 (11.3)	43.9 (10.6)	0.661
Fat mass (kg)	10.5 (4.5)	15.5 (8.5)	**0.002**
Fat mass (%)	19.3 (8.0)	24.5 (11.3)	**0.032**
Training variables			
Engagement period (months)	68.00 (41.52)	–	–
Weekly frequence (days/week)	5.97 (0.18)		
Training volume (min/month)	1794.1 (583.1)	–	–
Training Intensity (RPE/month)	59.8 (18.7)	–	–
Training load (RPE x min)	6305.8 (2229.7)	–	–

SD, standard deviation; GEE, generalized estimating equation, MO, maturity offset; PHV, peak height velocity; RPE, Rating of perceived exertion.
Significant results are presented in bold.

Finally, the mediation analyses presented in Table 3 were performed to confirm the absence of a mediating effect of inflammatory markers on the association between training load and aBMD among swimmers. In the mediation models of IL-6, a direct effect was found between training load and aBMD in the lower limbs (β=-0.153, p=0.025) and TBLH (β=-0.098, p=0.034), while no indirect effect of IL-6 was found (p>0.05). The mediation models of CRP showed no indirect effect (p>0.05), while the training load directly affected aBMD in the upper limbs (β=-0.013, p=0.019), lower limbs (β=-0.024, p=0.009), total spine (β=-0.015, p=0.034), and TBLH (β=-0.017, p=0.005).

4 Discussion

This cross-sectional study aimed to analyse whether adolescent swimmers present different concentration patterns of inflammatory, immunological, anabolic, and bone markers

10.3389/fendo.2025.1602551

TABLE 2 Comparison of markers by swimming participation (n=61).

Independent variables	Swimming group (n=30) Mean ± SD (95%CI)	Non-Sports group (n=31) Mean ± SD (95%CI)	GEE-p	Cohen's d
Bone mineral density #				
Upper Limbs (g/cm^2)	0.828 ± 0.037 (0.815, 0.842)	0.839 ± 0.084 (0.810, 0.869)	0.501	0.17
Lower Limbs (g/cm^2)	1.175 ± 0.075 (1.148, 1.202)	1.223 ± 0.089 (1.192, 1.255)	**0.026**	0.59
Total Spine (g/cm^2)	0.941 ± 0.069 (0.916, 0.966)	1.042± 0.111 (1.004, 1.082)	**<0.001**	1.09
WBLH (g/cm^2)	0.983 ± 0.047 (0.966, 1.000)	1.033 ± 0.076 (1.007, 1.060)	**0.002**	0.80
Bone markers ‡				
Calcium (mg/dL)	10.0 ± 0.30 (9.9, 10.1)	9.7± 0.44 (9.5, 9.8)	**0.007**	0.74
25-hydroxy vitamin D (ng/mL)*	42.6 ± 10.4 (39.0, 46.5)	24.2 ± 5.9 (22.2, 26.4)	**<0.001**	2.18
Bone turnover markers ‡				
CTX (ng/mL)	0.831 ± 0.270 (0.739, 0.933)	0.990 ± 0.394 (0.860, 1.139)	0.070	0.47
Osteocalcin	55.2 ± 23.4 (47.4, 64.2)	48.1 ± 28.8 (38.9, 59.3)	0.319	0.27
Hormones ‡				
Growth hormone (ng/mL)	2.42 ± 4.00 (1.34, 4.37)	1.24 ± 1.80 (0.74, 2.07)	0.123	0.38
IGF-1 (ng/mL)	397.2 ± 115.1 (358.0, 440.6)	220.3 ± 73.9 (195.8, 247.9)	**<0.001**	1.84
Inflammatory markers ‡				
IL-6 (pg/mL)	1.50 ± 0.41 (1.35, 1.66)	1.50 ± 0.36 (1.37, 1.63)	0.937	0.02
CRP (mg/L)	1.65 ± 2.05 (1.05, 2.57)	2.49 ± 2.23 (1.81, 3.41)	0.073	0.04
Immunological Markers ‡				
Total Leukocytes (cells/uL)	6316.3 ± 1441.2 (5821.1, 6853.7)	6686.5 ± 1370.6 (6221.0, 7186.8)	0.297	0.26
Total Lymphocytes (cells/uL)	2473.8 ± 660.2 (2248.5, 2721.7)	2371.2 ± 692.8 (2139.5, 2628.1)	0.579	0.15
CD3+ T Lymphocytes (cells/uL)	1828.7 ± 525.5 (1650.0, 2026.8)	1791.1 ± 559.3 (1604.7, 1999.2)	0.797	0.07
CD4+ T Lymphocytes (cells/uL)	1006.6 ± 374.6 (881.2, 1149.9)	960.2 ± 327.4 (851.6, 1149.9)	0.627	0.13
CD8+ T Lymphocytes (cells/uL)	732.3 ± 251.4 (647.6, 828.0)	698.6 ± 234.9 (620.6, 786.3)	0.594	0.14

WBLH, whole body less head; CTX, C-terminal telopeptide; IGF-1, insulin-like growth factor 1; CRP, C-reactive protein. #Model adjusted for sex and age from PHV (MO) and LST. ‡Model adjusted by sex, age from PHV (MO), and fat mass (g). *One missing data in the non-sport group.
Significant results are presented in bold.

compared with adolescents who do not practice organised sports and whether inflammatory variables mediate the association between training load and aBMD in adolescent swimmers. The main findings showed that although swimmers present lower BMD values in most body regions, they have higher concentrations of calcium, 25-hydroxy vitamin D, and IGF-1. Finally, in addition to the groups showing similar values for bone metabolism, immunological markers, and inflammatory variables, these inflammatory markers did not mediate the negative association between training load and BMD in swimmers.

10.3389/fendo.2025.1602551

TABLE 3 Mediation models of the association between training load and aBMD by inflammatory markers (IL-6 and CRP).

IL-6	Total effect	Controlled direct effect	Reference interaction	Mediated Interaction	Pure indirect effect
	β (95%*CI*)	*β* (95%*CI*)	*β* (95%*CI*)	*β* (95%*CI*)	*β* (95%*CI*)
aBMD					
Upper limbs	-0.0386 (-0.1507 to 0.0735)	-0.0650 (-0.1444 to 0.0143)	-0.0259 (0.1373 to 0.0854)	0.0259 (-0.0321 to 0.0839)	0.0264 (-0.0342 to 0.0871)
Lower limbs	-0.0855 (-0.3534 to 0.1824)	**-0.1533 (-0.2875 to -0.0191)**	-0.0636 (-0.3280 to 0.2009)	0.0636 (-0.0616 to 0.1888)	0.0678 (-0.0661 to 0.2017)
Spine	-0.0491 (-0.1996 to 0.1013)	-0.0858 (-0.1838 to 0.0122)	-0.0350 (-0.1839 to 0.1139)	0.0350 (-0.0405 to 0.1106)	0.0367 (-0.0434 to 0.1167)
TBLH	-0.0559 (-0.2234 to 0.1115)	**-0.0978 (-0.1880 to -0.0076)**	-0.0396 (-0.2051 to 0.1260)	0.0396 (-0.0400 to 0.1192)	0.0419 (0.4289 to 0.1266)
CRP	**Total effect**	**Controlled direct effect**	**Reference interaction**	**Mediated Interaction**	**Pure indirect effect**
	β (95%*CI*)	*β* (95%*CI*)	*β* (95%*CI*)	*β* (95%*CI*)	*β* (95%*CI*)
aBMD					
Upper limbs	**-0.0130 (-0.0244 to -0.0016)**	**-0.0133 (-0.0246 to -0.0021)**	0.00008 (-0.0013 to 0.0014)	-0.00008 (-0.0007 to 0.0005)	0.0003 (-0.0017 to 0.0022)
Lower limbs	**-0.0227 (0.0421 to -0.0033)**	**-0.0238 (-0.0417 to -0.0060)**	0.00010 (-0.0015 to 0.0017)	-0.0010 (-0.0009 to 0.0007)	0.0011 (-0.0063 to 0.0086)
Spine	**-0.0146 (-0.0287 to -0.0006)**	**-0.0146 (-0.0287 to -0.0006)**	0.0003 (-0.0041 to 0.0047)	-0.0003 (-0.0022 to 0.0016)	-0.00005 (-0.0009 to 0.0008)
TBLH	**-0.0168 (-0.0298 to -0.0039)**	**-0.0174 (-0.0296 to -0.0053)**	0.0001 (-0.0017 to 0.0019)	-0.0001 (-0.0009 to 0.0007)	0.0006 (0.0036 to 0.0048)

Adjusted by chronological age and age at peak height velocity (PHV). TBLH, total-body less head. Analysis were carried with swimmers only (n=30).
Significant results are presented in bold.

The literature consistently states that swimming does not appear to be an effective sport for improving BMD (4), and our findings corroborate this statement. However, while some studies have shown a neutral effect of sports compared to controls (24) or a gain but with lower magnitude (25), others have reported a considerable negative effect, (5, 26) including the present study, where swimmers presented lower BMD compared to the non-sports group, except for in the upper limbs. To support this statement, a recent meta-analyses (27), demonstrated that in human models, swimming can present a neutral or negative effect on bone depending to anatomical region. The negative effect seems to occurs mainly in studies that include swimmers with a higher frequency of weekly training and consequently, a higher training load. Therefore, it was speculated that the physiological and inflammatory consequences of training could partially explain this phenomena, in addition to the environment without mechanical stimulation. Nonetheless, our results do not confirm these hypotheses and reinforce the fact that swimmers have lower aBMD, especially in the hypogravitational environment (4).

Competitive swimmers have a higher training load and consequently, higher daily training volume (i.e., time in water) (2). Therefore, the longer the time in the water (hypogravitational environment), the shorter the daily duration of mechanical stimulation from weight-bearing activities on land, even those not directly linked to sports practice. Consequently, less stimulation of bone tissue and lower BMD were observed in adolescents who did not practice sports. This result is interesting because it reinforces the idea that despite the high muscle activity during swimming, which is a significant predictor of BMD (28, 29), these muscle contractions do not seem to be effective in bone tissue, mainly in the lower limbs and whole body. In fact, studies have found that the relationship between the muscle and bone unit is different in swimmers (24), because the sport does not involve eccentric muscle contractions, in addition to low strain magnitude/strain during practice (30–32). Thus, dryland training should be recommended for swimmers, which can assist performance and is beneficial for the accumulation of bone mass (4, 33).

Furthermore, calcium, vitamin D, and IGF-1 were the only blood variables that showed concentration differences in the swimmers. Young athletes at a competitive level usually receive nutritional monitoring of calcium and vitamin D to improve the athlete's health performance and avoid growth and developmental delays (34). Therefore, although we did not control for food intake, a diet rich in these nutrients justifies these results (34). In contrast,

high IGF-1 concentrations appear to be associated with swimming practice. The concentrations of peptide and protein hormones, such as IGF-1, increase after physical exercise (35, 36); therefore, it is expected that swimmers will have higher concentrations of these hormones. However, despite its anabolic effect on different tissues such as muscle and bone, swimmers had lower BMD.

Despite the innovative aspects of the study, such as comparisons of different blood markers and testing the possible mediating effect of inflammatory markers, some limitations need to be acknowledged. First, the cross-sectional design prevented cause-and-effect interpretations. Second, the study did not analyse the food intake of the participants, which could indirectly affect any of the analysed markers. In addition, the sample size did not allow for analysis stratified by sex and age groups. Future studies are encouraged to explore the association between training load and BMD, as well as its potential mediators, in adolescents of different age groups (e.g., 10–14 and 15–19 years), stratified by sex and considering athletes with higher levels of sport engagement. The IL-6 assessment also had limitations, as the kit sensitivity did not detect values below 1.5. Lastly, the method used to estimate the training load was subjective, and therefore presents greater limitations compared to objective methods previously applied in studies involving swimmers (37).

In summary, although adolescent swimmers at the competitive level had lower BMD in most body segments than those in the non-sports group, they did not show differences in bone turnover, inflammatory, or immunological markers. In contrast, swimmers presented with higher concentrations of IGF-1, calcium, and 25-hydroxy vitamin D. Furthermore, although the training load was negatively associated with the aBMD, IL-6 and CRP levels did not mediate this association. These results have two possible explanations. First, other biological markers need to be checked for an association between the training load and bone to confirm the findings. In contrast, this could reinforce the hypothesis that swimmers have lower aBMD, especially due to the hypogravitational environment, and should be encouraged to include dryland training in their training routines.

Data availability statement

The raw data supporting the conclusions of this manuscript will be made available by the authors, without undue reservation, to any qualified researcher.

Ethics statement

The studies involving humans were approved by Ethical Research Committee of the São Paulo State University-UNESP. The studies were conducted in accordance with the local legislation and institutional requirements. Written informed consent for participation in this study was provided by the participants' legal guardians/next of kin.

Author contributions

RA: Writing – review & editing, Writing – original draft. PN: Writing – review & editing, Writing – original draft. MC-e-S: Writing – review & editing. RB: Writing – review & editing. LG: Writing – review & editing. BT: Writing – review & editing. RF: Writing – review & editing. DV: Writing – original draft, Writing – review & editing.

Funding

The author(s) declare that financial support was received for the research and/or publication of this article. This study was supported by the São Paulo Research Foundation-FAPESP (2017/09182-5, 2018/24164-6, and 2015/19710-3). Pedro Henrique Narciso received a grant from the FAPESP (2022/08875-5). This study was financed in part by PROPG/UNESP through call № 00/2025.

Acknowledgments

The authors gratefully acknowledge São Paulo Research Foundation (FAPESP), Coordenação de Aperfeicoamento de Pessoal de Nível Superior- Brasil (CAPES), and Conselho Nacional de Desenvolvimento Científico e Tecnológico (CNPq). Finally, the authors acknowledge the efforts of the participants and their parents, coaches, and all researchers from the Laboratory of Investigation in Exercise (LIVE) for their support in data collection.

Conflict of interest

The authors declare that the research was conducted in the absence of any commercial or financial relationships that could be construed as a potential conflict of interest.

Correction note

A correction has been made to this article. Details can be found at: 10.3389/fendo.2025.1686139.

Generative AI statement

The author(s) declare that Generative AI was used in the creation of this manuscript. The Generative AI was used only to check English grammar when necessary and to perform equations. All content was written by the authors.

Publisher's note

References

1. Yan C, Moshage SG, Kersh ME. Play during growth: the effect of sports on bone adaptation. *Curr Osteoporos Rep*. (2020) 18:684–95. doi: 10.1007/s11914-020-00632-0

2. Agostinete RR, Fernandes RA, Narciso PH, Maillane-Vanegas S, Werneck A, Vlachopoulos D. Categorizing 10 sports according to bone and soft tissue profiles in adolescents. *Med Sci Sports Exerc*. (2020) 52:2673–81. doi: 10.1249/MSS.0000000000002420

3. Baxter-Jones AD, Faulkner RA, Forwood MR, Mirwald RL, Bailey DA. Bone mineral accrual from 8 to 30 years of age: An estimation of peak bone mass. *J Bone Mineral Res*. (2011) 26:1729–39. doi: 10.1002/jbmr.412

4. Gomez-Bruton A, Montero-Marín J, González-Agüero A, García-Campayo J, Moreno LA, Casajús JA, et al. The effect of swimming during childhood and adolescence on bone mineral density: A systematic review and meta-analysis. *Sports Med*. (2016) 46:365–79. doi: 10.1007/s40279-015-0427-3

5. Agostinete RR, Vlachopoulos D, Werneck AO, Maillane-Vanegas S, Lynch KR, Naughton G, et al. Bone accrual over 18 months of participation in different loading sports during adolescence. *Arch Osteoporos*. (2020) 15:64. doi: 10.1007/s11657-020-00727-2

6. Agostinete RR, Maillane-Vanegas S, Lynch KR, Turi-Lynch B, Coelho-e-Silva MJ, Campos EZ, et al. The impact of training load on bone mineral density of adolescent swimmers: A structural equation modeling approach. *Pediatr Exerc Sci*. (2017) 29:520–8. doi: 10.1123/pes.2017-0008

7. Ribeiro-Dos-Santos MR, Lynch KR, Agostinete RR, Maillane-Vanegas S, Turi-Lynch B, Ito IH, et al. Prolonged practice of swimming is negatively related to bone mineral density gains in adolescents. *J Bone Metab*. (2016) 23:149–55. doi: 10.11005/jbm.2016.23.3.149

8. Lancaster GI, Halson SL, Khan Q, Drysdale P, Wallace F, Jeukendrup AE, et al. Effects of acute exhaustive exercise and chronic exercise training on type 1 and type 2 T lymphocytes. *Exerc Immunol Rev*. (2004) 10:91–106.

9. Walsh NP, Gleeson M, Pyne DB, Nieman DC, Dhabhar FS, Shephard RJ, et al. Position statement. Part two: Maintaining immune health. *Exerc Immunol Rev*. (2011) 17:64–103.

10. Cerqueira É, Marinho DA, Neiva HP, Lourenço O. Inflammatory effects of high and moderate intensity exercise-A systematic review. *Front Physiol*. (2020) 10:1550. doi: 10.3389/fphys.2019.01550

11. Nemet D, Oh Y, Kim H-S, Hill M, Cooper DM. Effect of intense exercise on inflammatory cytokines and growth mediators in adolescent boys. *Pediatrics*. (2002) 110:681–9. doi: 10.1542/peds.110.4.681

12. Locatelli V, Bianchi VE. Effect of GH/IGF-1 on bone metabolism and osteoporsosis. *Int J Endocrinol*. (2014) 2014:235060. doi: 10.1155/2014/235060

13. Hashizume M, Hayakawa N, Mihara M. IL-6 trans-signalling directly induces RANKL on fibroblast-like synovial cells and is involved in RANKL induction by TNF-alpha and IL-17. *Rheumatol (Oxford)*. (2008) 47:1635–40. doi: 10.1093/rheumatology/ken363

14. Rincon M. Interleukin-6: from an inflammatory marker to a target for inflammatory diseases. *Trends Immunol*. (2012) 33:571–7. doi: 10.1016/j.it.2012.07.003

15. Bermudez EA, Rifai N, Buring J, Manson JE, Ridker PM. Interrelationships among circulating interleukin-6, C-reactive protein, and traditional cardiovascular risk factors in women. *Arterioscler Thromb Vasc Biol*. (2002) 22:1668–73. doi: 10.1161/01.ATV.0000029781.31325.66

16. Cayres SU, Werneck AO, Urban JB, Turi-Lynch BC, Barbosa MF, Fernandes RA. Sports participation is inversely associated with C-reactive protein levels in adolescents: ABCD Growth Study. *Scand J Med Sci Sports*. (2019) 29:1000–5. doi: 10.1111/sms.13418

17. McKay AKA, Stellingwerff T, Smith ES, Martin DT, Mujika I, Goosey-Tolfrey VL, et al. Defining training and performance caliber: A participant classification framework. *Int J Sports Physiol Perform*. (2022) 17:317–31. doi: 10.1123/ijspp.2021-0451

18. Moore SA, McKay HA, Macdonald H, Nettlefold L, Baxter-Jones ADG, Cameron N, et al. Enhancing a somatic maturity prediction model. *Med Sci Sports Exerc*. (2015) 47:1755–64. doi: 10.1249/MSS.0000000000000588

19. Narciso PH, Werneck AO, Luiz-de-Marco R, Ventura Faustino-da-Silva YDS, Maillane-Vanegas S, Agostinete RR, et al. Influential role of lean soft tissue in the association between training volume and bone mineral density among male adolescent practitioners of impact-loading sports: ABCD Growth study. *BMC Pediatr*. (2020) 20:496. doi: 10.1186/s12887-020-02402-4

20. Foster C, Florhaug JA, Franklin J, Gottschall L, Hrovatin LA, Parker S, et al. A new approach to monitoring exercise training. *J Strength Cond Res*. (2001) 15:109–15.

21. Higgins J, Deeks J. Chapter 7: Selecting studies and collecting data. In: *Cochrane Handbook for Systematic Reviews of Interventions*. John Wiley & Sons, Chichester, UK (2008).

22. Hopkins WG, Marshall SW, Batterham AM, Hanin J. Progressive statistics for studies in sports medicine and exercise science. *Med Sci Sports Exerc*. (2009) 41:3–13. doi: 10.1249/MSS.0b013e31818cb278

23. Valeri L, VanderWeele TJ. Mediation analysis allowing for exposure–mediator interactions and causal interpretation: Theoretical assumptions and implementation with SAS and SPSS macros. *Psychol Methods*. (2013) 18:137–50. doi: 10.1037/a0031034

24. Gomez-Bruton A, Gonzalez-Aguero A, Matute-Llorente A, Gomez-Cabello A, Casajus JA, Vicente-Rodríguez G. Longitudinal effects of swimming on bone in adolescents: a pQCT and DXA study. *Biol Sport*. (2017) 34:361–70. doi: 10.5114/biolsport.2017.69824

25. Ferreira FA, Santos CC, Palmeira AL, Fernandes RJ, Costa MJ. Effects of swimming exercise on early adolescents' Physical conditioning and physical health: A systematic review. *J Funct Morphol Kinesiol*. (2024) 9:158. doi: 10.3390/jfmk9030158

26. Maillane-Vanegas S, Agostinete RR, Lynch KR, Ito IH, Luiz-de-Marco R, Rodrigues-Junior MA, et al. Bone mineral density and sports participation. *J Clin Densitometry*. (2020) 23:294–302. doi: 10.1016/j.jocd.2018.05.041

27. Freitas L, Bezerra A, Boppre G, Amorim T, Fernandes RJ, Fonseca H. Does swimming exercise impair bone health? A systematic review and meta-analysis comparing the evidence in humans and rodent models. *Sports Med*. (2024) 54:2373–94. doi: 10.1007/s40279-024-02052-x

28. Ubago-Guisado E, Vlachopoulos D, Fatouros IG, Deli CK, Leontsini D, Moreno LA, et al. Longitudinal determinants of 12-month changes on bone health in adolescent male athletes. *Arch Osteoporos*. (2018) 13:106. doi: 10.1007/s11657-018-0519-4

29. Vlachopoulos D, Ubago-Guisado E, Barker AR, Metcalf BS, Fatouros IG, Avloniti A, et al. Determinants of bone outcomes in adolescent athletes at baseline: the PRO-BONE study. *Med Sci Sports Exerc*. (2017) 49:1389–96. doi: 10.1249/MSS.0000000000001233

30. Gomez-Bruton A, Gonzalez-Aguero A, Matute-Llorente A, Lozano-Berges G, Gomez-Cabello A, Moreno LA, et al. The muscle-bone unit in adolescent swimmers. *Osteoporos Int*. (2019) 30:1079–88. doi: 10.1007/s00198-019-04857-3

31. Hawkins SA, Schroeder ET, Wiswell RA, Jaque SV, Marcell TJ, Costa K. Eccentric muscle action increases site-specific osteogenic response. *Med Sci Sports Exerc*. (1999) 31:1287–92. doi: 10.1097/00005768-199909000-00009

32. Meakin LB, Price JS, Lanyon LE. The contribution of experimental *in vivo* models to understanding the mechanisms of adaptation to mechanical loading in bone. *Front Endocrinol (Lausanne)*. (2014) 5:154. doi: 10.3389/fendo.2014.00154

33. Agostinete RR, Werneck AO, Narciso PH, Ubago-Guisado E, Coelho-e-Silva MJ, Bielemann RM, et al. Resistance training presents beneficial effects on bone development of adolescents engaged in swimming but not in impact sports: ABCD Growth Study. *BMC Pediatr*. (2024) 24:247. doi: 10.1186/s12887-024-04634-0

34. Smith JW, Jeukendrup A. Performance nutrition for young athletes. In: Bagchi D, Nair S, Sen CK, editors. *Nutrition and Enhanced Sports Performance*. London: Elsevier (2013). p. 523–9. doi: 10.1016/B978-0-12-396454-0.00055-2

35. Moghetti P, Bacchi E, Brangani C, Donà S, Negri C. Metabolic effects of exercise. *Front Horm Res*. (2016) 47:44–57. doi: 10.1159/000445156

36. Rojas Vega S, Knicker A, Hollmann W, Bloch W, Strüder HK. Effect of resistance exercise on serum levels of growth factors in humans. *Horm Metab Res*. (2010) 42:982–6. doi: 10.1055/s-0030-1267950

37. Morgado JM, Rama L, Silva I, de Jesus Inácio M, Henriques A, Laranjeira P, et al. Cytokine production by monocytes, neutrophils, and dendritic cells is hampered by long-term intensive training in elite swimmers. *Eur J Appl Physiol*. (2012) 112:471–82. doi: 10.1007/s00421-011-1966-4

frontiers | Frontiers in Endocrinology

TYPE Original Research
PUBLISHED 04 September 2025
DOI 10.3389/fendo.2025.1598344

OPEN ACCESS

EDITED BY
Fátima Baptista,
Universidade de Lisboa, Portugal

REVIEWED BY
Edyta Łuszczki,
University of Rzeszow, Poland
Md. Abdul Alim Al-Bari,
University of Rajshahi, Bangladesh

*CORRESPONDENCE
Marta C. Erlandson
marta.erlandson@usask.ca

RECEIVED 23 March 2025
ACCEPTED 11 August 2025
PUBLISHED 04 September 2025

CITATION
Erlandson MC, Chapelski MS, Adam MEK, Zaluski AJ and Baxter-Jones ADG (2025) Longitudinal effects of childhood recreational gymnastics participation on bone development: The Young Recreational Gymnast Study. *Front. Endocrinol.* 16:1598344. doi: 10.3389/fendo.2025.1598344

Longitudinal effects of childhood recreational gymnastics participation on bone development: The Young Recreational Gymnast Study

Marta C. Erlandson[1*], Matthew S. Chapelski[1], Margo E. K. Adam[2], Alexandra J. Zaluski[1] and Adam D. G. Baxter-Jones[1]

[1]College of Kinesiology, University of Saskatchewan, Saskatoon, SK, Canada, [2]Faculty of Kinesiology, Sport, and Recreation, University of Alberta, Edmonton, AB, Canada

Purpose: Previous research in the Young Recreational Gymnast Study (2006–2014) found bone benefits from involvement in recreational gymnastics during young childhood. The purpose of this study was to identify any longitudinal effects of recreational gymnastics exposure during childhood on adolescent bone health.

Methods: For the present analysis, longitudinal data were available from 118 participants (66 female participants; 33 gymnasts) of the original 178 who were recruited and assessed on between one and five measurement occasions (median 3) between 2008 and 2020. Peripheral quantitative computed tomography (pQCT) scans were completed at both the distal and shaft sites of their non-dominant radius and tibia. Multilevel random-effects models were constructed to assess differences in the development of bone content, density, and estimated bone strength between those exposed and not exposed to recreational gymnastics while controlling for biological age, sex, body weight, limb length, and physical activity.

Results: Individuals who were exposed to recreational gymnastics during childhood were found to have greater total area, total content, bone strength index, trabecular area, trabecular content, and trabecular density at the distal radius compared to physically active controls. There were no differences at the radial shaft, distal tibia, or tibial shaft.

Conclusion: Involvement in childhood recreational gymnastics may provide long-term benefits at the distal radius as individuals enter young adulthood.

KEYWORDS

recreational gymnastics, bone health, peripheral quantitative computed tomography, physical activity, childhood, adolescence

1 Introduction

Bone development during childhood is an essential part of growth and can impact a child's risk of osteoporosis and life-threatening fractures as they age (1). Factors that influence bone development include the environment, genetics, and physical activity participation (2, 3). While the greatest predictor of bone health is genetics (3), physical activity is a modifiable factor that may have the greatest positive influence on bone mineral accrual (4, 5). For example, being physically active during childhood was found to result in an increase in boys' and girls' total body bone mineral content (BMC) by 9% and 17%, respectively, 1 year after peak growth in BMC, when compared to inactive peers (6). Additionally, childhood and adolescence have been shown to be the ideal time to optimize bone mineral accrual and increase peak bone mass.

Approximately 40% of an individual's bone mass is acquired during a 5-year period in adolescence (7). More precisely, 22% of total body BMC is accrued 3 years surrounding a child's peak height velocity (7). Furthermore, researchers have found a strong relationship between maturity and bone architecture, bone mineral density (BMD), and strength in both male and female adolescents (8). These findings suggest that physical activity may have the greatest impact on bone mineral accrual during the time around a child's peak height velocity. While adolescence appears to be the premier time to accrue bone, studies have shown that childhood involvement in physical activity may have long-term bone health benefits. Gunter and colleagues completed a 7-month jumping intervention in children 9 years of age and found that 3 years after study completion, the intervention group had significantly higher BMC at the hip, lumbar spine, and total body when compared to controls (9). At follow-up 8 years later, it was found that the hip BMC remained significantly greater during adolescence (10). In alignment with Gunter and colleagues, we evaluated the influence of repeated impacts on children's bone health using a recreational gymnastics model.

In terms of long-term bone health, participation in elite gymnastics has been shown to provide gymnasts with greater bone strength years after cessation of gymnastics participation (11, 12). However, elite gymnastics is not attainable for every child; thus, participation in recreational gymnastics has been studied and has also been found to improve bone health in young children (13–16). Elite gymnasts have been found to experience peak magnitudes of 3.6–10.4 times their body weight on their upper and lower limbs during standard training (17), while ground reaction forces from recreational gymnastics skills have been reported to vary from 1/3 to 6 times their body weight (18). Initially, in a study of recreational gymnasts [the Young Recreational Gymnast Study (YRGS)] between 4 and 6 years of age, we found that exposure to recreational gymnastics increased their total body BMC by 3% and their femoral neck BMC by 7% when compared to physically active controls using dual-energy X-ray absorptiometry (19). Additionally, in different cohorts, recreational gymnastics was shown to improve lumbar spine and forearm areal BMD (20) and distal radius BMC (16). Furthermore, using peripheral quantitative computed tomography (pQCT), the YRGS cohort had significantly greater total bone content (ToC), total bone density (ToD), total cross-sectional bone area (ToA), and estimated bone strength index (BSIc) during young childhood at the distal radius when compared to physically active controls (21, 22). Lastly, Dowthwaite et al. found that ex-gymnasts involved in premenarchal competitive gymnastics training for a minimum of 5 hours/week had radius bone size and strength that were at least 20% greater when compared to those of controls at both the distal and mid-shaft of the radius post-menarche (23). This suggests that involvement in gymnastics in the pre-pubertal years may have long-term bone health benefits.

Previous studies in the YRGS cohort have shown that childhood involvement in recreational gymnastics provides positive bone benefits at the distal radius in the short term. However, it is unknown if these benefits are still present in adolescence when bone accrual accelerates. Therefore, the purpose of the present study was to assess whether baseline bone health benefits observed in childhood recreational gymnasts are still retained after the children enter adolescence. We hypothesized that the difference observed in the recreational gymnasts would be maintained at the distal radius.

2 Methods

2.1 Participants

Participants were drawn from the YRGS conducted at the University of Saskatchewan between 2006 and 2020. The details of the YRGS have been previously published (19, 22). In brief, 178 participants (4 to 6 years of age) were recruited between 2006 and 2009 into a mixed longitudinal study examining the influence of early-life exposure to recreational gymnastics participation on body composition development. pQCT was acquired at the University of Saskatchewan and added to the study protocol in 2008. In 2008–2009, baseline pQCT measurements were obtained for 127 participants (68 female and 59 male participants), with 69 exposed to recreational gymnastics (35 female and 34 male participants) (71%) of the original sample (21). Thus, the data for this analysis span the 2008–2020 data collection periods. Recreational gymnasts had to participate in recreational gymnastics for at least 45 minutes/week for at least 4 months and were recruited from the recreational and precompetitive gymnastics programs at four gymnastics clubs in Saskatoon, Saskatchewan. The controls were recruited from other recreational sport programs at the University of Saskatchewan, such as swimming, soccer, and "sports 'r' fun" summer sport camps. Controls had no exposure to recreational gymnastics but did have exposure to other weight-bearing sports such as ice hockey, basketball, soccer, and volleyball. Thus, participants were divided into two groups: recreational gymnasts and controls. For the present analysis, participants were measured over a maximum of five visits between

2008 and 2020, for a total of 428 measurements. Participants were removed from the present analysis if they did not have full data at a measurement occasion, as well as if they had any condition that inhibited them from performing physical activity safely or any health condition that is known to affect bone development (i.e., heart disease or musculoskeletal disease). A total of 118 participants (66 female participants; 33 gymnasts) (93% of participants with a baseline pQCT scan) fulfilled these criteria and were measured between one and five occasions (median of three visits) for a total of 282 measurements. Informed consent was obtained from their parents or guardians, and verbal assent was obtained from children before study initiation. This study was approved by the University of Saskatchewan's Biomedical Research Ethics Board.

2.2 Anthropometry

Anthropometric measurements included height, body weight and limb length. Demographics such as age and sex were also collected. Height and sitting height were measured using a wall-mounted stadiometer to the nearest 0.5 cm (Holtain Ltd., Crosswell, UK). Body weight was measured using a calibrated digital scale to the nearest 0.5 kg (Model 1631, Tanita Corp., Tokyo, Japan). Left tibia length was measured from the base of the medial malleolus to the superior margin of the medial epicondyle and left ulna length was measured from the distal tip of the styloid process to the proximal endplate using an anthropometric caliper (Rosscraft Lufkin, Canada). All measurements were taken twice, and if the difference was >0.4 (cm or kg), a third measurement was performed (24). Then, the mean or median was reported depending on whether two or three measurements were taken (24).

2.3 Biological age

A biological age, indicating years from peak height velocity (PHV), was estimated. Many equations can be used to predict when a child will or if they have attained their PHV. The most commonly cited equation is the Mirwald et al. equation (25). This tool is non-invasive and can be applied to both male and female individuals. The calculation only requires the participant's sex, age, height, sitting height, and body weight to calculate years from PHV. A negative number indicates how many years away the child is from reaching their PHV. A positive number shows how many years past their PHV the child is. Finally, this equation is more accurate the closer the child is to attaining their PHV (25).

The equations are as follows:

Male Years from PHV

$$= -9.236 + (0.0002708*\text{Leg Length}*\text{Sitting Height}) + (-0.001663*\text{Age}*\text{Leg Length}) + (0.007216*\text{Age}*\text{Sitting Height}) + (0.02292*\text{Weight by Height Ratio}),$$

Female Years from PHV

$$= -9.376 + (0.0001882*\text{Leg Length}*\text{Sitting Height}) + (0.0022*\text{Age}*\text{Leg Length}) + (0.005841*\text{Age}*\text{Sitting Height}) - (0.002658*\text{Age}*\text{Weight}) + (0.07693*\text{Weight by Height Ratio}).$$

For each individual, an age from PHV was estimated at each measurement occasion, and the estimate closest to age at PHV was then used to represent a participant's age at PHV across the study duration.

2.4 Peripheral quantitative computed tomography

pQCT was used to assess cross-sections of bone health for the non-dominant radius and tibia. If the participants had ever had a fracture in the non-dominant limb, then the dominant limb was scanned (XCT, Stratec Medizintechnik GmbH, Pforzheim, Germany). Two trained technicians performed scans with a voxel size of 0.4 mm and a scan speed of 20 mm/s for every site. For all sites, a scout view scan was first performed to visualize the distal growth plate and identify the medial point of the distal endplate, which is where the reference line was placed. Radius scans were conducted at the distal and shaft sites at 4% and 65% of the limb length, respectively, while tibia scans were conducted at the distal and shaft of the tibia at 4% and 66% of the limb length, respectively. Scans were analyzed using the Stratec software, Version 6.0, and standard variables at each site were reported according to manufacturer recommendations. At the distal sites (4% sites), bone was separated from the surrounding tissues using contour mode 1 with a threshold of 280 mg/cm^3. This process allowed us to assess ToC (mg), ToD (mg/cm^3), and ToA (mm^2), as well as trabecular bone area (TrA; mm^2), trabecular bone content (TrC; mg), and trabecular bone density (TrD; mg/cm^3) at the distal radius and tibia. Additionally, BSIc (mg/mm^4) was calculated (ToA × ToD^2) to estimate the bone's resistance to compression (26). At the shaft sites (65% radius and 66% tibia), separation mode 4 with an outer threshold of 280 mg/cm^3 and an inner threshold of 540 mg/cm^3 was used to separate bone and determine cortical bone content (CoC; mg/mm), cortical bone density (CoD; mg/cm^3), cortical bone cross-sectional area (CoA; mm^2), cortical thickness (CoTHK; mm), and polar stress strain index (SSIp; mm^3), which is an estimate of bone's resistance to torsion. Short-term precision (CV% root mean square) for repeated bone measurements has been reported previously from our group and ranged from 1.8% to 6.3% at the radius and tibia (27).

2.5 Physical activity

The Netherlands Physical Activity Questionnaire (NPAQ) asks parents to report their child's current physical activity levels. It has

questions about activity preferences and everyday activity choices rather than recalling physical activity levels. Questionnaire scores range from 7 (low physical activity levels) to 35 (high physical activity levels). The NPAQ has been documented to be a reliable and valid method to assess a child's physical activity levels for children 4 to 7 years of age (28).

Additionally, the Physical Activity Questionnaire for Children (PAQ-C; 8 to 14 years of age) and for Adolescents (PAQ-A; 14 to 18 years of age) were used once participants were older. The PAQ-C and PAQ-A are nine- and eight-item questionnaires that ask children about how much physical activity they engaged in the previous 7 days (29). The only difference between the two questionnaires is that the PAQ-C asks about how active the child was at recess, while the PAQ-A does not ask about recess. Both give scores ranging from 1 to 5. A score of 1 means a child participated in a low amount of physical activity the previous week, while a score of 5 means a child participated in a high amount of physical activity the week prior. Both these tools have been found to be reliable and valid (30–32). We employed these different questionnaires due to the age-appropriate validation of the tools.

2.6 Statistical analysis

Descriptive statistics were analyzed by an independent t-test using SPSS (Version 29). For the longitudinal analyses, multilevel (hierarchical) random-effects models were constructed using a multilevel modeling approach (MlwiN Version 3.13, Centre for Multilevel Modelling, University of Bristol, UK) (33). A detailed description of the multilevel modeling procedures is presented elsewhere (34). In brief, bone parameters (ToA, ToC, ToD, TrA, TrC, TrD, BSIc, CoA, CoC, CoD, CoTHK, and SSIp) were measured repeatedly in individuals (level 1 of the hierarchy) and between individuals (level 2 of the hierarchy). Analysis models that contain variables measured at different levels of a hierarchy are known as multilevel regression models. Additive random-effects multilevel regression models were adopted to describe the developmental changes in bone parameters with biological age and are described in detail previously (22). Furthermore, since physical activity was measured using tools with different scales, a physical activity z-score was calculated and used in the model using the equation z-score = $(x - \mu)/\sigma$, where x is the individual score, μ is the mean, and σ is the standard deviation.

Models were built in a stepwise procedure; i.e., predictor variables were added one at a time, and the log-likelihood ratio statistics were used to judge the fit of the model. Biological age was added as both a random variable (level 1) and a fixed variable. This permits individuals to have independent intercepts and slopes and a calculation of the intercept–slope covariance relationship. A significant biological age coefficient at level 1 of the models indicates that a bone measurement is increasing significantly at each measurement occasion within individuals. Significant coefficients at the individual variance matrix (level 2) in each model indicate that individuals have significantly different growth curves for bone measurements, in terms of both their intercepts and the slopes, and that there is a relationship between intercepts and slopes in the model. Fixed predictor variables were accepted as significant if the estimated mean coefficient was greater than twice the standard error of the estimate (SEE; i.e., $p < 0.05$). If the retention criteria were not met, the predictor variable was discarded. The power functions of biological age^2 were introduced into the linear models to allow for the non-linearity of growth and were retained whether or not it was significant so as to shape the developmental curves. The predictor variable coefficients were used to predict bone development for ToA, ToC, ToD, TrA, TrC, TrD, BSIc, CoA, CoC, CoD, and SSIp with biological age, body weight, limb length, physical activity, sex, and group (gymnastics exposure versus no exposure) controlled in the prediction equations. A total of 11 independent multilevel (hierarchical) random-effects models were constructed for each bone parameter (ToA, ToC, ToD, TrA, TrC, TrD, BSIc, CoA, CoC, CoD, and SSIp).

3 Results

3.1 Participant characteristics

The anthropometric characteristics of children exposed and not exposed to recreational gymnastics from 5 to 19 years of age are displayed in Table 1. At 15 years of age, children not exposed to recreational gymnastics participated in more physical activity than children exposed to recreational gymnastics ($p = 0.01$). There were no other differences within any other age category ($p > 0.05$). The average recreational gymnastics participation was 45 minutes/week (median, 1.5 hours/week), while the years of exposure on average was 3 years (median, 2 years).

3.2 Distal radius (4% site)

Table 2 displays the results from the multilevel model for the distal radius bone measurements of ToA, ToC, ToD, BSIc, TrA, TrC, and TrD. Specifically, exposure to recreational gymnastics was a significant contributor to greater ToA, ToC, BSIc, TrA, TrC, and TrD. No differences were found for ToD for children exposed to recreational gymnastics. Biological age^2, sex, body weight, radius length, and physical activity contributed to the prediction of ToA, while biological age, biological age^2, sex, body weight, radius length, and physical activity contributed to the prediction of ToC and TrC. Furthermore, the constant, biological age, biological age^2, and body weight contributed to ToD. BSIc was contributed to by the constant, sex, and body weight, while TrA was predicted by biological age^2, sex, body weight, radius length, and physical activity. Finally, the constant, biological age, and body weight predicted TrD.

3.3 Radial shaft (64% site)

Table 3 summarizes the multilevel model output for the radial shaft; exposure to recreational gymnastics was not significant for any bone measurement at the radial shaft. We found that biological

10.3389/fendo.2025.1598344

TABLE 1 Descriptive characteristics for children not exposed and exposed to recreational gymnastics.

Age	5	6	7	8	9	10	11	12
Not exposed								
N	10	12	23	33	28	13	19	4
Sex (male/%)	6 (60%)	6 (50%)	11 (48%)	15 (45%)	11 (39%)	4 (31%)	13 (68%)	0 (0%)
Height (cm)	111.89 ± 6.99	117.75 ± 5.62	124.26 ± 5.66	129.49 ± 5.88	133.11 ± 6.79	137.07 ± 8.58	144.42 ± 6.47	146.93 ± 10.35
Weight (kg)	20.83 ± 3.65	21.74 ± 2.55	26.71 ± 4.82	28.71 ± 6.54	30.09 ± 4.76	33.78 ± 9.18	38.17 ± 6.29	42.63 ± 7.93
BMI (kg/m^2)	16.53 ± 1.08	15.67 ± 1.35	17.19 ± 2.04	16.95 ± 2.62	16.91 ± 1.71	17.75 ± 3.04	18.20 ± 1.97	19.61 ± 2.04
Bio Age (years)	−5.83 ± 0.71	−5.12 ± 0.66	−4.469 ± 0.88	−3.74 ± 0.74	−3.22 ± 0.76	−2.71 ± 1.06	−2.13 ± 0.92	0.23 ± 1.48
PA score	25.10 ± 2.81	23.75 ± 3.91	26.35 ± 2.93	25.30 ± 3.99	25.14 ± 3.96	26.85 ± 3.51	22.19 ± 8.967	21.03 ± 11.46
Exposed								
N	2	5	10	9	11	7	1	1
Sex (male/%)	0 (0%)	2 (40%)	3 (30%)	2 (22%)	3 (27%)	3 (43%)	0 (0%)	0 (0%)
Height (cm)	108.80 ± 6.79	118.18 ± 4.96	121.84 ± 6.96	127.43 ± 7.99	131.65 ± 7.12	139.62 ± 5.79	138.10	145.90
Weight (kg)	18.20 ± 2.26	23.64 ± 2.16	24.74 ± 4.79	26.16 ± 3.77	27.97 ± 3.31	33.67 ± 6.99	31.50	31.50
BMI (kg/m^2)	15.35 ± 0.01	16.93 ± 1.28	16.53 ± 1.87	16.05 ± 1.17	16.10 ± 0.89	17.16 ± 2.79	16.52	14.78
Bio Age (years)	−5.45 ± 0.42	−5.02 ± 0.79	−4.35 ± 0.57	−3.66 ± 0.34	−3.25 ± 0.63	−2.94 ± 0.99	−1.84	−1.15
PA score	27.50 ± 0.71	24.80 ± 1.64	25.20 ± 2.09	26.11 ± 3.92	26.09 ± 2.95	25.71 ± 2.36	25.00	34.00
Age	**13**	**14**	**15**	**16**	**17**	**18**	**19**	
Not exposed								
N	9	20	15	10	10	6	8	
Sex (male/%)	3 (33%)	10 (50%)	6 (40%)	2 (20%)	3 (30%)	3 (50%)	5 (63%)	
Height (cm)	160.77 ± 10.68	163.96 ± 8.66	166.86 ± 8.35	167.30 ± 10.69	169.70 ± 8.74	173.08 ± 10.23	175.48 ± 7.01	
Weight (kg)	54.99 ± 16.0	53.09 ± 10.17	59.73 ± 11.71	61.60 ± 8.312	61.75 ± 8.089	69.62 ± 9.29	77.41 ± 14.70	
BMI (kg/m^2)	20.94 ± 4.05	19.59 ± 2.55	21.32 ± 3.19	22.09 ± 3.24	21.47 ± 2.64	23.19 ± 1.77	25.01 ± 3.46	
Bio Age (years)	0.61 ± 1.23	0.80 ± 1.06	1.88 ± 0.99	2.89 ± 0.52	3.49 ± 0.67	3.72 ± 0.45	4.63 ± 1.04	
PA score	2.99 ± 0.33	2.76 ± 0.59	**2.86* ± 0.62**	2.57 ± 0.71	2.22 ± 0.87	2.79 ± 0.86	1.75 ± 0.73	
Exposed								
N	3	3	3	2	1	2	2	
Sex (male/%)	1 (33%)	2 (66%)	0 (0%)	2 (100%)	1 (100%)	0 (0%)	0 (0%)	
Height (cm)	166.13 ± 4.37	170.13 ± 11.76	162.40 ± 2.29	167.90 ± 15.27	187.85	168.63 ± 2.09	170.43 ± 3.36	
Weight (kg)	53.23 ± 7.51	57.90 ± 4.61	57.77 ± 5.42	58.90 ± 17.39	68.90	61.35 ± 1.77	57.20 ± 4.81	
BMI (kg/m^2)	19.41 ± 3.81	20.07 ± 1.68	21.89 ± 1.85	20.59 ± 2.41	19.53	21.57 ± 0.09	19.74 ± 2.43	
Bio Age (years)	0.89 ± 0.867	1.17 ± 1.24	2.389 ± 0.13	1.44 ± 1.28	3.53	4.10 ± 0.23	5.189 ± 0.49	
PA score	2.87 ± 0.55	2.82 ± 0.32	1.74 ± 0.48	2.86 ± 1.29	1.00	1.87 ± 0.04	2.53 ± 0.70	

*indicates a difference between children not exposed to and exposed to recreational gymnastics within a given age category (bolded).
BMI, body mass index; Bio Age, biological age; PA, physical activity.

age^2, body weight, and radius length predicted ToA. The constant, biological age, and body weight were significant contributors to ToC and CoC. The constant, biological age, biological age^2, body weight, and radius length were significant contributors to CoD, while the constant, body weight, and radius length predicted CoA. CoTHK was predicted by the constant, biological age, body weight, and radius length. Finally, SSIp was contributed to by biological age, biological age^2, body weight, radius length, and physical activity.

TABLE 2 Multilevel regression models for total cross-sectional bone area (ToA), total bone content (ToC), total bone density (ToD), bone strength index (BSIc), trabecular area (TrA), trabecular content (TrC), and trabecular bone density (TrD) at the 4% distal radius site.

Distal radius (4%)							
Variable	ToA (mm^2)	ToC (mg)	ToD (mg/cm^3)	BSIc (mg/mm^4)	TrA (mm^2)	TrC (mg)	TrD (mg/cm^3)
Fixed effects							
Constant	NS	NS	289.05 ± 28.11	14.82 ± 6.59	NS	NS	242.44 ± 33.11
Biological age	NS	−5.52 ± 0.79	0.94 ± 1.16	NS	NS	−2.52 ± 0.79	−6.71 ± 1.61
Biological age^2	−0.34 ± 0.17	−0.23 ± 0.06	0.30 ± 0.11	NS	−0.64 ± 0.19	−0.23 ± 0.07	NS
Sex	−21.40 ± 6.67	−4.68 ± 2.49	NS	−2.57 ± 1.17	−16.51 ± 7.31	−4.68 ± 2.49	NS
Weight	2.14 ± 0.47	0.84 ± 0.17	1.14 ± 0.34	0.44 ± .81	1.91 ± 0.51	0.84 ± 0.17	1.18 ± 0.34
Radius length	0.73 ± 0.19	0.17 ± 0.07	NS	NS	0.81 ± 0.21	0.17 ± 0.07	NS
PA	7.13 ± 52.59	2.05 ± 0.96	NS	NS	7.80 ± 2.80	2.05 ± 0.96	NS
Gymnastic exposure	20.38 ± 7.39	9.44 ± 2.74	NS	4.51 ± 1.18	17.77 ± 7.81	9.44 ± 2.74	19.29 ± 6.52
Random effects							
Level 1							
Constant	1,022.14 ± 135.94	163.62 ± 21.11	285.55 ± 40.04	27.24 ± 3.59	1,239.69 ± 163.55	163.62 ± 21.11	762.94 ± 83.26
Level 2							
Constant	1,112.56 ± 251.88	111.61 ± 29.96	1,482.74 ± 233.84	45.18 ± 8.89	1,447.24 ± 320.52	111.61 ± 29.96	468.63 ± 111.43
Biological age	28.23 ± 9.42	2.63 ± 1.15	13.20 ± 3.84	0.81 ± 0.25	38.40 ± 11.96	2.63 ± 1.15	NS
Constant * Biological age	146.64 ± 40.49	14.95 ± 4.75	88.04 ± 24.63	5.62 ± 1.32	213.14 ± 53.18	14.95 ± 7.75	NS

All numerical values are reported as significant, $p < 0.05$ (mean > 2 * SEE). NS, not significant.
Fixed-effects values are estimated mean coefficients ± standard error estimate (SEE) of total cross-sectional bone area (ToA; mm^2), total bone content (ToC; mg/mm), total bone density (ToD; mg/cm^3), bone strength index (BSIc), trabecular bone area (TrA; mm^2), trabecular bone content (TrC; mg/mm), and trabecular bone density (TrD; mg/cm^3) at the distal radius (4% site). Random-effects values are estimated mean variance ± SEE. Biological age [at peak height velocity (PHV) = 0], radius length (cm), physical activity score (z-score), sex (male = 0, female = 1), and gymnastic exposure (0 = no exposure, 1 = exposed to gymnastics).

3.4 Distal tibia (4% site)

Table 4 shows the multilevel model for outputs for the distal tibia. Once again, exposure to recreational gymnastics was not significant for any bone measurement at the distal tibia. ToA was predicted by biological age^2, sex, body weight, and tibia length, while ToC was predicted by the constant, biological age, biological age^2, sex, body weight, tibia length, and physical activity. The constant, body weight, and tibia length were significant predictors of ToD. BSIc was contributed to by the constant, biological age, sex, body weight, tibia length, and physical activity. Sex, body weight, tibia length, and physical activity were predictors of ToA, while TrC was contributed to by biological age^2, sex, body weight, and tibia length. Finally, TrD was predicted by the constant, body weight, and tibia length.

3.5 Tibial shaft (65% site)

Table 5 displays the outputs from the multilevel model for the tibial shaft. Like the radial shaft and distal tibia, exposure to recreational gymnastics was not a contributor to any bone measurements. ToA was predicted by the constant, biological age, biological age^2, sex, body weight, and tibia length, while ToC was significantly contributed to by the constant, biological age, biological age^2, body weight, tibia length, and physical activity. The constant, biological age, body weight, and tibia length contributed to CoC. CoD was predicted by the constant, biological age, biological age^2, and tibia length, while CoA was contributed to by biological age^2, body weight, and tibia length. Finally, the constant, biological age^2, and body weight predicted CoTHK, while the constant, biological age, body weight, tibia length, and physical activity contributed to SSIp.

4 Discussion

The purpose of our study was to evaluate whether individuals who participated in recreational gymnastics during childhood had any bone health benefits in adolescence when measured by pQCT. We found that recreational gymnasts had significantly higher ToA, ToC, BSIc, TrA, TrC, and TrD at the distal radius but no difference at the radial shaft or tibia when compared to physically active controls. This is important, as it demonstrates that distal radius

10.3389/fendo.2025.1598344

TABLE 3 Multilevel regression models for cortical cross-sectional total bone area (ToA), total bone content (ToC), cortical bone content (CoC), cortical bone density (CoD), cortical bone area (CoA), cortical thickness (CoTHK), and polar stress strain index (SSIp) at the 65% radial shaft.

Radial shaft (65%)							
Variable	ToA (mm^2)	ToC (mg)	CoC (mg/mm)	CoD (mg/cm^3)	CoA (mm^2)	CoTHK (mm)	SSIp (mm^3)
Fixed effects							
Constant	NS	40.31 ± 6.97	43.00 ± 6.72	1,101.1 ± 53.29	30.52 ± 8.82	3.04 ± 0.28	NS
Biological age	NS	1.73 ± 0.39	1.89 ± 0.38	20.91 ± 2.68	NS	0.05 ± 0.02	6.29 ± 1.57
Biological age^2	0.12 ± 0.05	NS	NS	−1.18 ± 0.22	NS	NS	0.37 ± 0.11
Sex	NS	NS	NS	NS	NS	NS	NS
Weight	0.31 ± 0.15	0.69 ± 0.08	0.70 ± .08	1.23 ± 0.53	0.52 ± 0.09	0.02 ± 0.001	1.58 ± 0.33
Radius length	0.47 ± 0.06	NS	NS	−0.95 ± 0.25	0.13 ± 0.04	−0.004 ± 0.001	0.67 ± 0.11
PA	NS	NS	NS	NS	NS	NS	2.89 ± 1.68
Gymnastic exposure	NS	NS	NS	NS	NS	NS	NS
Random effects							
Level 1							
Constant	85.77 ± 11.51	23.86 ± 3.21	21.66 ± 2.94	1,727.71 ± 227.96	44.45 ± 5.80	0.04 ± .001	287.97 ± 40.02
Level 2							
Constant	191.46 ± 33.65	64.49 ± 11.13	64.45 ± 11.03	808.55 ± 259.18	60.39 ± 12.04	0.06 ± 0.01	1,361.08 ± 220.99
Biological age	NS	0.56 ± 0.21	0.70 ± 0.22	32.64 ± 13.1	NS	0.02 ± 0.01	21.01 ± 4.98
Constant * Biological age	NS	4.86 ± 1.29	5.53 ± 1.35	NS	NS	0.01 ± 0.00	146.32 ± 29.68

All numerical values are reported as significant, $p < 0.05$ (mean > 2 * SEE). NS, not significant.
Fixed-effects values are estimated mean coefficients ± standard error estimate (SEE) of total cross-sectional bone area (ToA; mm^2), total bone content (ToC; mg/mm), cortical bone content (CoC; mg/mm), cortical bone density (CoD; mg/cm^3), cortical bone area (CoA; mm^2), cortical thickness (CoTHK), and polar stress strain index (SSIp) at the radial shaft (65% site). Random-effects values are estimated mean variance ± SEE. Biological age [at peak height velocity (PHV) = 0], radius length (cm), physical activity score (z-score), sex (male = 0, female = 1), and gymnastic exposure (0 = no exposure, 1 = exposed to gymnastics).

bone health can be improved in the long term by involvement in recreational gymnastics during young childhood, even when compared to children involved in other weight-bearing activities and sports. Previous research demonstrated that participation in elite gymnastics provides long-term bone benefits in female individuals (35–37); however, as previously mentioned, elite gymnastics participation is not attainable on a population level. To the authors' knowledge, this is the first study to show long-term bone benefits from involvement in childhood recreational gymnastics in both male and female individuals.

The results from this study are aligned with those of previous research in the YRGS cohort, which found that children involved in recreational gymnastics during young childhood had significantly higher ToC, ToD, and BSIc in a baseline cross-sectional analysis (21) and higher ToA and ToC longitudinal during childhood (22) at the distal radius compared to controls; both studies also found no changes at the radial shaft or the tibia. Research from other cohorts of gymnasts has also found involvement in gymnastics to have positive effects on bone health. In contrast to our findings, other researchers have found differences at the shaft site in both the radius and tibia. A study analyzing bone health in non-elite female gymnasts aged 6 to 12 years found that they had higher ToA and SSI than controls but lower ToD at the ulnar shaft (38). Ward and colleagues (39) compared gymnasts and controls aged 5 to 14 years and found that gymnasts had greater CoA and SSIp at the 50% radius length as well as greater CoA, CoTHK, and SSIp at the 65% tibia site. Another study assessing pre-menopausal retired elite artistic gymnasts found that they had higher BMC, ToA, and BSIc at the distal radius and higher BMC, ToA, CoA, CoD, and SSIp at the radial shaft (40). Part of this could be due to muscle mass, as muscle area was significantly associated with improvements in cortical BMC, area, and SSIp (41). Another explanation may be that the control group in the current study was an active group involved in other sports, which loads the lower limb and potentially also the upper limb in some sports such as basketball and volleyball. Additionally, there may be a dose response to long-term bone benefits. Burt et al. found that female individuals engaging in more than 5 hours/week of non-elite gymnastics have greater bone health than female individuals engaged in under 5 hours/week of non-elite gymnastics (38). Additionally, another study found that years of training was positively correlated with cortical BMC, area, and thickness (41). To be included in the current study, individuals only had to be participating in recreational gymnastics for 45 minutes/week, and

TABLE 4 Multilevel regression models for total cross-sectional bone area (ToA), total bone content (ToC), total bone density (ToD), bone strength index (BSIc), trabecular area (TrA), trabecular content (TrC), and trabecular bone density (TrD) at the 4% distal tibia site.

Distal tibia (4%)							
Variable	ToA (mm^2)	ToC (mg)	ToD (mg/cm^3)	BSIc (mg/mm^4)	TrA (mm^2)	TrC (mg)	TrD (mg/cm^3)
Fixed effects							
Constant	NS	107.45 ± 30.53	355.05 ± 29.83	45.03 ± 139.66	NS	NS	310.09 ± 26.68
Biological age	NS	4.02 ± 1.60	NS	1.56 ± 7.51	NS	NS	NS
Biological age^2	−1.71 ± 0.39	−0.49 ± 0.13	NS	NS	−1.74 ± 0.45	−0.55 ± 0.15	NS
Sex	−66.99 ± 16.91	−25.81 ± 6.73	NS	−7.75 ± 0.62	−51.29 ± 17.85	−16.18 ± 6.61	NS
Weight	4.79 ± 1.09	2.44 ± 0.36	1.46 ± 0.34	1.15 ± 1.71	3.90 ± 1.25	1.65 ± 0.42	0.75 ± 0.28
Tibia length	1.88 ± 0.25	0.21 ± 0.09	−0.35 ± 0.09	NS	2.13 ± 0.28	0.46 ± 0.10	−0.19 ± 0.08
PA	NS	4.97 ± 1.75	NS	2.14 ± 0.82	NS	NS	NS
Gymnastic exposure	NS	NS	NS	NS	NS	NS	NS
Random effects							
Level 1							
Constant	3,242.81 ± 440.75	295.98 ± 41.43	261.12 ± 36.87	66.6 ± 9.34	4,833.78 ± 641.44	573.49 ± 75.99	256.02 ± 34.93
Level 2							
Constant	14,865.6 ± 2,380.1	111.61 ± 29.96	1,493.01 ± 235.89	368.15 ± 58.13	17,299.64 ± 2,868.40	1,840.22 ± 306.24	721.08 ± 121.16
Biological age	174.82 ± 44.64	1,858.5 ± 286.7	13.06 ± 3.71	4.46 ± 1.10	219.32 ± 58.09	15.64 ± 5.26	NS
Constant * Biological age	1,503.26 ± 296.02	145.6 ± 31.43	89.98 ± 24.29	33.62 ± 7.05	1,895.37 ± 373.26	162.50 ± 35.53	NS

All numerical values are reported as significant, $p < 0.05$ (mean > 2 * SEE). NS, not significant.
Fixed-effects values are estimated mean coefficients ± standard error estimate (SEE) of total cross-sectional bone area (ToA; mm^2), total bone content (ToC; mg/mm), total bone density (ToD; mg/cm^3), bone strength index (BSIc), trabecular bone area (TrA; mm^2), trabecular bone content (TrC; mg/mm), and trabecular bone density (TrD; mg/cm^3) at the distal tibia (4% site). Random-effects values are estimated mean variance ± SEE. Biological age [at peak height velocity (PHV) = 0], tibia length (cm), physical activity score (z-score), sex (male = 0, female = 1), and gymnastic exposure (0 = no exposure, 1 = exposed to gymnastics).

the median exposure throughout the study duration to gymnastics was 1.5 hours/week, which may not have been a high-enough dose of ground reaction force to elicit greater bone health benefits, as seen in other studies (38, 39).

The reason that the bone health differences may only have been maintained at the distal radius is that gymnastics is one of the few sports to put high-impact strains/loads on the forearm, while most other sports put strain/load on the lower body. In fact, gymnasts experience more ground reaction forces compared to other recreational athletes (42). The lack of a difference in any of the bone variables at the radial shaft is surprising given the aforementioned load that recreational gymnastics puts on the forearm; however, no differences in the shaft were observed in the earlier investigations of this cohort either (21, 22). This could be because the variables assessed at the distal radius and radial shaft were different, or the distal radius is more susceptible to changes from loading. Finally, since our controls were physically active and engaged in a similar amount of physical activity (as assessed by the NPAQ and PAQ-C/A), it can be assumed that our controls and recreational gymnasts are continuing to accrue bone with mechanical stimulus, which may also explain why no differences existed at the radial shaft and tibia bone sites. Additionally, increases in BMC at the distal site are thought to be due to axial compression, while those in the shaft sites are more responsive to bending forces from muscle activity (43). Therefore, recreational gymnastics skills may put more axial compression on distal sites and not enough bending force to elicit change at shaft sites. Finally, elite male gymnasts have peak load magnitudes of 4 and 10 times their body weight for their upper and lower bodies, respectively (17). However, it is unlikely that recreational gymnastics reaches the same peak loads, in turn reducing some of the impact that it may have on long-term bone development (17). Additionally, body weight may not be the only factor influencing impact forces, as other factors such as landing technique have been reported to influence ground reaction forces experienced (18). Despite this, the ground reaction forces experienced during recreational gymnastics participation were maintained into adolescence, highlighting the potential of this type of activity on long-term bone health at the wrist.

Our physical activity assessment shows that the current cohort was continuing their engagement in physical activity. When comparing our physical activity scores to those of the Saskatchewan Pediatric Bone Mineral Accrual Study, our participants would be average in their activity levels (44). Baxter-

10.3389/fendo.2025.1598344

TABLE 5 Multilevel regression models for cortical cross-sectional total bone area (ToA), total bone content (ToC), cortical bone content (CoC), cortical bone density (CoD), cortical bone area (CoA), cortical thickness (CoTHK), and polar stress strain index (SSIp) at the 65% tibial shaft.

Tibial shaft (65%)							
Variable	ToA (mm^2)	ToC (mg)	CoC (mg/mm)	CoD (mg/cm^3)	CoA (mm^2)	CoTHK (mm)	SSIp (mm^3)
Fixed effects							
Constant	−163.88 ± 54.57	118.78 ± 32.09	48.71 ± 18.37	1,133.49 ± 43.29	NS	2.91 ± 0.36	−377.67 ± 165.57
Biological age	−18.91 ± 2.94	28.74 ± 2.12	5.29 ± 1.03	19.85 ± 1.84	NS	NS	43.48 ± 9.65
Biological age^2	−2.43 ± 0.28	2.76 ± 0.19	NS	−0.67 ± 0.19	−0.22 ± 0.09	−0.01 ± 0.002	NS
Sex	−15.25 ± 9.46	NS	NS	NS	NS	NS	NS
Weight	3.69 ± 0.67	1.80 ± 0.43	3.39 ± 0.23	NS	2.99 ± 0.24	0.04 ± 0.004	22.54 ± 2.17
Tibia length	1.37 ± 0.17	0.29 ± 0.09	0.18 ± 0.05	−0.57 ± 0.13	0.36 ± 0.06	NS	2.98 ± 0.49
PA	NS	6.39 ± 2.25	NS	NS	NS	NS	21.41 ± 10.39
Gymnastic exposure	NS	NS	NS	NS	NS	NS	NS
Random effects							
Level 1							
Constant	1,792.71 ± 242.93	794.58 ± 106.58	134.21 ± 18.69	1,205.36 ± 150.95	155.13 ± 21.71	0.05 ± 0.01	11,967.43 ± 1,664.16
Level 2							
Constant	2,448.03 ± 516.54	2,988.88 ± 517.10	630.89 ± 102.58	599.82 ± 168.22	523.18 ± 90.26	0.19 ± 0.03	57,892.06 ± 9,451.28
Biological age	56.97 ± 18.19	144.07 ± 25.72	10.10 ± 2.36	NS	10.31 ± 2.53	0.002 ± 0.001	1,165.37 ± 249.94
Constant * Biological age	291.21 ± 80.22	656.61 ± 111.33	70.29 ± 14.01	−87.65 ± 20.47	59.93 ± 13.19	0.014 ± 0.004	7,579.32 ± 1,417.31

All numerical values are reported as significant, $p < 0.05$ (mean > 2 * SEE). NS, not significant.
Fixed-effects values are estimated mean coefficients ± standard error estimate (SEE) of total cross-sectional bone area (ToA; mm^2), total bone content (ToC; mg/mm), cortical bone content (CoC; mg/mm), cortical bone density (CoD; mg/cm^3), cortical bone area (CoA; mm^2), cortical thickness (CoTHK), and polar stress strain index (SSIp) at the tibial shaft (65% site). Random-effects values are estimated mean variance ± SEE. Biological age [at peak height velocity (PHV) = 0], tibia length (cm), physical activity score (z-score), sex (male = 0, female = 1), and gymnastic exposure (0 = no exposure, 1 = exposed to gymnastics).

Jones and colleagues measured boys and girls at 1 year past their PHV and categorized their participants' physical activity levels into three groups: inactive, average, and active (44). Our average PAQ-C score was 3, which would put our participants in the average physical activity level group. Therefore, the current participants would have continued to accrue BMC in the loaded bones and would have increased their BMC as seen in Bailey and associates' study (6). In fact, physical activity predicts adolescents' bone strength at 8% and 50% of their tibia length (45). Also, it has been found that physical activity engagement may be declining at approximately 5 to 7 years of age (46, 47), and participation in sports helps mediate this decrease (47). This may explain why there are no differences at the tibia since our control group was involved in sports and would load the tibia. However, recreational gymnastics, unlike most sports, loads the wrist. Therefore, we can assume that the difference at the distal radius is due to involvement in recreational gymnastics in young childhood and not from participation in other sports.

Finally, if involvement in recreational gymnastics only improves bone variables at the wrist, there is still clinical importance to increasing bone at that site. Childhood fracture incidence rates range from 20 to 36 per 1,000 (48, 49), with fractures at the radius and ulna making up 36% of upper body fractures (49). Recent research has shown that the highest fracture incidence rates continue to be at the distal forearm, clavicle, and distal humerus (50). Furthermore, with wrist fracture incidence rates slightly decreasing for women while remaining stable for men (51), it is important to strengthen the wrist during childhood to reduce the risk of fracture later in life. Additionally, the upper limb accounts for 65% of all childhood fractures and is a common site of fracture later in life (52–54). Therefore, participation in recreational gymnastics may provide a way to improve bone health during childhood and reduce the risk of wrist fractures later in life. Lastly, participating in recreational gymnastics has been shown to benefit bone health even in older adults (55–57), highlighting the potential of recreational gymnastics as a modality for bone health.

4.1 Strengths and limitations

A strength of this study is the use of pQCT to measure bone health instead of dual-energy X-ray absorptiometry (DXA). pQCT allows us to look at trabecular and cortical bone independently and together, which DXA is unable to do. Additionally, pQCT allows us

to evaluate a three-dimensional perspective of the bone rather than a two-dimensional perspective. This was also the first study, to the authors' knowledge, to examine the longer-term influence of recreational gymnastics participation on bone health.

A limitation of this study is, first, the variability when participants were tested. Not every individual was present at all five measurement occasions. Second, we were unable to conduct a sex-specific analysis due to our limited power. Additionally, the physical activity questionnaires did not specifically assess osteogenic loads of the activities that participants engaged in over the years. We were also unable to quantify the exact loads experienced during all the different recreational gymnastics classes, as they occurred at different locations and over 12 years. However, our group has previously quantified the loads experienced while performing different recreational gymnastics skills after observing the classes occurring at these different recruitment locations (18). Lastly, our control group was a physically active group rather than a sedentary control group. While this potentially limits our ability to assess the full influence of recreational gymnastics participation on bone health, we believe that the physically active control group allows us to highlight that, compared to an active group of peers, recreational gymnastics participation imparts a benefit above and beyond other forms of physical activity and sport participation at the wrist.

4.2 Future directions

Future research should be conducted comparing recreational gymnasts to sedentary controls, which would provide more insight into the potential benefits of involvement in recreational gymnastics during childhood. Furthermore, studies should examine if there is a dose-response threshold for recreational gymnastics benefits on bone health.

4.3 Conclusion

In conclusion, individuals who were involved in recreational gymnastics during childhood had higher ToA, ToC, BSIc, TrA, TrC, and TrD at the distal radius but no difference at the radial shaft or the tibia when compared to physically active controls. Should this difference progress into adulthood, it may reduce the risk of obtaining a wrist fracture. Previous research in the same cohort has shown that there are short-term benefits from being involved in recreational gymnastics during childhood; however, this analysis adds to the knowledge base by extending the results through adolescence up to 19 years of age. This study highlights the long-term impact of early childhood exposure to weight-bearing activity, such as recreational gymnastics participation.

Data availability statement

The raw data supporting the conclusions of this article will be made available by the authors, without undue reservation.

Ethics statement

The studies involving humans were approved by University of Saskatchewan's Biomedical Research Ethics Board. The studies were conducted in accordance with the local legislation and institutional requirements. Written informed consent for participation in this study was provided by the participants' legal guardians/next of kin.

Author contributions

MCE: Project administration, Data curation, Visualization, Conceptualization, Methodology, Supervision, Writing – review & editing, Funding acquisition, Writing – original draft, Investigation, Formal analysis. MSC: Data curation, Visualization, Writing – original draft, Writing – review & editing. MEKA: Writing – review & editing, Writing – original draft, Data curation. AJZ: Writing – review & editing, Writing – original draft, Data curation, Investigation. ADGBJ: Methodology, Data curation, Formal Analysis, Conceptualization, Writing – review & editing, Funding acquisition, Writing – original draft.

Funding

The author(s) declare financial support was received for the research and/or publication of this article. My (MCE) University of Saskatchewan New Faculty Start-Up funds were used for partial funding of this project.

Acknowledgments

The authors would like to acknowledge the participants and families involved in the Young Recreational Gymnast Study and their continued support of this project.

Conflict of interest

The authors declare that the research was conducted in the absence of any commercial or financial relationships that could be construed as a potential conflict of interest.

Generative AI statement

The author(s) declare that no Generative AI was used in the creation of this manuscript.

Any alternative text (alt text) provided alongside figures in this article has been generated by Frontiers with the support of artificial intelligence and reasonable efforts have been made to ensure accuracy, including review by the authors wherever possible. If you identify any issues, please contact us.

Publisher's note

References

1. Bonjour JP, Chevalley T, Ferrari S, Rizzoli R. The importance and relevance of peak bone mass in the prevalence of osteoporosis. *Salud Publica Mex*. (2009) 51:s5–s17. doi: 10.1590/s0036-36342009000700004

2. Baxter-Jones ADG, McKay H, Burrows M, Bachrach LK, Lloyd T, Petit M, et al. International longitudinal paediatric reference standard for bone mineral content. *Bone*. (2010) 23:1–7. doi: 10.1038/jid.2014.371

3. Chestnut CH. Is osteoporosis a pediatric disease? Peak bone mass attainment in the adolescent female. *Public Health Rep Supplement*. (1989) 104:50–4.

4. Nikander R, Sievänen H, Heinonen A, Daly RM, Uusi-Rasi K, Kannus P. Targeted exercise against osteoporosis: A systematic review and meta-analysis for optimising bone strength throughout life. *BMC Med*. (2010) 8:1–16. doi: 10.1186/1741-7015-8-47

5. Turner CH, Robling AG. Designing exercise regimens to increase bone strength. *Exerc Sport Sci Rev*. (2003) 31:45–50. doi: 10.1097/00003677-200301000-00009

6. Bailey DA, McKay HA, Mirwald RL, Crocker PRE, Faulkner RA. A six-year longitudinal study of the relationship of physical activity to bone mineral accrual in growing children: The University of Saskatchewan Bone Mineral Accrual Study. *J Bone Mineral Res*. (1999) 14:1672–9. doi: 10.1359/jbmr.1999.14.10.1672

7. Baxter-Jones ADG, Faulkner RA, Forwood MR, Mirwald RL, Bailey DA. Bone mineral accrual from 8 to 30 years of age: An estimation of peak bone mass. *J Bone Mineral Res*. (2011) 26:1729–39. doi: 10.1002/jbmr.412

8. Gabel L, McKay HA, Nettlefold L, Race D, Macdonald HM. Bone architecture and strength in the growing skeleton: The role of sedentary time. *Med Sci Sports Exerc*. (2015) 47:363–72. doi: 10.1249/MSS.0000000000000418

9. Gunter KB, Baxter-Jones ADG, Mirwald RL, Almstedt H, Fuller A, Durski S, et al. Jump starting skeletal health: A 4-year longitudinal study assessing the effects of jumping on skeletal development in pre and circum pubertal children. *Bone*. (2008) 42:710–8. doi: 10.1016/j.bone.2008.01.002

10. Gunter KB, Baxter-Jones ADG, Mirwald RL, Almstedt H, Fuchs RK, Durski S, et al. Impact exercise increases BMC during growth: An 8-year longitudinal study. *J Bone Mineral Res*. (2008) 23:986–93. doi: 10.1359/jbmr.071201

11. Kort L, Laing E, Pollock N, Lewis R, Georgia GA, Vingren JL, et al. Former collegiate gymnasts maintain higher bone mineral density after A 34-year retirement: A twenty-year follow-up. *Med Sci Sports Exercise*. (2015) 47:704.

12. Gannon L, Hind K. Skeletal loading: Lean and bone mass development in young elite male gymnasts, swimmers, and nonathletes aged 6–24 years. *Pediatr Exerc Sci*. (2024) 36:224–32. doi: 10.1123/pes.2024-0029

13. Jürimäe J, Gruodyte-Raciene R G, Baxter-Jones AD. Effects of gymnastics activities on bone accrual during growth: A systematic review. *J Sports Sci Med*. (2018) 17:245–58.

14. Burt LA, Greene DA, Naughton GA. Bone health of young male gymnasts: A systematic review. *Pediatr Exerc Sci*. (2017) 29:456–64. doi: 10.1123/pes.2017-0046

15. Dowthwaite JN, Flowers PPE, Spadaro JA, Scerpella TA. Bone geometry, density, and strength indices of the distal radius reflect loading via childhood gymnastic activity. *J Clin Densitometry*. (2007) 20:65–75. doi: 10.1016/j.jocd.2006.10.003

16. Scerpella TA, Dowthwaite JN, Rosenbaum PF. Sustained skeletal benefit from childhood mechanical loading. *Osteoporosis Int*. (2011) 22:2205–10. doi: 10.1007/s00198-010-1373-4

17. Daly RM, Rich PA, Klein R, Bass S. Effects of high-impact exercise on ultrasonic and biochemical indices of skeletal status: A prospective study in young male gymnasts. *J Bone Mineral Res*. (1999) 14:1222–30. doi: 10.1359/jbmr.1999.14.7.1222

18. Erlandson MC, Hounjet S, Treen T, Lanovaz JL. Upper and lower limb loading during weight-bearing activity in children: reaction forces and influence of body weight. *J Sports Sci*. (2018) 36:1640–7. doi: 10.1080/02640414.2017.1407438

19. Erlandson MC, Kontulainen SA, Chilibeck PD, Arnold CM, Baxter-Jones ADG. Bone mineral accrual in 4- to 10-year-old precompetitive, recreational gymnasts: A 4-year longitudinal study. *J Bone Mineral Res*. (2011) 26:1313–20. doi: 10.1002/jbmr.338

20. Laing EM, Wilson AR, Modlesky CM, O'Connor PJ, Hall DB, Lewis RD. Initial years of recreational artistic gymnastics training improves lumbar spine bone mineral accrual in 4- to 8-year-old females. *J Bone Mineral Res*. (2005) 20:509–19. doi: 10.1359/JBMR.041127

21. Erlandson MC, Kontulainen SA, Baxter-Jones ADG. Precompetitive and recreational gymnasts have greater bone density, mass, and estimated strength at the distal radius in young childhood. *Osteoporosis Int*. (2011) 22:75–84. doi: 10.1007/s00198-010-1263-9

22. Jackowski SA, Baxter-Jones ADG, Gruodyte-Raciene R, Kontulainen SA, Erlandson MC. A longitudinal study of bone area, content, density, and strength development at the radius and tibia in children 4–12 years of age exposed to recreational gymnastics. *Osteoporosis Int*. (2015) 26:1677–90. doi: 10.1007/s00198-015-3041-1

23. Dowthwaite JN, Scerpella TA. Distal radius geometry and skeletal strength indices after peripubertal artistic gymnastics. *Osteoporosis Int*. (2010) 22:207–16. doi: 10.1007/s00198-010-1233-2

24. Stewart A, Marfell-Jones M, Olds T, De Ridder JH. *International standards for anthropometric assessment*. Sydney, Austrailia: International Society for the Advancement of Kinanthropometry. (2001). p. 1.

25. Mirwald RL, Baxter-Jones ADG, Bailey DA, Beunen GP. An assessment of maturity from anthropometric measurements. *Med Sci Sports Exerc*. (2002) 34:689–94. doi: 10.1097/00005768-200204000-00020

26. Kontulainen S, Johnston J, Lui D, Leung C, Oxland T, McKay H. Strength indices frompQCT imaging predict up to 85% of variance in bone failure properties at the tibial epiphysis and diaphysis. *J Musculoskelet Neuronal Interact*. (2008) 8:401–9.

27. Duckham RL, Frank AW, Johnston JD, Olszynski WP, Kontulainen SA. Monitoring time interval for pQCT-derived bone outcomes in postmenopausal women. *Osteoporosis Int*. (2013) 24:1917–22. doi: 10.1007/s00198-012-2242-0

28. Janz KF, Broffitt B, Levy SM. Validation evidence for the Netherlands physical activity questionnaire for young children: The Iowa bone development study. *Res Q Exerc Sport*. (2005) 76:363–9. doi: 10.1080/02701367.2005.10599308

29. Kowalski KC, Crocker PRE, Columbia B, Donen RM. The physical activity questionnaire for older children (PAQ-C) and adolescents (PAQ-A) manual. (2004).

30. Kowalski KC, Crocker PRE, Kowalski N. Convergent validity of the physical activity questionnaire for adolescents. *Pediatr Exerc Sci*. (1997) 9:342–52. doi: 10.1123/pes.9.4.342

31. Kowalski KC, Crocker PRE, Faulkner RA. Validation of the physical activity questionnaire for older children. *Pediatr Exerc Sci*. (1997) 9:174–86. doi: 10.1123/pes.9.2.174

32. Crocker PR, Bailey DA, Faulkner RA, Kowalski KC, McGrath R. Measuring general levels of physical activity: Preliminary evidence for the Physical Activity Questionnaire for Older Children. *Med Sci Sports Exerc*. (1997) 29:1344–9. doi: 10.1097/00005768-199710000-00011

33. Goldstein H, Browne W, Rasbash J. Multilevel modelling of medical data. *Stat Med*. (2002) 21:3291–315. doi: 10.1002/sim.1264

34. Baxter-Jones ADG, Mirwald R. Multilevel modelling. In: Hauspie R, Cameron N, Molinari L, editors. *Methods in Human Growth Research*. Cambridge University Press, Cambridge, UK (2004). p. 306–30. doi: 10.1017/CBO9780511542411

35. Erlandson MC, Kontulainen SA, Chilibeck PD, Arnold CM, Faulkner RA, Baxter-Jones ADG. Higher premenarcheal bone mass in elite gymnasts is maintained into young adulthood after long-term retirement from sport: A 14-year follow-up. *J Bone Mineral Res*. (2012) 27:104–10. doi: 10.1002/jbmr.514

36. Eser P, Hill B, Ducher G, Bass S. Skeletal benefits after long-term retirement in former elite female gymnasts. *J Bone Mineral Res*. (2009) 24:1981–8. doi: 10.1359/jbmr.090521

37. Zanker CL, Osborne C, Cooke CB, Oldroyd B, Truscott JG. Bone density, body composition and menstrual history of sedentary female former gymnasts, aged 20–32 years. *Osteoporosis Int*. (2004) 15:145–54. doi: 10.1007/s00198-003-1524-y

38. Burt LA, Naughton G, Courteix D, Greene D. Gymnastics participation is associated with skeletal benefits in the distal forearm: A 6-month study using peripheral Quantitative Computed Tomography. *J Musculoskelet Neuronal Interact*. (2013) 13:395–404.

39. Ward KA, Roberts SA, Adams JE, Mughal MZ. Bone geometry and density in the skeleton of pre-pubertal gymnasts and school children. *Bone*. (2005) 36:1012–8. doi: 10.1016/j.bone.2005.03.001

40. Ducher G, Hill BL, Angeli T, Bass SL, Eser P. Comparison of pQCT parameters between ulna and radius in retired elite gymnasts: The skeletal benefits associated with long-term gymnastics are bone- and site-specific. *J Musculoskelet Neuronal Interact*. (2009) 9:247–55. doi: 10.1530/endoabs.63.p470

41. Tournis S, Michopoulou E, Fatouros IG, Paspati I, Michalopoulou M, Raptou P, et al. Effect of rhythmic gymnastics on volumetric bone mineral density and bone geometry in premenarcheal female athletes and controls. *J Clin Endocrinol Metab*. (2010) 95:2755–62. doi: 10.1210/jc.2009-2382

42. Seegmiller JG, McCaw ST. Ground reaction forces among gymnasts and recreational athletes in drop landings. *J Athletic Training 311 J Athletic Training*. (2003) 38:311–4.

43. Burt LA, Naughton GA, Greene DA, Courteix D, Ducher G. Non-elite gymnastics participation is associated with greater bone strength, muscle size, and function in pre- and early pubertal girls. *Osteoporosis Int*. (2012) 23:1277–86. doi: 10.1007/s00198-011-1677-z

44. Baxter-Jones ADG, Kontulainen SA, Faulkner RA, Bailey DA. A longitudinal study of the relationship of physical activity to bone mineral accrual from adolescence to young adulthood. *Bone*. (2008) 43:1101–7. doi: 10.1016/j.bone.2008.07.245

45. Tan VP, Macdonald HM, Gabel L, McKay HA. Physical activity, but not sedentary time, influences bone strength in late adolescence. *Arch Osteoporos*. (2018) 13:1–9. doi: 10.1007/s11657-018-0441-9

46. Farooq MA, Parkinson KN, Adamson AJ, Pearce MS, Reilly JK, Hughes AR, et al. Timing of the decline in physical activity in childhood and adolescence: Gateshead Millennium Cohort Study. *Br J Sports Med*. (2018) 52:1002–6. doi: 10.1136/bjsports-2016-096933

47. Kwon S, Janz KF, Letuchy EM, Burns TL, Levy SM. Developmental trajectories of physical activity, sports, and television viewing during childhood to young adulthood: Iowa bone development study. *JAMA Pediatr*. (2015) 169:666–72. doi: 10.1001/jamapediatrics.2015.0327

48. Rennie L, Court-Brown CM, Mok JYQ, Beattie TF. The epidemiology of fractures in children. *Injury*. (2007) 38:913–22. doi: 10.1016/j.injury.2007.01.036

49. Lyons RA, Delahunty AM, Kraus D, Heaven M, McCabe M, Allen H, et al. Children's fractures: A population based study. *Injury Prev*. (1999) 5:129–32. doi: 10.1136/ip.5.2.129

50. Larsen AV, Mundbjerg E, Lauritsen JM, Faergemann C. Development of the annual incidence rate of fracture in children 1980–2018: a population-based study of 32,375 fractures. *Acta Orthop*. (2020) 91:1–5. doi: 10.1080/17453674.2020.1772555

51. De Putter CE, Selles RW, Polinder S, Hartholt KA, Looman CW, Panneman MJM, et al. Epidemiology and health-care utilisation of wrist fractures in older adults in the Netherlands, 1997-2009. *Injury*. (2013) 44:421–6. doi: 10.1016/j.injury.2012.10.025

52. Clark EM. The epidemiology of fractures in otherwise healthy children. *Curr Osteoporos Rep*. (2014) 12:272–8. doi: 10.1007/s11914-014-0227-y

53. Moustaki M, Lariou M, Petridou E. Cross country variation of fractures in the childhood population. Is the origin biological or "accidental"? *Injury Prev*. (2001) 7:77–9. doi: 10.1136/ip.7.1.77

54. Polinder S, Iordens GI, Panneman MJ, Eygendaal D, Patka P, Den Hartog D, et al. Trends in incidence and costs of injuries to the shoulder, arm and wrist in the Netherlands between 1986 and 2008. *BMC Public Health*. (2013) 13. doi: 10.1186/1471-2458-13-531

55. Uusi-Rasi K, Karinkanta S, Kannus P, Tokola K, Sievänen H. Does long-term recreational gymnastics prevent injurious falls in older women? A prospective 20-year follow-up. *BMC Geriatr*. (2020) 20. doi: 10.1186/s12877-020-1428-0

56. Uusi-Rasi K, Sievänen H, Heinonen A, Vuori I, Beck TJ, Kannus P. Long-term recreational gymnastics provides a clear benefit in age-related functional decline and bone loss. A prospective 6-year study. *Osteoporosis Int*. (2006) 17:1154–64. doi: 10.1007/s00198-006-0108-z

57. Uusi-Rasi K, Sievänen H, Vuori I, Heinonen A, Kannus P, Pasanen M, et al. Long term recreational gymnastics, estrogen use, and selected risk factors for osteoporotic fractures. *J Bone Mineral Res*. (1999) 14:1231–8. doi: 10.1359/jbmr.1999.14.7.1231

Frontiers in Endocrinology

Explores the endocrine system to find new therapies for key health issues

The second most-cited endocrinology and metabolism journal, which advances our understanding of the endocrine system. It uncovers new therapies for prevalent health issues such as obesity, diabetes, reproduction, and aging.

Discover the latest Research Topics

See more →

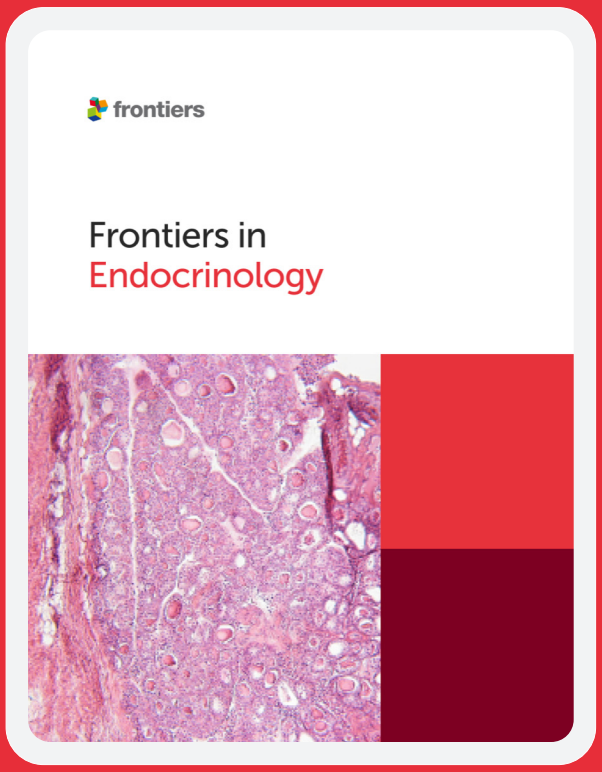

Frontiers

Avenue du Tribunal-Fédéral 34
1005 Lausanne, Switzerland
frontiersin.org

Contact us

+41 (0)21 510 17 00
frontiersin.org/about/contact